CHARACTERIZATION OF SELECTED PETROLEUM SOURCE ROCKS AND RESERVOIR ROCKS OF BENGAL BASIN (BANGLADESH) BASED ON GEOCHEMICAL, PETROGRAPHICAL AND PETROPHYSICAL METHODS

MD. FARHADUZZAMAN

THESIS SUBMITTED IN FULFILLMENT OF THE REQUIREMENTS FOR THE DEGREE OF DOCTOR OF PHILOSOPHY

DEPARTMENT OF GEOLOGY
FACULTY OF SCIENCE
UNIVERSITY OF MALAYA
KUALA LUMPUR

2013

UNIVERSITI MALAYA

ORIGINAL LITERARY WORK DECLARATION

Name of Candidate: Md. Farhaduzzaman (I.C/Passport No: AD7162597)

Registration/Matric No: SHC100036

Name of Degree: Doctor of Philosophy

Title of Project Paper/Research Report/Dissertation/Thesis ("this Work"):

CHARACTERIZATION OF SELECTED PETROLEUM SOURCE ROCKS AND RESERVOIR ROCKS OF BENGAL BASIN (BANGLADESH) BASED ON GEOCHEMICAL, PETROGRAPHICAL AND PETROPHYSICAL METHODS

Field of Study: Coal / Petroleum Geology

1) I do solemnly and sincerely declare that:
2) I am the sole author/writer of this Work;
3) This Work is original;
4) Any use of any work in which copyright exists is done by way of fair dealing and for permitted purposes and any excerpt or extract from, or reference to or reproduction of any copyright work has been disclosed expressly and sufficiently and the title of the Work and its authorship have been acknowledged in this Work;
5) I do not have any actual knowledge nor do I ought reasonably to know that the making of this work constitutes an infringement of any copyright work;
6) I hereby assign all and every rights in the copyright to this Work to the University of Malaya ("UM"), who henceforth shall be owner of the copyright in this Work and that any reproduction or use in any form or by any means whatsoever is prohibited without the written consent of UM having been first had and obtained;
7) I am fully aware that if in the course of making this Work I have infringed any copyright whether intentionally or otherwise, I may be subject to legal action or any other action as may be determined by UM.

Candidate's Signature Date

Subscribed and solemnly declared before,

Witness's Signature Date

Name: Dr. Wan Hasiah Binti Abdullah
Designation: Professor and Supervisor

ABSTRACT

Nine gas fields and two coal fields of Bengal Basin, Bangladesh are studied in the current research based on geochemical, petrographical and petrophysical methods. The Surma Group of Bengal Basin is composed of the Bhuban and Boka Bil Formations. Both formations are composed of sandstones and shales interpreted to have been deposited in a deltaic to shallow-marine environment. This is the most important geological unit of the basin since the entire hydrocarbon accumulations so far discovered in Bangladesh is found within these sandstones. These two formations also contain shale intervals with important source rock potential. Together with coal and coaly samples, shales and sandstones of the Surma Group are the key subjects of the present study. Around 151 core samples of shale, sandstone and coal were investigated for this project. Shale and sandstone cores were chosen from ten wells of respective nine gas fields. Five bore holes of the Barapukuria and Dighipara Basins were selected for coal, carbargillite and mudstone sampling. All shale, coal and coaly samples are subjected to a Source Rock Analyzer (SRA). After SRA screening, different standard geochemical methods (e.g., PyGC, GC, GCMS, AAS, TG-DTA, EA and proximate analysis) were employed for the current study. Many shale and coal and coaly samples are examined with UV-facilitated microscope for maceral and vitrinite reflectance analyses. Poor to fair quality source rock potential is estimated for the studied Bhuban and Boka Bil shales. The organic matter found in both formations is thermally immature to early mature for hydrocarbon generation. The organic matters of the analyzed shales are derived from land plants of terrestrial environmental settings with minor contribution from marine sources. The siliciclastic sandstone samples are studied using both petrographic microscope, SEM and XRD for reservoir quality and diagenetic control analysis. Very good to excellent reservoir quality is evaluated by the present study.

Together with petrography, petrophysical analysis is also carried out for one well (Rashidpur 4) and four potential hydrocarbon bearing zones are identified.

The depositional environment and hydrocarbon generation potential is another focus of the present study, emphasizing the biomarker characteristics of Permian coals of the Barapukuria and Dighipara half-graben basins. In this project, organic facies distributions within the Permian succession are investigated focusing on coals, carbargillites and mudstones in the half-graben basins. The studied bituminous B rank coal consists dominantly of inertinite macerals followed by vitrinite and liptinite. The various facies models used commonly indicate forest swamps with mixed oxic-anoxic conditions under terrestrial settings with periodic flooding. Organic facies characteristics suggest that the coals are dominantly terrestrial with minor contributions from marine sources. The carbargillites correspond to a mixture of terrestrial and marine sources, whereby the mudstones being terrestrial with no marine influences. Very good hydrocarbon generation potential is estimated for the analyzed coal and coaly samples, ranging from fair to excellent. The carbargillites possess good potential for both oil and gas and followed by coals (mainly gas with minor oil) and mudstones (predominantly gas). Along with $\%R_o$ and T_{max}, the presence of exsudatinite, fluorinite and solid bitumen suggests the analyzed coal and coaly samples have already expelled hydrocarbons.

ABASTRAK (Bahasa Malaysia)

Kajian terhadap sembilan lapangan gas and dua lapangan arang batu telah dijalankan menggunakan kaedah-kaedah geokimia, petrografi and petrofizik. Kumpulan Surma yang terletak di Lembangan Bengal terdiri daripada Formasi Bhuban and Formasi Boka Bil. Kedua-dua formasi ini terdiri daripada batu pasir dan batuan syal yang ditafsirkan telah dienapkan di persekitaran delta hingga ke laut cetek. Unit geologi ini adalah amat penting bagi lembangan ini berdasarkan jumlah himpunan hidrokarbon yang telah dijumpai. Kedua-dua formasi ini juga mengandungi beberapa ketebalan batuan syal yang amat penting berpotensi sebagai batuan punca bagi hidrokarbon tersebut. Kesemua sampel arang batu, sampel yang mengandungi arang batu, batuan syal dan batu pasir ini merupakan keutamaan bagi kajian ini. Lebih kurang 151 sampel teras bagi batuan syal, batu pasir dan arang batu telah diselidik bagi projek ini. Teras-teras bagi batuan syal dan batu pasir telah dipilih daripada sepuluh telaga daripada sembilan lapangan gas di kawasan tersebut. Lima lubang teras daripada Lembangan Barapukuria dan Lembangan Dighipara telah dipilih bagi persampelan arang batu, batuan berkarbon (carbargillites) dan batu lumpur. Kesemua sampel-sampel batuan syal, arang batu dan batuan yang mengandungi arang batu ini tertakluk kepada kaedah Analisis Batuan Sumber (SRA). Selepas analisis SRA dijalankan, beberapa kaedah geokimia standard seperti PyGC, GC, GCMS, AAS, TG-DTA, EA dan anggaran atau analisis mutlak dan sebagainya telah dijalankan bagi kajian ini. Beberapa sampel batuan syal dan arang batu telah diuji dengan mikroskop yang mempunyai UV untuk analisis maseral dan vitrinit reflectans. Keputusan ujian bagi syal Bhuban dan Boka Bil ini menunjukkan kualiti potensi arang batu yang lemah kepada baik. Bahan organik yang dijumpai di dalam kedua-dua formasi menunjukkan yang ianya tidak matang hingga ke tahap awal kematangan bagi penjanaan hidrokarbon. Bahan-bahan organik daripada batuan syal ini terhasil daripada tumbuhan daratan daripada persekitaran daratan dengan hanya sedikit sumbangan daripada sumber lautan. Sampel-sampel batu pasir silisiklastik

dikaji menggunakan kaedah mikroskop petrografi, SEM dan XRD untuk menentukan kualiti takungan hidrokarbon dan kawalan diagenetik di mana hasil kajian menunjukkan kualiti takungan adalah sangat bagus hingga cemerlang. Bersama-sama dengan petrografi, analisis petrofizik juga dijalankan bagi telaga Rashidpur 4 dan empat zon lagi yang dikenalpasti mempunyai potensi menghasilkan hidrokarbon.

Persekitaran enapan dan potensi penjanaan hidrokarbon juga merupakan tumpuan bagi kajian ini dengan penekanan pada ciri-ciri biomarker bagi arang batu Permian bagi Lembangan Barapukuria dan Lembangan separa-graben Dighipara. Di dalam projek ini, taburan fasies organik bagi batuan Permian telah diselidiki dengan keutamaan pada arang batu, batuan berkarbon (carbargillites) dan batu lumpur di kawasan lembangan separa-graben. Arang batu berbitumen kelas B yang telah dikaji mengandungi kebanyakannya adalah maseral inertinit diikuti oleh vitrinit dan liptinit. Kajian model fasies yang digunakan menunjukkan kebanyakannya adalah hutan paya bakau dengan campuran keadaan oksid-anoksid kawasan daratan dengan banjir berkala. Ciri-ciri fasies organik arang batu menunjukkan kebanyakannya adalah dari daratan dengan sedikit sumbangan daripada lautan. Batuan berkarbon (carbargillites) pula menunjukkan campuran punca daratan dan lautan manakala batu lumpur pula adalah daratan sahaja tanpa dipengaruhi lautan. Dianggarkan potensi penghasilan hidrokarbon bagi sampel arang batu adalah sangat baik manakala bagi sampel yang mengandungi arang batu adalah baik hingga cemerlang. Batuan berkarbon (carbargillites) mempunyai potensi minyak dan gas, diikuti arang batu kebanyakannya adalah berpotensi untuk gas dan sedikit minyak, manakala batu lumpur pula kebanyakannya adalah berpotensi untuk gas. Bersama-sama dengan $\%R_o$ and T_{max}, kehadiran beberapa maseral yang penting seperti liptinit menunjukkan bahawa sampel arang batu dan sampel yang mengandungi arang batu yang dianalisis ini telah mengeluarkan hidrokarbon.

ACKNOWLEDGEMENTS

The motherly behavior of my supervisor Prof. Dr. Wan Hasiah Binti Abdullah has made me very easy to accomplish this research work very successfully. I pass the times here at UM like my own home at Bangladesh just because of the brotherly behavior of my co-supervisor Dr. Md. Aminul Islam. Because of their very friendly cooperation and guidance I have never felt the home sickness. I am really very lucky for being a research student of these two excellent academicians with unique personalities. Mr. Zamri Rashid, Mr. Abdul Rahman, Mrs. Maisarah, Mrs. Zaitun and Mrs. Zaleha have assisted a lot during the laboratory analysis. The cooperation from Mrs Zurina Marzuki, Physics Department, University of Malaya (Malaysia) and School of Geoscience, University of Tsukuba (Japan) is acknowledged for providing their supports on FESEM and SEM respectively. Prof. Dr. Michael J. Pearson, Aberdeen University, UK and Mr. Peter Abolin, PETRONAS, Malaysia have assisted in different arenas of the present work. The cooperation from Mr Joyanta Dutto (Chulalongkorn University) and Afzal Hossain (Geokinetics) is acknowledged for petrophysical analysis. Dr. Aqueel Ashraf helped to carry out the elemental analyses. Minerals and Geoscience Department Malaysia (JMG) has analyzed the coal samples for proximate analyses. Mrs. Norishah Hashim of UM Geology assisted for translating the English Abstract to Bahasa Malaysia. SRA and RE analyses have been carried out in the Weatherford Laboratories (USA) and Geotechnical Services (Australia) respectively. Special thank goes to Dr. Rahman and Dr. Zakia (Ireland) who have helped a lot for English editing with the thesis.

I am grateful to Prof. Dr. Md. Hussain Monsur, Chairman of Bangladesh Oil, Gas and Mineral Corporation (Petrobangla) and Mrs. Monira Akhter Chowdhury, Director General of the Geological Survey of Bangladesh (GSB) for permitting the usage of the samples and data for this study. Mr. Mortuza Ahmad Faruque, Managing Director, Bangladesh Petroleum Exploration and Production Co. Ltd. deserves the cordial thanks for providing the necessary shale and sandstone samples and related reports for the present research. During the official and sampling procedures, the friendly cooperation from the Petrobangla personnel Mr. R. A. Khan Kayas, Mr. Mahfuzul Haque, Mr. Fazlul Karim, Mr. Faisal

Ahmed, Mr. Akhtaruzzaman and Mrs. Zebunnahar Moly is cordially acknowledged. The BAPEX personnel Mr. Ruhul Chowdhury, Mrs. Nahar Begum, Mr. Babul Akhtar, Mr. Mamun Rony and Mr. Mozammel Haque have cooperated greatly in the official and sampling systems. Dr. Nehel Uddin (GSB), Mr. Abdul Hannan (BCMCL), Mr. Zahangir Alam (BCMCL) and Mr. Kamal Uddin (BCMCL) have helped a lot during the coal core collection. Sylhet Gas Fields Limited (A Company of Petrobangla) deserves the appreciation for providing the official supports including the required leave for the present research. Especial thank goes to Mr. Tofazzal Hossain, Managing Director of SGFL and his colleagues. I always remember the cooperation and mental supports form Mr. Shamsul Islam, Mr. Mozammel Chowdhury, Mr. N. A. Haider, Mr. Abdul Qadir, Mr. Rawnakul Islam Opu, Mr. Akbar Ali Tula, Mr. Ekramul Haque, Mr. Helal Uddin, Mr. Abdur Rahman Rumi, Mr. Nazrul Islam, Mr. Nuruzzaman Khan, Group-09 members, other colleagues of SGFL and former colleagues of Asia Energy Corporation (Bangladesh) Pty Ltd. I am cordially acknowledging the cooperation and motivation provided by Prof. Dr. Khalil R. Chowdhury and his colleagues at Jahangirnagar University while carrying out this study. I recall the inspirations delivered by Mr. Frans Boss, Mr. Ben Jonsen, Mr. John Anderson and Mr. Tony Armstrong (former colleagues) from GHD Australia. The examiners Prof. Dr. James C. Hower (University of Kentucky, USA), Prof. Dr. M. P. Singh (Banaras Hindu University, India) and Prof. Dr. Mohammad Y. Bakr (University of Malaya) deserve the sincere gratitude for their fruitful suggestions while reviewing the thesis. The Bright Sparks Fellowship BSP-APP-1080-2012, IPPP grant PV100-2011A and UMRG grants RG121/10AFR and RG145/11AFR from the University of Malaya for financial support are acknowledged.

Mrs. Murshida Khanam Ratna (my wife) has always supported me in order to carry out this research. Without her great sacrifices, the present PhD project would not have accomplished successfully. I am also grateful to those known and unknown peoples who have helped me in any stage of this research. Finally I am thankful to Almighty Allah who has powered me to accomplish this research successfully.

Md. Farhaduzzaman July 2013

Dedicated to

my family members and late father

CONTENTS OF THESIS

	Page no.
Abstract	ii
Abstrak (Bahasa Malaysia)	iv
Acknowledgements	vi
Dedication	viii
CHAPTER 1: INTRODUCTION	1
1.1 Background	1
1.2 Exploration History, Petroleum System and Study Design	5
1.3 Aims and Objectives	9
1.4 Limitations of the Study	10
1.5 Outline of the Thesis	10
CHAPTER 2: LITERATURE REVIEW AND STUDY AREAS	12
2.1 Previous Studies	12
2.1.1 Shale	12
2.1.2 Coal	13
2.1.3 Reservoir sandstone	15
2.2 Regional Geology and Tectonics	16
2.3 Study Areas and their Stratigraphic Frameworks	20
2.3.1 Structure and Stratigraphy of the Barapukuria Coal Basin	20
2.3.1.1 Basement Complex (Archaean) in Barapukuria	22
2.3.1.2 Gondwana Group (Permian) in Barapukuria	22
2.3.1.3 Dupi Tila Formation (Mio-Pliocene) in Barapukuria	26
2.3.1.4 Barind Clay (Pleistocene to Recent) in Barapukuria	28
2.3.2 Structure and Stratigraphy of the Dighipara Coal Basin	28
2.3.2.1 Basement Complex (Archaean) in Dighipara	31
2.3.2.2 Gondwana Group (Permian) in Dighipara	32
2.3.2.3 Dupi Tila Formation (Mio-Pliocene) in Dighipara	32
2.3.2.4 Barind Clay (Pleistocene to Recent) in Dighipara	33
2.3.3 Stratigraphy of the Deep Basin unit of the Bengal Basin	33
2.3.3.1 Jaintia Group (Paleocene-Eocene)	35
2.3.3.2 Barail Group (Oligocene)	35
2.3.3.3 Surma Group (Mio-Pliocene)	37
2.3.3.4 Tipam Group (Pliocene)	39
2.3.3.5 Madhupur Clay Formation (Plio-Pleistocene)	39
2.4 Coal Resources in the Bengal Basin, Bangladesh	41
2.5 Hydrocarbons in the Bengal Basin, Bangladesh	41
CHAPTER 3: MATERIALS AND METHODS	43
3.1 Fieldwork and sampling	43
3.2 Laboratory work	44
3.2.1 SRA and RE	46
3.2.2 EA	49
3.2.3 Bitumen extraction (EOM)	49
3.2.4 Liquid column chromatography	50
3.2.5 PyGC	51
3.2.6 GC and GCMS	53
3.2.7 AAS	55
3.2.8 Polished block preparation (shale/coal) for microscopic study	56
3.2.9 Petrographic study of shale, coal and other coaly samples	58

Page no.
3.2.10 Themrogravimetry-differential thermal analysis (TG-DTA) 60
3.2.11 Thin section preparation for sandstone samples 61
3.2.12 Petrographic study of sandstone samples 64
3.2.13 XRD analysis 65
3.3 Software Used 67
3.3.1 ProSim 67
3.3.2 Didger 4 68
3.3.3 Excel for petrophysical analysis 68
3.3.4 EndNote, StyleWriter and Turnitin 73
CHAPTER 4: RESULTS AND DISCUSSION 74
4.1 Petroleum Source Rock- Shales 75
4.1.1 Source rock properties 75
4.1.2 Maceral characteristics and kerogen type 79
4.1.3 Soluble extract and biomarker distributions 88
4.1.3.1 GC: TIC 89
4.1.3.2 GCMS: m/z 191 92
4.1.3.3 GCMS: m/z 217 97
4.1.4 Discussion 98
4.1.4.1 Thermal maturity 98
4.1.4.2 Hydrocarbon generation potential 100
4.1.4.3 Environment of deposition 103
4.1.4.4 Stratigraphic correlation 108
4.2 Petroleum Source Rock- Permian Coals 110
4.2.1 Macroscopic study of coals 111
4.2.1.1 Seam characteristics 111
4.2.1.2 Proximate analysis 112
4.2.1.3 Discussion 114
4.2.1.3.1 Moisture content 116
4.2.1.3.2 Volatile matters 117
4.2.1.3.3 Ash yield 117
4.2.1.3.4 Fixed carbon 117
4.2.1.3.5 Elemental concentrations 118
4.2.2 Microscopic study of coals 122
4.2.2.1 Macerals 122
4.2.2.1.1 Vitrinite group 122
4.2.2.1.2 Liptinite group 127
4.2.2.1.3 Inertinite group 135
4.2.2.1.4 Mineral matters 137
4.2.2.2 Microlithotypes 137
4.2.2.3 Discussion 141
4.2.2.3.1 Facies models 141
4.2.2.3.1.1 Mukhopadhyay (1986) facies model 142
4.2.2.3.1.2 Singh and Singh (1996) facies model 142
4.2.2.3.1.3 Diessel (1986) facies model 142
4.2.2.3.1.4 Calder et al. (1991) facies model 143
4.2.2.3.1.5 Hacquebard and Donaldson (1969) model 145
4.2.2.3.2 Depositional environment of the Barapukuria and Dighipara Basin coals 148

Page no.
4.2.3 Organic geochemical study of coals and associated sediments 154
4.2.3.1 Source rock properties 154
4.2.3.2 Macerals and kerogen type 157
4.2.3.3 Soluble extract and biomarker distributions 161
4.2.3.3.1 GC: TIC 164
4.2.3.3.2 GCMS: m/z 191 168
4.2.3.3.3 GCMS: m/z 217 169
4.2.3.4 Discussion 170
4.2.3.4.1 Thermal maturity of organic matter 170
4.2.3.4.2 Organic facies characteristics 172
4.2.3.4.3 Hydrocarbon generation and expulsion 176
4.3 Petroleum Reservoir Rock- Sandstones 184
4.3.1 Petrography and diagenesis of sandstones 185
4.3.1.1 Sandstone texture and sorting 185
4.3.1.2 Sandstone composition 185
4.3.1.3 Sandstone classification 193
4.3.1.4 Diagenetic constituents 196
4.3.1.4.1 Quartz cements 196
4.3.1.4.2 Clay mineral authigenesis 197
4.3.1.4.3 Carbonate cements 200
4.3.1.4.4 Feldspar authigenesis 200
4.3.1.4.5 Dissolution and replacement 204
4.3.1.5 Compaction and grain packing 204
4.3.1.6 Discussion and reservoir implications 205
4.3.1.6.1 Implications to reservoir porosity and permeability 210
4.3.2 Petrophysical study of the well Rashidpur 4 213
4.3.2.1 Data analysis and interpretation 213
4.3.2.2 Identification of HC bearing zones 214
4.3.2.3 Shale distribution 215
4.3.2.4 Porosity distribution 216
4.3.2.5 Water saturation distribution 216
4.3.2.6 HC saturation distribution 226
4.3.2.7 Permeability distribution 226
4.3.2.8 HC moveability index 227
4.3.2.9 Bulk volume of water 227
4.3.2.10 Discussion 227
CHAPTER 5: CONCLUSIONS AND RECOMMENDATION 231

List of Figures xii
List of Tables xvii
List of Symbols and Abbreviations xviii
List of Appendices xix
Bibliography 271

LIST OF FIGURES

Page no.

Fig.1.1. Location map shows the studied nine gas fields and two coal basins (Imam, 2005). 3
Fig.1.2. The essential petroleum system elements of any sedimentary basin (AAPG, 2011). 7
Fig.1.3. Flow chart of the research approach and outlines of the current project. 8
Fig.2.1. Location map of study areas including Barapukuria and Dighipara Coal Basins and nine gas fields. It shows the major tectonic elements of the Bengal Basin (modified after Khan, 1991; Reimann, 1993; Alam, et al., 2003; Shamsuddin et al., 2004; Imam, 2005). 18
Fig.2.2. The positions of Gondwana basins in the vicinity of the Barapukuria and Dighipara Coal Basins (after Uddin and Islam, 1992; Imam, 2005; Islam and Hayashi, 2008; Farhaduzzaman et al., 2012a). 22
Fig.2.3. (a) Sampling locations shown in the study area of the Barapukuria Basin, Bangladesh. Two cross-sections have also been added- (b) west to east, and (c) north to south (Imam, 2005; Islam and Hayashi, 2008; Farhaduzzaman et al., 2013c and 2013d). The analyzed samples are collected from Seam VI, Seam V and Seam IV. 23
Fig.2.4. Generalized lithostratigraphic succession of the Barapukuria Basin, Bangladesh. (a) represents the central north-western part of the basin, and (b) represents the central south-eastern part of the basin (Fig.2.3 for its location). The sampling locations are also shown. 27
Fig.2.5. Sampling locations in the study area of the Dighipara Coal Basin, Bangladesh. 29
Fig.2.6. Generalized lithostratigraphic columns of two investigated bore holes GDH60 and GDH62 of Dighipara Basin. Sampling positions are shown here (Farhaduzzaman et al., 2012a). 31
Fig.2.7. Correlation of the studied ten wells (from north to south) of respective nine gas fields, the Bengal Basin, Bangladesh. All of the analyzed samples are collected from Boka Bil and Bhuban Formations lying at the bottom part (Moinul et al, 1977; Nazim et al., 1982; Khan, 1991; Alam et al., 2003; Imam, 2005; Farhaduzzaman et al., 2012b and 2013b). 36
Fig.2.8. Geological cross-section through the Platform (Province 1) unit and southern part of the Deep Basin (Province 2) unit of the Bengal Basin. The location of cross-section line has been shown in Fig.2.1 (after Alam et al., 2003). 38
Fig.2.9. The petroleum systems of the Bengal Basin, Bangladesh. The estimated hydrocarbon resource is added (modified after Jamaluddin et al., 2001; Shamsuddin et al., 2004). 82 shale (SH), 33 sandstone (ST) and 36 coaly (CL) sampling numbers are also shown. 40
Fig.3.1.1. (A) Shale and sandstone core samples stored in core-box of BAPEX; (B) and (C) Shale core samples; (D) Sandstone core samples; (E) Coal core samples of the Dighipara Basin; (F) Coal core samples with organic-rich mudstone (top left at F) sample of the Barapukuria Basin. 45
Fig.3.2.1. A Weatherford Source Rock Analyzer (SRA:TPH/TOC) installed at the petroleum geochemistry laboratory of the Geology Department, University of Malaya. 47
Fig.3.2.2. A Perkin Elmer 2400 elemental analyzer (CHNS/O) operated at the Chemistry Department of the University of Malaya. 48
Fig.3.2.3. Bitumen (EOM) extraction in progress; the sample is placed in a thimble. 50
Fig.3.2.4. Long column chromatography in progress for separating aliphatic (SAT) fraction. Petroleum ether solvent, silica gel, alumina and slurry are also shown at table. 51
Fig.3.2.5. An Agilent 6890N Series gas chromatograph (GC) and gas chromatography mass spectrometer (GCMS). The Frontier Laboratories PY-2020iD model pyrolysis gas chromatograph (PyGC) unit shown here is also installed at the Geology Department, University of Malaya as an attachment 52
Fig.3.2.6. The analytikjena contrAA®700 High Resolution Continuum Source Atomic Absorption Spectrometer (HR-CS AAS) installation at the Department of Geology of the University of Malaya. 54
Fig.3.2.7. Polishing in progress with Buehler Beta Grinder-Polisher automatic polishing machine (A) and the polished coal/shale blocks (B). 58
Fig.3.2.8. A LEICA DM6000M microscope and LEICA CTR6000 photometry system equipped with fluorescence illuminators used at the Geology Department of the University of Malaya. 59
Fig.3.2.9. A PerkinElmer Diamond TG-DTA installed at the Geology Department of the University of Malaya (A); A typical TGA profile whereby the moisture content, volatile matter and fixed carbon of the analyzed coal sample are represented by the first, second and third weight loss steps respectively; The remaining weight at 950 ºC in oxygen corresponds to the ash content in % (B). 62

Page no.
Fig.3.2.10. Thin section preparation in progress operated at the Geology Department, University of Malaya. 63
Fig.3.2.11. A Leica DMLP optical microscopes installed at the Geology Department of the University of Malaya; The PixeLINK digital cameras are attached for capturing images. 64
Fig.3.2.12. A JEOL JSM-7600F field emission scanning electron microscope (FESEM) operated at the Physics Department of the University of Malaya. 66
Fig.3.2.13. A PANalytical X-ray Diffraction (XRD) machine working at the Geology Department of the University of Malaya. 67
Fig.4.1.1 Cross-plot of total organic carbon (TOC in wt.%) and remaining hydrocarbon potential (S2 in mg HC/g rock) of the studied samples. Bhuban formation shows poor to fair quality source potential while Boka Bil shows mostly poor quality (adopted by Peters and Cassa, 1994; Dembicki, 2009). 78
Fig.4.1.2. Distribution of vitrinite reflectance (%Ro) and Tmax (°C) plotting with hydrogen index (HI) of the analyzed samples. Bhuban formation depicts Type III/II (gas-oil prone) kerogen whereas Boka Bil is of Type III. Both formations are within immature to early mature oil window (see Appendices B1 and B3 for definitions) (modified from Peters and Cassa, 1994; Koeverden et al., 2011; cited by Farhaduzzaman et al., 2013a and 2013e). 80
Fig.4.1.3. Photomicrographs showing macerals in shale samples under microscope. 83
Fig.4.1.4 Photomicrographs showing macerals in shale samples under microscope. 84
Fig.4.1.5 Photomicrographs showing macerals in shale samples under microscope. 85
Fig.4.1.6. PyGC pyrograms of Boka Bil and Bhuban shales (RP4SH1 and FN2SH9) display a mixed kerogen of Types III and II. 87
Fig.4.1.7. Gas chromatogram (TIC) and mass fragmentograms m/z 191 and m/z 217 of aliphatic fraction of a studied Boka Bil sample (SB1SH29). It represents immature oil window (peak i.d. in Appendix B2). 93
Fig.4.1.8. Gas chromatogram (TIC) and mass fragmentograms m/z 191 and m/z 217 of aliphatic fraction of a studied Boka Bil sample (SB1SH48). It represents mature oil window (peak i.d. in Appendix B2). 94
Fig.4.1.9. Gas chromatogram (TIC) and mass fragmentograms m/z 191 and m/z 217 of aliphatic fraction of a studied Bhuban sample (KM1SH2). It represents immature oil window (peak i.d. in Appendix B2). 95
Fig.4.1.10. Gas chromatogram (TIC) and mass fragmentograms m/z 191 and m/z 217 of aliphatic fraction of a studied Bhuban sample (T11SH68). It represents mature oil window (peak i.d. in Appendix B2). 96
Fig.4.1.11. A cross-plot of Tmax (˚C) and production index (PI). Both of the studied Bhuban and Boka Bil shale samples fall within and outside the hydrocarbon generation regime. But Bhuban shows relatively higher maturity (c.f., Powell, 1978). 102
Fig.4.1.12. A cross-plot of HC yield and hydrocarbon in extract. The studied Bhuban and Boka Bil shale samples correspond mostly to marginal-good quality petroleum source rock potential with marginal to early mature thermogenic condition (e.g., Powell, 1978). 102
Fig.4.1.13. A triangular diagram from visual kerogen analysis (vol %). The analyzed Bhuban and Boka Bil shales represent the generation potential for dry gas (gas-prone) (adopted after Tissot and Welte, 1978). 103
Fig.4.1.14. Relationship between sterane compositions, source input and depositional environment. Both of the analyzed Bhuban and Boka Bil Formation shales are dominated by terrestrial organic matter input. A minor contribution is from marine sources (e.g., Waples and Machihara, 1991). 104
Fig.4.1.15. A plot of pristane/nC17 versus Phytane/nC18 for the examined samples infer oxicity and organic matter the source rock depositional environment (e.g., Peters et al., 2005; Koeverden et al., 2011). The analyzed Bhuban and Boka Bil samples support the terrigenous Type III and mixed Type III/II source regions under oxic-anoxic condition. 105
Fig.4.1.16. A cross-plot of Pr/Ph ratios and sterane C27/(C27+C29) values related to deposition environment and source. Both of the analyzed Bhuban and Boka Bil shales suit terrestrial (oxic-anoxic) depositional setting and minor influence from pelagic source (c.f., Waseda and Nishita, 1998; Sawada, 2006; Hossain et al., 2009). 106

Page no.
Fig.4.2.1.1. Photographs of coal samples collected from the Barapukuria and Dighipara basins. (A) and (B) are the bulk samples of Barapukuria Basin whereby (C) and (D) are the core samples of Dighipara Basin. The samples show different bands of coal, e.g., dull band (db) and bright parting (bp) along with a joint (j) in photograph D. This is a characteristic feature of a bituminous coal. 112
Fig.4.2.1.2. The elemental concentration of the analyzed coal samples from the Dighipara Basin. Mostly all of the identified elements cross their Clarke values which point to the environmental hazards while combustion. 116
Fig.4.2.1.3. Photomicrograph shows iron and sulfur bearing mineral pyrite which is of syngenetic (spy, A) or epigenetic (epy, B) origin. It is associated with vitrinite macerals observed under microscope with normal reflected white light under oil immersion. 121
Fig.4.2.2.1. A triangular diagram illustrating peat-forming depositional environments based on maceral compositions. The studied samples represent forest swamp, mildly oxic to anoxic conditions, with good tissue preservation (adopted by Mukhopadhyay, 1986). 141
Fig.4.2.2.2. Environmental depositional conditions of the coals based on the composition of the macerals and mineral matter contents. The explored samples fall within an alternation of oxic-anoxic moor (c.f., Singh and Singh, 1996). 143
Fig.4.2.2.3. A cross-plot of the Gelification Index (GI) and Tissue Preservation Index (TPI) showing the depositional settings of the peat mires. The analyzed samples fall mostly within terrestrial dry forest swamp and piedmont plain (e.g., Diessel, 1986). 144
Fig.4.2.2.4 A cross-plot of the Ground Water Index (GWI) and Vegetation Index (VI) showing the palaeoenvironments of the coal mires. The studied samples also imply mostly bog forest environment and swamp forest (adopted by Calder et al., 1991). 145
Fig.4.2.2.5. A double triangular diagram based on microlithotypes, illustrating the coal facies. The examined samples indicate a facies range from reed moor to forest moor (adopted by Hacquebard and Donaldson, 1969; Cited by Singh and Shukla, 2004). 147
Fig.4.2.2.6. Coal depositional environments based on the composition of microlithotypes (free of mineral matter). The analyzed coal samples indicate deltaic-lacustrine-fluvial environments (e.g., Singh and Singh, 1996; Singh and Shukla, 2004; Smyth, 2009). 148
Fig.4.2.2.7. A triangular diagram based on microlithotypes, illustrating the depositional environments. The analyzed samples represent the upper delta plain (mostly) to lower delta plain deposits (adopted by Hunt, 1982). 149
Fig.4.2.2.8. The variation of different maceral indices (TPI, GI, VI and GWI) with vertical depth patterns at the Barapukuria (BA, BB, BC and BD) and Dighipara (DA, DB, DC and DD). TPI, GI and VI values increase with depth in both basins. However, the GWI value decreases with depth at Barapukuria but increases with depth at Dighipara. It indicates that a similar depositional condition prevailed at the time of deposition for both basins, while the groundwater level is fluctuating. 152
Fig.4.2.2.9. Schematic block diagram represents the palaeodepositional environments of the Permian Gondwana coal deposits of the Barapukuria and Dighipara Basins, NW Bangladesh (Farhaduzzaman et al., 2012a). 153
Fig.4.2.3.1. Pictorial comparison of Tmax, HI and OI values found from two different methods SRA and RE. It shows a good agreement one another (see Appendix E1). 156
Fig.4.2.3.2. Organic facies distribution from HI versus Tmax plot. The analyzed coals are dominated by Type III-II, carbargillites by Type II-III and mudstones by Type III organic matter. All the samples being early to mid-maturity thermal conditions (see Appendices B1 and B3 for definitions) (minor modification from Bjorøy et al., 1981; Davies and Nassichuk, 1988; Goodarzi et al., 1987; van Koeverden et al., 2011). 159
Fig.4.2.3.3. PyGC pyrograms of the analyzed coal, carbargillite and mudstone samples representing Type III/II (dominant Type III), Type II/III mixture and Type III kerogen respectively (c.f., Dembicki, 2009). 163
4.2.3.4. Gas chromatogram (TIC) and mass fragmentograms m/z 191 and m/z 217 of aliphatic fraction of a studied coal sample (BPCL15) of the Barapukuria Basin (peak i.d. in Appendix B2). 165

Page no.
4.2.3.5. Gas chromatogram (TIC) and mass fragmentograms m/z 191 and m/z 217 of aliphatic fraction of a studied carbargillite sample (DPCR42) of the Dighipara Coal Basin (peak i.d. in Appendix B2). 166
4.2.3.6. Gas chromatogram (TIC) and mass fragmentograms m/z 191 and m/z 217 of aliphatic fraction of a studied mudstone sample (BPMT22) of the Barapukuria Coal Basin (peak i.d. in Appendix B2). 167
Fig.4.2.3.7. Organic facies related triangular diagram based on C27, C28 and C29 regular sterane epimers. The analyzed coal samples correspond to mainly terrestrial organic matter with minor contribution from marine source. The carbargillite samples indicate mixed terrestrial and marine influenced sources and mudstones to terrestrial organic source (e.g., Waples and Machihara, 1991). 171
Fig.4.2.3.8. A cross-plot of pristane/nC17 versus phytane/nC18 for the currently explored coal, carbargillite and mudstone samples. It represents the sub-oxic depositional conditions with dominantly terrestrial organic matter (c.f., Peters et al., 2005). 172
Fig.4.2.3.9. Environmental depositional conditions of coals and carbargillites based on the macerals and mineral matter contents (adopted by Singh and Singh, 1996). The analyzed coal samples fall within alternating oxic-anoxic swamp. The carbargillite samples fall within the wet swamp with intermittent and moderate to high flooding. 174
Fig.4.2.3.10. A cross-plot of TOC versus S2 while all the analyzed samples fall within the range of fair to excellent hydrocarbon generation potential. Mudstone indicates the lowest potential and followed by carbargillite and coals (adopted by Peters and Cassa, 1994; Dembicki, 2009; cited by Farhaduzzaman, 2012a). 182
Fig.4.3.1.1 A tri-plot of the modal composition of the studied Surma Group sandstones of the Bengal Basin, Bangladesh. The sandstones place within the sublithic arenite to subfeldspathic arenite class (adopted by Folk, 1980). 195
Fig.4.3.1.2. XRD analysis of clay minerals identified in the analyzed reservoir sandstones and interlayered shales. (A) Non-treated air-dried diffractogram of sandstone samples. (B) Glycol saturated diffractogram of sandstone samples. It shows relative high abundance of clay mineral chlorite compared to others. Both air-dried and glycol-treated diffractograms show the similar responses due to the absence of smectite swelling clay. (C) 550 °C heated diffractogram of sandstone sample and hence the kaolinite peak is disappeared remained a small peak for chlorite. (D) Non-treated air-dried diffractogram of the interlayered shale sample is also shown which indicates the similar clay responses compared to those found in sandstone sample (A and B). It suggests the similar genetic origin for the clay minerals found both in sandstones and shales (e.g., Moore and Reynolds, 1979). 201
Fig.4.3.1.3. Paragenetic sequence of the important diagenetic events observed in the studied Surma Group sandstone reservoirs, the Bengal Basin, Bangladesh. 210
Fig.4.3.1.4. A cross-plot of porosity and depth observed in the Tertiary reservoir sandstones of the Bengal Basin, Bangladesh. It shows the overall porosity decreases with depth. 211
Fig.4.3.2.1. Composite log responses of the hydrocarbon bearing Zone 1 (1447-1522 m) identified in Surma Group of well Rashidpur 4, the Bengal Basin, Bangladesh. 218
Fig.4.3.2.2. Graphical presentation of the petrophysical parameters of the hydrocarbon bearing Zone 1 (1447-1522 m) identified in Surma Group of well Rashidpur 4, the Bengal Basin, Bangladesh. 219
Fig.4.3.2.3. Composite log responses of the hydrocarbon bearing Zone 2 (2337-2350 m) identified in Surma Group of well Rashidpur 4, the Bengal Basin, Bangladesh. 220
Fig.4.3.2.4. Graphical presentation of the petrophysical parameters of the hydrocarbon bearing Zone 2 (2337-2350 m) identified in Surma Group of well Rashidpur 4, the Bengal Basin, Bangladesh. 221
Fig.4.3.2.5. Composite log responses of the hydrocarbon bearing Zone 3 (2466-2483 m) identified in Surma Group of well Rashidpur 4, the Bengal Basin, Bangladesh. 222
Fig.4.3.2.6. Graphical presentation of the petrophysical parameters of the hydrocarbon bearing Zone 3 (2466-2483 m) identified in Surma Group of well Rashidpur 4, the Bengal Basin, Bangladesh. 223

Page no.
Fig.4.3.2.7. Composite log responses of the hydrocarbon bearing Zone 4 (2668-2731 m) identified in Surma Group of well Rashidpur 4, the Bengal Basin, Bangladesh. 224
Fig.4.3.2.8. Graphical presentation of the petrophysical parameters of the hydrocarbon bearing Zone 4 (2668-2731 m) identified in Surma Group of well Rashidpur 4, the Bengal Basin, Bangladesh. 225

Photomicrograph 4.2.2.1. Show macerals in coal samples under microscope. 129
Photomicrograph 4.2.2.2. Show macerals in coal samples under microscope. 130
Photomicrograph 4.2.2.3. Show macerals in coal samples under microscope. 131
Photomicrograph 4.2.2.4. Show macerals in coal samples under microscope. 132
Photomicrograph 4.2.2.5. Show macerals in coal samples under microscope. 133
Photomicrograph 4.2.2.6. Show macerals in coal samples under microscope. 138
Photomicrograph 4.2.2.7. Show maceral associations in coal samples under microscope. 139
Photomicrograph 4.2.2.8. Show maceral associations in coal samples under microscope. 140
Photomicrograph 4.2.3.1. Show macerals in coal, carbargillite and mudstones samples under microscope. 178
Photomicrograph 4.2.3.2. Show macerals in coal, carbargillite and mudstones samples under microscope. 180
Photomicrograph 4.2.3.3. Show macerals in coal, carbargillite and mudstones samples under microscope. 181
Photomicrograph 4.3.1.1. Show minerals, cements and pores in sandstones in thin sections under microscope. 188
Photomicrograph 4.3.1.2. Show minerals, cements and pores in sandstones in thin sections under microscope. 194
Photomicrograph 4.3.1.3. Show minerals, cements and pores in sandstones under SEM. 198
Photomicrograph 4.3.1.4. Show minerals, cements and pores in sandstones under SEM. 202
Photomicrograph 4.3.1.5. Show minerals, cements and pores in sandstones under SEM. 203

LIST OF TABLES

Page no.

Table 2.1. Stratigraphic succession of Barapukuria Basin (modified after Armstrong, 1991; Alam et al., 2003; Islam and Islam, 2005). 21

Table 2.2. Stratigraphic succession of Dighipara Basin (modified after Hasan and Islam, 2003; Alam et al., 2003). 30

Table 2.3. Generalized stratigraphic succession of Deep Basin unit or Province 2 (including study area) of Bengal Basin (modified after Alam et al., 2003; Imam, 2005). 34

Table 4.1.1. Source Rock Analyzer (of Rock-Eval equivalent) parameters and vitrinite reflectance data of the analyzed shale samples (refer to Appendix B1). 76

Table 4.1.2. Comparison between SRA and RE results of the analyzed shale samples (refer to Appendix B1). 79

Table 4.1.3. Elemental analysis (CHNS) results of the studied samples. 81

Table 4.1.4. A summary of the maceral contents (mineral free basis) of the studied shale samples from Bhuban and Boka Bil Formations, Bengal Basin, Bangladesh. 82

Table 4.1.5. Solubale extract yield and alkane parameters of the studied shale samples, Bengal Basin (refer to Appendix B1). 88

Table 4.1.6. Hopane biomarker parameters (measured from m/z 191) of the analyzed shale samples (refer to Appendix B2). 90

Table 4.1.7. Sterane and diasterane biomarker parameters (measured from m/z 217) of the analyzed shale samples (refer to Appendix B2). 91

Table 4.2.1.1. The proximate analysis results (air dried, ad-basis) obtained from TG-DTA (ASTM D5800-96) method (UM Geology Lab; denoted by TGA) and ASTM D2013-07 (Geoscience Malaysia Lab; denoted by JMG) of the studied coal samples. Sulfur content (%) and gross calorific value (GCV, kcal/kg) are also added. 'Arms' denotes the results taken after Armstrong (1991). 113

Table 4.2.1.2. Ash yield (%, ad basis) and elemental concentration (ppm, ad basis) with Clarke values or world average of Dighipara Basin coals. 115

Table 4.2.2.1. A summary of maceral and mineral matter contents (vol. %) of the analyzed coal samples (22 cores and 5 bulks) of Barapukuria and Dighipara Basins. GI - TPI and GWI -VI values are also shown. 123

Table 4.2.2.2. A summary of maceral concentrations in mineral free basis (vol. %) of the analyzed coal samples (22 cores and 5 bulks) of Barapukuria and Dighipara Basins. 124

Table 4.2.2.3. A summary of concentrations of microlithotype and carbominerite (vol. %) of the analyzed coal samples (22 cores and 5 bulks) of Barapukuria and Dighipara Basins. 125

Table 4.2.2.4. A summary of concentrations of microlithotypes in mineral free basis (vol. %) of the analyzed coal samples (22 cores and 5 bulks) of Barapukuria and Dighipara Basins. 126

Table 4.2.3.1. Source Rock Analyzer (of Rock-Eval equivalent) parameters and vitrinite reflectance data of the analyzed samples- coal, carbargillite and mudstone (refer to Appendix B1). 155

Table 4.2.3.2. A summary of maceral and mineral matter (MM) contents (vol.%) of the analyzed samples- coal, carbargillite and mudstone. 158

Table 4.2.3.3. Soluble extract yield and alkane parameters of the studied coal, carbargillite and mudstones (refer to Appendix B1). 162

Table 4.2.3.4. Hopane biomarker parameters (measured from m/z 191) of the analyzed coal, carbargillite and mudstones (refer to Appendix B2). 164

Table 4.2.3.5. Sterane and diasterane biomarker parameters (measured from m/z 217) of the analyzed coal, carbargillite and mudstone samples (refer to Appendix B2). 169

Table 4.3.1.1. Petrographic results (%) of Surma Group reservoir sandstones of the Bengal Basin, Bangladesh. 186

Table 4.3.2.1. Permeable zones identified from the log based petrophysical analysis of the well Rashidpur 4, the Bengal Basin, Bangladesh. 215

Table 4.3.2.2. Log based petrophysical analysis results of 4 hydrocarbon (HC) bearing zones identified in well Rashidpur 4 of Bengal Basin, Bangladesh. 217

LIST OF SYMBOLS AND ABBREVIATIONS

AAS : Atomic absorption spectrometry
ASTM : American Society for Testing and Materials
BAPEX : Bangladesh Petroleum Exploration and Production Company Limited (A Company of Petrobangla)
BCMCL : Barapukuria Coal Mining Company Limited (A Company of Petrobangla)
BB : Boka Bil Formation
BBS : Bangladesh Bureau of Statistics
BG : Begumganj Gas Field
Bh : Bhuban Formation
BK : Bakhrabad Gas Field
BP : Barapukuria Coal Basin
BVW : Bulk volume water
BWDB : Bangladesh Water Development Board
CL : Coal
CR : Carbargillite
DP : Dighipara Coal Basin
FESEM : Field emission scanning electron microscope
Fm : Formation
FN : Fenchuganj Gas Field
GC/GCMS : Gas chromatography / Gas chromatography mass spectrometry
GDH/DOB : Geological Drill Hole
GIIP 2P : Gas Initially In Place Proven + Probable
GR_{log} : Gamma ray reading from formation
GR_{max} : Gamma ray reading from shale (gamma ray maximum)
GR_{min} : Gamma ray reading from clean sand (gamma ray minimum)
GSB : Geological Survey of Bangladesh
HCU : Hydrocarbon Unit
I_{GR} : Gamma ray index
K : Permeability of formation
KM : Kamta Gas Field
KT : Kailas Tila Gas/Oil Field
m : Cementation exponent
MMSCFD : Million Standard Cubic Feet per Day
MT : Mudstone
Φ : Porosity
Φ_N : Neutron porosity
Φ_D : Density porosity
NPD : Norwegian Petroleum Directorate
Petrobangla : Bangladesh Oil, Gas and Mineral Corporation (BOGMC)
P_b : Bulk density of formation
P_f : Density of the fluid in the borehole
P_h : Hydrocarbon density
P_{ma} : Density of the formation matrix
PT : Patharia Gas Field / Structure
PyGC : Pyrolysis gas chromatography
RE : Rock-Eval pyrolysis 6
R_{ILD} : Resistivity induction log deep
R_{SFL} : Resistivity of spherically focused log
R_m : Resistivity of drilling mud
R_{mc} : Resistivity of mudcake
R_{mf} : Resistivity of mud filtrate
R_t : Resistivity of uninvaded zone
R_w : Resistivity of formation water
R_{xo} : Resistivity of flushed zone
RP : Rashidpur Gas Field
SEM : Scanning Electron Microscope

SB	: Shahbazpur Gas Field
SGFL	: Sylhet Gas Fields Limited (A Company of Petrobangla)
SH	: Shale
S_h	: Hydrocarbon saturation ($1 - S_w$)
SP	: Spontaneous potential
SSP	: Static spontaneous potential
SRA	: Source Rock Analyzer
ST	: Sandstone
STOIIP	: Stock Tank Oil Initially In Place
STOOIP	: Stock Tank Original Oil In Place
S_{wirr}	: Irreducible water saturation
S_w	: Water saturation
S_{xo}	: Water saturation of flushed zone
T	: Titas Gas Field
TCF	: Trillion Cubic Feet
T_f	: Formation temperature
XRD	: X-ray Diffraction
UM	: University of Malaya
V_{sh}	: Volume of shale

LIST OF APPENDICES

Page no.

Appendix A1. Published in International Journal of Coal Geology (ISI-cited; Q1; IF = 2.70). 239
Appendix A2. Published in Journal of Petroleum Geology (ISI-cited; Q2; IF = 1.01). 240
Appendix A3. Published in Journal of Asian Earth Sciences (ISI-cited; Q1; IF = 2.42). 241
Appendix A4. Published in Journal of Petroleum Geology (ISI-cited; Q2; IF = 1.01). 242
Appendix A5. Accepted in Journal of the Geological Society of India (ISI-cited; Q4; IF = 0.59). 243
Appendix A6. Under review in Geosciences Journal (ISI-cited; Q2; IF = 0.81). 244
Appendix A7. Under review in J. of the Geological Society of India (ISI-cited; Q4; IF = 0.59). 245
Appendix A8. Under review in Sains Malaysiana (ISI-cited; Q3; IF = 0.27). 246
Appendix A9. Under review in Malaysian Journal of Science (Scopus-cited). 247
Appendix B1: Some definitions and measurement terms used in the literature. 248
Appendix B2: Peak assignments for alkane HCs in the gas chromatograms of the aliphatic fractions (i) in the m/z 191 mass fragmentogram and (ii) m/z 217 mass fragmentogram. 249
Appendix B3: Some important standard parameters used for petroleum source rock screening in the thesis. 250
Appendix C1: TOC (wt.%) of both Boka Bil and Bhuban shales plotted with vertical depth profile (m) of the study area. It shows TOC increases with overall depth increasing irrespective of any particular wells. 251
Appendix C2: Modified van Krevelen diagram (HI versus OI) shows that the analyzed both Bhuban and Boka Bil samples consist of a mixture of Type III and II kerogens. 252
Appendix C3: PyGC pyrograms of Boka Bil and Bhuban shales (PT5SH14 and KM1SH4) display a mixed kerogen of Types III and II. 253
Appendix C4: Pictorial presentation of CPI values shows that the members of odd-numbered and even-numbered n-alkanes alternately predominate each other in both of the analyzed Bhuban and Boka Bil samples. 254
Appendix C5: Gas chromatogram (TIC) and mass fragmentograms m/z 191 and m/z 217 of aliphatic fraction of a studied Boka Bil sample (PT5SH10). It represents immature oil window (peak i.d. in Appendix B). 255
Appendix C6: Gas chromatogram (TIC) and mass fragmentograms m/z 191 and m/z 217 of aliphatic fraction of a studied Boka Bil sample (BK9SH71). It represents mature oil window (peak i.d. in Appendix B). 256
Appendix C7: Gas chromatogram (TIC) and mass fragmentograms m/z 191 and m/z 217 of aliphatic fraction of a studied Bhuban sample (FN2SH7). It represents immature oil window (peak i.d. in Appendix B). 257

Page no.

Appendix C8: Gas chromatogram (TIC) and mass fragmentograms m/z 191 and m/z 217 of aliphatic fraction of a studied Bhuban sample (BG1SH6). It represents mature oil window (peak i.d. in Appendix B). 258

Appendix C9: Cross-plot of bc/C_{30}-hopane and ol/C_{30}-hopane (oleanane index) with respective depth (samples) shows that bc/C_{30}-hopane ratio decreases and ol/C_{30}-hopane ratio increases with depth. It indicates the relative maturity increase with depth. 259

Appendix C10: The identified similar organic geochemical and organic petrological properties of the analyzed Bhuban and Boka Bil Formations, Bengal Basin, Bangladesh. 260

Appendix D1: Bar diagram displaying the concentrations of macerals and minerals (vol. %) of the studied Permian coals of Bangladesh. 261

Appendix D2: Bar diagram displaying the concentrations of microlithotypes (maceral associations) and carbominerites (vol. %) of the studied Permian coals of Bangladesh. 262

Appendix E1: Comparison between SRA and RE results of the analyzed coal, carbargillite and mudstone samples (refer to Appendix B1). 263

Appendix E2: Gas chromatogram (TIC) and mass fragmentograms m/z 191 and m/z 217 of aliphatic fraction of a studied coal sample (DPCL35) of Dighipara Coal Basin (peak i.d. in Appendix B2). 264

Appendix E3: Gas chromatogram (TIC) and mass fragmentograms m/z 191 and m/z 217 of aliphatic fraction of a studied carbargillite sample (BPCR11) of Barapukuria Coal Basin (peak i.d. in Appendix B2). 265

Appendix E4: Pictorial presentation of CPI values whereby all of the analyzed coal, carbargillite and mudstone samples show the dominance of odd carbon numbered n-alkanes. It indicates the terrestrial dominated organic facies in the depositional system. 266

Appendix F1: A sample report of a reference management software EndNote X5 that has been used for the thesis. 267

Appendix F2: A standard report of StyleWriter 4.0 software for checking English Language. It shows the status of English used in the thesis is “Excellent”. 268

Appendix F3: A sample report for checking the originality using Turnitin software. It reports 19% similarity index with the thesis whereas more than 5% comes from the publication of author himself based on present research. 269

Appendix G: Contributors of the thesis. 270

CHAPTER 1: INTRODUCTION

1.1 Background

Bangladesh is a country covering an area of 147570 square kilometers. It lies between latitudes of 20°N-27°N and longitudes of 88°E-93°E and borders India and with a small part of Myanmar (Bangladesh Bureau of Statistics, 2011). The Bengal Basin is located at the northeast-southeast corner of the Indian subcontinent (Fig.1.1). Geographically two-thirds of the basin is covered by on- and offshore Bangladesh. The rest one-third lies within India surrounding Bangladesh on three sides- east, west and north (Banerji, 1984). To the south, the basin extends to the Bay of Bengal. So far, twenty five (25) gas fields and only one minor oil field have been discovered in the Bengal Basin, Bangladesh. The Miocene Surma Group has been found as a host for the discovered gas (28 trillion cubic feet) and oil (137 million barrels) in Bangladesh (Shamsuddin et al., 2004; Hossain, 2012).

Northward migration of the Indian plate and convergence with Eurasian plate about 55 Ma resulted in developing the Bengal Basin in the west and the Burmese Basin in the east. The Eastern Petroleum Province and the Western Petroleum Province are the main two petroleum systems in the Bengal Basin, Bangladesh. So far, the entire hydrocarbon discovery is demarcated in the Eastern Petroleum Province. The coal is found in the Western Petroleum Province. Stratigraphy of the Eastern Petroleum Province (22km thick sediments) is different from that of the Western Petroleum Province (400m thick sediments). In general, the Basement Complex (at bottom), Gondwana Group, Dupi Tila Formation and Barind Clay Formation are the major stratigraphic units in the Western Province. On the other hand, the Eastern Petroleum Province includes Jaintia Group (bottom unit), Barail Group, Surma Group, Tipam Group, Dupi Tila Formation and Madhupur Clay Formation (Alam et al., 2003).

Natural gas is the most important energy resource in Bangladesh. Around 94.96% power generation is based on hydrocarbons (mostly gas with oil). The share of coal in power is only 2.41% (BPDB, 2012). The national industry, agriculture, business, investment, sustainable development and infrastructure are mostly dependent on the natural gas. Several workers have already carried out their researches on natural gas and petroleum systems. However, the research is still inadequate compared to the huge coverage of the basin and increasing demand of natural gas. The national policy makers and the experts of Bangladesh are looking forward to improve the gas and oil sector. Therefore, they are trying to encourage more research based on petroleum systems. Accordingly, there is initiative and effort to carry out more focused research on oil and gas and its related petroleum systems.

The Surma Group, up to 5 km thick, consists of the Bhuban and Boka Bil Formations. This is exposed in the Sylhet and Chittagong hills, Bangladesh. Both formations, consisting of sandstones and shales, are interpreted to have been deposited in a deltaic to shallow-marine environment (Holtrop and Keiser, 1970). All the hydrocarbons so far discovered in Bangladesh have been found within the Bhuban and Boka Bil Formation sandstones. This is the most important geological unit of the basin. These formations also contain shale intervals showing important source rock potential (Imam, 2005). Overlying marine shale acts as a basin-wide seal.

Many authors have recently reported the organic geochemical and petrological evidences as diagnostic for characterizing extracts and oils gained from different organic matter and environment.

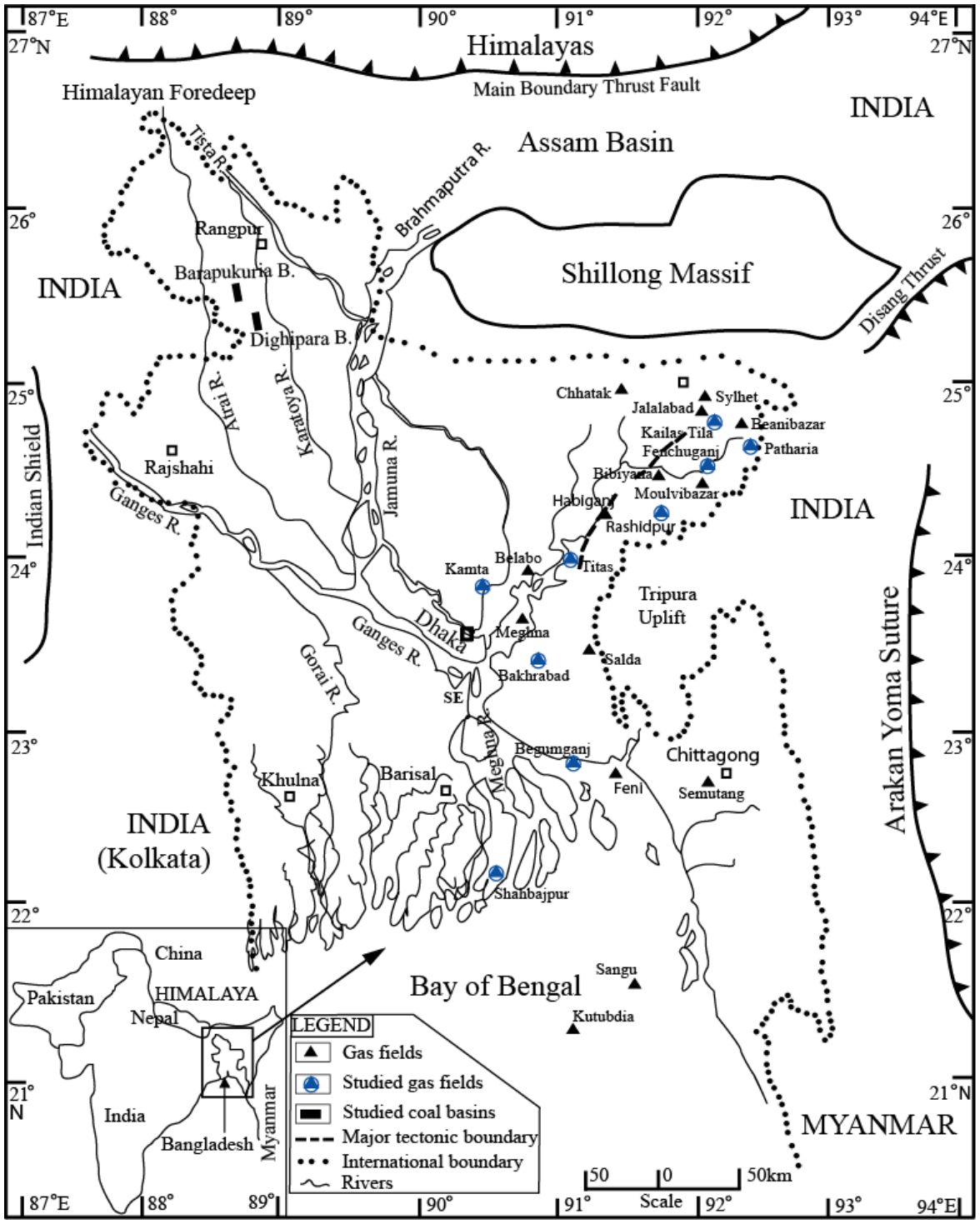

Fig.1.1. Location map shows the studied nine gas fields and two coal basins (Imam, 2005).

For example, Espitalie et al. (1977), Mukhopadhyay et al. (1991), Hunt (1991), Wan Hasiah (1999a), Wan Hasiah and Abolins (1998), Farrimond et al. (1998), Petersen et al. (2005), Banerjee et al. (2006) and Dutta et al. (2011) have worked on different topics of

petroleum source rock. Considering the Bengal Basin, none of the works, however, are based on detail organic geochemistry and petrography of the Surma Group shales of Bangladesh. Now, it is worthwhile to carry out more research on Surma Group shales in the Bengal Basin. The focus of the present work is on the hydrocarbon source potential and environmental conditions using organic matter quantity, quality and thermal maturity. The petrographic characteristics of the Surma Group shales covering almost whole eastern Bengal Basin (nine gas fields), Bangladesh, have also been discussed.

In the current research, the reservoir quality and diagenetic controls of the Surma Group sandstones are carried out using petrographical methods, x-ray diffraction (XRD) and scanning electron microscopy (SEM). The well log based petrophysical evaluation of the reservoir sandstones is accomplished for assessing the reservoir properties. Although there are some publications on the reservoir sandstones, they are not enough. Therefore, the findings of the current analysis will supplement the present understanding of the related petroleum systems of the Bengal Basin, Bangladesh.

The geophysical surveys, including gravity and magnetic anomaly maps, identified five Permian coal-bearing half-graben basins found in the western Platform area of the Bengal Basin, northwest Bangladesh (Hasan and Islam, 2003). Later detail seismic and geological drilling with geophysical logging confirmed these coals (about 3 billion tons) including the Barapukuria and Dighipara Basins. The Permian Gondwana succession consists of sandstones and mudstones with thick coal seams and carbargillites. Sandstone with cross-bedding was deposited in high-energy based fluvial environments.

The mudstone was deposited in low-energy delta plain whereby coal and carbargillites in calm and quiet (low-energy) swamp settings (Alam et al., 2003; Imam, 2005). Thus, the organic facies developed in these rock units are different. So far, no previous work on assessing organic petrology, organic geochemistry and hydrocarbon source potential has published for Bangladesh coals. Now, it is an urgent issue to carry out further research on coals. The depositional environment and hydrocarbon generation potential is the focus of the present study. It highlights the biomarker characteristics of the Permian coals of the Barapukuria and Dighipara basins. No published papers included analyses of the coals and their relationship with other fine-grained sediments. In present study, organic facies distributions within the Permian succession are examined, concentrating on the coals, carbargillites and mudstones in the half-graben basins of Bangladesh. The term 'carbargillite' used here refers to clay-rich coals (20-60% of clay minerals by volume as defined by Mackowsky, 1982).

1.2 Exploration History, Petroleum System and Study Design

The term petroleum originates from Latin word '*petroleum'* from Latin '*petra*' means rock and Latin '*oleum*' means oil. It is a naturally occurring flammable liquid consisting of a complex mixture of hydrocarbons of various molecular weights and other liquid organic compounds. Petroleum, the fossil fuel, is found in geologic formations beneath the Earth's surface. It is formed when large quantities of dead organisms (e.g. zooplankton and phytoplankton) are buried underneath rock and undergo extensive heat and pressure (Tissot and Welte, 1984). It occurs as three phases including oil, gas and condensate. Oil is a liquid at surface temperature and pressure and it consists of compounds containing six or more carbon atoms. Natural gas exists as vapor phase at surface temperature and pressure and it consists of compounds containing five or fewer carbon atoms.

Condensate exists as gaseous phase in reservoir sediments underneath the Earth's surface but it converts liquid phase when brought to the surface. Petroleum has a long history for its discovery, identification, technology and use. It is now important across the society, encompassing economics, politics and technology. The rise in importance is mostly because of the invention of the internal combustion engine, the rise in commercial aviation and the increasing use of plastic and pesticides. More than 4000 years ago, according to Herodotus and Diodorus Siculus, asphalt was used for constructing the walls and towers of Babylon. Ancient Persian tablets indicate the medicinal and lighting uses of petroleum in the upper levels of their society. By 347 AD, oil was produced from bamboo-drilled wells in China (Chisholm and Hugh, 1911). Edwin Drake's 1859 well in Pennsylvania is popularly considered the first modern well for which a steam engine was used for drilling. However, in mid-19th century, there was considerable activity before Drake in various parts of the world. A hand-drilled well in the Baku region in 1848 has been documented. An early commercial well was hand dug in Poland in 1853 and another in nearby Romania in 1857. Romania was the first country in the world to have its crude oil output officially recorded in international statistics, namely 275 tones in 1857. Access to petroleum was and still is a major factor in several military conflicts of the twentieth century, including World War II, during which petroleum was a major strategic asset and were extensively bombed. Petroleum exploration in North America during the early 20th century later led to the U.S. becoming the leading producer by mid-century. Petroleum's worth as a portable, dense energy source powering most of vehicles and as the base of many industrial chemicals makes it one of the world's most important commodities. The top three petroleum producing countries are Saudi Arabia, Russia and the United States (IEA, 2010).

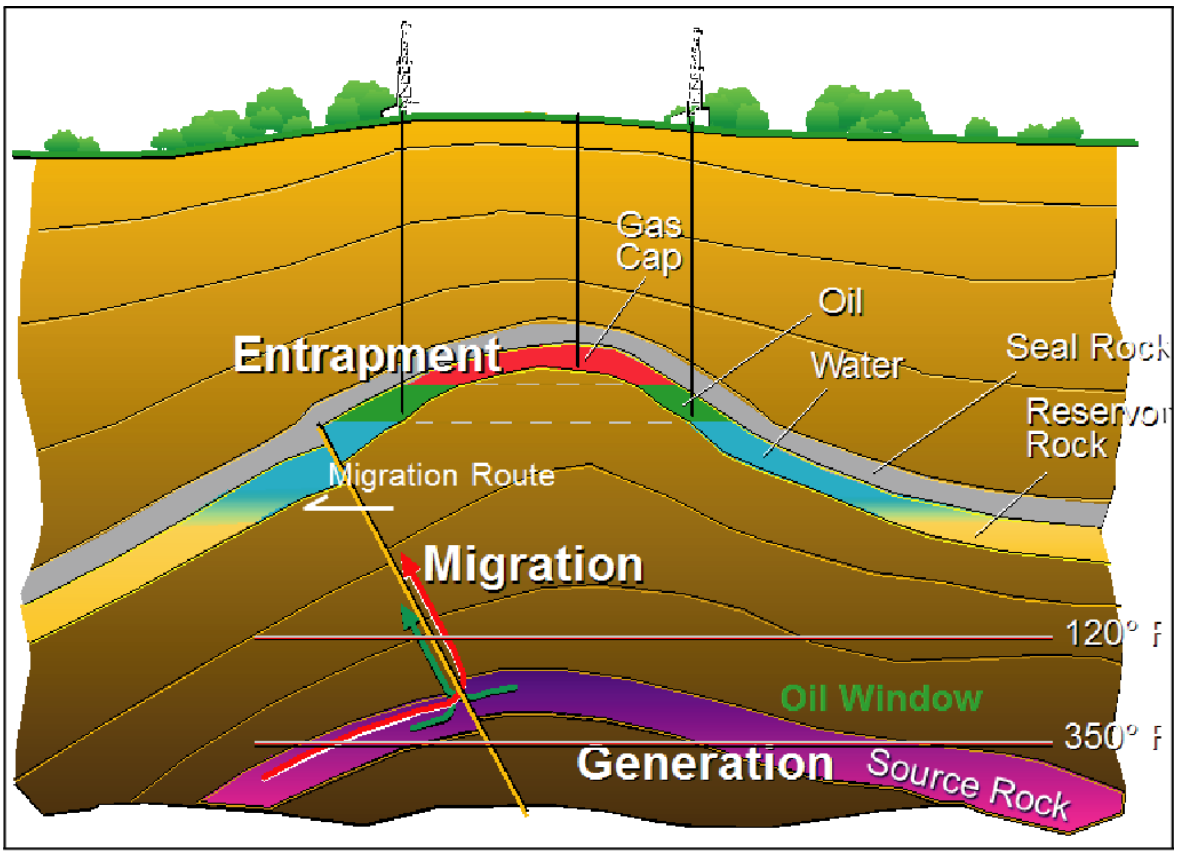

Fig.1.2. The essential elements (source, reservoir, migration route, trap and seal) of a petroleum system of any sedimentary basin (AAPG, 2011).

The techniques used for petroleum exploration first involve the assessment of the petroleum systems of the associated sedimentary basin. The formation of hydrocarbons depends on the coexistence of all the petroleum essential elements (source rock, reservoir rock, seal rock, trap and migration route) and processes (generation, migration, accumulation, preservation and timing) whose origin is a single pod of active source rock in the sedimentary basin, known as petroleum system (Fig.1.2). Absence of any of these elements and processes results no hydrocarbon accumulation in the subsurface (Tissot and Welte, 1984; AAPG, 2011). 'Source rock' and 'reservoir rock', the two essential petroleum system elements of the Bengal Basin, Bangladesh, are the focus of the current project.

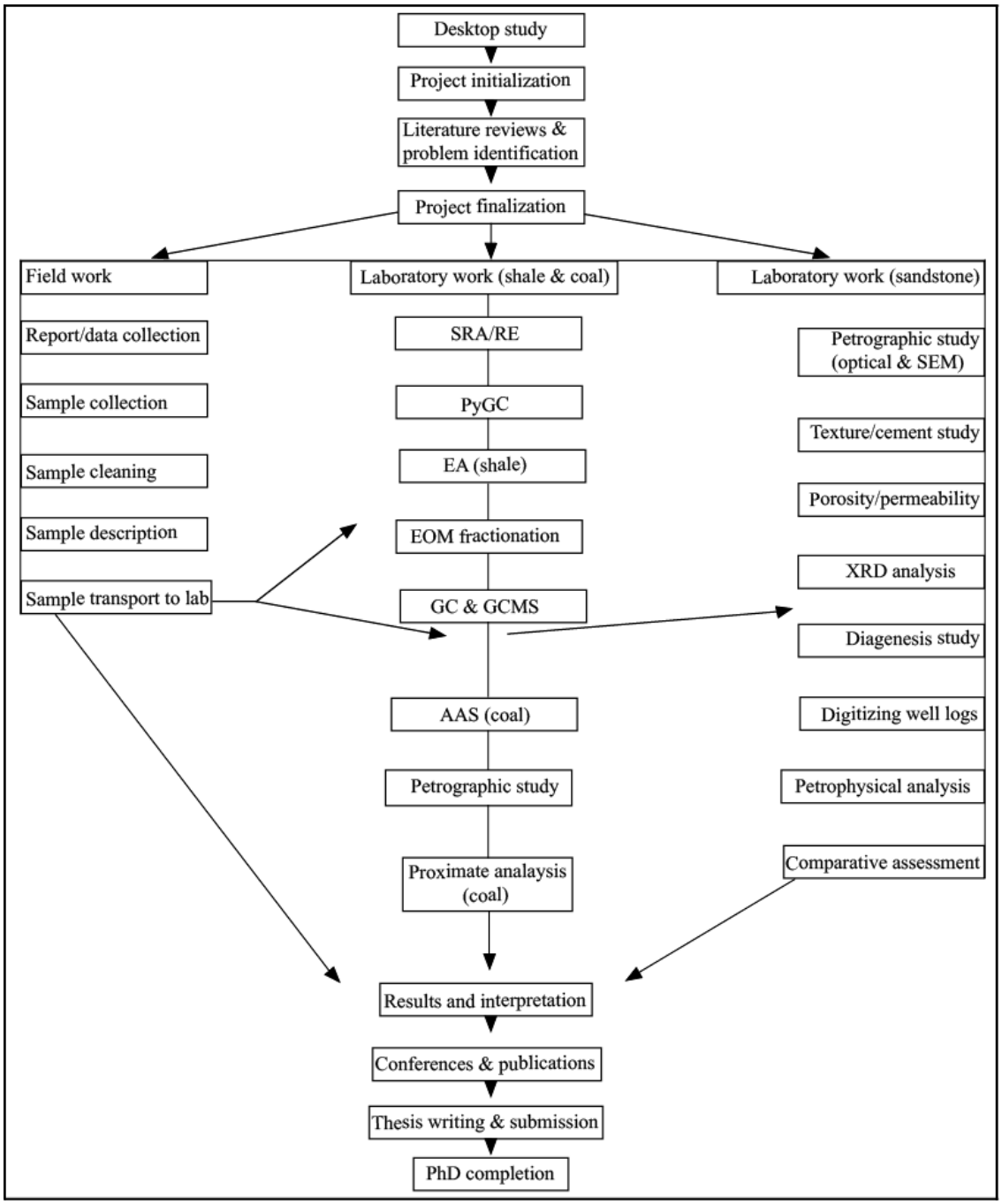

Fig.1.3. Flow chart of the research approach and outlines of the current project.

After project finalization, the research design is prepared for the selected Shale, Coal and Sandstone samples of the Bengal Basin, Bangladesh. The whole project is divided mainly into two parts including field work and laboratory work.

Once the laboratory work is finished, then the study concentrates for data analysis, publications and finally thesis writing. The research approach and design is shown in the flow chart (Fig.1.3).

1.3 Aims and Objectives

The aims and objectives of the current project can be showed briefly below:

a) To measure quantity, quality and thermal maturity of organic matter in shales, coals and associated fine grained sediments.

b) To characterize biomarker distributions of the shales, coals and fine grained sediments involved and to comment on their organic facies variations.

c) To identify kerogen types (organic matter) of the shales, coals and related fine grained sediments.

d) To study macerals, microlithotypes and vitrinite reflectance of the shales, coals and related fine grained sediments.

e) To explore depositional facies models of the coals.

f) To evaluate petroleum source rock potential and hydrocarbon generation-expulsion of the shales, coals and fine grained sediments.

g) To examine the coal quality.

h) To characterize palaeodepositional environments of the shales, coals and related fine grained sediments.

i) To identify minerals, cements, textures and thin section porosity in the sandstones.

j) To measure porosity, permeability and hydrocarbon saturation of sandstones using well logs.

k) To evaluate reservoir quality based on petrography, diagenesis and petrophysical study of the sandstones.

l) To put forward a final observation about the potential of the source rocks and reservoir rocks of the Bengal Basin.

1.4 Limitations of the Study

The current research deals with nine gas fields and two coal basins of the Bengal Basin, Bangladesh. However, considering the size of the Bengal Basin, the collected core samples of the studied gas fields and coal fields are not enough to evaluate the elements of petroleum system of the Bengal Basin. Sometimes, the collected core samples were old, broken and distorted which could have affected its insitu condition. The petrophysical analysis is dependent mostly on wire line log data with the help of limited core data. Detailed analysis of some insitu properties (e.g., porosity, permeability, hydrocarbon saturation and water saturation of sandstone reservoirs; proximate analyses of coals) need more core samples from different depths to supplement the present study.

1.5 Outline of the Thesis

The Chapter 1 introduces the major issues concerning the current research project based on the Bengal Basin, Bangladesh. The background study with literature survey results are described in the Chapter 2. It is summarized separately on Shale, Coal and Sandstone aspects since different methodologies and explanations are drawn independently for each of them. The petroleum and coal resources of the study area and its related description are included in this Chapter 2. The sampling methods, sample size, sample cleaning, sampling depths and all laboratory analytical techniques are illustrated in Chapter 3. The detail results of the current project are described and discussed in Chapter 4. It is described in three sections, including ‘Shale’ as a petroleum source rock (4.1), ‘Coal’ as a petroleum source rock (4.2) and ‘Sandstone’ as a petroleum reservoir rock (4.3). Different

experiments and study methods are used for the current research based on different study materials. Accordingly, a section on 'Discussion' is added at the end of each of these sub-chapters. The major findings of the current research are summarized in Chapter 5. Nonetheless, the future research is also suggested in the recommendation sub-chapter at the end followed by the Appendices and Bibliography.

The output of this research would add to the existing knowledge of the source rocks and reservoir rocks of the Bengal Basin, Bangladesh. It should be noted that a large portion of the findings of the current research project have already been published/accepted (including review stages) in different ISI/WoS (web of science) indexed journals (Appendices A1, A2, A3, A4 and A5; A6, A7, A8 and A9) and also in several conference proceedings.

CHAPTER 2: LITERATURE REVIEW AND STUDY AREAS

Literature review offers an outline of the relevant and important current literature on the planned research area. The following review includes description and summary with their critical evaluations of the relevant materials. Finally, it finds the 'gap' where the special attention needs to address during the present study.

2.1 Previous Studies

2.1.1 Shale

Publications on shale of the Bengal Basin (Bangladesh) are scanty. A systematic study on the presence of bicadinanes and other terrestrial terpenoids in Oligocene Jenum Formation of the Bengal Basin was analyzed by Pearson and Alam (1993). Curiale et al. (2002) studied on the origin of petroleum in Bangladesh mostly based on molecular and isotopic compositions of the natural gas and condensates. They compiled a report on petroleum systems of the Bengal Basin, Bangladesh. Based on optical microscopy and XRD, the mineralogical composition of Surma Group shales was explored by Rahman and Faulp (2003). A provenance study of the Surma Group shale has been carried out by Rahman and Suzuki (2007a) on the basis of chemical and mineralogical compositions. Hossain et al. (2009 and 2010) published papers on characterization of organic matter, depositional environments and provenance of the Tertiary mudstones from the Sylhet sub-basin of the Bengal Basin. Geochemical methods (organic and inorganic) were used for identifying the quantity, quality and thermal maturity of the studied mudstones samples ranging from Eocene Kopili to Pliocene Dupi Tila Formations. Takeda et al. (2011) worked on the geochemistry of the natural gas and condensates collected from the Surma sub-basin, Bengal Basin. They found the coaly or terrestrial organic matter as the sources for these gas and condensates. None of the workers published any paper considering the detail

geochemistry and petrology of the Surma Group shales. The present research establishes the need for a detailed study on the geochemical and petrological characteristics of the Surma Group shales, the Bengal Basin, Bangladesh.

2.1.2 Coal

There are several publications and reports on the Permian Gondwana coals of Bangladesh. The Barapukuria and Dighipara Coal Basins were discovered by the Geological Survey of Bangladesh (GSB) in 1985 and 1995, respectively. On the basis of exploration work including geophysical surveys and drilling results, Armstrong (1991) prepared a detail feasibility study report for the Barapukuria coal deposit, Bangladesh. The coal is now being extracted from the Barapukuria Basin using underground mining methods. The Dighipara Coal Basin is still in the exploration stage. There is no published scientific work on Dighipara before the present study. Bostick et al. (1991) published on petrography (macerals assemblages) of the Barapukuria coal on the basis of semiautomated reflectance scanning. Akhtar and Kosanke (2000) and Akhtar (2001) analyzed the palynomorphs of Permian Gondwana coals of the Barapukuria and discussed its paleoenvironments. As a partial study on Petroleum Systems of Bangladesh, Shamsuddin et al. (2001) discussed the source rock potential of the Gondwana coals of Bangladesh. They stated that coals in Gondwana formations are at sufficient thermal maturity for hydrocarbon generation. Imam et al. (2002) published a paper on coal bed methane (CBM) prospect of the Permian Gondwana coal of the Jamalganj Coal Basin, Bangladesh.

Hossain et al. (2002) worked on the sedimentary facies and palaeodepositional histories of the Permian Gondwana succession of the Khalaspir Coal Basin, northwest Bangladesh. Rahman (2004) published on the importance of the utility of the Permian coal resources of

Bangladesh. From a structural and mining point of view, Islam and Islam (2005) worked on the water inrush hazard in the Barapukuria underground coal mine. Hasan and Islam (2003) published on the generalized subsurface geology and mineral resources of the Barapukuria, Dighipara and Khalaspir coal basins of northwest Bangladesh. Based on elemental compositions, Islam and Kamruzzaman (2006) studied the geochemistry and techno-environmental issues related to mining and uses of Barapukuria coals. Islam and Hossain (2006) worked on the lithofacies and Embedded Markov Chain analysis of the Gondwana sequence of the Barapukuria Basin, Bangladesh, dealing with the identification of lithofacies, their upward transition, cyclicity within the sequence and environments of deposition of the Gondwana sequences.

Islam and Hayashi (2008) published on geology and coal bed methane resource potential of the Gondwana Barapukuria Basin. The methane content of the bituminous coal at Barapukuria ranges from 6.51 to 12.68 m^3/t and it is represented as a potential resource of more than 5 Gm^3 of gas. Farhaduzzaman et al. (2008) and Farhaduzzaman (2010) studied Gondwana coal properties of Bangladesh. Measured ash, sulfur, calorific value, fixed carbon, volatile matter, moisture, average seam thickness and seam depth of Phulbari coal are 15%, < 1%, 6600 kcal/kg, 51.9%, 30.5%, 2.7%, 36m and 165-270m, respectively (Farhaduzzaman et al., 2008). The total coal resource is 572 Mt at Phulbari. The coal is ranked as sub-bituminous to bituminous rank. They also showed the property of the Barapukuria coal is quite similar with the Phulbari coal. Frielingsdorf et al. (2008) published a paper on tectonic subsidence modeling and basin development from a structural point of view based on the Gondwana coals from Kuchma, Singra and Hazipur wells of northwest Bangladesh. Recently, based on comprehensive desktop studies, UNDP (2008), Muller (2009), Hildebrand (2010), Alam (2010) and Khalequzzaman (2010) discussed the

coal resources. They raised possibility of the challenges for coal bed methane (CBM), underground coal gasification (UCG) and mining development issues in northwest Bangladesh.

There is no comprehensive analysis of the Permian Gondwana coals (Bangladesh) and its relation to other fine grained sediments based on organic geochemical and petrographical methods. The current study aims to fill this gap and undertakes to characterize the organic facies distributions within the Permian succession. It concentrates on the comprehensive analyses of coals, carbargillites and mudstones covering mostly all of the identified important seams of the Barapukuria and Dighipara Basins.

2.1.3 Reservoir sandstone

Several workers have published papers on sandstone analysis of the Bengal Basin, Bangladesh. The petroleum reservoir sandstone of the Bengal Basin is primarily analyzed for reservoir quality as well as the diagenetic controls by Imam and Shaw (1985 and 1987) and Imam (1986 and 1989). Subsequently, Imam and Hossain (2002) discussed the hydrocarbon habitats in the Bengal Basin, Bangladesh. The reserves of natural gas and oil and the acting petroleum systems are highlighted in this dissertation. Based on formation velocity evaluation, Zahid and Uddin (2005) discussed the overpressure effect for the Neogene strata of eastern Bengal Basin. Islam et al. (2006) have done petrophysical analysis of the reservoir sandstones from Titas Gas Field, the Bengal Basin. Rahman and Suzuki (2007b) studied the provenance and tectonic settings on the basis of Surma Group sandstone geochemistry of the Bengal Basin. Najman et al. (2008) worked on the Paleogene record of the Himalayan erosion based on the biostratigraphy and geochemistry of the Paleogene sediments of the Bengal Basin, Bangladesh.

Islam (2009) published on reservoir quality and diagenesis of the Bhuban Formation sandstones. Petrophysical evaluation of subsurface reservoir sandstones of the Bengal Basin is carried out by Islam (2010a). Rahman et al. (2009) worked on the tidal sedimentation record of the Neogene Surma Group of the Sylhet Trough, the Bengal Basin. Islam and Rahman (2009) carried out a geochemical analysis of the Miocene Surma Group sediments from Meghna Gas Field. Islam (2010b) studied the petrography and provenance of the subsurface Neogene sandstone reservoirs of the basin. A study on diagenetic history of the Surma Group sandstones of the Bengal Basin has recently been carried out by Rahman and McCann (2012). Hossain (2012) published the latest oil reserves, albeit limited, of the Bengal Basin, Bangladesh. In the present research, sandstone petrography and XRD are used to study on reservoir quality and diagenesis effects to supplement all these studies. The petrophysical evaluation of the reservoir sandstone is also carried out and compared with the findings obtained from petrographic results.

2.2 Regional Geology and Tectonics

Guha (1978), Banerji (1984), Khan (1991), Reimann (1993), Khan and Chouhan (1996), Alam et al. (2003), Uddin and Lundberg (2004), Imam (2005) and Steckler et al. (2008) studied the general geology and tectonics of Bengal Basin. Bangladesh lies in the northeastern corner of the Indian subcontinent at the head of the Bay of Bengal. It has 144,000 km^2 of onshore and 63,000 km^2 of offshore area. The basin occupies major part of the Ganges-Brahmaputra delta- the largest of its kind in the world by sediment load (some 1.6 billion tones per annum) carried to the sea (Reimann, 1993; Alam et al., 2003). The Bengal Basin includes, in addition to Bangladesh, part of the Indian state of West Bengal in the west and Tripura in the east.

The basin is bordered to the west by the Precambrian Indian shield, to the north by the Shillong Massif and to the east by the frontal fold belt of the Indoburman Range. It is open to the south for some distance to the Bay of Bengal (Fig.2.1).

Tectonically, the Bengal Basin evolved from collision of the Indian plate and the Asian plate. According to plate tectonic theory, the northwestern part of Bangladesh was initially joined along with Indian landmass, including Antarctica, Australia and others, forming a vast southern hemisphere super continent named Gondwanaland (Guha, 1978; Banerji, 1984; Khan, 1991). The southern part of the landmass of Bangladesh did not exist at that time. During the Cretaceous time (110 Ma), the Gondwanaland super continent began to break up and India began to drift towards north (Imam, 2005). The Bengal Basin was initiated during this time (Cretaceous) with rifting of the Indian plate from Antarctica. However, the basin did not become center of deposition of thick clastic sediments until the northward drifting Indian plate collided with the relatively passive Asian plate (Khan and Chouhan, 1996; Alam et al., 2003). It is only after this collision and minor uplift of Himalayan Mountains that the remaining landmass of Bangladesh began to form.

The collision between Indian plate and Asian plate took place in stages beginning in Eocene (55 Ma) when an initial uplift of the Himalayas occurred. By late Eocene (40 Ma), the last remnant of intervening Tethys Sea between Indian plate and Asian plate probably disappeared as a result of the collision (Uddin and Lundberg, 2004). During this time, the direction of Indian plate convergence changed from north to northeast with increasing collision with Asia. Since Oligocene (35 Ma), major sediments were shed off the rising Himalayas as large river system started filling up the basin.

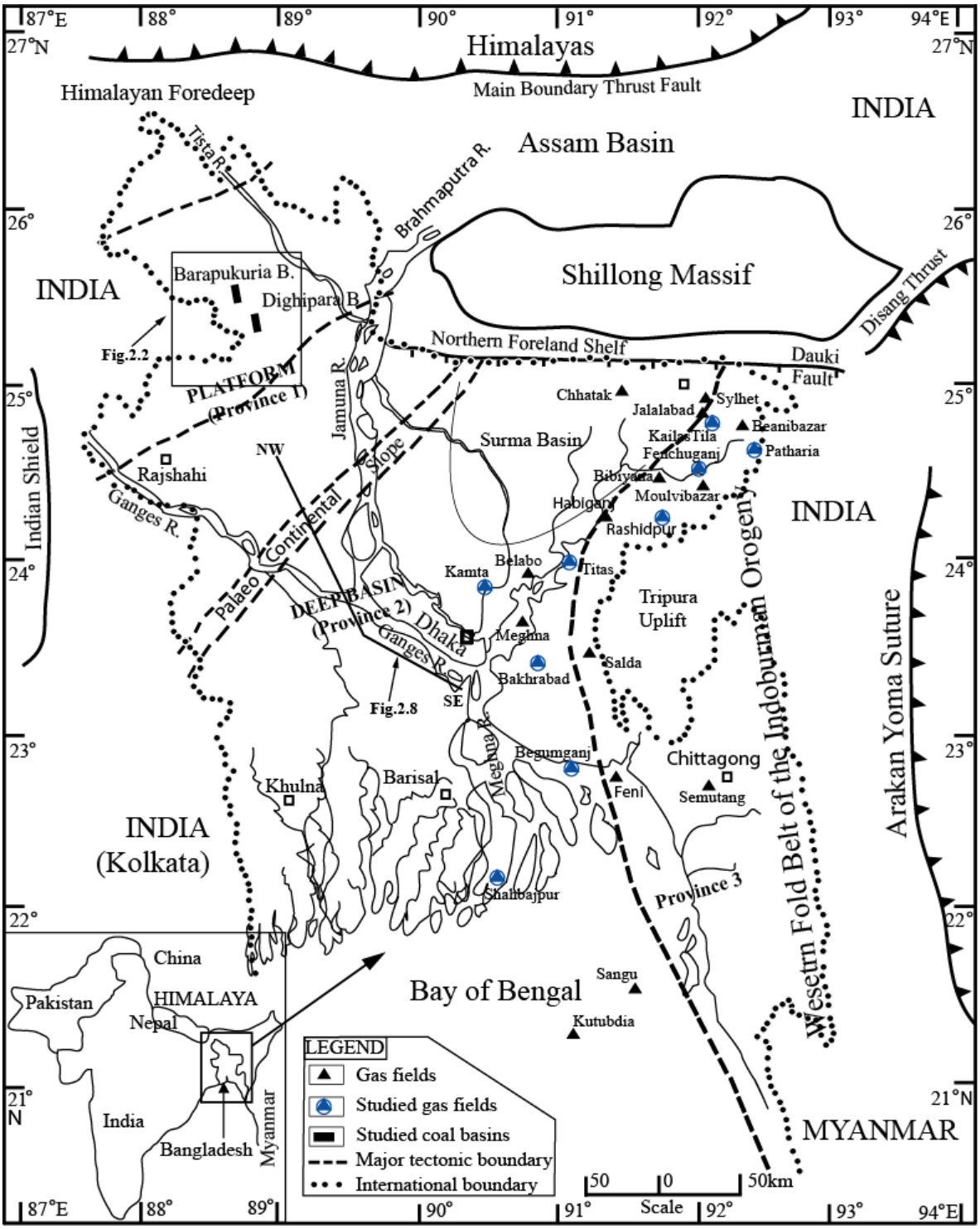

Fig.2.1. Location map of study areas including Barapukuria and Dighipara Coal Basins and nine gas fields. It shows the major tectonic elements of the Bengal Basin (modified after Khan, 1991; Reimann, 1993; Alam, et al., 2003; Shamsuddin et al., 2004; Imam, 2005).

During Neogene (onwards from 25 Ma), rapid rise in the Himalayas, accompanied by rapid subsidence in the basin to the south, resulted in deposition of a huge sedimentary pile with the simultaneous development of a mega delta. This became the land mass we now know as the Ganges-Brahmaputra delta.

The delta building activities continued along the central part of the basin, although the eastern part of the basin has since been uplifted into a folded mountain belt, i.e., Sylhet-Chittagong Hills. It represents the frontal or outer western part of a more extensive orogeny, namely the 'Indoburman Range'. The folded mountain belt resulted as a direct consequence of the subduction of the Indian plate beneath the Asian (Burmese) plate to the east. Alam et al. (2003) described the Bengal Basin as a 'Remnant Ocean Basin' which continued subduction along its eastern margin and incorporation of sediment complex into a westward migrating orogenic belt (Indoburman)- a process which will presumably result in the eventual closure and destruction of the basin. The tectonic framework of the Bengal Basin can broadly be divided into two main units: (a) Stable Platform unit (Province 1) in the northwest, which further comprises two subunits- Rangpur Saddle and Bogra Shelf; and (b) Deep Basin unit (Province 2) to the southwest-northeast, which also includes the Surma basin, Madhupur-Tripura Threshold, Faridpur Trough, Barisal High and Hatiya Trough in the west and the Fold Belt (Province 3) in the east. A third unit, a narrow northeast-southwest trending zone called 'Hinge Zone' (also known as Palaeocontinental Slope), separates the above two units diagonally almost through the middle of the country (Fig.2.1). Above the basement in northwest Bangladesh, a number of half graben small basins like Barapukuria, Phulbari, Khalaspir, Dighipara and Jamalganj occurred where sediments of the coal bearing Gondwana formations are present (Fig.2.2).

2.3 Study Areas and their Stratigraphic Frameworks

The Permian coal bearing Barapukuria and Dighipara Basins, northwest Bangladesh, are investigated in the present research. Also, nine gas fields covering the entire Deep Basin unit of the Bengal Basin, eastern Bangladesh, are examined in the current study (Figs.2.1 and 2.2). The detail of the study areas is discussed below.

2.3.1 Structure and Stratigraphy of the Barapukuria Coal Basin

The Barapukuria Basin is a north-south elongated coal bearing half-graben basin bounded by a major N-S oriented eastern boundary fault (Fig.2.3). The Gondwana sedimentary succession within the basin forms a singular asymmetric synclinal fold with ca. N10˚W trending axis. The axial plane dips towards the east (Imam, 2005). Stratigraphically, the Barapukuria Basin includes Archaean, Permian, Tertiary and Quaternary formations representing the Basement Complex, Gondwana Group, Dupi Tila Formation and Barind Clay (Madhupur Clay) Formation, respectively (Fig.2.4). The coal deposit is found within the Permian Gondwana Group (Armstrong, 1991; Islam and Islam 2005, Islam and Hossain, 2006; Islam and Kamruzzaman, 2006; Islam and Hayashi, 2008). This sedimentary half-graben basin lies above the basement complex within which Permian age formations preserved by down faulting and subsequently infilled with unconsolidated Tertiary and Quaternary sediments (Table 2.1). The lithostratigraphic description of the Barapukuria Basin is stated below (from oldest upward).

Table 2.1. Stratigraphic succession of the Barapukuria Basin (modified after Armstrong, 1991; Alam *et al.*, 2003; Islam and Islam, 2005).

Age	Group	Formation	Simplified lithology	Thickness (m)	Depositional environment
Holocene		Alluvium	Silt, clay, sand and gravels.	0-1	Fluvial-alluvial and rapidly prograding delta.
Plio-Pleistocene		Barind Clay	Yellowish to reddish brown silty clay.	3-15	
Late Pliocene	Dupi Tila	Upper Dupi Tila	Micaceous fine to medium grained grey sands and gravels with occasional bands of silt and clay.	107	Fluvial and prograding delta-shelf.
Early Pliocene to Late Miocene		Lower Dupi Tila	Firm light grey and white clayey sand and kaolinitic clays.	0-81	
Permian	Gondwana	Upper Coals Sequence	Interlaminated fine to coarse quartzo-feldspathic sandstones with some coal seams (Seams I to V) and occasional beds of siltstones and mudstones.	upto 180	
		Seam VI Sandstone Sequence	Light grey to white medium to coarse grained sandstones, gritstones and conglomerates with tickest Seam VI.	75-125	Fluvial to delta plain, coal swamps.
		Lower Sandstone Sequence	Interbanded sandstones, siltstones and mudstones with occasional thin coal bands. Tillites at the basal part.	-	
Archaean	Pre-Cambrian	Basement Complex	Various veined gneissic metamorphic and meta-igneous rocks with weathered top (5-10m).	-	Stable Gondwana continent.

2.3.1.1 Basement Complex (Archaean) in Barapukuria

The Archaean Basement Complex consists of various veined gneissic metamorphic and metaigneous rocks. There is some weathering at the top (5-10m), but below, these rocks are very strong and fresh. It has been considered to be eminently suitable for a wide range of uses as industrial aggregates.

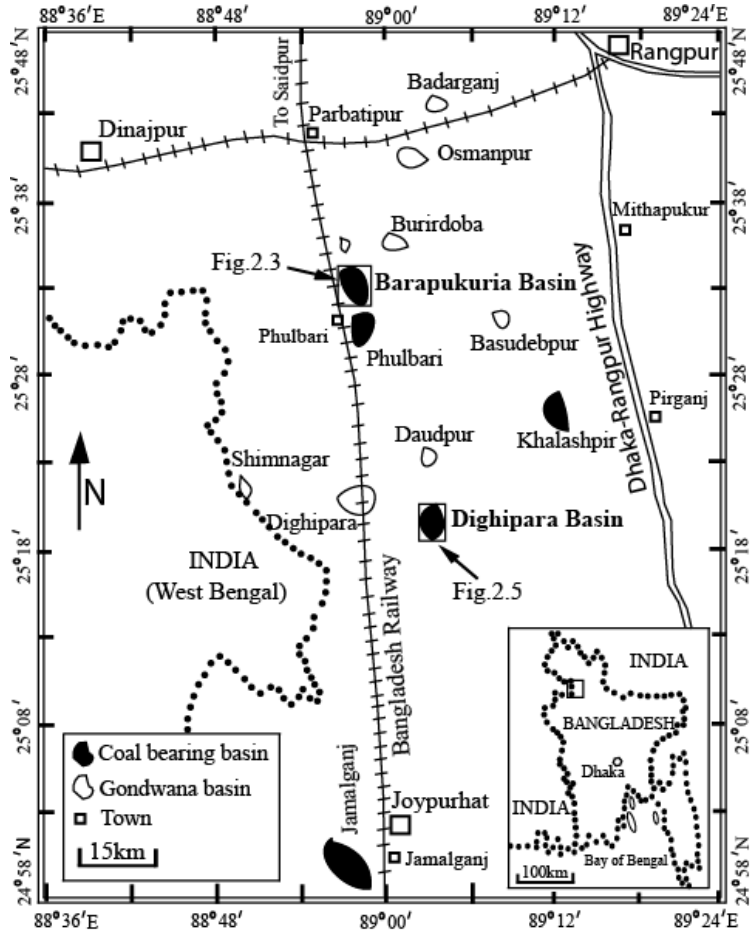

Fig.2.2. The positions of Gondwana basins in the vicinity of the Barapukuria and Dighipara Coal Basins (after Uddin and Islam, 1992; Imam, 2005; Islam and Hayashi, 2008; Farhaduzzaman et al., 2012a).

2.3.1.2 Gondwana Group (Permian) in Barapukuria

The Permian Gondwana Group occupies an elongated sedimentary basin to the immediate west of a north-south geological fault, to the east of which is Archaean basement.

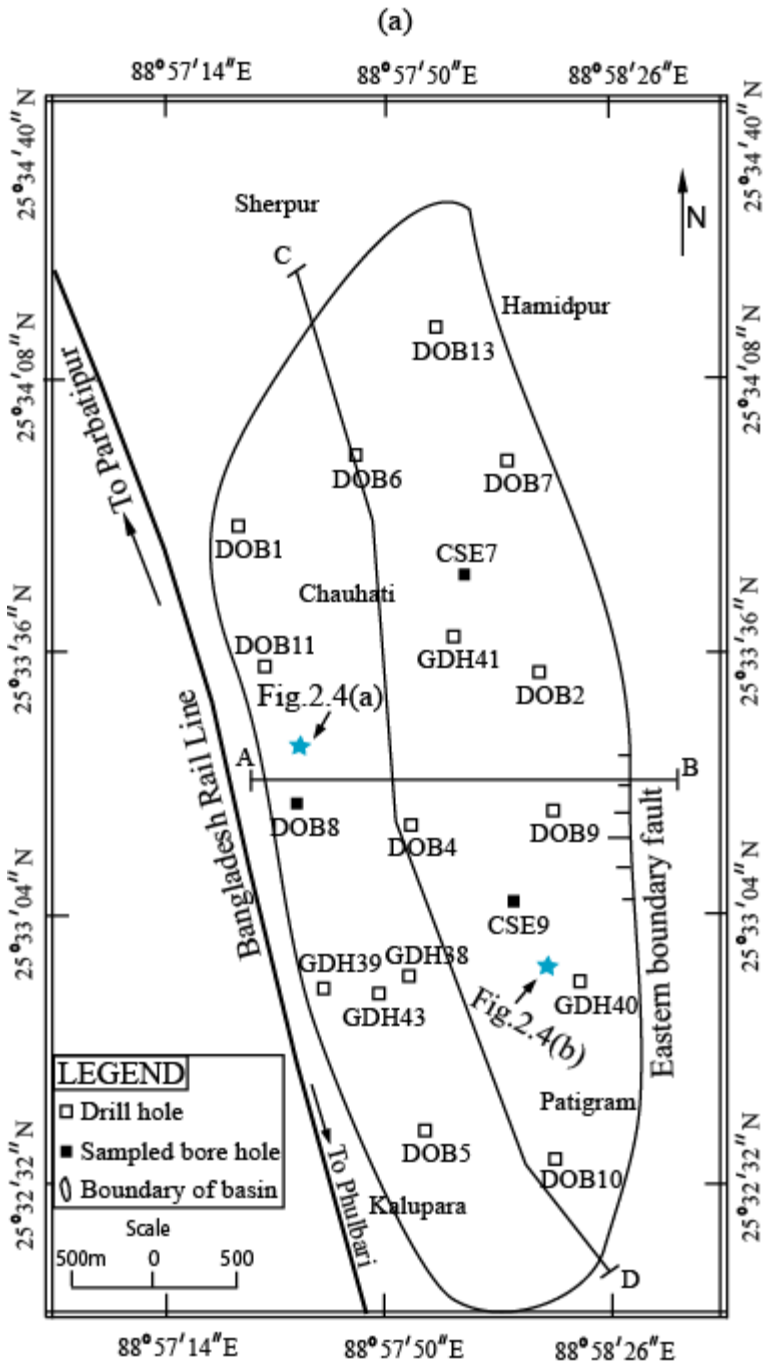

Note: The cross-sections of the lines A-B and C-D are shown in Fig.2.3 (b) and Fig.2.3 (c).

Fig.2.3. (a) Sampling locations shown in the study area of the Barapukuria Basin, Bangladesh. Two cross-sections have also been added- (b) west to east, and (c) north to south (Imam, 2005; Islam and Hayashi, 2008; Farhaduzzaman et al., 2013c and 2013d). The analyzed samples are collected from Seam VI, Seam V and Seam IV (Continued).

Fig.2.3 (Continued).

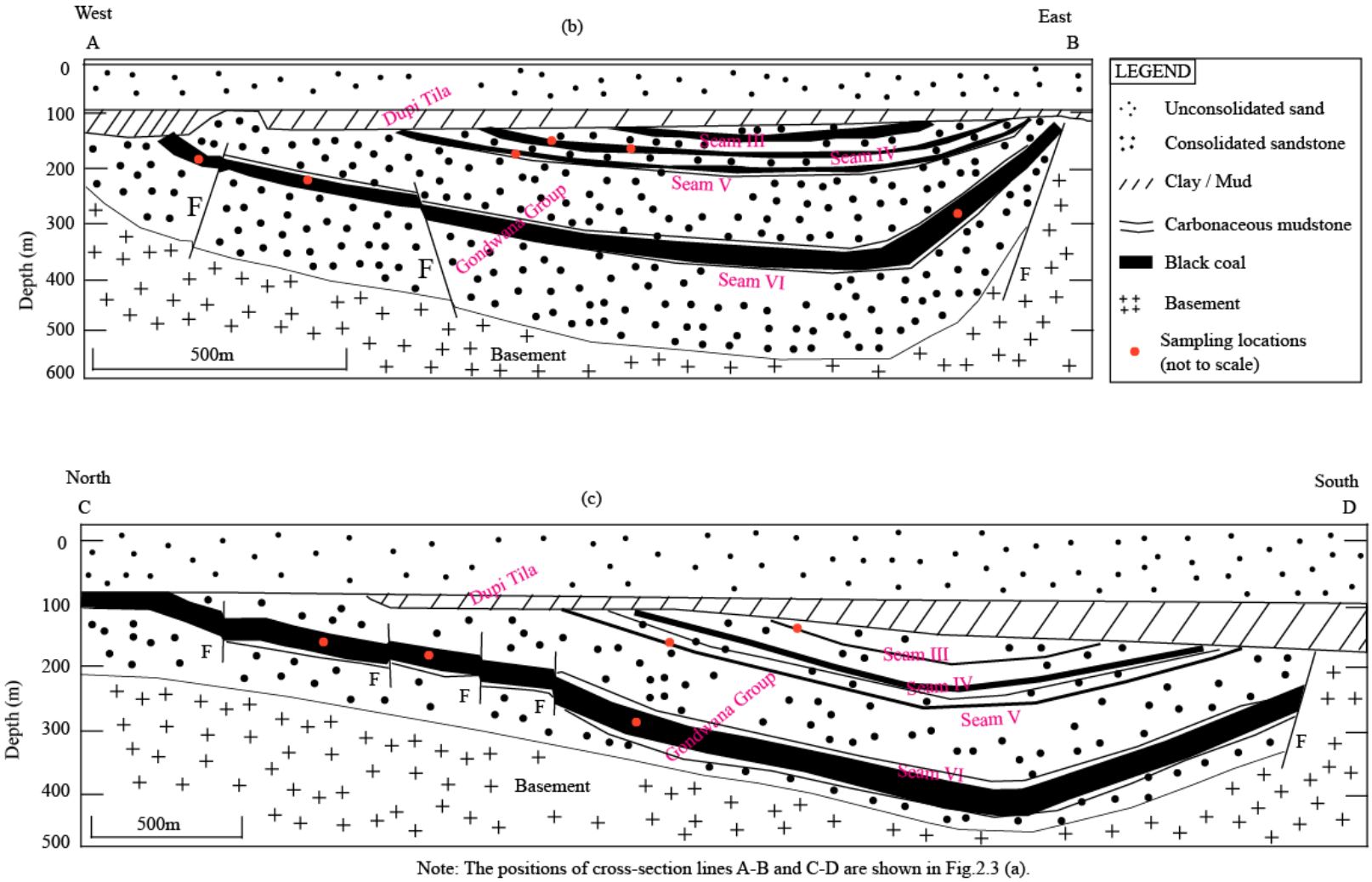

Note: The positions of cross-section lines A-B and C-D are shown in Fig.2.3 (a).

The full sequence is found only in the deepest part of the half-graben basin (approximately 450m) whilst in the peripheries only Seam VI and the underlying sediments are present.

Gondwana- 'Lower Sandstone Sequence'

The sequence below Seam VI is substantially different from the Gondwana sequence above (Table 2.1). It consists of a rapidly interbanded sequence of sandstones, siltstones and mudstones with occasional thin coal bands. Most of the sandstones above Seam VI are, to some extent, weathered and moderately weak, with slight to complete decomposition of the feldspars to kaolinitic clay. The sandstones below Seam VI, on the other hand, are mostly unweathered, less feldspathic and moderately strong. There are frequent units of fluviatile sandstones and interbanded sandstone-siltstone sequences with occasional thin bands of coals and isolated fossil plants. Tillites of glacial origin form the lowest part of the Gondwana sedimentary sequence are generally considered to be of Upper Carboniferous age. They consist of variable thickness boulder-bed tillites containing clasts of unsorted sedimentary, igneous and metamorphic rocks, interbedded with occasional units of mudstone, siltstone and coal indicative of periods of interglacial sedimentation and occasional minor peat accumulations.

Gondwana- 'Seam VI Sandstone Sequence'

This sequence varies from 75m to 125m in thickness and is of relatively homogeneous and massive light grey and white, medium to coarse grained sandstones, gritstones and conglomerates (Imam, 2005). The originally arkosic sandstones are strongly kaolinized, resulting in a white clay matrix almost throughout, greatly reducing their primary permeability. All of the sandstones in the Gondwana sequence contain occasional high angle joints.

These joints are generally tight or infilled, further limiting the sandstone's secondary permeability, an important factor in terms of hydrogeology. Seam VI is the thickest seam (average 36m) and apart from some thin impersistent bands of coal below, it is the basal coal seam in this sequence. It contains > 90% of the Barapukuria coal reserves.

Gondwana- 'Upper Coals Sequence'

The sequence is up to 180m thick and consists of an interlaminated sequence of fine to coarse quartzo-feldspathic sandstones with a number of coal seams (Seam I to Seam V) and occasional beds of siltstone and mudstone. The interlaminated nature of this sequence is very noticeable on the seismic sections. The sandstones close to the the base of the Dupi Tila Formation are extremely weathered and there is slight to moderate weathering and kaolinization of the sandstones throughout the sequence.

2.3.1.3 Dupi Tila Formation (Mio-Pliocene) in Barapukuria

The Gondwana Group is unconformably overlain by Dupi Tila Formation (Table 2.1). This is comprised of grey to yellowish brown, medium to coarse, loose unconsolidated sands with clay-silt layers or gravels. The thickness is around 100-200m and it is the regional groundwater aquifer. The formation is divided into two units, namely, Lower Dupi Tila and Upper Dupi Tila. The Lower Dupi Tila is characterized by firm, light grey and white clayey sands and kaolinitic clays which were probably derived from the weathering of the weak kaolinized Gondwana sandstones immediately below. Lower Dupi Tila is absent from the northern parts of the basin and generally thickens to the south where the main clay beds are interlaminated with loose silts and sands. Upper Dupi Tila is 107m thick on average and is divisible into lower and upper parts.

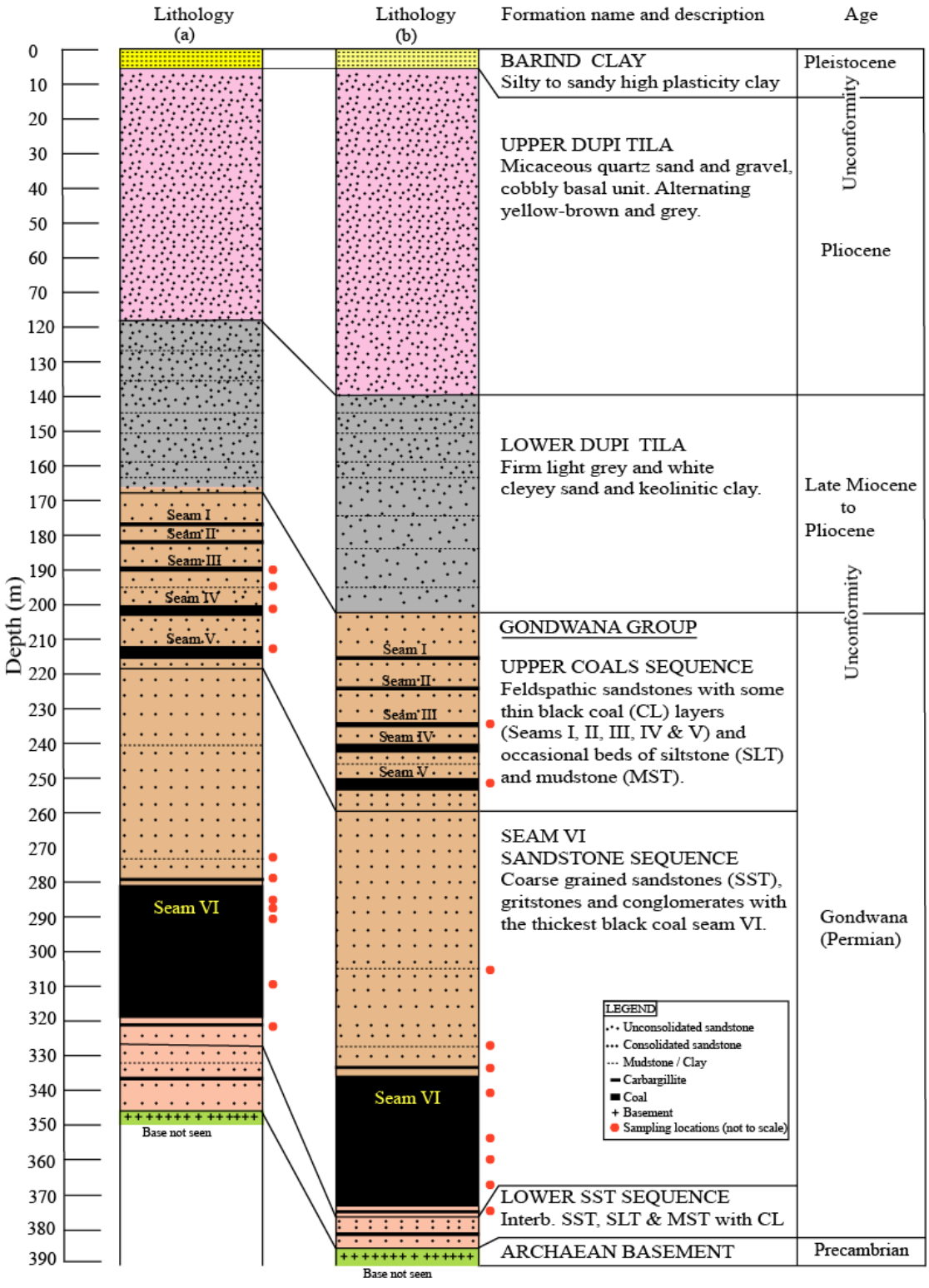

Fig.2.4. Generalized lithostratigraphic succession of the Barapukuria Basin, Bangladesh. (a) represents the central north-western part of the basin, and (b) represents the central south-eastern part of the basin (Fig.2.3 for its location). The sampling locations are also shown (Farhaduzzaman et al., 2012a).

The lower part of Upper Dupi Tila is approximately 40m thick and is composed of organic-brown, slightly micaceous sandstone, generally finer than the upper part with more frequent thin beds of silt and clay. The upper part of Upper Dupi Tila is 65m thick and is composed of micaceous grey sands and gravels with occasional bands of silt and clay.

2.3.1.4 Barind Clay (Pleistocene to Recent) in Barapukuria

The Upper Dupi Tila is overlain by the 3-15m thick Barind Clay (also known as Madhupur Clay) that consists of yellow to reddish brown silty clay and overlain by a thin mantle (less than 1m) of alluvium and silty soil.

2.3.2 Structure and Stratigraphy of the Dighipara Coal Basin

Stratigraphy of the Dighipara coal basin has not been well established and it is still under exploration. However, on the basis of lithological logging and data collection while sampling (for current research) and during drilling, the following description has been prepared. The Dighipara Coal Basin is located within the southern slope of the Platform unit. The Dighipara Basin is a north-south elongated oval-shaped and fault bounded basin. The eastern side of the basin might be fault bounded, as evidenced from the Bouger gravity anomaly map. The northeast-southwest trending fault may be the northern limit of the basin. The basin might have formed by faulting in the crystalline basement during Permo-Carboniferous time (Banerjee, 1984). Later on, these basins were reshaped and basin marginal adjustments took place from time to time due to the Himalayan upheavals (Uddin, 1996). Subsequently, the Tertiary and Quaternary sediments were deposited over the crystalline basement within the half-graben basin. The quality of the Dighipara coal is similar to that of the Barapukuria coal (Alam, 2010). The Geological Survey of Bangladesh drilled four holes (as of December 2011) in the Dighipara and found coal in all holes.

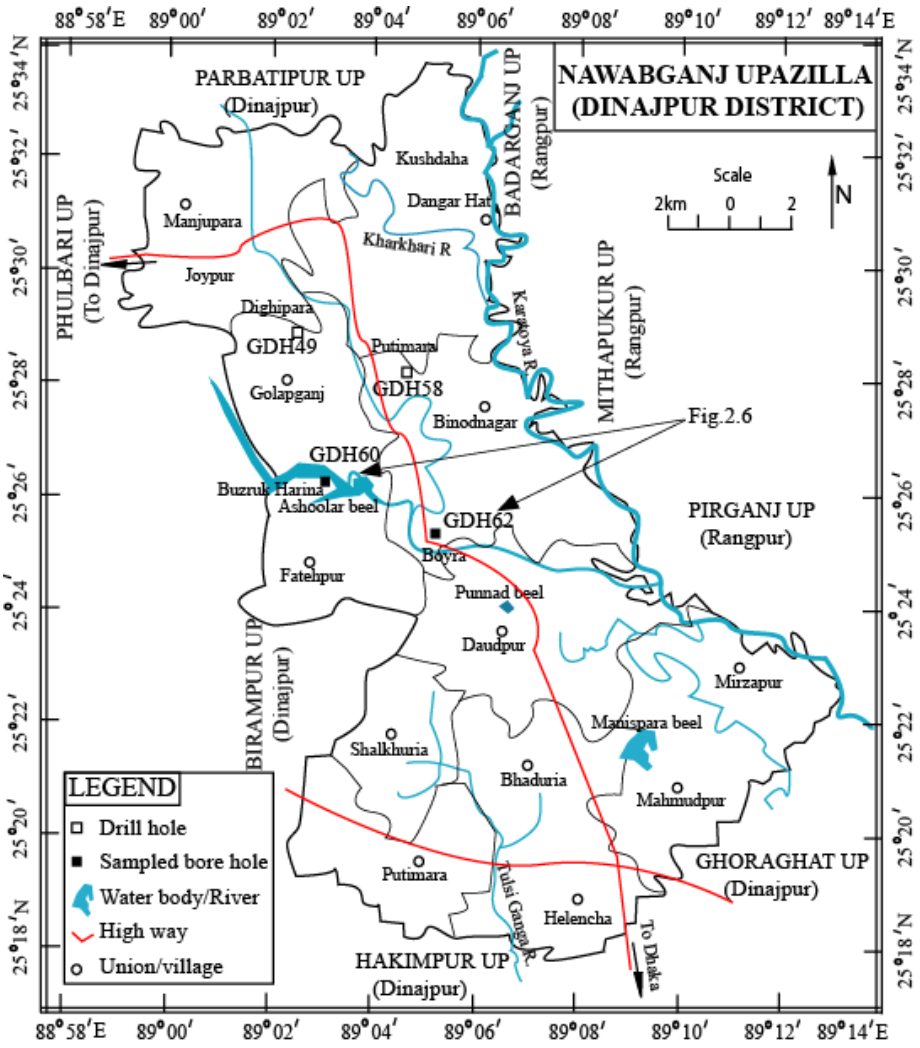

Fig.2.5. Sampling locations in the study area of the Dighipara Coal Basin, Bangladesh.

The number of coal seams varies from three to seven whereby the top seams, A, B and C, constitute the majority of the resources. The coal is found at depths of 323-383m, which indicates the resource identified here is comparatively deeper than the Barapukuria. The cumulative thickness of the coal seams ranges from 47.32m to 71.07m, whilst the average thickness is 61 meters. The probable basin area is about 15 km^2. The Bangladesh Government has recently granted an exploration license to the Petrobangla. The Delta Pacific Mining PLC has expressed their interest to have joint venture with Petrobangla.

Table 2.2. Stratigraphic succession of the Dighipara Basin (modified after Hasan and Islam, 2003; Alam et al., 2003).

Age	Group	Formation	Simplified lithology	Max. thickness (m)	Depositional environment
Holocene		Alluvium	Silt, clay, sand, soft and rootlets.	1	Fluvial-alluvial and rapidly prograding delta.
Plio-Pleistocene		Barind Clay	Reddish brown silty sticky clay.	8	
Late Pliocene	Dupi Tila	Upper Dupi Tila	Yellowish brown fine to coarse poorly consoliadted sands and pebbles with occasional claystone bands.	320	Fluvial and prograding delta-shelf.
Early Pliocene to Late Miocene		Lower Dupi Tila	Grey to bluish gery plastic clayey sand. Bottom part soft and white kaolinitic clays.		
? Up. Eocene	? Jaintia	? Kopili	Reworked shale and sandstones with fossils.	61	Deltaic to slope.
? Paleocene		? Tura	Mainly silica sandstone and occasional clay beds.	61	Deltaic to outer shelf.
Permian	Gondwana	Gondwana	Feldspathic sandstone, carbonaceous sandstone and shale, conglomerate with coal beds.	167	Fluvial to delta plain, coal swamps.
Archaean	Pre-Cambrian	Basement Complex	Gneissic and schistose metamorphic and meta-igneous rocks with weathered top.	41	Stable Gondwana continent.

The lithological descriptions and their corresponding stratigraphic positions of the geological formations are similar in comparison to those of the Barapukuria (Hasan and Islam, 2003). The sampling locations, boreholes and a simplified lithostratigraphic succession of representative bore holes of the Dighipara have been shown in Figs.2.5 and 2.6. The simplified lithostratigraphic descriptions of the Dighipara Basin are stated below (from bottom upward).

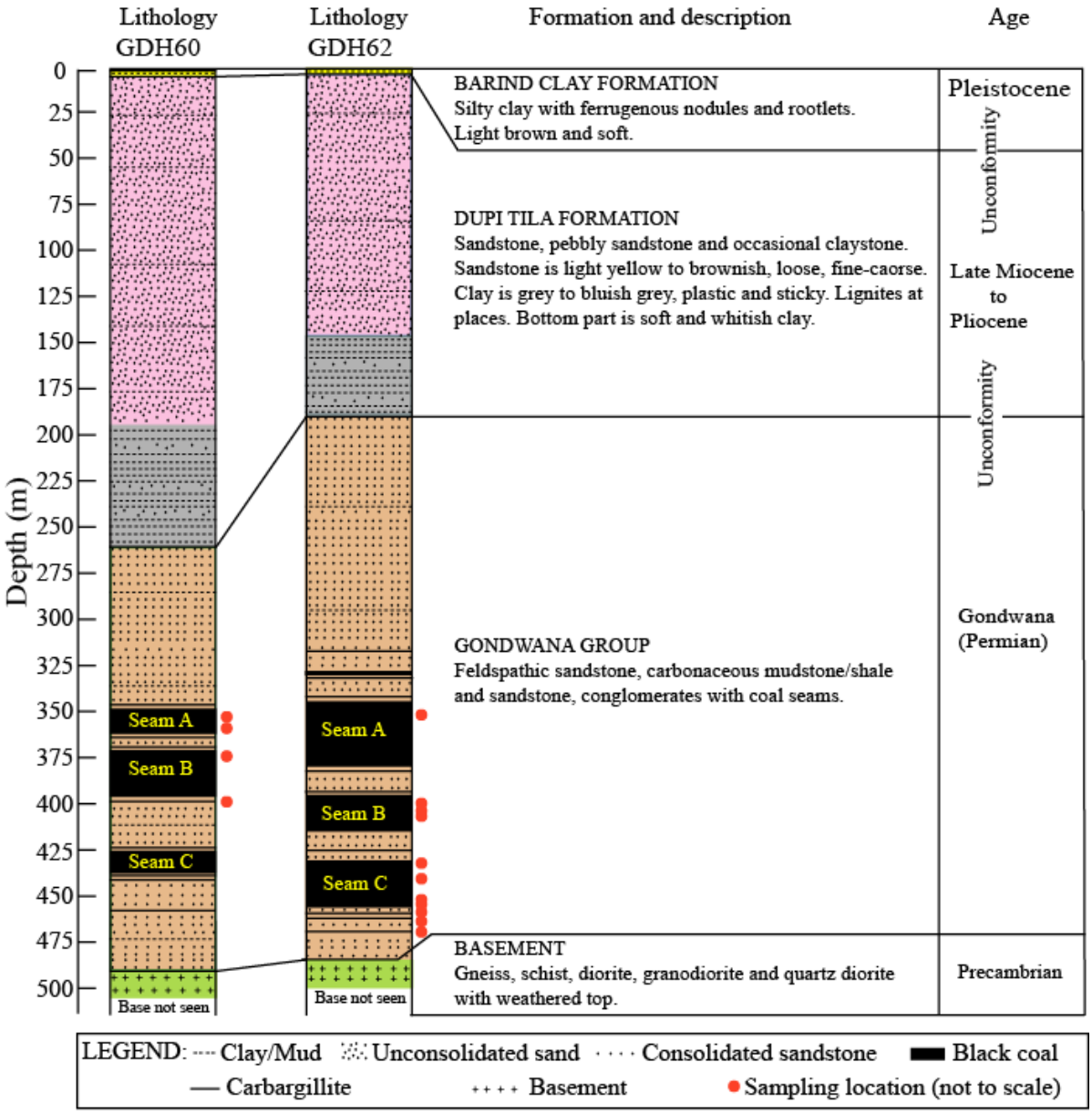

Fig.2.6. Generalized lithostratigraphic columns of two investigated bore holes GDH60 and GDH62 of the Dighipara Basin. Sampling positions are also shown here.

2.3.2.1 Basement Complex (Archaean) in Dighipara

Gneissic and schistose metamorphic and meta-igneous rocks are the main constituents of the Basement Complex. Kaolinized weathering top is observed in this group whereas it is strong and fresh at deeper part. Gneiss, schist, granodiorite and quartz diorite are the common rock types.

2.3.2.2 Gondwana Group (Permian) in Dighipara

The Dighipara Gondwana Group consists of relatively homogeneous and massive light grey and white, medium to coarse grained feldspathic sandstones, gritstones and conglomerates. Carbonaceous sandstone and carbonaceous shale is very common especially as roof and floor of the coal seams. The important Permian coal seams are hosted by this group of sediments.

Overlying the Gondwana Group, a silica sandstone with occasional clay beds, are observed in few of the GSB drill holes (Table 2.2) [Assumed to be the Paleocene Tura Formation (?) (Hasan and Islam, 2003)]. On the other hand, reworked sandstone and shale with fossils is identified in some cases underlying this so-called Tura Formation. This is assumed to be Kopili Formation (?) as stated by Hasan and Islam (2003). There is a great possibility that these so-called Tura and Kopili Formations could be the part of huge Gondwana Group sediments. However, it requires more study (palynology, geochemistry, isotopes) for further clarifications.

2.3.2.3 Dupi Tila Formation (Mio-Pliocene) in Dighipara

The Dupi Tila Formation unconformably overlies the Gondwana Group sediments (Table 2.2). It is basically unconsolidated sandstone, pebbly sandstone and occasional claystone. The sandstone is light yellow to brown, white at places, fine to coarse and loose. The pebbly sandstone is grey with various shades of colour, sub-angular, mostly quartzite embedded in a sand matrix and is poorly consolidated. The clay is grey to bluish grey with reddish tints, sticky and plastic when wet, hard on drying, and at places, with lignitic material present. The bottom part is white and soft.

2.3.2.4 Barind Clay (Pleistocene to Recent) in Dighipara

The Barind Clay is red and brown, variegated, sticky and plastic when wet and hard on drying. Ferruginous nodules are present within this formation. It is overlain by a thin layer of Recent Alluvium consisting of silty clay with rootlets at the top.

2.3.3 Stratigraphy of the Deep Basin unit of the Bengal Basin

In contrast to Platform unit (a 400m thick sedimentary pile), the stratigraphy of the Deep Basin unit of the Bengal Basin is characterized by an enormous thickness (up to 22km) of Tertiary succession, the largest sedimentary accumulation in the world. In Platform unit (Province 1), the stratigraphic succession includes Permian, Cretaceous and Tertiary rocks overlying Precambrian basement. On the other hand, in the Deep Basin unit (Province 2), this succession can be divided into the Jaintia Group (Paleocene to Eocene), Barail Group (Oligocene), Surma Group (Miocene to Early Pliocene), Tipam Group (Middle Pliocene) and overlying Dupi Tila (Late Pliocene) and Madhupur Clay Formations (Plio-Pleistocene) (Fig.2.7) (Alam et al., 2003; Imam, 2005). During the Tertiary period (2-65 Ma), the Bengal Basin as it is today, started to form and a major part of the sedimentary succession was deposited in this time (Fig.2.8). Stratigraphy of the Deep Basin unit is dominated by deltaic to terrestrial (continental) clastic sedimentary rocks comprising mostly sandstone and shale. Recently, the open marine to shelf marine depositional environmental signatures have also been documented, especially for the Neogene sediments. However, the sedimentary succession encountered in the Deep Basin unit, described below, ranged from Paleocene to Recent (Alam et al., 2003; Imam, 2005).

Table 2.3. Generalized stratigraphic succession of the Deep Basin unit or Province 2 of the Bengal Basin (modified after Alam *et al*., 2003; Imam, 2005). The currently investigated formations are in bold fonts.

Age	Group	Formation	Simplified lithology	Formation base (m)	Thickness (m)	Depositional environment
Holocene		Alluvium	Silt, clay, sand and gravels.	2	2	Fluvial system.
Plio-Pleistocene		Madhupur Clay	Yellowish brown silty clay.	13	11	Fluvial system.
Late Pliocene	Dupi Tila	Upper Dupi Tila	Fine to medium grained poorly consolidated sandstones, silty, with lignite fragments and fossil woods, intercalations of mottled clay horizons.	2515	2500	Fluvial system.
		Lower Dupi Tila	Lower unit shows fining upward sequences.			Meandering river.
Middle Pliocene	Tipam	Girujan Clay	Mottled clay.	3515	1000	Lacustrine and fluvial overbank.
		Tipam Sandstone	Coarse grained sandstone with wood fragments and coal interbeds.	6015	2500	Braided fluvial systems.
Early Pliocene	**Surma**	**Boka Bil**	**Alternating shale and sandstone with minor siltstone.**	**7515**	**1500**	**Subaerial to brackish with marine influence.**
Miocene		**Bhuban**	**Alternating and repetetive sandstones and shales with minor conglomerate and siltstone.**	**11015**	**3500**	**Pro-delta and delta front of mud rich delta system.**
Oligocene	Barail	Renji	Predominantly sandstone with minor shale.	11715	700	Predominantly tide dominated shelf.
		Jenum	Predominantly shale with minor siltstone and sandstone.	12515	800	Predominantly tide dominated shelf.
Upper Eocene	Jaintia	Kopili Shale	Fossiliferous shale.	12565	50	Deep sea fan.
Middle Eocene		Sylhet Limestone	Nummulitic fossiliferous limestone with minor sandstone.	12815	250	Shallow marine.
Paleocene		Tura Sandstone	Poorly sorted sandstone, mudstone and fossiliferous marl, with minor carboniferous material and impure limestone.	13025	210	Shallow marine to marine.
Pre-Paleocene	Undifferentiated sedimentary rocks (?volcanic) on the continental basement complex.			22000	8975	Not determined.

2.3.3.1 Jaintia Group (Paleocene-Eocene)

The Paleocene-Eocene marine Jaintia Group that is deposited under marine conditions can be divided into three formations (from bottom upward): Tura (Paleocene), Sylhet Limestone (Middle Eocene) and Kopili (Upper Eocene) (Table 2.3). The Tura Formation is composed mainly of whitish sandstone with little shale and occasional coal beds near the top. The unit is drilled in several wells in the Platform area of the Bengal Basin and it is 150-350m thick. Only one isolated outcrop of this unit has been recorded in Sylhet-Meghalaya (India) border and it represents the oldest exposed rock in Bangladesh. The overlying Sylhet Limestone Formation is a fossiliferous (Nummulitic) limestone unit with an average thickness of 250m. It is extensively developed and can be traced as a seismic marker horizon in Platform area of the Bengal Basin. Scattered small outcrops of this formation are observed along the Sylhet-Meghalaya (India) border close to Dauki fault. The overlying Kopili Formation is composed of dark grey to black fossiliferous shale with few limestone beds. This formation is around 40-90m thick and marks the end of open marine condition of deposition at the top.

2.3.3.2 Barail Group (Oligocene)

The Oligocene Barail Group is composed of alternating sandstone, shale, siltstone and occasional carbonaceous rich layers. In neighboring Assam, about 3000m of Barail sediments are recorded and this group is divided into three units from bottom upward: (a) the arenaceous Laisong Formation, (b) the argillaceous Jenum Formation and (c) the arenaceous Renji Formation. Most of the Barail Group sediments are deeply buried in Bangladesh.

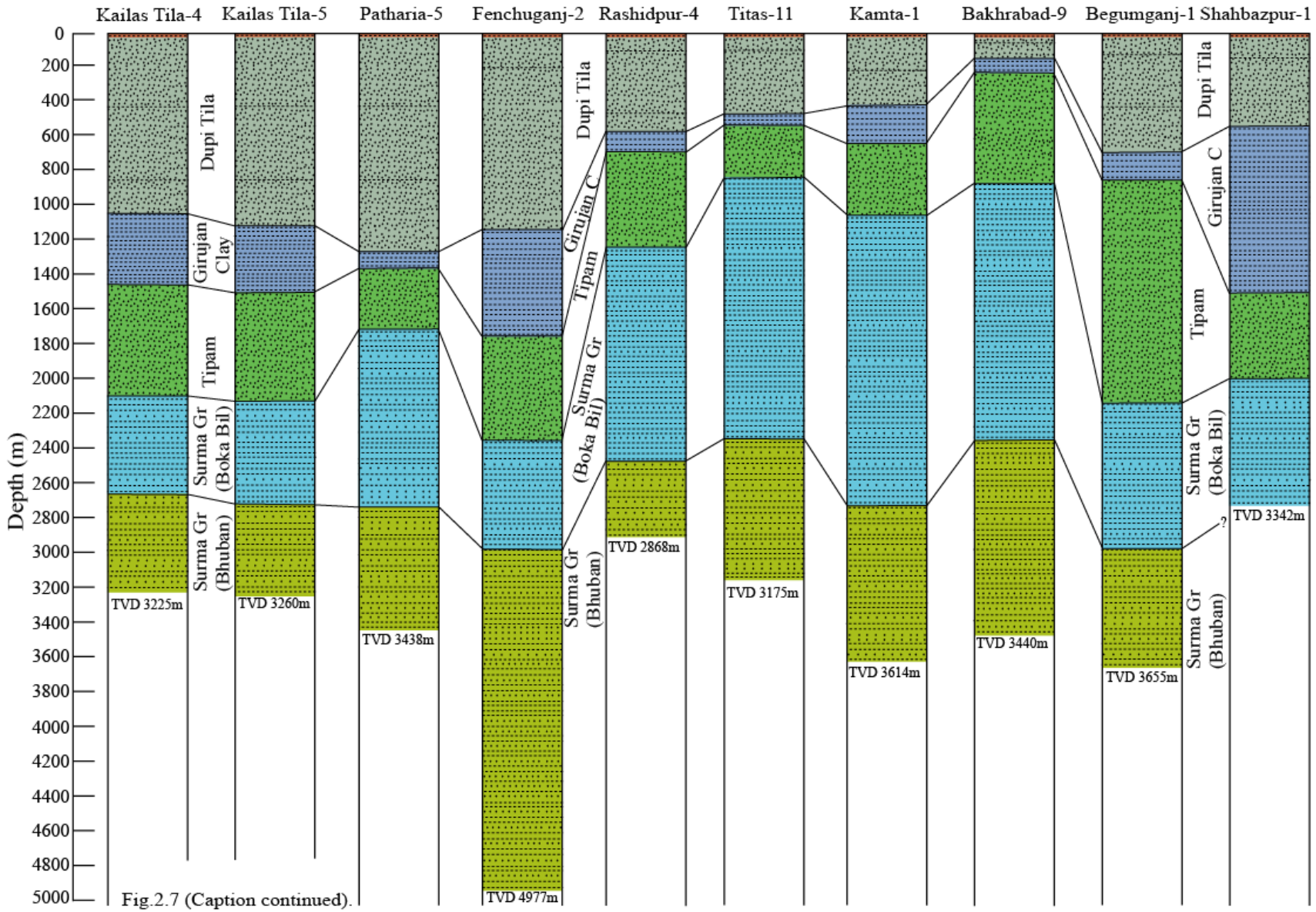

Fig.2.7 (Caption continued).

Fig.2.7 (Continued). Correlation of the studied ten wells (from north to south) of respective nine gas fields, the Bengal Basin, Bangladesh. All of the analyzed samples are collected from Boka Bil and Bhuban Formations lying at the bottom part (Moinul et al, 1977; Nazim et al., 1982; Khan, 1991; Alam et al., 2003; Imam, 2005; Farhaduzzaman et al., 2012b and 2013b).

Only two wells, i.e., Atgram IX and Rashidpur 2, penetrated 960m and 460m Barail sediments, respectively, at depths more than 4000m below the surface (Reimann, 1993). A small trip of land at Jaintia (Sylhet)-India border exposes about 350m of Barail (Renji Formation) sediments and it represents the only Oligocene outcrop in Bangladesh.

2.3.3.3 Surma Group (Bhuban and Boka Bil Formations) (Mio-Pliocene)

The Surma Group, up to 5km thick, is composed of the Bhuban and Boka Bil Formations and is exposed in the Sylhet and Chittagong hills. Both formations are composed of sandstones and shales with siltstone and some conglomerates interpreted to have been deposited in a deltaic to shallow-marine environment (Holtrop and Keiser, 1970). All of the hydrocarbon accumulations so far discovered in Bangladesh have been found within the Bhuban and Boka Bil Formation sandstones. The formations also contain shale intervals with important source rock potential (Imam, 2005). The overlying marine shale acts as a basin-wide seal.

The Tertiary succession in the Bengal Basin in Bangladesh can be correlated with outcrops in Lower and Upper Assam (India) which were studied and interpreted by Evans (1932). However, this stratigraphic classification is based almost exclusively on lithologic characteristics (Das Gupta, 1977).

The subdivision of the monotonous and repetitive sand-shale sequence of Surma Group into the Bhuban and Boka Bil formations is often ambiguous in absence of diagnostic lithology (Johnson and Alam, 1991; Alam et al., 2003; Imam, 2005). Correlation between the basins is made difficult because of the absence of marker horizons (Khan and Muminullah, 1980), diachronism of the units and lithological and facies variations (Das Gupta, 1982; Reimann, 1993). The deltaic Tipam Sandstone, for example, has been dated as Miocene in the Upper Assam Basin, but as Pliocene in the eastern portion of the Surma sub-basin in the Bengal Basin, Bangladesh. Within the Surma Group, the Bhuban Formation is in general more sand-rich and the Boka Bil Formation more argillaceous. Both formations show extensive lateral facies changes and vertical variations in sand: shale ratios, making difficult to correlate them across the basin (Johnson and Alam, 1991; Imam, 2005). Alam et al. (2003) emphasized that the contact between the formations is often difficult to recognize based on Evan's (1932) lithostratigraphic scheme.

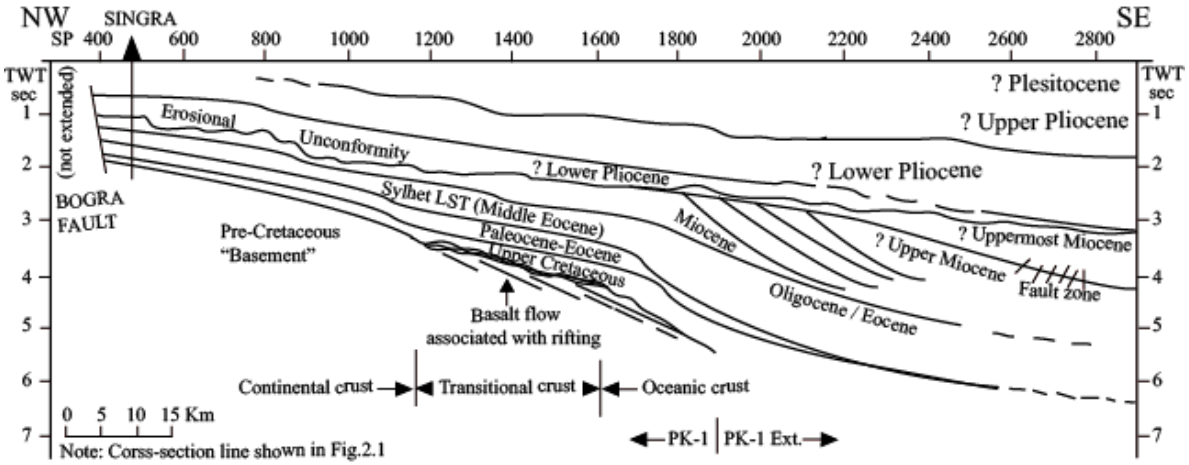

Fig.2.8. Geological cross-section through the Platform (Province 1) unit and southern part of the Deep Basin (Province 2) unit of the Bengal Basin. The location of cross-section line has been shown in Fig.2.1 (after Alam et al., 2003).

2.3.3.4 Tipam Group (Pliocene)

Following the basin filling by deltaic deposits, a broad front of river plain environment was established under which sand dominating (arenaceous) units are deposited. This is recognized as Tipam Group, which can further be divided into three formations including (from bottom upward) Tipam Sandstone Formation, Girujan Clay Formation and Dupi Tila Formation (Imam, 2005). The Middle Pliocene Tipam Sandstone Formation (1200-2500m) is typically a grey brown, medium to coarse grained, cross-bedded to massive sandstone with minor intervals of clay layers. Overlying the Surma Group, it is extensively exposed in Chittagong Hill Tracts area. The overlying Girujan Clay Formation (100-1000m) is a sticky bluish-grey clay unit that has a local extent and represents deposition in lake environments. This unit is conformably overlain by sand dominating Dupi Tila Formation (500-3000m). The Late Pliocene Dupi Tila is the sand dominated unit with minor interbedded claystone. The sandstone within this formation is red to brown, medium to coarse grained, loosely compacted, cross-bedded, occasionally pebbly and contain petrified wood in places. This formation was deposited under fluvial/river plain environments. This is the regional and major groundwater aquifer in Bangladesh. The Dupi Tila Formation is sometimes considered to be a separate group (Alam et al., 2003).

2.3.3.5 Madhupur Clay Formation (Plio-Pleistocene)

Quaternary sediments are represented by the Madhupur Clay Formation overlying the Dupi Tila Formation (Table 2.3). It is composed of reddish to brownish clay with subordinate silt and typically occurs in the uplifted terraces as well as in the subsurface. This unit is covered by a thin layer of Recent Alluvium sediments.

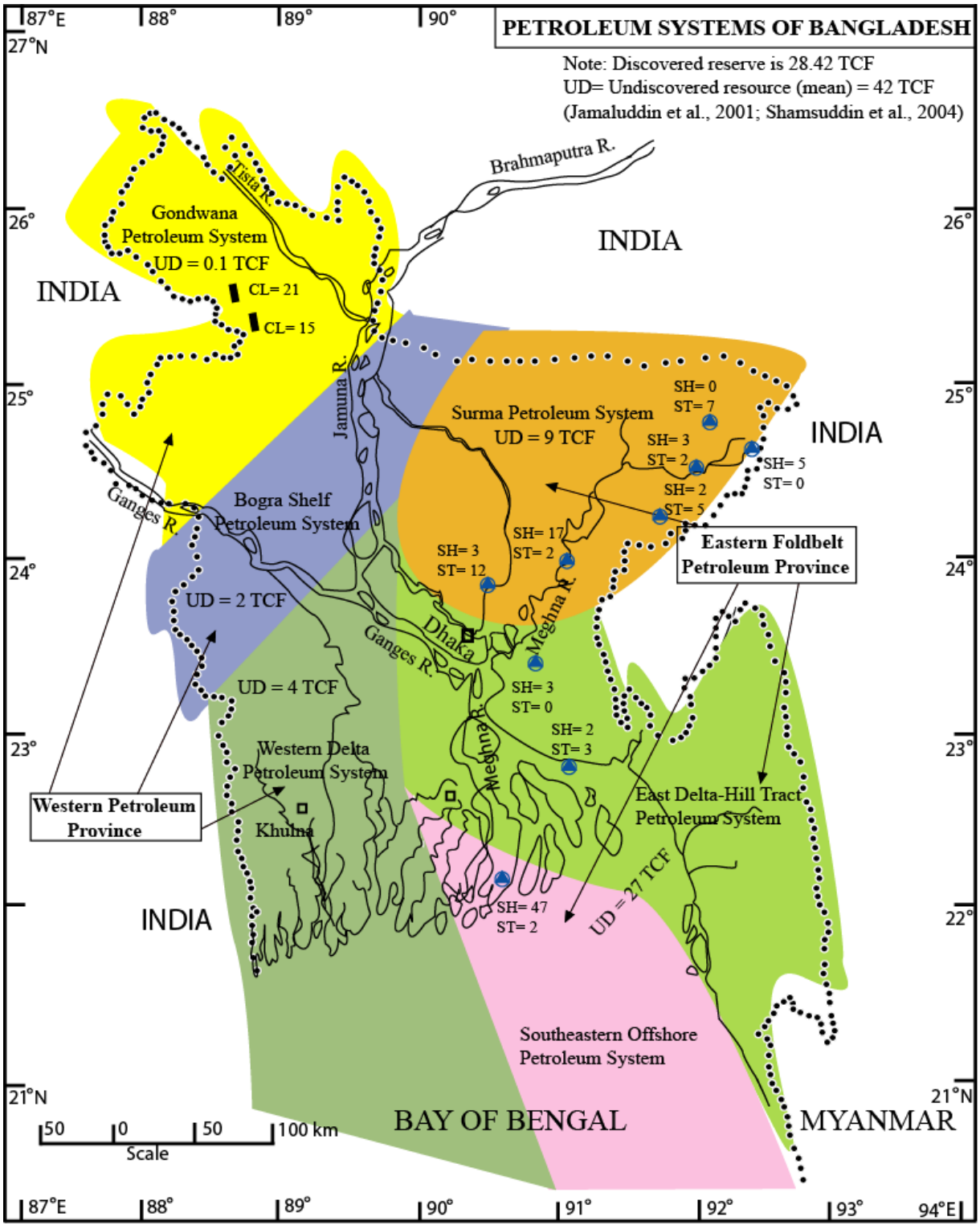

Fig.2.9. The petroleum systems of the Bengal Basin, Bangladesh. The estimated hydrocarbon resource is added (modified after Jamaluddin et al., 2001; Shamsuddin et al., 2004). 82 shale (SH), 33 sandstone (ST) and 36 coaly (CL) sampling numbers are also shown.

2.4 Coal Resources in the Bengal Basin, Bangladesh

Approximately three billion tons of Permian Gondwana coal resources (70 TCF gas equivalent) has been estimated in five coal basins discovered so far in Bangladesh. All of the recognized coal basins have been identified in the Platform unit of the Bengal Basin, northwest Bangladesh. The estimated coal resources include 1053 million tons (Mt) in Jamalganj, 390 Mt in Barapukuria, 572 Mt in Phulbari, 685 Mt in Khalaspir and 600 Mt in Dighipara Coal Basin (Farhaduzzaman et al., 2008). The identified coal is low ash, low sulfur and high volatile bituminous to sub-bituminous in rank (Imam, 2005). Together with power plant uses, it has the property to make coke which is an important fuel for steel industries. Starting from 2007, coal has been continuously extracted (1 Mt/a) from the Barapukuria Underground Coal Mine, the only coal mine in the country.

2.5 Hydrocarbons in the Bengal Basin, Bangladesh

The Bengal Basin (Bangladesh) comprises two major petroleum provinces: (a) The Eastern Foldbelt Petroleum Province and (b) The Western Petroleum Province (Fig.2.9). The Eastern Foldbelt Petroleum Province is, so far, the only known proved petroleum system in the basin. The natural gas and condensates currently produced in Bangladesh come from anticlinal structures in the Eastern Foldbelt Petroleum Province of the Bengal Basin (Jamaluddin et al., 2001). Here, Middle to Late Miocene reservoir sandstones are capped by Upper Marine shales in the upper part of the Surma Group. Source rock intervals occur in the Middle Oligocene Jenum shales and the Miocene Surma Group shales. Estimated gas reserve (GIIP P+P) in Bangladesh is 28.42 TCF with 42 TCF undiscovered (Jamaluddin et al., 2001; Shamsuddin et al., 2004). Petrobangla re-estimated the total recoverable oil reserve of 137 million barrels STOIIP or STOOIP (Hossain, 2012).

Crude oil production took place here from 1987 to 1997. Currently, out of 25 gas fields (including one minor oil field) so far discovered, only 20 are producing. The gas production started in 1959. Now the daily production of gas and condensate is approximately 2283 MMCFD (million cubic feet per day) and 7338 BBLD (barrels per day) respectively (04 April 2013, Petrobangla). The majority of gasfields in Bangladesh produce dry gas with a significant proportion of condensate (up to 18 barrels per million cubic feet of gas).

CHAPTER 3: MATERIALS AND METHODS

Assuming the nature of the working procedure, the materials and methods were divided into two main sections: (a) field work and sampling and (b) laboratory work.

3.1 Fieldwork and Sampling

After a through literature review, the project plan was finalized and accordingly, fieldwork was carried out in the Bengal Basin, Bangladesh. The rationale of the field work was to cover the entire Deep Basin unit and major coal fields of the Bengal Basin. Fifty six Boka Bil shale, 26 Bhuban shale, 33 sandstone, 22 coal, 10 carbargillite and four mudstone core samples (full core with dimensions of 50mm x 45mm) were collected (all together 151 core samples) from the core laboratories controlled by Bangladesh Oil Gas and Mineral Corporation (Petrobangla). However, some of the core laboratories (e.g., coal cores of Dighipara Basin) were controlled by the Geological Survey of Bangladesh (GSB). In addition for a purpose of comparative assessment, five bulk coal samples were also collected from a stockpile of the Barapukuria half-graben basin whereas coal is currently being extracted through underground mining method. Each core sampling location was considered as a single depth instead of 'from-to'.

Core samples were chosen from ten wells of respective nine gas fields. However, shale samples are chosen from eight wells of respective eight gas fields (Rashidpur, Patharia, Fenchuganj, Bakhrabad, Titas, Kamta, Begumganj and Shahbazpur). Similarly sandstones are from eight wells of respective seven gas fields (Kailas Tila, Rashidpur, Fenchuganj, Titas, Kamta, Begumganj and Shahbazpur). Five bore holes of two coal basins (DOB8, CSE7 and CSE9 at Barapukuria; GDH60 and GDH62 at Dighipara) were selected for coal, carbargillite and mudstone sampling. The depth of shale sampling ranged from 998 to

3572m, 2398-3620m for sandstones and 133-469m for coals/coaly samples. All of the core samples and bulk samples were air dried and stored in core boxes made with tin or plastic. Each core box contained one meter of core sample of shale, coal or sandstones. All of the core samples are cleaned properly after drilling. The collected core samples were again cleaned with wire brush and penknife for removing the surface contamination. Fig.3.1.1 displays typical samples of some of the shale (A, B and C), sandstone (A and D), coal (E and F) and mudstone (F) cores.

3.2 Laboratory Work

The core samples collected from the field were subjected to laboratory work using different modern standard analytical methods and techniques.

All 82 shale (Boka Bil 56 and Bhuban 26) and 36 coal and coaly samples were crushed into fine powder for analysis with a Source Rock Analyzer (SRA) in the Weatherford Laboratories, USA. After SRA screening, 32 shale samples and 16 coal and coaly samples were selected for Soxhlet extraction followed by liquid column chromatography for fractionations. Subsequently, 30 shale (Boka Bil 16 and Bhuban 14) and 16 coal and coaly samples were investigated using gas chromatography mass spectrometry (GCMS). Ten shale, six coal, three carbargillite and two mudstone samples were analyzed by pyrolysis gas chromatography (PyGC) for kerogen quality. Among these samples, 11 shale and 15 coal samples were chosen for Rock-Eval pyrolysis for comparing with the results of SRA. Forty shale (Boka Bil 20 and Bhuban 20) samples were used in parallel for elemental analysis. Eleven coal samples of the Dighipara Basin were analyzed by Atomic Absorption Spectrometry (AAS) for elemental concentrations. 48 shale (Boka Bil 29 and Bhuban 19) and 36 coal and coaly samples were examined microscopically for maceral analysis.

Every coal samples were used for proximate analysis. All 33 sandstone samples were studied using petrographic microscope. Ten representative sandstone samples were analyzed with scanning electron microscope and XRD.

Fig.3.1.1. (A) Shale and sandstone core samples stored in core-box of BAPEX; (B) and (C) Shale core samples; (D) Sandstone core samples; (E) Coal core samples of the Dighipara Basin; (F) Coal core samples with organic-rich mudstone (top left at F) sample of the Barapukuria Basin.

The elemental analysis (EA), pyrolysis gas chromatography (PyGC), gas chromatography (GC), gas chromatography mass spectrometry (GCMS), atomic absorption spectrometry (AAS), thermogravimetry-differential thermal analysis (TG-DTA), XRD and microscopic studies were performed in different relevant laboratories at the University of Malaya, Malaysia.

3.2.1 SRA and RE

The Weatherford Laboratories Instruments Source Rock Analyzer^{TM} (SRA) is designed to help identify and characterize source rock and reservoir rock by heating small amount (50-100mg powder) of geologic samples (i.e., outcrops, cuttings, conventional cores and sidewall cores) to a programmed temperature in an inert atmosphere. Like Rock-Eval (RE) pyrolysis, SRA also determines the quantity, quality and thermal maturity of organic matter in sediments. Hence, the pyrolysis oven temperature is 750 ºC (850 ºC maximum) whereby the ramp rate is 25 ºC/minute (range 0.1 to 50 ºC/minute). The composition of the column is special tungsten alloy. The gas helium (GC zero grade), hydrogen (GC zero grade) or air (GC zero grade) are used for the different required purposes during the analysis. Nitrogen or dry air is used for cleaning and cooling. It has a 100 position autosampler capacity which makes the procedure fast. The SRA quantitatively determines the amount of free hydrocarbons (S1) and the amount of hydrocarbons generated through thermal cracking of nonvolatile organic matter (S2) using a Flame Ionization Detector (FID). The amount of CO_2 produced during pyrolysis of kerogen (S3) is determined using an IR (infrared) detector. The SRA also determines the temperature at which the maximum release of hydrocarbons from cracking of kerogen occurs during pyrolysis (T_{max}) and Total Organic Carbon (TOC). Furthermore, it measures the hydrogen index (HI) and oxygen index (OI)

with good accuracy. A Weatherford SRA installed at the Geology Department, University of Malaya, is shown in Fig.3.2.1.

Fig.3.2.1. A Weatherford Source Rock Analyzer (SRA:TPH/TOC) installed at the petroleum geochemistry laboratory of the Geology Department, University of Malaya.

Rock-Eval 6 (RE-6) pyrolysis method was performed in the laboratory of Geotechnical Services Pty Ltd, Australia. Rock-Eval pyrolysis has been widely used in the industry as a standard method in petroleum exploration (Espitalié et al., 1977 and 1984; Larter and Douglas, 1980; Tissot and Welte, 1984; Peters, 1986). Like SRA, it is used to measure quantity, quality and thermal maturity of organic matter in sediments. This technique consists of the temperature programmed heating of a small amount of rock (100mg powder) in an inert atmosphere (Helium or Nitrogen) so as to determine the quantity of free hydrocarbons present in the sample (S1) and the amount of hydrocarbons (S2) and carbon

dioxides (S3) produced during the thermal cracking of the insoluble organic matter (kerogen) in the rock. Nonetheless, Total Organic Carbon (TOC) content of the rock is determined by oxidation under air, in a second oven, of the residual organic carbon after pyrolysis (S4). In Rock-Eval 6, programmed heating of both the pyrolysis and the oxidation ovens is conducted from 100°C (instead of 180°C in the previous versions) up to 850°C (instead of 600°C in the previous versions). By increasing the maximum pyrolysis temperature in Rock-Eval 6, the measure of the Hydrogen Index (HI) and oxygen index (OI) are more accurate and the range of validity of T_{max} is extended to higher values.

Fig.3.2.2. A Perkin Elmer 2400 elemental analyzer (CHNS/O) operated at the Chemistry Department of the University of Malaya.

3.2.2 Elemental Analysis (EA)

The powder samples are treated with 1M HCL in order to remove the inorganic carbonate. The samples are then dried (Sia and Wan Hasiah, 2011). A small amount (1.5-2 mg) of dried sample is used for elemental analysis with a Perkin Elmer 2400 Elemental Analyzer (CHNS/O) (Fig.2.2.2). The procedure is fully automated and includes a 60 position autosampler. In addition, it includes an intuitive, easy-to-use, EA Data Manager Software. The EA Data Manager software adds a powerful capability that assists in streamlining the data collection and analyses. The CHNS analysis is accomplished by combustion at 925 ºC, reduction at 640 ºC, detector oven at 82.6 ºC, pressure 15 mmHg and a detector for 4000 counts. The sample is burned in an excess of high purity oxygen and various traps collected the combustion products namely carbon to carbon dioxide, hydrogen to water, sulfur to sulfur dioxide and nitrogen to nitric oxide. The masses of these combustion products are used to calculate the composition of the unknown samples. Helium is used as purge gas.

3.2.3 Bitumen (EOM) extraction

Extractable organic matter (EOM) or bitumen extraction is performed on approximately 15g of the powder samples using Soxhlet's apparatus with an azeotropic mixture of dichloromethane (DCM) and methanol (CH_3OH) (93:7) for 72 hours (Fig.3.2.3). Together with solvents (DCM and CH_3OH), the EOM is evaporated using a water-bath evaporator until the majority of the solvent evaporates. After evaporation from water-bath, the EOM (with some remaining solvent) is transferred to a measuring vial or in 10ml measuring cylinder. This vial (with EOM) is blowing with nitrogen gas until the rest little amount of solvent evaporates. Once all the solvent evaporates, then the EOM is measured.

3.2.4 Liquid column chromatography

The extracts (EOM) are separated by liquid column chromatography into aliphatic, aromatic and polar (NSO) fractions using the solvent petroleum ether, dichloromethane (DCM) and methanol (CH_3OH) respectively (Harwood and Moody, 1989) (Fig.3.2.4).

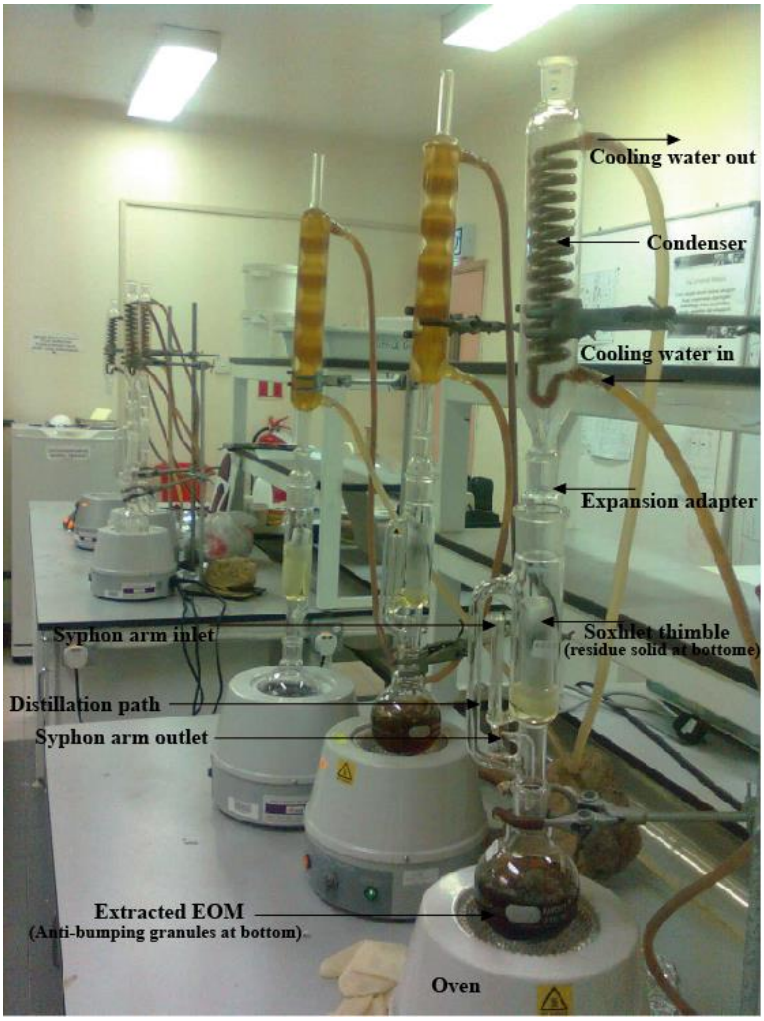

Fig.3.2.3. Bitumen (EOM) extraction in progress using Soxhlet's apparatus; the sample is placed in a thimble.

However, at the start of this fractionation, the slurry is prepared by mixing silica gel and petroleum ether (petroleum benzine). A small volume of cotton wool is inserted at the bottom of the long column before pouring the EOM solution in the column. A small amount of alumina (2-3 cm) is also poured above the slurry inside the column. After this,

using 100ml petroleum benzine, the EOM solution is allowed to fractionate only the aliphatic fraction that is collected and weighed after blowing. Similar procedure is followed for separating aromatic and NSO fractions using the solvents DCM and CH_3OH, respectively

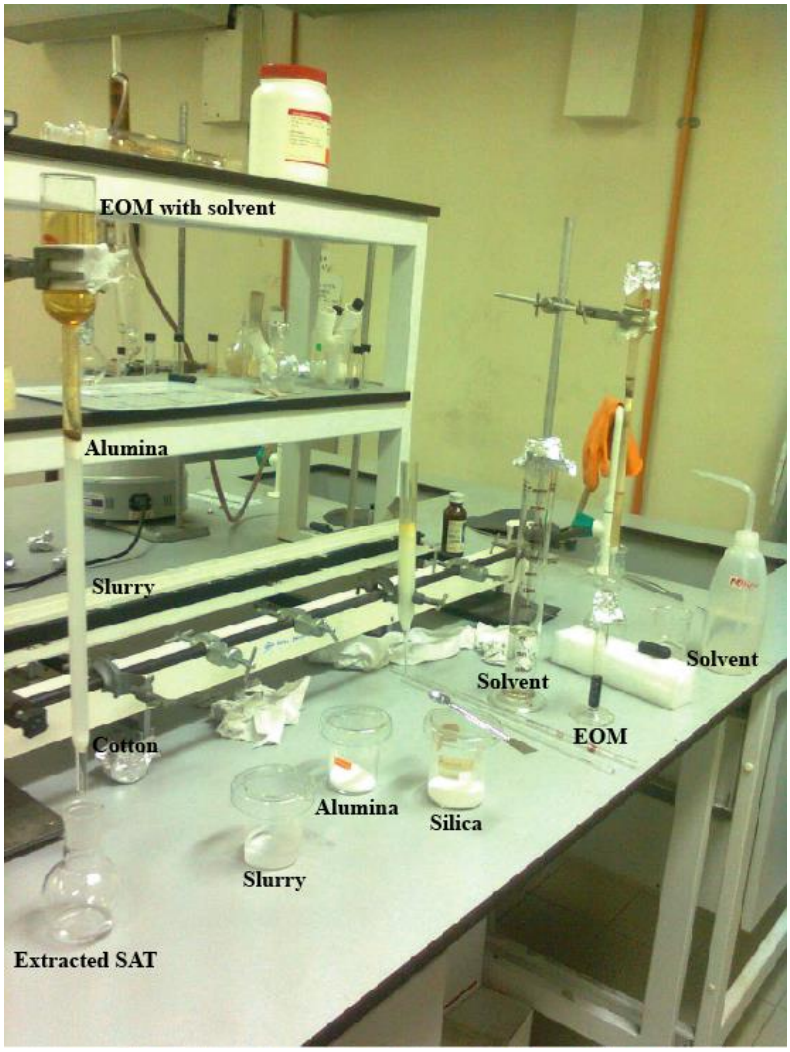

Fig.3.2.4. Long column chromatography in progress for separating aliphatic (SAT) fraction. Petroleum ether solvent, silica gel, alumina and slurry are also shown at table.

3.2.5 Pyrolysis gas chromatography (PyGC)

Pyrolysis is simply the breaking apart of large and complex molecules into smaller and more analytically useful fragments by the application of heat (Harwood and Moody, 1989). When heat energy applied to the molecule is greater than the energy of specific bonds,

those bonds will dissociate in a predictable and reproducible way. The smaller molecules generated by this bond-breaking are identified by the analytical tool selected with the help of understanding of the original macromolecule.

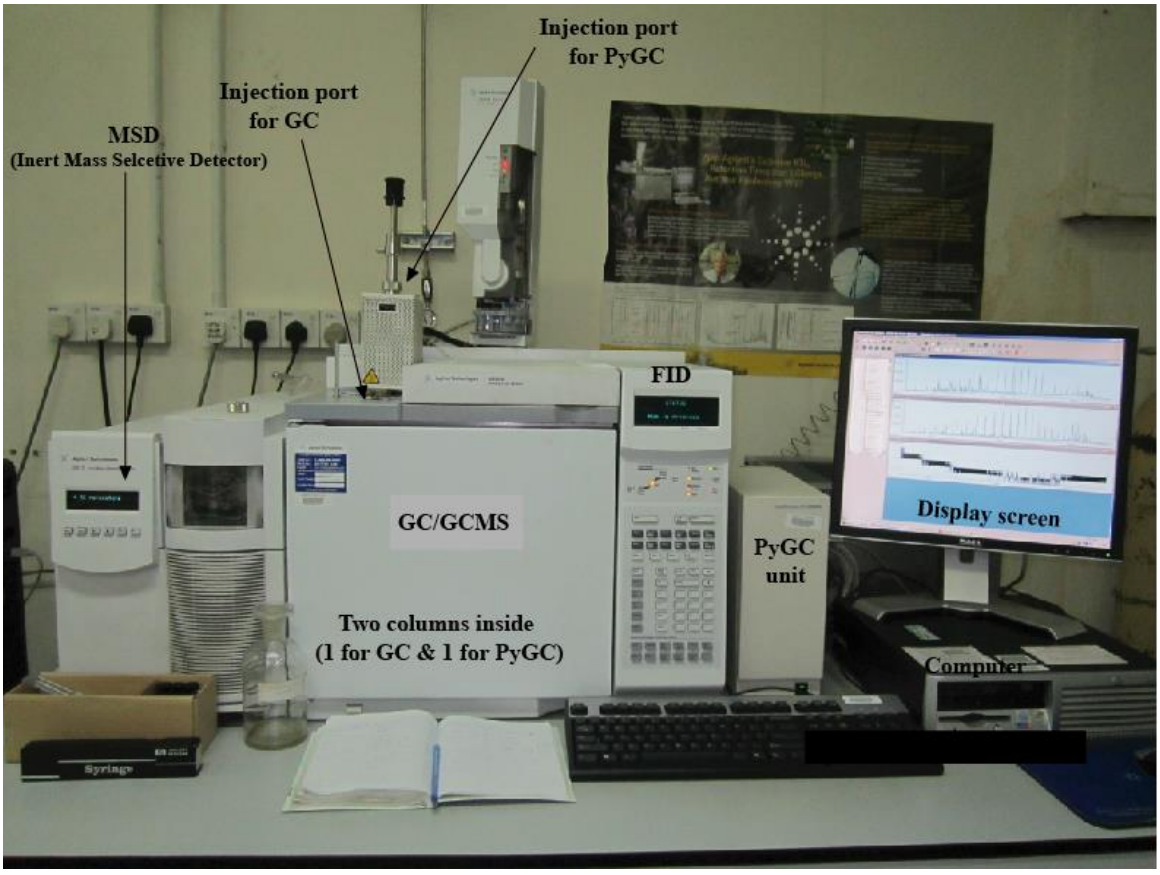

Fig.3.2.5. An Agilent 6890N Series gas chromatograph (GC) and gas chromatography mass spectrometer (GCMS). The Frontier Laboratories PY-2020iD model pyrolysis gas chromatograph (PyGC) unit shown here is also installed at the Geology Department, University of Malaya as an attachment.

In pyrolysis-gas chromatography (PyGC), the fragments generated by pyrolysis are passed through the GC for separation and identification. Frequently the major peaks in the resulting chromatogram (pyrogram) are easily identifiable and give direct structural information about the material being pyrolyzed. The pyrograms are more complex and serve as 'fingerprints' which may be used to distinguish related materials for identification or for quality control.

The number of peaks, the resolution by capillary GC and the relative intensities of the peaks permit discrimination among many similar formulations, making pyrolysis-GC a powerful tool in the identification of unknown samples.

Frontier Laboratories double-shot pyrolyzer PY-2020iD was used in this study. A 4-8mg (4mg coal; 6mg carbargillite; 8mg shale/mudstone) solid whole rock sample (crushed powder) is used for the present analysis. The powder sample is inserted manually into the sample insertion port. An ultra-alloy capillary column specified with 30m length, 250µm nominal diameter and 0.25 µm nominal film thickness is used. A flow of helium flushes the pyrolyzates into the column where components are separated. The initial flow is 1.2 µL/min, with an initial pressure and average velocity of 13.3 psi and 29 cm/sec, respectively. The initial temperature is 54 ºC, ramping to the pyrolysis temperature of 600 ºC at a rate of 20 ºC/min. The total run time for analyzing a single sample is 95 minutes. The detection method used is mass spectrometry and it is attached with GC/GCMS as described below (Fig.3.2.5).

3.2.6 Gas chromatography and gas chromatography mass spectrometry

Gas chromatography mass spectrometry (GCMS) is a method that combines the features of gas-liquid chromatography and mass spectrometry to identify different substances within a test sample. The aliphatic hydrocarbon fractions were analyzed using an Agilent 6890N Series gas chromatography (GC) and gas chromatography mass spectrometry (GCMS). A manual syringe is used to inject small amount (1.0 µL) of the dissolved sample. The injected sample is vaporized and mixed with the He carrier gas. The vaporized mixture of sample and carrier gas is then moved through the capillary column.

The column is HP-5MS 5% phenyl methyl siloxane specified with 30m length, 250 µm nominal diameter and 0.25 µm nominal film thickness. The initial flow is 1.9 µL/min while nominal initial pressure and average velocity are 14.99 psi and 49 cm/sec, respectively. Hydrogen, air and nitrogen gases are used for combustion for FID. A FID gas chromatograph with HP-5MS column, temperature programmed from 40 to 300 °C at a rate of 4 °C/min and then held for 30 min at 300 °C is used for GC analysis. GCMS analysis is performed using an Agilent V 5975B MSD mass spectrometer with a gas chromatograph attached directly to the ion source (70 eV EI mode). The total run time for GC/GCMS is 95 minutes. Fig.3.2.5 displays a GCMS together with Frontier Laboratories PY-2020iD model pyrolysis gas chromatograph (PyGC) unit installed at UM Geology Department.

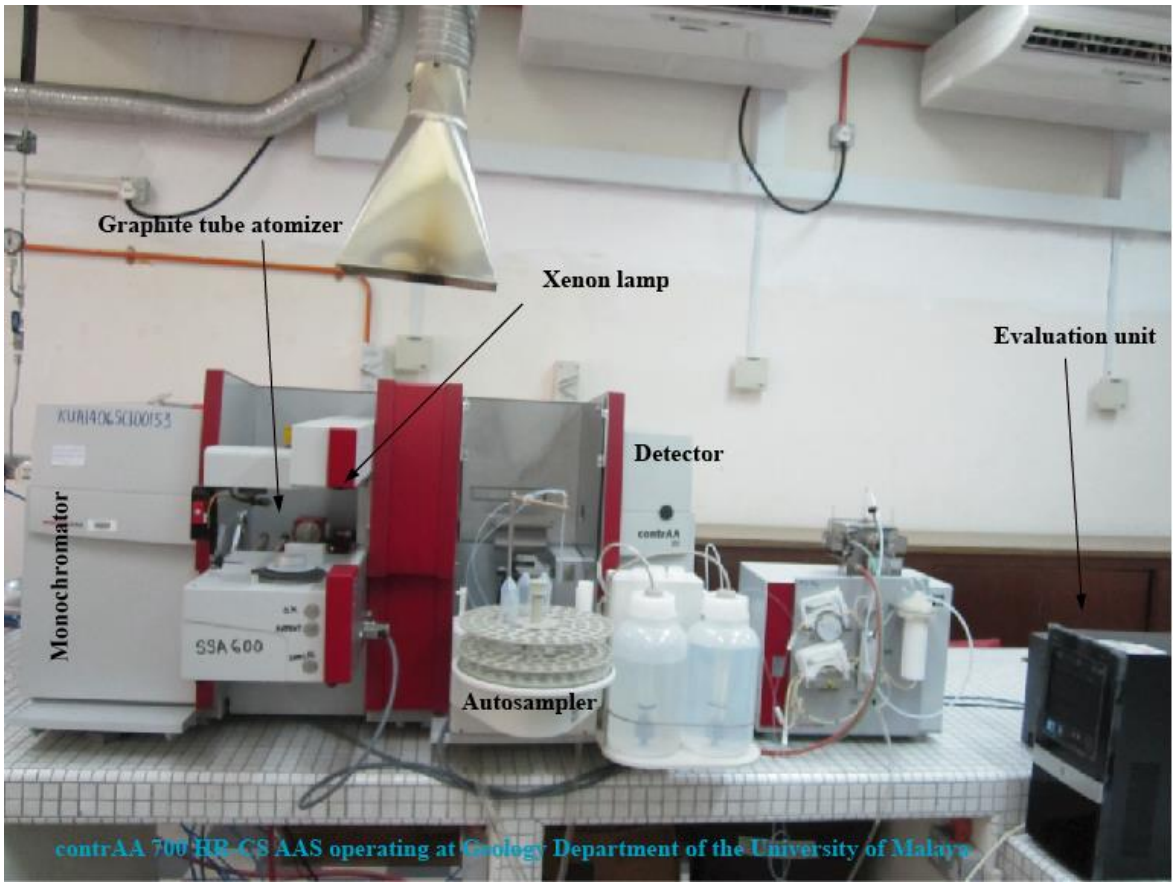

Fig.3.2.6. The analytikjena contrAA®700 High Resolution Continuum Source Atomic Absorption Spectrometer (HR-CS AAS) installation at the Department of Geology of the University of Malaya.

3.2.7 Atomic absorption spectrometry (AAS)

Atomic absorption spectroscopy (AAS) is a spectroanalytical procedure for the quantitative determination of chemical elements employing the absorption of optical radiation (light) by free atoms in the gaseous state (Welz and Sperling, 2007). In analytical chemistry, the technique is used for determining the concentration of a particular element (the analyte) in a sample to be analyzed. In principle, it requires standards with known analyte content to establish the relation between the measured absorbance and the analyte concentration and relies therefore on the Beer-Lambert Law. In short, the electrons of the atoms in the atomizer can be promoted to higher orbitals (excited state) for a short period of time (nanoseconds) by absorbing a defined quantity of energy (radiation of a given wavelength). This amount of energy (i.e., wavelength) is specific to a particular electron transition in a particular element. In general, each wavelength corresponds to only one element and the width of an absorption line is only of the order of a few picometers (pm) which gives the technique its elemental selectivity. The radiation flux without a sample and with a sample in the atomizer is measured using a detector and the ratio between the two values (the absorbance) is converted to analyte concentration or mass using the Beer-Lambert Law.

The currently investigated samples are crushed into fine powder and then digested for AAS analysis. A small amount of sample (25mg) is dissolved with a mixture of hydrofluoric acid (2ml HF), nitric acid (4ml HNO_3) and hydrogen peroxide (2ml H_2O_2) using a Perkin Elmer Microwave Reaction System. The power is 1000W with ramp of 10min. It is held on 50 minutes and then cooled for 20 minutes. Boric acid (12ml H_3BO_3) is also added for completion with 1200w power. It is held on for 10 minutes and then cooled for 5 minutes. Nitric acid (6ml HNO_3) is used for cleaning the digested solution.

Hence the power is 800W and held on for 5 minutes. It is finally cooled for 20 minutes in order to use in AAS.

The analytikjena contrAA®700 High Resolution Continuum Source Atomic Absorption Spectrometer (HR-CS AAS) is used for the present analysis (Fig.3.2.6). Combined with an autosampler, the contrAA®700 works as a multi-element automatic setup for routine analytical jobs. An initial calibration is carried out on the elements under analysis by sequentially processing the related calibration standards at first and sequentially processing the actual samples in a second step. Hence, after each sample measurement, the results are available for all elements that are subject to analysis. The HR-CS AAS device consists of five basic modules such as light source, atomizer, monochromator, detector and evaluation unit (PC). A xenon short-arc lamp is used as the light source. It ensures the high radiation density and continuous emission throughout the entire spectral range (190-900 nm). The graphite tube atomizer and the burner and nebulizer system (BZS) are firmly installed in the sample compartment of the contrAAR®700. The selectivity of the analysis is realized by a high resolution double-monochromator (F=380mm) based on a prism and an Echelle grating monochromator. A low-noise and UV-sensitive semiconductor detector is used (CCD line detector). ASpect CS 1.5 software is used for data analysis installed with the evaluation module. It supports the unique features of HR-CS AAS such as simultaneous background correction by acquiring spectral information in the vicinity of the analysis line, fast element/line change and the fast sequential multi-element measurement.

3.2.8 Polished block preparation for shale and coal samples for microscopic study

ICCP (1963) is followed for preparing the polished blocks. Approximately 20g hard coal (or shale) is crushed into fine grains (2-3 mm diameter) using a mortar.

The crushed grains are then taken onto the bottom plate of a plastic mold and upper plate is placed surrounding the coal grains onto the bottom plate of the mold. The resin mixed with 2% - 3% hardener is poured onto the coal (or shale) grains in the mold as soon as possible. The mold remains at room temperature for 24 hours so that the mold (coal or shale block) becomes ready for grinding and polishing. After 24 hours, the coal (or shale) block is removed from the mold. This block is then ground followed by polishing and shining. The coal (or shale) block is grinded using a diamond grinder in three stages: firstly, with coarse grains of carborundum so that the shale/coal surface becomes visible; secondly, with medium carborundum grains; and thirdly with fine carborundum grains. Finally, the block is smoothed with the finest powder used on a glass-plate. Water is slowly poured onto the block continuously during grinding/smoothing.

After grinding, the coal (or shale) block is polished manually sequentially using the 1 μm carborundum plate (with 1 μm powder), 0.3 μm carborundum plate (with 0.3 μm powder) and 0.05 μm carborandum plate (with 0.05 μm powder). Water is used with the powder when polishing. Finally, using the spongy plate with colloidal silica suspension, the coal/shale block is smoothed and shined for microscopic study. Nevertheless, the polishing is also carried out mechanically using the Buehler Beta Grinder-Polisher automatic polishing machine (Fig.3.2.7A). Firstly, three carborandum plates of different sizes (1 μm, 0.3 μm and 0.05 μm, progressively) are used onto the right wheel of the machine. In case of shale blocks, 2-propynol (iso-propynol) is used whereby water is used on coal blocks while polishing. Secondly, three similar carborundum plates of different sizes (1 μm, 0.3 μm and 0.05 μm, progressively) are used onto the left wheel of the machine. Thereafter, the 1 μm, 0.3 μm and 0.05 μm (respectively) suspension/gel is used on the corresponding plate while polishing. The force per unit area selected here is below 4 lbs in the machine.

The time is fixed at 20 seconds for each step. The coal/shale block is balanced and pressured using the legs of the machine. Some typical polished blocks are shown in Fig.3.2.7B.

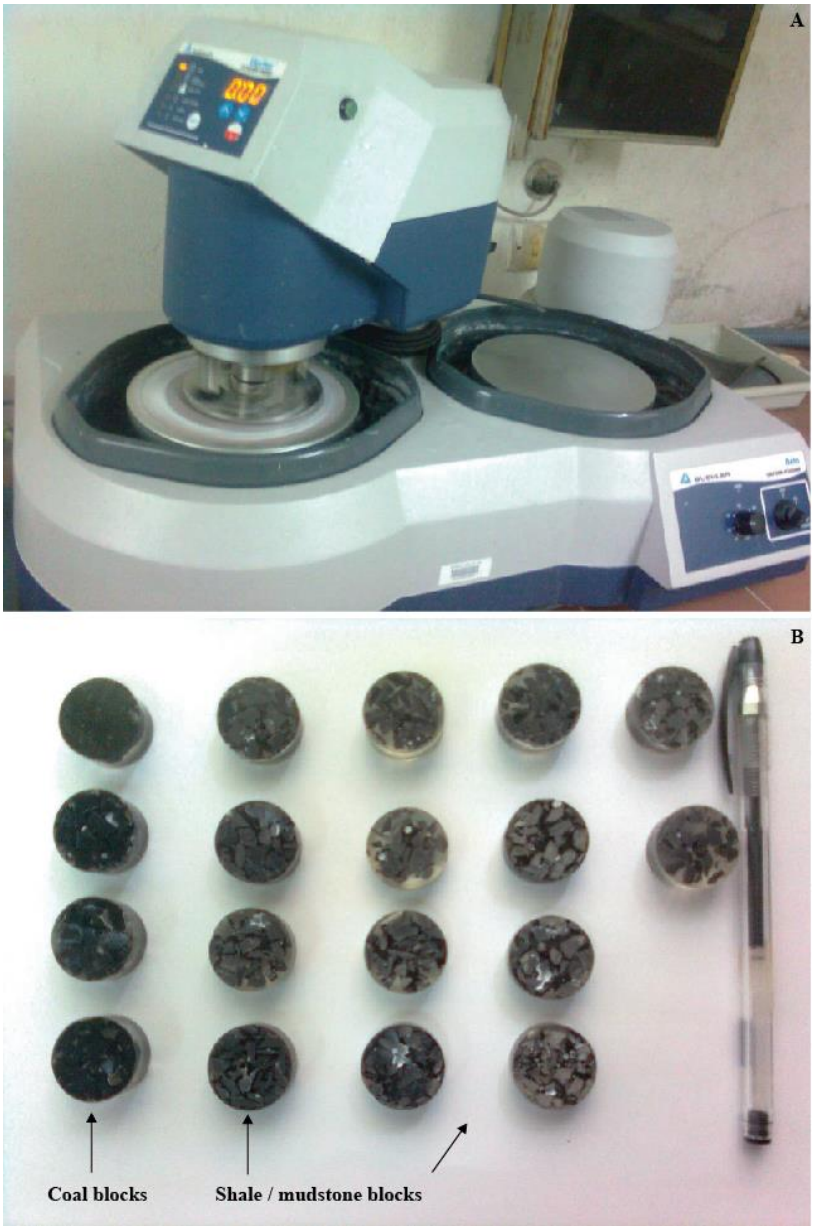

Fig.3.2.7. Polishing in progress with Buehler Beta Grinder-Polisher automatic polishing machine (A) and the polished coal/shale blocks (B).

3.2.9 Petrographic study of shale, coal and other coaly samples

The procedures, descriptions and analysis published by ICCP (1963 and its supplements 1985, 1986 and 1993) and ICCP System 1994 (1998 and 2001) are followed for

petrographic study of shale, coal and other organic-rich sediments. Petrographic examination is carried out using polished blocks (preparation details in subsection 3.2.8) under oil immersion in plane polarised reflected light.

Fig.3.2.8. A LEICA DM6000M microscope and LEICA CTR6000 photometry system equipped with fluorescence illuminators used at the Geology Department of the University of Malaya.

The LEICA DM6000M microscope and LEICA CTR6000 photometry system equipped with fluorescence illuminators was used for the present study (Fig.3.2.8). The filter system consists of BP 340-380 excitation filters, a RKP 400 dichromatic mirror and a LP425 suppression filter. Maceral compositions, based on a 1000 point count, are determined under both normal reflected 'white' light and ultraviolet light. Random vitrinite reflectance (%VR_r or %R_o) measurements in oil immersion are carried out in reflected 'white' light using the windows-based DISKUS Fossil software together with a Basler camera.

The DISCUS Macerals software attached with Basler camera is also used for point counting of different macerals and microlithotypes. Leica software along with Leica DFC camera is used for random analysis of macerals and for capturing photomicrographs. Alternatively JENOPTIK ProGres® C3 is also chosen for capturing the photomicrographs. At least 20, 500 and 1000 measurements per sample for shale/mudstone, carbargillite and coal samples respectively are taken while examination. The conventions of the 5% rule and the minimum band width (50×50 μm) are maintained during the microlithotype identification while the distances between points and between the lines of points are 0.5mm.

3.2.10 Themrogravimetry-differential thermal analysis (TG-DTA)

Thermogravimetric analysis or thermal gravimetric analysis (TGA) is a type of testing performed on samples that determines changes in weight in relation to a temperature program in a controlled atmosphere. A PerkinElmer Diamond TG-DTA is used for the proximate analysis (moisture, volatiles, fixed carbon and ash in percentages as stated by Earnest, 1988) of the studied coal samples. The simultaneous TG-DTA measures both heat flow and weight changes in a material as a function of temperature or time in a controlled atmosphere. The PerkinElmer Diamond TG-DTA analyzer consists of a high-precision balance with a platinum pan loaded with the sample. This pan resides in a furnace and is heated up to 1000 ºC with different required rates 10 and 20 ºC/minute or cooled during the experiment. The atmosphere is purged with inert gas helium to prevent oxidation or other undesired reactions. The gas (N, O, air) is used for the analysis. A computer is used to control the instrument. TGA is the process that utilizes heat and stoichiometry ratios to determine the percent by mass of a solute. After the data are obtained, curve smoothing and other operations are done to find the exact points of inflection. Fig.3.2.9A shows the

PerkinElmer Diamond TG-DTA analyzer installed at the Geology Department of the University of Malaya. Fig.3.2.9B represents a typical TGA profile whereby the moisture content (%), volatile matter (%) and fixed carbon (%) of the analyzed coal sample are represented by the first, second and third weight loss steps respectively. The remaining weight at 950 ºC in oxygen corresponds to the ash content (%).

The coal samples were also analyzed from the laboratory of Minerals and Geoscience Department Malaysia (ASTM D2013-07; denoted by JMG) for comparative assessments. It increases the data accuracy with high confidence.

3.2.11 Thin section preparation for sandstone samples

The procedure specified by Adams et al. (1988) is followed for thin section preparation. A slab of rock (1-2 mm thick) from the sandstone core is cut using a diamond saw. This slab is thoroughly cleaned and vacuum impregnated with low viscosity epoxy to fill the pores and mechanically support the specimen material. Using 100 micron particle size (120 grade) carborandum abrasive, one surface of the rock slab is ground flat on a piece of glass measuring about 30cm x 30cm and up to 1 cm in thickness. Only a small amount of carborandum (half a teaspoonful), just moistened with water, is used for grinding. After grinding with a rotary movement for about half a minute, the glass plate is washed and cleaned and fresh slurry of carborundum is placed on the plate.

When the surface of the rock sample becomes flat, it is thoroughly cleaned with a jet of water before grinding with the finer grade of carborundum. The second stage of grinding is carried out using 60 micron size (220 grade) carborundum and two periods of grinding, for about a minute each, with a fresh quantity of carborundum as required. After washing the

sample, a final grinding of one surface is made for about a minute with 12 micron size (3F grade) carborundum. Again after cleaning, the rock sample is polished using cerium oxide (0.8 micron size).

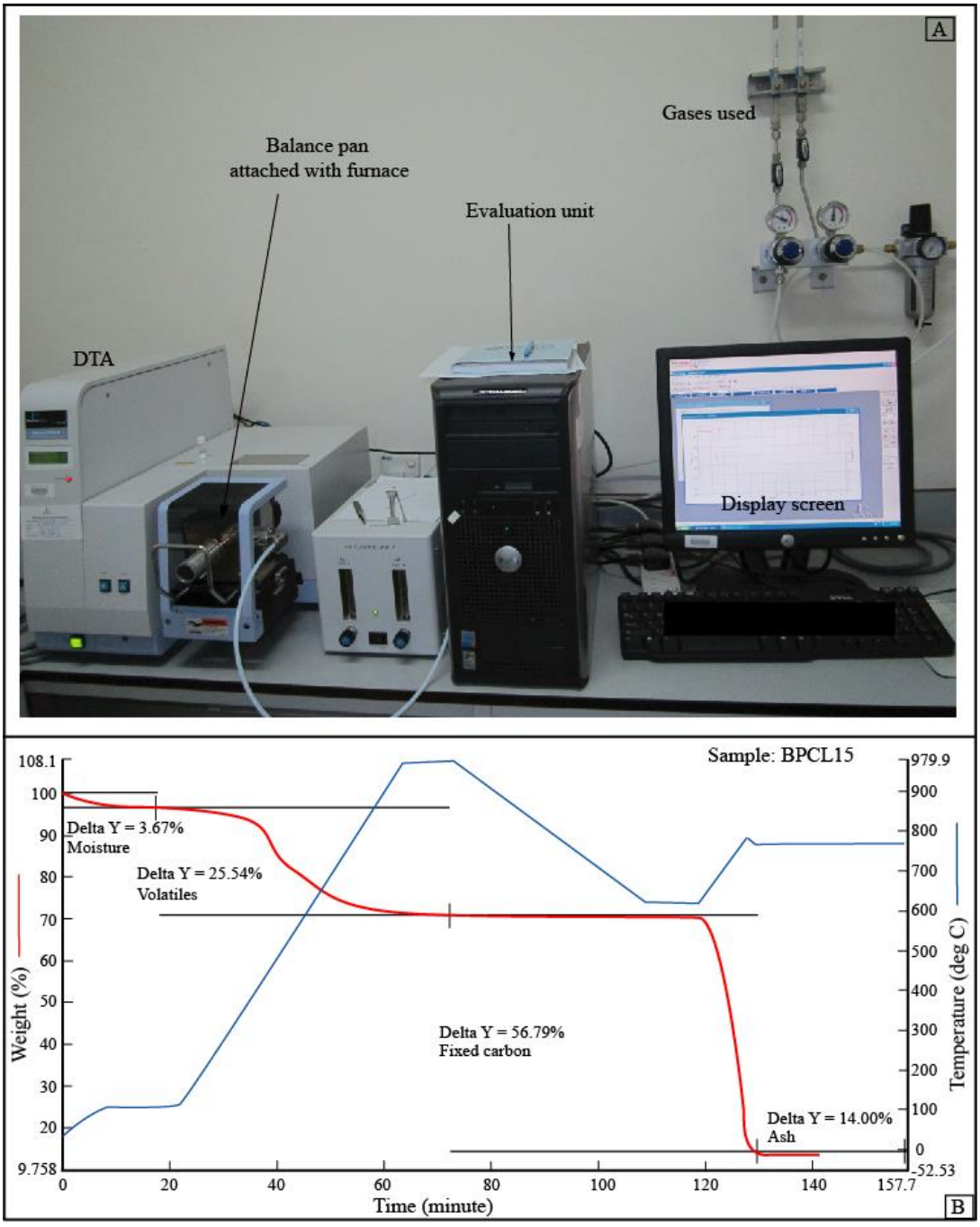

Fig.3.2.9. A PerkinElmer Diamond TG-DTA installed at the Geology Department of the University of Malaya (A); A typical TGA profile whereby the moisture content, volatile matter and fixed carbon of the analyzed coal sample are represented by the first, second and third weight loss steps respectively; The remaining weight at 950 ºC in oxygen corresponds to the ash content in % (B).

Fig.3.2.10. Thin section preparation in progress operated at the Geology Department, University of Malaya.

The smooth surface of the rock sample is glued to a microscope slide using epoxy resin (mixture of two fluids) with refractive index higher than 1.54. In case of few samples, the cover glass is attached with the help of the same epoxy resin. Moreover, in the process of fixing the rock to the microscope slide, care is taken to ensure that no air or gas bubbles are trapped between the cover glass and the rock. A thin section preparation in progress is displayed in Fig.3.2.10.

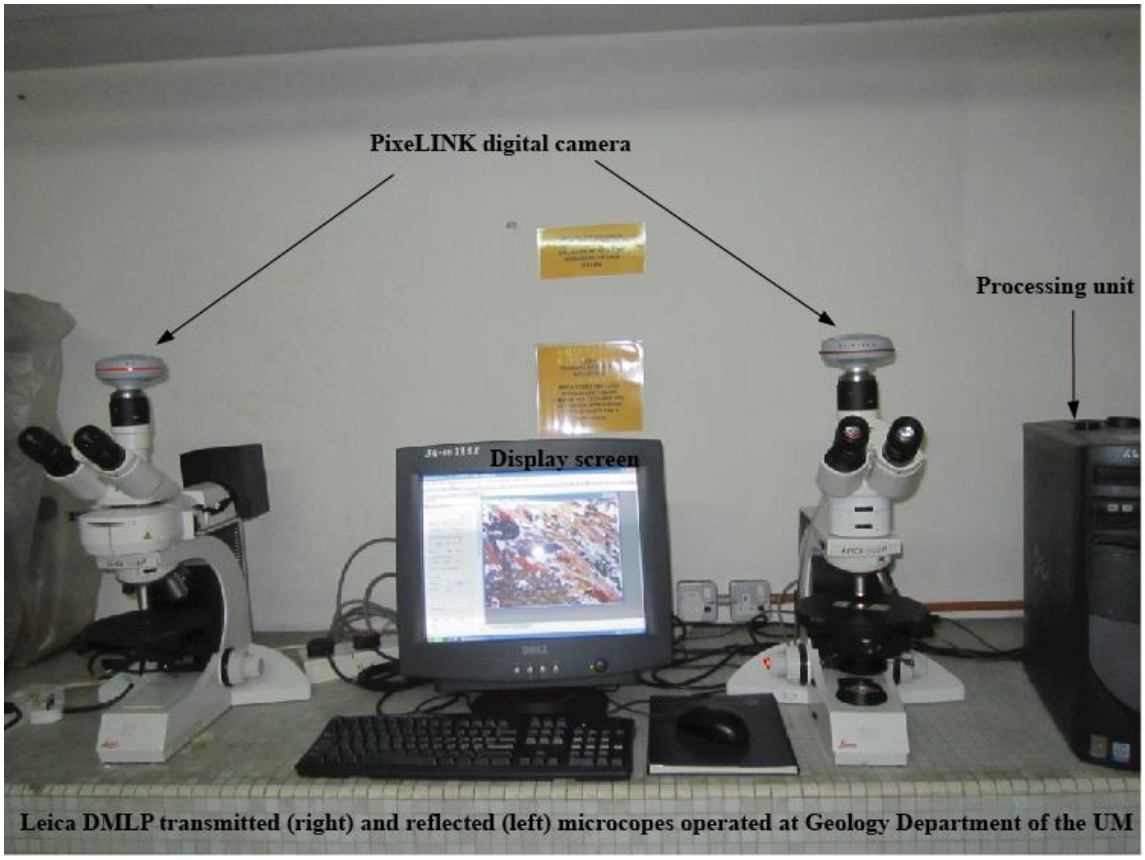

Fig.3.2.11. A Leica DMLP optical microscopes installed at the Geology Department of the University of Malaya; The PixeLINK digital cameras are attached for capturing images.

3.2.12 Petrographic study of sandstone samples

Petrography is the study of rocks and minerals using a microscope. In this study, thin sections were analyzed with a Leica DMLP microscope for polarization techniques in transmitted and incident light (please see 3.2.11 for thin section preparation). The PixeLINK digital camera attached with the Leica DMLP microscope is used for capturing the images of the samples studied. The SWIFT (Model F) is used for point counting while the modal composition is achieved based on 600-point modal analysis per thin section.

SEM: Some of the selected sandstone samples were analyzed with JEOL JSM-7600F field emission scanning electron microscope (FESEM) operated in the Physics Department of the University of Malaya (Fig.3.2.12). The secondary electron detector mode is used for

capturing the images for the current analyses. Some of the images were taken with a HITACHI 3000S scanning electron microscope (SEM) fitted with back scattered electron detector operated at the University of Tsukuba, Japan. It images a sample by scanning it with a beam of electron in a raster scan pattern. The electrons interact with the atoms that make up the sample producing signals that contain information about the sample's surface topography, composition and other properties such as electrical conductivity. High resolution examinations, up to 1,000,000 times magnifications with a resolution of up to 1.5 nanometers at 1.0 kV in GB mode, are carried out. The clay minerals, pore geometry, permeability, dissolution effect, cements, quartz overgrowth, texture and other related diagenetic imprints were investigated using the SEM.

3.2.13 XRD analysis

The clay minerals of the Tertiary sandstone and shale samples are studied using a PANalytical Empyrean XRD equipped with PIXcel^{3D} detection system located at the Geology Department, UM. The PANalytical's XRD software package (X'Pert HighScore) is used for identification, data collection and analysis of the clay minerals. Initially the samples are gently crushed into fine powder. The < 2 μm fractions are then separated by centrifugation and are subsequently placed into a test tube mixed with distilled water. The dispersing reagent ammonia solution is mixed with the sample in test tube in order to prevent flocculation. The test tube (with sample solution) was kept at room temperature for 24 hours so that the finer clay fractionation settles at the top of the suspension.

Fig.3.2.12. A JEOL JSM-7600F field emission scanning electron microscope (FESEM) operated at the Physics Department of the University of Malaya.

The clay fraction at the top is then transferred by pipetting onto a small glass slide to prepare the XRD mounts. These mounts are then analyzed after air-drying and vapor saturation with ethylene glycol at 80 °C for one hour. The samples were also heated in two steps, to 350 °C and to 550 °C, in order to observe the changes in the XRD responses for different clay minerals present in the sandstones studied.

Fig.3.2.13. A PANalytical X-ray Diffraction (XRD) machine working at the Geology Department of the University of Malaya.

3.3 Software Used

3.3.1 ProSim ternary diagram

ProSim ternary diagram (France) is used to easily and quickly trace series of points or lines resulting from experimental data or calculations. It is always tiresome to plot a ternary diagram (tri-plot or triangular diagram) by hand. For this reason, ProSim develops for us an easy to use but powerful application enabling to create these diagrams in a few mouse clicks. In this case, the data used are always normalized. In order to have a relevant position of a point in the diagram, the sum of its coordinates must be equal to 1 (one). However, if we paste data from another software, the data can be provided in term of percentage. The 'normalize data' button leads to convert the whole series of points.

3.3.2 Didger 4

The printed hard copies of the studied well logs are scanned first using high quality scanner and then is made TIFF images for each logs required. The Golden Software's Didger® 4 is used to calibrate and digitize geophysical well logs and export the information to an LAS file for the purpose of current analysis. In this case, well logs in TIFF format are converted to LAS files and subsequently studied by Excel software for petrophysical interpretation.

3.3.3 Excel software for petrophysical analysis

Archie (1942) introduced a classic empirical formula that is essentially related to formation conductivity, formation water conductivity and the formation resistivity factor (a function of porosity and cementation exponent) to the formation water saturation (S_w) and conversely hydrocarbon saturation (S_h). This formula applies satisfactorily to clean sands, whereas the presence of clay minerals (amount, type and distribution modes) has detrimental effect on the water saturation calculation. More than 30 water saturation models have been proposed to overcome the effect of shale for shaly sand reservoir evaluation (Fertl, 1987). In most cases, hydrocarbon bearing clastic reservoirs are not free of clay minerals. The significant effects of these minerals on geophysical log responses are well recognized. The presence of shale (i.e., clay minerals) in a reservoir can cause erroneous values for water saturation and porosity derived from logs (Asquith and Gibson, 1982). Hilchie (1978) notes that the most significant effect of shale in a formation is to reduce the resistivity contrast between oil or gas and water. The net result is that if considerable shale is present in a reservoir, it may be very difficult or perhaps impossible to determine if a zone is productive. He also suggests that shale content must be greater than 10 to 15% to significantly affect the log derived water saturation. The current analysis is based on the following procedures and formulas.

The hard copies of gamma (GR), resistivity (deep and shallow), sonic, SP, neutron, density, temperature and caliper logs were examined at the data center of the Bangladesh Petroleum Exploration and Production Company Ltd (BAPEX), Petrobangla. Initial study regarding data quality, depth adjustment, sand and shale zone identification and quick look observation have been carried out on paper based logs. The scanned images (TIFF format) of all these well logs of Rashidpur 4 were collected from BAPEX for the present study. These TIFF images have been converted to digital data (LAS format) using Didger®4 software. Subsequently, the digitized LAS files were transferred to Excel software and used for current analysis covering total gross thickness of 1463 m (depth 1310 – 2774 m) of the well Rashidpur 4.

Shale volume: Quantitative calculations of shale volume have been performed with the help of conventional techniques and formula introduced by Dresser Atlas (1979). Gamma ray logs are very good shale indicators and hence, calculation of the gamma ray index (I_{GR}) is the first step needed to determine the volume of shale (V_{sh}) from a gamma ray log.

$$I_{GR} = \frac{GR_{\log} - GR_{\min}}{GR_{\max} - GR_{\min}} \quad \text{----------} \quad (1)$$

The volume of shale can be calculated mathematically from the gamma ray index for Tertiary rocks (Dresser Atlas, 1979). This is a conventional formula that is used frequently to calculate shale volume in the petroleum industry and written as:

$$V_{sh} = 0.083\left[2^{(3.7\times I_{GR})} - 1.0\right] \quad \text{----------} \quad (2)$$

[Note: Please see the list of Symbols and Abbreviations for the descriptions of the symbols used here]

Porosity: After determining the volume of shale, it has been used to correct the porosity logs for shale effect. The density logs are used for porosity determination.

Dresser Atlas (1979) used the following equation to calculate porosity from density log:

$$\phi_{Den} = \left(\frac{\rho_{ma} - \rho_b}{\rho_{ma} - \rho_f} \right) - V_{sh} \left(\frac{\rho_{ma} - \rho_{sh}}{\rho_{ma} - \rho_f} \right) \text{----------} (3)$$

Subsequently, the combined neutron and density log is used for getting the corrected porosity values (Schlumberger 1975):

$$\phi_{Ncorr} = \phi_N - \left[\left(\frac{\phi_{Nclay}}{0.45} \right) \times 0.30 \times V_{sh} \right] \text{----------} (4)$$

$$\phi_{Dcorr} = \phi_D - \left[\left(\frac{\phi_{Nclay}}{0.45} \right) \times 0.13 \times V_{sh} \right] \text{----------} (5)$$

$$\phi_{N-D} = \sqrt{\frac{\phi_{Ncorr^2} + \phi_{Dcorr^2}}{2.0}} \text{----------} (6)$$

Thickness weighted average porosity (Bradley, 1987) is also measured as below:

$$\Phi_{av} = \frac{\sum_{i=1}^{n} \Phi_i h_i}{\sum_{i=1}^{n} h_i} \text{----------} (7)$$

Water saturation: After the log derived porosity correction for shale effect, the water saturation was calculated using the neutron-density porosity (ϕ_{N-D}). Following are the three more commonly used shaly-sand formulas for calculating water saturation (S_w):

$$S_w = \left(\frac{0.4 \times R_w}{\phi^2}\right) \times \left[-\frac{V_{sh}}{R_{sh}} + \sqrt{\left(\frac{V_{sh}}{R_{sh}}\right)^2 + \frac{5\phi^2}{R_t \times R_w}}\right] \text{----------} (8)$$

$$S_w = \frac{1}{\phi} \times \left[\sqrt{\frac{R_w}{R_t} + \left(\frac{a \times V_{sh}}{2}\right)^2} - \frac{a \times V_{sh}}{2}\right] \text{----------} (9)$$

$$S_w = \frac{-\frac{V_{sh}}{R_{sh}} + \frac{\phi^2}{0.2 \times R_w \times (1.0 - V_{sh}) \times R_t}}{\frac{\phi^2}{0.4 \times R_w \times (1.0 - V_{sh})}} \text{----------} (10)$$

Equation (8), (9) and (10) were introduced by Simandoux (1963), Fertl (1975) and Schlumberger (1975), respectively. Thickness weighted average water saturation is calculated using the following formula given by Bradley (1987).

$$S_{wav} = \frac{\sum_{i=1}^{n} Sw_i \phi_i h_i}{\sum_{i=1}^{n} \phi_i h_i} \text{----------} (11)$$

Formation water resistivity: Formation water resistivity (R_w) of the hydrocarbon bearing zone has been calculated from the formula given by Bateman and Konen (1977).

$$R_w = 10^{\left\{\frac{SSP}{K} + \log R_{mf}\right\}} \text{----------} (12)$$

Where, SSP = Static spontaneous potential = – k×log (R_{mf} / R_w)

K= 60+ (0.133× Formation temperature)

$R_{mf} = R_{Temp} \times (Temp + 6.77)/(T_F + 6.77)$

R_{mf} or R_{Tf} = resistivity of mud filtrate at formation temperature

T_F =Formation temp = (Hole temp – Surface temp)× (Required depth / Total depth)

Permeability: Permeability (K) has been calculated from the following formula given by Coates and Dumanoir (1973):

$$K = \left(\frac{C \times \phi^{2w}}{w^4 \times (R_w / R_{tirr})} \right)^2 \text{----------} (13)$$

$$\text{Where, } W = \left[(3.75 - \phi) + \left\{ \frac{[\log\{R_w / R_{tirr}\} + 2.2]^2}{2} \right\} \right]^{\frac{1}{2}}$$

$$C = 23 + 465\rho_h - 188\rho_h^2$$

Permeability has also been calculated using Wyllie and Rose's (1950) formula:

$$K = (79 \times \phi^3 / S_{wirr})^2 (\text{dry gas}) \text{----------} (14)$$

Thickness weighted average permeability is measured as stated below (Bradely, 1987).

$$K_{av} = \frac{\sum_{i=1}^{n} k_i h_i}{\sum_{i=1}^{n} h_i} \text{ ---------- (15)}$$

Hydrocarbon moveability: Comparative analyses were carried out for the calculated water saturation, hydrocarbon saturation and permeability of the studied reservoir. The arguments in favour of suitable approach have also been put forward. Movability of hydrocarbon is

also brought to notice with the aid of water saturation ratio of uninvaded zone and flushed zone; the expression of the formula is as follows (Asquith and Gibbson, 1982):

$$\frac{S_w}{S_{xo}} = \left(\frac{R_{xo} / R_t}{R_{mf} / R_w} \right)^{1/2} \quad \text{----------} \quad (16)$$

Bulk volume of water: The bulk volume of water of the hydrocarbon bearing zones in the studied well has been calculated using Morris and Biggs (1967**)** formula:

$$BVW = S_w \times \phi \quad \text{----------} \quad (17)$$

3.3.4 EndNote, StyleWriter and Turnitin

EndNote X5 software is used for bibliography management. The English grammar is checked with StyleWriter 4. The originality of the write-up is evaluated using Turnitin which is an important tool for checking the plagiarism of the work. The related reports are attached in Appendices F1, F2 and F3.

CHAPTER 4: RESULTS AND DISCUSSION

4.1 Petroleum Source Rock- Shales

4.2 Petroleum Source Rock- Permian Coals

4.3 Petroleum Reservoir Rock- Sandstones

CHAPTER 4.1 PETROLEUM SOURCE ROCK- SHALES

With respect to petroleum geology, the Bhuban and Boka Bil Formations are the most important stratigraphic units of the Bengal Basin, Bangladesh. These formations contain all the petroleum resources discovered so far. They are composed mainly of alternating shales and sandstones. The shales have long been considered as source rocks and the sandstones as reservoirs. The present study reports on an investigation of potential source beds within these two formations. For the present study, 82 drill core samples were collected from eight gas fields of the basin. Kerogen facies and thermal maturity are studied using geochemical and petrographical techniques.

4.1.1 Source rock properties

The results gained from Source Rock Analyzer (SRA) are shown in Table 4.1.1. Rock-Eval pyrolysis (RE) results of some selected samples are also displayed in Table 4.1.2 for comparative assessment. There is a good agreement between the results obtained from SRA and those of RE, raising the confidence in the SRA results. Most samples are organic lean (<1%). TOC increases with depth (Appendix C1). The source rock potential of the analyzed shales is evaluated from the cross-plot of S2 (mg HC/g rock) versus TOC (wt.%) following the classification published by Peters and Cassa (1994) (Fig.4.1.1). HI values of Bhuban Formations and Boka Bil Formations vary from 55 to 231 and 55 to 162 mg HC/g TOC respectively. Poor to fair source poetical is estimated by the Bhuban Formation. The Boka Bil Formation shows mostly poor potential for hydrocarbon generation. Most of the Bhuban samples plot in the Type III range but a few containing mixtures of Type II show notable variations, inferring a mixture of kerogen types (III/II). The Boka Bil samples represent mostly Type III kerogen. (Fig.4.1.2). The recorded OI values of Bhuban and Boka Bil shales range from 60 to 228 and 62-228 mg CO_2/g TOC, respectively.

Table 4.1.1. Source Rock Analyzer (of Rock-Eval equivalent) parameters and vitrinite reflectane data of the analyzed shale samples (refer to Appendix B1).

Sample	Gas Filed	Well no.	Depth (m)	TOC	Tmax	S1	S2	S3	HI	OI	PI	%Ro
Boka Bil Fm												
RP4SH1	Rashidpur	4	1380	0.57	428	0.07	0.31	0.87	55	154	0.18	0.56
RP4SH2	Rashidpur	4	1385	0.55	430	0.06	0.33	0.89	60	162	0.15	0.57
PT5SH10	Patharia	5	1834	0.29	433	0.05	0.24	0.27	82	93	0.17	0.57
PT5SH11	Patharia	5	1835	0.30	435	0.05	0.23	0.28	77	94	0.18	0.59
PT5SH12	Patharia	5	1836	0.28	436	0.04	0.21	0.24	75	86	0.16	0.65
PT5SH13	Patharia	5	3104	0.32	437	0.12	0.28	0.22	88	69	0.30	0.69
PT5SH14	Patharia	5	3163	0.28	438	0.13	0.34	0.20	123	72	0.28	0.70
SB1SH1	Shahbazpur	1	997.5	0.26	420	0.04	0.16	0.42	62	162	0.20	na
SB1SH2	Shahbazpur	1	998.5	0.29	420	0.05	0.21	0.59	72	203	0.19	0.48
SB1SH3	Shahbazpur	1	1000.5	0.27	422	0.05	0.19	0.36	70	132	0.21	na
SB1SH4	Shahbazpur	1	1001.5	0.28	421	0.05	0.20	0.61	71	216	0.20	0.50
SB1SH5	Shahbazpur	1	1003.5	0.24	422	0.05	0.19	0.53	81	226	0.21	0.48
SB1SH6	Shahbazpur	1	1004.5	0.23	422	0.05	0.18	0.48	79	210	0.22	na
SB1SH7	Shahbazpur	1	1212.5	0.30	423	0.06	0.20	0.28	68	95	0.23	na
SB1SH9	Shahbazpur	1	1277	0.38	424	0.05	0.25	0.35	66	93	0.17	0.51
SB1SH10	Shahbazpur	1	1279.5	0.32	424	0.05	0.22	0.38	69	119	0.19	na
SB1SH11	Shahbazpur	1	1280.5	0.33	425	0.05	0.20	0.36	61	110	0.20	na
SB1SH12	Shahbazpur	1	1281.5	0.32	424	0.05	0.20	0.46	63	144	0.20	na
SB1SH13	Shahbazpur	1	1283.5	0.34	425	0.05	0.21	0.32	63	96	0.19	0.52
SB1SH13A	Shahbazpur	1	1284.5	0.29	425	0.05	0.21	0.36	74	126	0.19	na
SB1SH14	Shahbazpur	1	1285.5	0.36	425	0.07	0.21	0.68	58	187	0.25	na
SB1SH16	Shahbazpur	1	1570.9	0.19	426	0.05	0.19	0.44	98	228	0.21	na
SB1SH17	Shahbazpur	1	1571.4	0.19	426	0.06	0.21	0.39	111	205	0.22	0.53
SB1SH18	Shahbazpur	1	1572.4	0.30	427	0.05	0.22	0.40	73	132	0.19	na
SB1SH19	Shahbazpur	1	1574.4	0.21	427	0.05	0.20	0.38	95	180	0.20	na
SB1SH20	Shahbazpur	1	1575.4	0.28	428	0.06	0.22	0.42	78	149	0.21	na
SB1SH21	Shahbazpur	1	1576.4	0.26	428	0.05	0.21	0.49	81	188	0.19	na
SB1SH22	Shahbazpur	1	1577.4	0.25	429	0.06	0.23	0.44	92	177	0.21	na
SB1SH23	Shahbazpur	1	1578.4	0.19	429	0.04	0.16	0.13	84	68	0.20	0.54
SB1SH24	Shahbazpur	1	1597.4	0.30	430	0.06	0.24	0.46	80	153	0.20	0.54
SB1SH25	Shahbazpur	1	1769.8	0.17	430	0.07	0.24	0.38	140	222	0.23	na
SB1SH27	Shahbazpur	1	1771.8	0.19	429	0.07	0.23	0.42	122	223	0.23	na
SB1SH28	Shahbazpur	1	1773.8	0.24	430	0.06	0.23	0.33	97	139	0.21	na
SB1SH29	Shahbazpur	1	1774.3	0.23	430	0.06	0.22	0.33	94	142	0.21	0.54
SB1SH30	Shahbazpur	1	1775.3	0.23	431	0.05	0.21	0.31	92	135	0.19	na
SB1SH31	Shahbazpur	1	1776.8	0.20	430	0.05	0.22	0.33	110	165	0.19	na
SB1SH32	Shahbazpur	1	1777.3	0.17	431	0.04	0.17	0.37	99	216	0.19	0.55
SB1SH33	Shahbazpur	1	2012.5	0.27	430	0.08	0.36	0.41	132	150	0.18	0.55
SB1SH34	Shahbazpur	1	2014.5	0.15	432	0.04	0.16	0.27	106	179	0.20	na
SB1SH35	Shahbazpur	1	2015.5	0.22	432	0.04	0.17	0.25	79	116	0.19	0.55
SB1SH36	Shahbazpur	1	2016.5	0.22	431	0.05	0.19	0.27	85	121	0.21	na
SB1SH37	Shahbazpur	1	2091	0.28	432	0.05	0.22	0.21	79	75	0.19	na
SB1SH38	Shahbazpur	1	2091.5	0.18	431	0.04	0.18	0.22	99	122	0.18	na
SB1SH39	Shahbazpur	1	2092.5	0.14	433	0.04	0.17	0.26	119	182	0.19	0.56

(continued next page)

Table 4.1.1. (Continued).

Sample	Gas Filed	Well no.	Depth (m)	TOC	Tmax	S1	S2	S3	HI	OI	PI	%Ro
Boka Bil Fm												
SB1SH40	Shahbazpur	1	2093.94	0.26	434	0.04	0.19	0.29	72	110	0.17	0.56
SB1SH41	Shahbazpur	1	2094.5	0.31	434	0.04	0.21	0.19	69	62	0.16	na
SB1SH42	Shahbazpur	1	2095.5	0.18	435	0.04	0.19	0.24	107	135	0.17	0.57
SB1SH43	Shahbazpur	1	2096.5	0.25	435	0.04	0.18	0.22	72	88	0.18	na
SB1SH44	Shahbazpur	1	2097.5	0.20	435	0.03	0.17	0.24	87	122	0.15	0.57
SB1SH45	Shahbazpur	1	2293.5	0.23	436	0.04	0.17	0.41	75	180	0.19	0.58
SB1SH46	Shahbazpur	1	2294.5	0.22	438	0.03	0.17	0.39	79	181	0.15	na
SB1SH47	Shahbazpur	1	2296.5	0.15	438	0.06	0.18	0.18	120	120	0.25	0.64
SB1SH48	Shahbazpur	1	2316	0.28	440	0.06	0.24	0.50	85	177	0.20	0.65
BK9SH69	Bakhrabad	9	2301.2	0.18	430	0.05	0.20	0.20	109	109	0.20	0.56
BK9SH70	Bakhrabad	9	2318.6	0.19	432	0.06	0.31	0.39	162	204	0.16	0.58
BK9SH71	Bakhrabad	9	2329.6	0.34	437	0.07	0.40	0.45	118	132	0.15	0.65
Range			998-3163	0.14-0.57	420-440	0.03-0.13	0.16-0.40	0.13-1.29	55-162	62-228	0.15-0.30	0.48-0.70
Bhuban Fm												
KM1SH2	Kamta	1	3138	0.26	433	0.05	0.22	0.36	85	139	0.19	0.59
KM1SH3	Kamta	1	3139	0.27	433	0.06	0.26	0.39	96	143	0.19	0.60
KM1SH4	Kamta	1	3377	0.39	434	0.11	0.33	0.42	84	107	0.25	0.63
BG1SH5	Begumganj	1	3100	0.28	435	0.05	0.22	0.29	80	105	0.19	0.68
BG1SH6	Begumganj	1	3571.5	0.32	439	0.05	0.24	0.25	75	78	0.17	0.71
FN2SH7	Fenchuganj	2	3142	0.29	433	0.06	0.23	0.48	81	168	0.21	0.57
FN2SH8	Fenchuganj	2	3172	0.36	435	0.05	0.23	0.44	63	121	0.18	0.59
FN2SH9	Fenchuganj	2	3173	0.40	436	0.05	0.24	0.36	60	90	0.17	0.60
SB1SH50	Shahbazpur	1	3409.2	0.17	441	0.04	0.17	0.10	102	60	0.19	0.66
T11SH52	Titas	11	2710.9	1.37	433	0.52	3.76	0.97	274	71	0.12	0.56
T11SH53	Titas	11	2712.7	0.33	433	0.09	0.35	0.31	106	94	0.20	na
T11SH54	Titas	11	2714.2	0.30	433	0.10	0.38	0.27	127	90	0.21	0.57
T11SH55	Titas	11	2715.8	0.44	435	0.09	0.74	0.42	169	96	0.11	na
T11SH56	Titas	11	2719.4	0.50	435	0.14	0.88	0.54	176	108	0.14	0.59
T11SH57	Titas	11	2720.6	0.38	435	0.07	0.43	0.40	115	107	0.14	na
T11SH57A	Titas	11	2721.5	0.35	436	0.06	0.25	0.31	71	89	0.19	0.60
T11SH58	Titas	11	2723.1	0.35	434	0.10	0.71	0.45	202	128	0.12	na
T11SH59	Titas	11	2727.4	0.90	435	0.51	2.48	0.83	277	93	0.17	0.65
T11SH61	Titas	11	2737.7	1.42	435	0.90	3.70	0.85	260	60	0.20	0.66
T11SH62	Titas	11	2739.2	0.36	434	0.08	0.44	0.39	121	107	0.15	na
T11SH63	Titas	11	2740.5	0.21	436	0.05	0.21	0.17	99	80	0.19	na
T11SH64	Titas	11	2740.8	0.49	437	0.33	1.20	0.76	244	155	0.22	0.66
T11SH65	Titas	11	2783.1	0.34	439	0.03	0.13	0.22	39	65	0.19	0.67
T11SH66	Titas	11	2788.6	0.35	439	0.03	0.13	0.21	37	61	0.19	na
T11SH67	Titas	11	2791.7	0.16	438	0.04	0.14	0.12	90	77	0.22	0.67
T11SH68	Titas	11	2792.4	0.61	439	0.33	1.41	0.81	231	133	0.19	0.68
Range			2711-3572	0.14-1.42	420-441	0.03-2.52	0.13-3.76	0.10-1.29	55-231	60-228	0.11-0.40	0.48-0.71

Note: na = not analyzed.

The cross-plot of HI versus OI (modified van Krevelen diagram) reveals mostly Type III character of both formations (Appendix C2). T_{max} values vary considerably ranging from 420 to 441 °C in Bhuban and 420 to 440 °C in Boka Bil Formation.

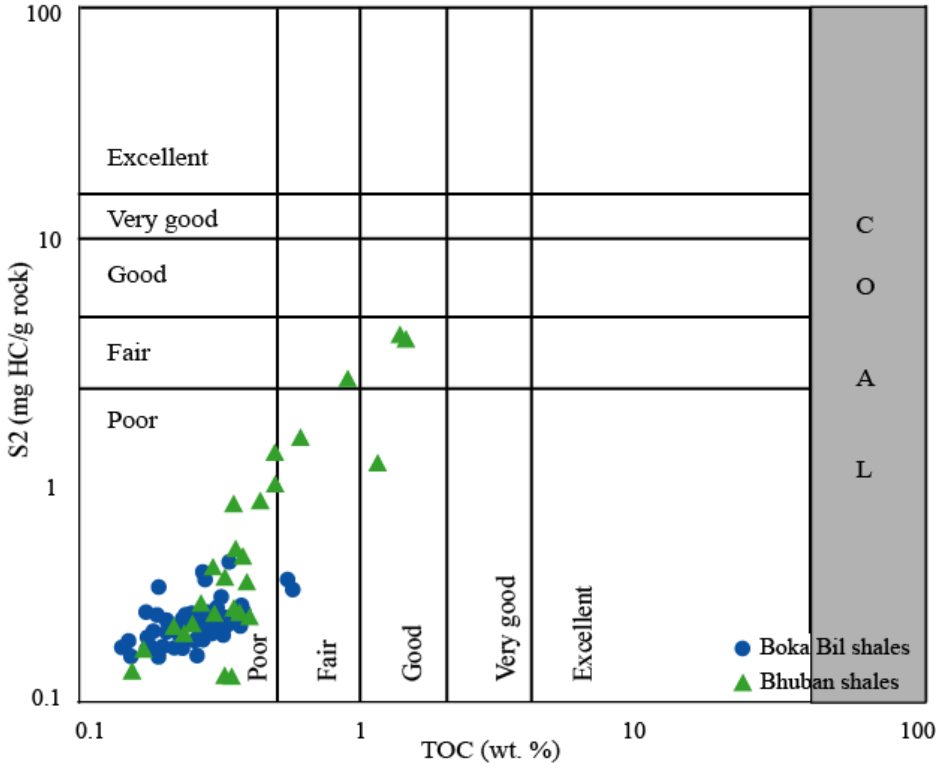

Fig.4.1.1 Cross-plot of total organic carbon (TOC in wt.%) and remaining hydrocarbon potential (S2 in mg HC/g rock) of the studied samples. Bhuban formation shows poor to fair quality source potential while Boka Bil shows mostly poor quality (adopted from Peters and Cassa, 1994; Dembicki, 2009).

The measured total sulfur percentage of the analyzed shale samples is very low. It ranges from 0.01 to 0.08% (Bhuban Formation) and 0.01 to 0.02% (Boka Bil Formation). Total nitrogen varies from 0.07 to 0.43% in the Bhuban and 0.12 to 0.43% in the Boka Bil. The ratio of C/S ranges from 4.2 to 128.6% in the analyzed Bhuban shales whereas 2.4 to 53.3% in the Boka Bil shales (Table 4.1.3). The measured C/N ratio varies from 0.6 to 13.3% and 0.8 to 4.2% in the Bhuban and Boka Bil, respectively. These values are typical of terrestrial organic matter deposited in a non-marine environment. Environment implications are discussed more thoroughly in section 4.1.4.3.

Table 4.1.2. Comparison between SRA and RE results of the analyzed shale samples (refer to Appendix B1).

Sample no.	TOC		Tmax		S1		S2		S3		HI		OI	
	SRA	RE	SRA	RE	SRA	RE	SRA	RE	SRA	RE	SRA	RE	SRA	RE
RP4SH1	0.57	0.53	428	427	0.07	0.08	0.31	0.30	0.87	0.76	54	57	153	143
RP4SH2	0.55	0.53	430	428	0.06	0.08	0.33	0.30	0.89	0.77	60	57	162	145
KM1SH2	0.26	0.41	433	433	0.05	0.06	0.22	0.25	0.36	0.27	85	61	138	66
BG1SH5	0.28	0.31	435	434	0.05	0.07	0.22	0.24	0.29	0.25	79	77	104	81
FN2SH7	0.29	0.22	433	433	0.06	0.06	0.23	0.22	0.48	0.38	79	100	166	173
PT5SH13	0.32	0.33	437	438	0.12	0.14	0.28	0.30	0.22	0.18	88	91	69	55
SB1SH35	0.22	0.21	432	431	0.04	0.05	0.17	0.16	0.25	0.20	77	76	114	95
SB1SH48	0.28	0.25	440	439	0.06	0.05	0.24	0.23	0.50	0.45	86	92	179	180
T11SH59	0.90	1.21	435	434	0.51	0.55	2.48	2.42	0.83	0.86	276	200	92	71
T11SH68	0.61	0.75	439	437	0.33	0.35	1.41	1.30	0.81	0.77	231	173	133	103
BK9SH70	0.19	0.21	432	431	0.06	0.06	0.31	0.34	0.39	0.37	163	162	205	176

4.1.2 Maceral characteristics and kerogen type

Vitrinite is the dominant maceral group found in both of the analyzed Bhuban and Boka Bil samples followed by liptinite and inertinite (Table 4.1.4). Vitrinite is identified by its moderate grey color reflectance under normal reflected white light. In mineral free basis, it ranges from 62 to 80 (vol.%) and 64 to 83 (vol.%) in the studied Bhuban and Boka Bil shale samples, respectively. Vitrinite macerals are mostly distorted because of the bitumen staining, which is commonly observed in association with vitrinites (Fig. 4.1.3A and B). Wood fragments are present in all the analyzed samples (Fig. 4.1.3C and D). Inertinite maceral ranges 7-14 vol.% in the studied Bhuban Formation and 5-15 vol.% in Boka Bil Formation. Inertinite is distinguished by its higher reflectance and characteristic whitish color under normal reflected white light. Fusinite, semifusinite and inertodetrinite are the most common inertinite macerals observed in the studied samples (Fig.4.1.3E and F).

Both vitrinite and inertinite macerals are dark under ultraviolet light. But liptinite macerals show characteristic fluorescence under ultraviolet light (Figs.4.1.4 and 4.1.5).

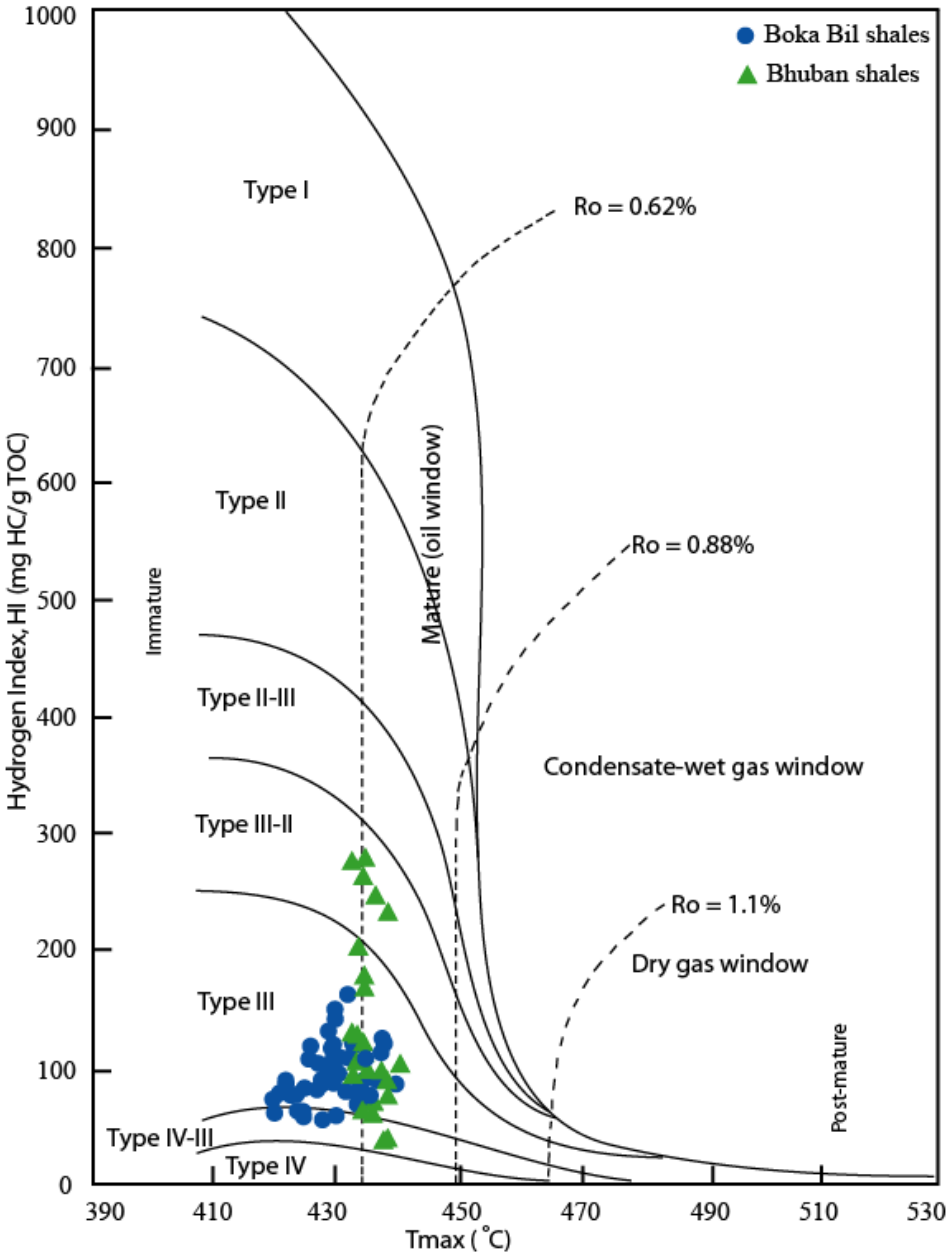

Fig.4.1.2. Distribution of vitrinite reflectance (%R_o) and T_{max} (°C) plotting with hydrogen index (HI) of the analyzed samples. Bhuban formation depicts Type III/II (gas-oil prone) kerogen whereas Boka Bil is of Type III. Both formations are within immature to early mature oil window (see Appendices B1 and B3 for definitions) (modified from Peters and Cassa, 1994; Koeverden et al., 2011; cited by Farhaduzzaman et al., 2013a and 2013e).

Table 4.1.3. Elemental analysis (CHNS) results of the studied samples (TS = total sulfur; TN = total nitrogen; TH = total hydrogen; TOC = total organic carbon).

Sample ID	TOC	TH	TS	TN	C/S	C/N
Boka Bil Fm						
RP4SH1	0.57	0.912	0.150	0.135	3.80	4.22
PT5SH10	0.29	0.931	0.047	0.115	6.17	2.52
PT5SH11	0.30	0.874	0.012	0.158	25.00	1.90
PT5SH12	0.28	0.929	0.012	0.178	23.33	1.57
PT5SH13	0.32	0.862	0.044	0.142	7.27	2.25
PT5SH14	0.28	0.399	0.014	0.246	20.14	1.14
SB1SH3	0.27	1.146	0.015	0.228	18.00	1.18
SB1SH9	0.38	1.283	0.024	0.230	15.83	1.65
SB1SH11	0.33	0.766	0.017	0.259	19.08	1.27
SB1SH12	0.32	1.233	0.006	0.265	53.33	1.21
SB1SH13	0.34	0.750	0.022	0.428	15.60	0.79
SB1SH23	0.19	1.246	0.024	0.146	7.92	1.30
SB1SH24	0.30	0.860	0.016	0.220	18.75	1.36
SB1SH29	0.23	0.690	0.008	0.148	28.75	1.55
SB1SH32	0.17	1.068	0.007	0.136	24.29	1.25
SB1SH45	0.23	1.352	0.036	0.164	6.39	1.40
SB1SH47	0.15	0.850	0.008	0.137	18.75	1.09
BK9SH69	0.18	1.012	0.069	0.139	2.61	1.29
BK9SH70	0.19	0.956	0.080	0.170	2.38	1.12
BK9SH71	0.34	1.101	0.064	0.152	5.31	2.24
Range	0.15-0.57	0.40-1.35	0.01-0.15	0.12-0.43	2.4-53.3	0.8-4.2
Bhuban Fm						
KM1SH2	0.26	0.691	0.024	0.370	10.97	0.70
KM1SH3	0.27	0.850	0.015	0.292	18.62	0.92
KM1SH4	0.39	0.539	0.055	0.116	7.09	3.36
BG1SH5	0.28	0.554	0.016	0.110	17.50	2.55
BG1SH6	0.32	0.903	0.045	0.163	7.11	1.96
FN2SH7	0.29	1.747	0.066	0.141	4.39	2.06
FN2SH8	0.36	0.532	0.032	0.119	11.25	3.03
FN2SH9	0.40	0.779	0.018	0.184	22.22	2.17
T11SH52	1.37	1.157	0.016	0.358	87.82	3.83
T11SH56	0.50	0.115	0.008	0.184	62.50	2.72
T11SH57	0.38	0.841	0.012	0.175	31.67	2.17
T11SH58	0.35	0.644	0.028	0.430	12.68	0.81
T11SH59	0.90	0.963	0.007	0.327	128.57	2.75
T11SH61	1.42	0.491	0.016	0.107	88.75	13.27
T11SH62	0.36	0.761	0.006	0.180	60.00	2.00
T11SH63	0.21	0.609	0.034	0.068	6.18	3.09
T11SH65	0.34	0.688	0.057	0.293	5.96	1.16
T11SH66	0.35	0.705	0.084	0.334	4.17	1.05
T11SH67	0.16	0.766	0.017	0.259	9.25	0.62
T11SH68	0.61	0.150	0.041	0.116	14.88	5.26
Range	0.16-1.42	0.12-1.75	0.01-0.08	0.07-0.43	4.2-128.6	0.6-13.3

Table 4.1.4. A summary of the maceral contents (mineral free basis) of the studied shale samples from Bhuban and Boka Bil Formations, Bengal Basin, Bangladesh.

Sample no.	Vitrinite	Liptinite	Inertinite	Remarks/Observatons
Boka Bil Fm				
RP4SH1	64	21	15	Woody fragments, amorphous, sporinite and bitumen stain.
RP4SH2	71	17	12	Woody fragments, amorphous, sporinite, bitumen stain and alginite (?).
PT5SH10	76	15	9	Woody fragments, amorphous, resinite, sporinite, and bitumen stain.
PT5SH11	70	18	12	Woody fragments, amorphous, sporinite, microcutinite and bitumen stain.
PT5SH12	68	19	13	Woody fragments, amorphous, resinite, cutinite and bitumen stain.
PT5SH13	76	15	9	Woody fragments, amorphous, sporinite, microcutinite and bitumen stain.
PT5SH14	79	14	7	Woody fragments, amorphous, resinite and bitumen stain.
SB1SH2	71	18	11	Woody fragments, amorphous, sporinite and bitumen stain.
SB1SH4	70	20	10	Woody fragments, amorphous, microcutinite and bitumen stain.
SB1SH9	75	19	6	Woody fragments, amorphous, sporinite and bitumen stain.
SB1SH11	83	10	7	Woody fragments, amorphous cutinite and bitumen stain.
SB1SH13	77	13	10	Woody fragments, sporinite, microcutinite and bitumen stain.
SB1SH17	76	15	9	Woody fragments, amorphous, resinite, sporinite, microcutinite and bitumen stain.
SB1SH23	67	18	15	Woody fragments, amorphous, sporinite and bitumen stain.
SB1SH24	85	10	5	Woody fragments, amorphous, sporinite, cutinite and bitumen stain.
SB1SH29	73	17	10	Woody fragments, amorphous, resinite, sporinite and bitumen stain.
SB1SH32	70	18	12	Woody fragments, amorphous, resinite, cutinitr and bitumen stain.
SB1SH33	77	14	9	Woody fragments, amorphous, sporinite, microcutinite and bitumen stain.
SB1SH35	69	20	11	Woody fragments, amorphous, sporinite and bitumen stain.
SB1SH39	67	20	13	Woody fragments, amorphous, sporinite and microcutinite.
SB1SH40	76	15	9	Woody fragments, amorphous, resinite, sporinite, microcutinite and bitumen stain.
SB1SH42	71	18	11	Woody fragments, amorphous, sporinite cutinitr and bitumen stain.
SB1SH44	78	14	8	Woody fragments, amorphous, resinite, sporinite and bitumen stain.
SB1SH45	71	19	10	Woody fragments, amorphous, sporinite, microcutinite and bitumen stain.
SB1SH47	79	16	5	Woody fragments, amorphous, sporinite and bitumen stain.
SB1SH48	72	19	9	Woody fragments, amorphous, sporinite, microutinite and bitumen stain.
BK9SH69	72	14	14	Woody fragments, amorphous, sporinite, alginite (?) and bitumen stain.
BK9SH70	67	19	14	Woody fragments, amorphous, resinite, sporinite and bitumen stain.
BK9SH71	69	19	12	Woody fragments, amorphous, sporinite and bitumen stain.
Range	64-83	10-21	5-15	
Mean	73	17	10	
Bhuban Fm				
KM1SH2	70	19	11	Woody fragments, amorphous, sporinite, microcutinite and bitumen stain.
KM1SH3	80	11	9	Woody fragments, amorphous, resinite, sporinite and bitumen stain.
KM1SH4	62	24	14	Woody fragments, amorphous, cutinite and bitumen stain.
BG1SH5	73	17	10	Woody fragments, amorphous, resinite, sporinite and bitumen stain.
BG1SH6	74	15	11	Woody fragments, resinite, sporinite and bitumen stain.
FN2SH7	73	18	9	Woody fragments, amorphous, sporinite, cutinite and bitumen stain.
FN2SH8	72	18	10	Woody fragments, resinite, sporinite, cutinite and bitumen stain.
FN2SH9	79	13	8	Woody fragments, amorphous, sporinite and bitumen stain.
T11SH52	80	11	9	Woody fragments, amorphous, resinite, sporinite and bitumen stain.
T11SH54	73	20	7	Woody fragments, amorphous, resinite, sporinite, cutinite and bitumen stain.
T11SH56	72	19	9	Woody fragments, amorphous, sporinite and bitumen stain.
T11SH57	79	15	6	Woody fragments, amorphous, resinite, sporinite and bitumen stain.
T11SH59	73	16	11	Woody fragments, amorphous, resinite, sporinite, cutinite and bitumen stain.
T11SH61	78	16	6	Woody fragments, amorphous, sporinite and bitumen stain.
T11SH62	77	14	9	Woody fragments, amorphous, sporinite, cutinite and bitumen stain.
T11SH64	79	13	8	Woody fragments, amorphous, resinite, sporinite, cutinite and bitumen stain.
T11SH65	77	15	8	Woody fragments, amorphous, resinite, sporinite, alginite (?) and bitumen stain.
T11SH67	78	14	8	Woody fragments, amorphous, resinite, sporinite, cutinite and bitumen stain.
T11SH68	76	13	11	Woody fragments, amorphous, sporinite, microcutinite and bitumen stain.
Range	62-80	11-24	7-14	
Mean	74	17	9	

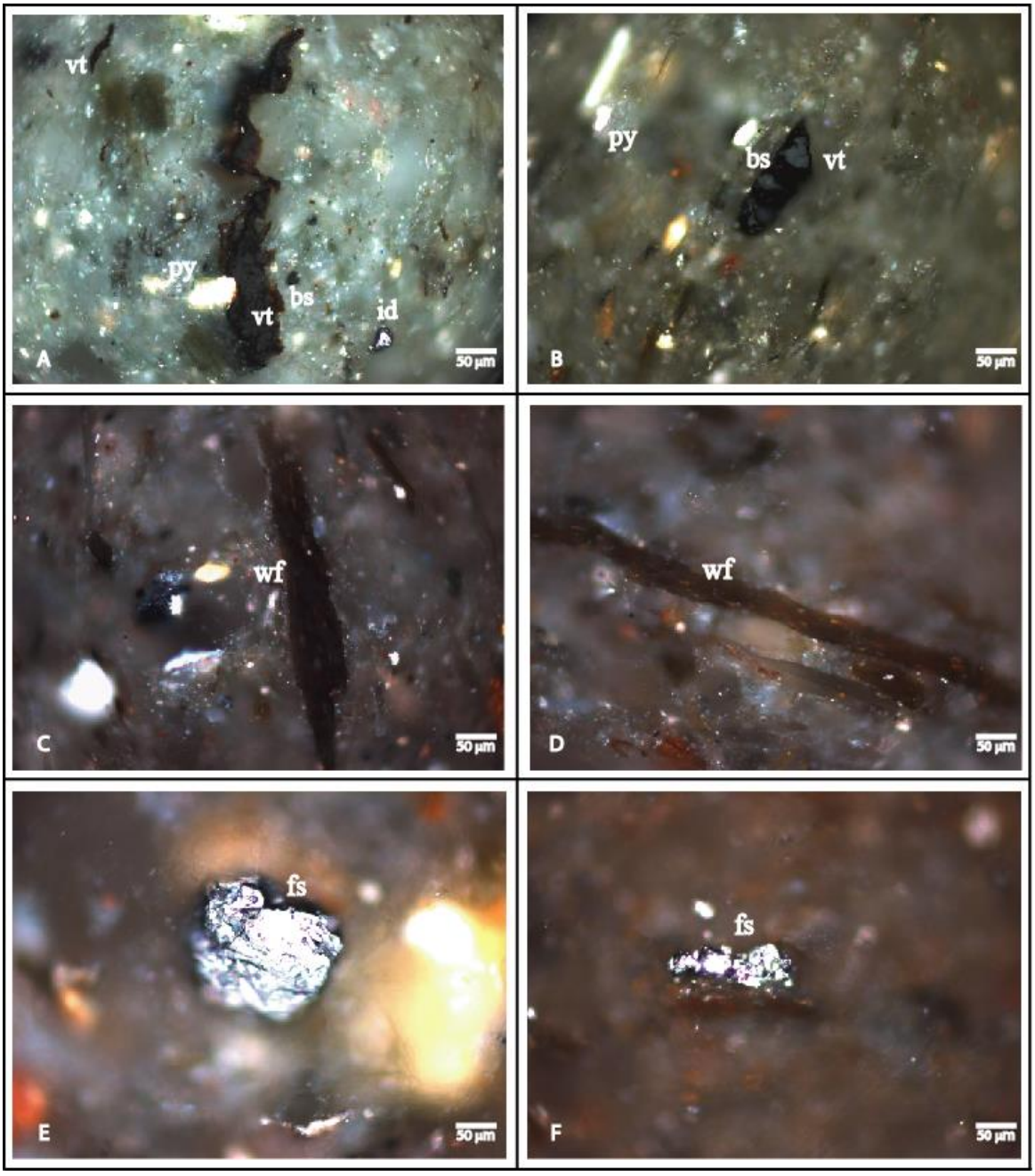

Fig.4.1.3. (A) Moderately reflecting vitrinite (vt) which is associated with bitumen staining (bs) and white color inertinite maceral inertodetrinite (id) and pyrite (py) observed in Bhuban Formation, depth 3173m in well Fenchuganj-2. (B) Bitumen stained vitrinite associated with pyrite (py) observed in Boka Bil Formation, depth 2301.2m in well Bakhrabad-9. (C) Dark brownish color woody fragment (wf) found in Bhuban Formation, depth 3100m in well Begumganj-1. (D) Light brownish color woody fragment observed in Boka Bil Formation, depth 2296.5m in well Shabazpur-1. (E) Whitish color inertinite maceral fusinite (fs) identified in Bhuban Formation, depth 3172m in well Fenchuganj-2. (F) Whitish color inertinite maceral fusinite (fs) identified in Boka Bil Formation, depth 1777.3m in well Shahbazpur-1 [all photomicrographs shown are taken in normal reflected white light using oil immersion objective].

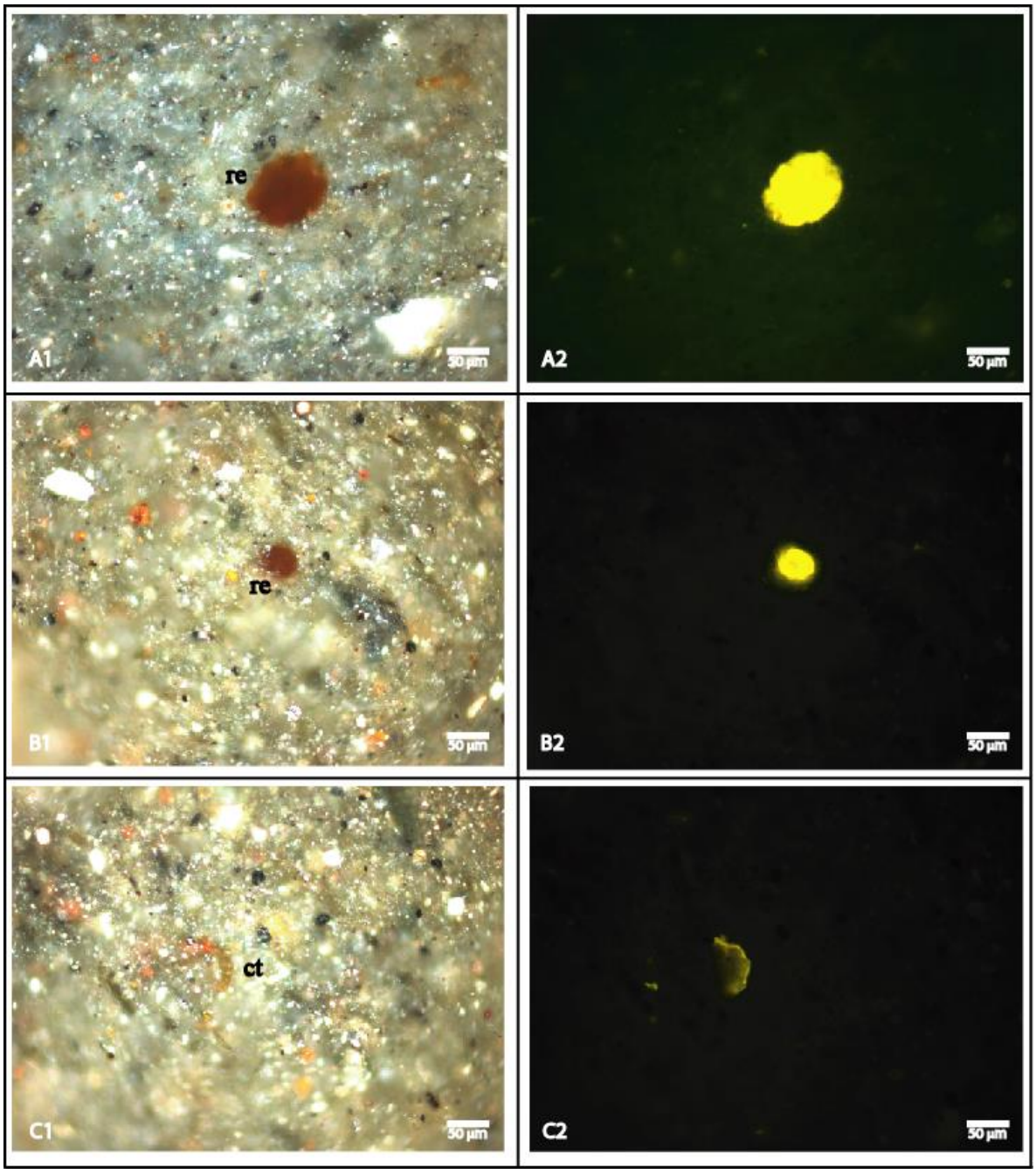

Fig.4.1.4 (A1) Moderate brown color liptinite maceral resinite (re) under normal reflected white light observed in Boka Bil Formation, depth 1834m in well Patharia-5. (A2) Same view as A1 under ultraviolet light which shows yellow fluorescence. (B1) Moderate brown color liptinite maceral resinite (re) under normal reflected white light observed in Bhuban Formation, depth 2714.2m in well Titas-11. (B2) Same view as B1 under ultraviolet light which shows yellow fluorescence. (C1) Brownish color liptinite maceral cutinite (ct) under normal reflected white light observed in Boka Bil Formation, depth 2329.6m in well Bakhrabad-9. (C2) Same view as C1 under ultraviolet light which shows yellow fluorescence.

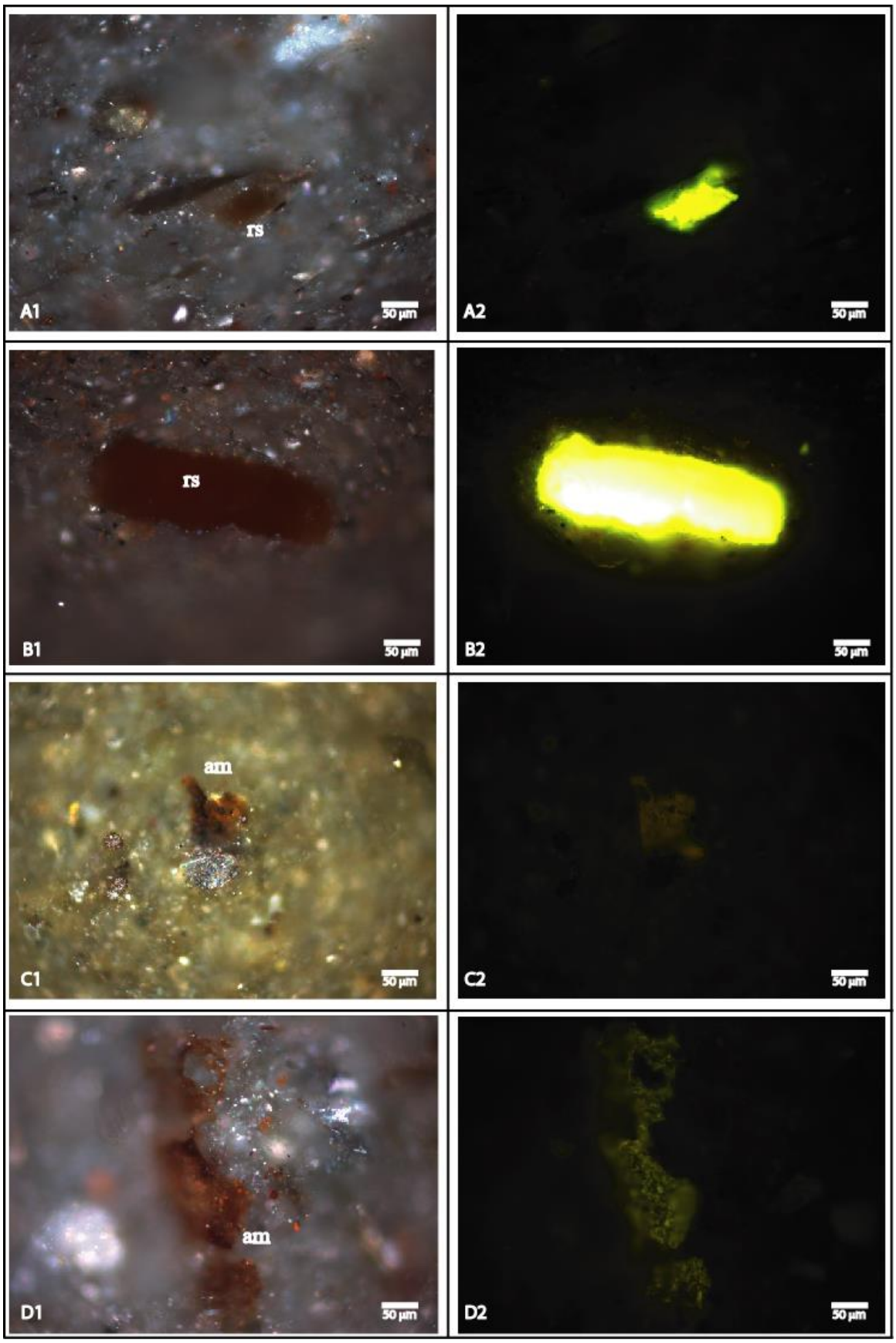

Fig.4.1.5 (Caption continued next page)

Fig.4.1.5 (Continued). (A1) Dark brown color liptinite maceral resinite (rs) under normal reflected white light observed in Bhuban Formation, depth 2727.4m in well Titas-11. (A2) Same view as A1 under ultraviolet light which shows greenish yellow fluorescence. (B1) Dark brown resinite (rs) under normal reflected white light noted in Boka Bil formation, depth 2316m in well Shahbazpur-1. (B2) Same view as B1 which shows intense yellow fluorescence under ultraviolet light. (C1) Brownish color liptinitic amorphous (am) component under normal reflected white light viewed in Bhuban Formation, depth 3139m in well Kamta-1. (C2) Same view as C1 under ultraviolet light and it shows brownish yellow fluorescence. (D1) Brownish color liptinitic amorphous (am) maceral which could be of alginite origin under normal reflected white light saw in Boka Bil Formation, depth 3163m in well Patharia-5. (D2) Same view as D1 under ultraviolet light and it shows greenish light yellow fluorescence.

Liptinite content was determined from petrography as 11 to 24 and 10 to 21 vol.% in the analyzed Bhuban and Boka Bil shales, respectively. The important liptinitic macerals include resinite (Fig.4.1.4 A1 and A2; B1 and B2; Fig.4.1.5 A1 and A2; B1 and B2), cutinite (Fig.4.1.4 C1 and C2), amorphous organic matter (Fig.4.1.5 C1 and C1; D1 and D2), liptodetrinite and alginite (trace amount). Nevertheless, similar types of maceral assemblages are observed in both of the analyzed Bhuban and Boka Bil Formations.

Giraud (1970), Larter and Douglas (1980), Dembicki et al. (1983) and Dembicki (2009) have all noted that pyrolysis-GC helps to interpret kerogen mixtures. This can give a direct indication of HC likely to be generated. According to the interpretation by Dembicki (2009), $<C_{10}$ mode dominates in PyGC traces of Type III kerogens with only a minor $>C_{15}$ mode. For Type I kerogens, the situation is reversed. An intermediate situation represents Type II kerogens (Dembicki, 2009). Unimodal fingerprints of predominantly n-alkane/alkene doublets with some specific abundant aromatic compounds displayed by whole rock PyGC pyrograms (Fig.4.1.6 and Appendix C3) suggest mixed kerogen sources of Bhuban and Boka Bil samples, possibly reflecting 75% Type III and 25% Type II input (Dembicki, 2009). The ratio of n-octene (C_8) to xylene (m+p) is applied as a measure of the comparative abundance of aliphatic to aromatic hydrocarbons (Aarssen et al., 1992).

The measured C_8/xylene ratio of the analyzed Bhuban and Boka Bil samples varies from very low to moderate (0.56-1.78) (c.f., Solli et al., 1984). The high relative abundance of specific aromatic hydrocarbons (benzene, toluene and xylene) and low ratio of cadalene to xylene (Cd/xylene) (0.06 to 0.12) are consistent with dominant input from vascular higher plants in a terrestrial depositional setting.

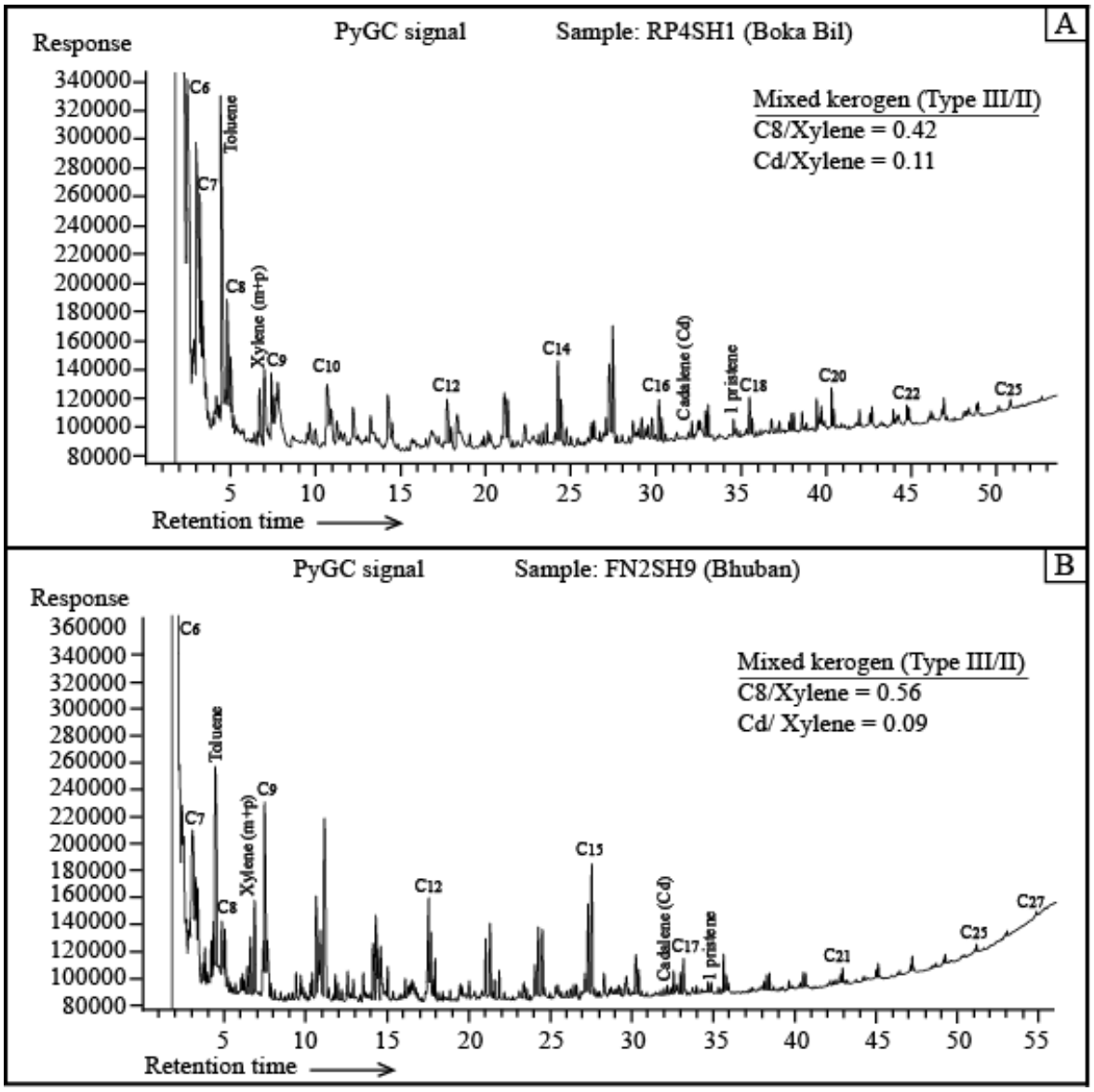

Fig.4.1.6. PyGC pyrograms of Boka Bil and Bhuban shales (RP4SH1 and FN2SH9) display a mixed kerogen of Types III and II.

Table 4.1.5. Solubale extract yield and alkane parameters of the studied shale samples, Bengal Basin (refer to Appendix B1).

Sample no.	EOM (ppm of whole rock)		EOM (mg EOM/g TOC)				n-alkane parameters					
	Tot extr	HC in extract(%)	Tot extr	Aliph	Arom	Total HC (yield)	n-alk max	CPI[1]	CPI[2]	Pr/Ph	Pr/nC17	Ph/nC18
Boka Bil Fm												
RP4SH1	649	34	113.88	14.13	24.94	39.07	16	0.99	1.07	1.26	0.32	0.32
RP4SH2	554	47	100.79	9.48	37.90	47.38	16	0.77	1.47	1.00	0.54	0.47
PT5SH10	255	39	88.04	1.98	32.73	34.72	18	1.38	1.61	2.24	1.38	0.50
PT5SH13	1100	62	343.82	92.92	120.90	213.82	20	1.05	1.11	1.10	1.10	0.93
PT5SH14	1458	54	520.57	72.67	209.12	281.79	21	1.00	1.12	0.58	1.39	1.17
SB1SH3	994	22	354.88	37.08	41.05	78.13	16	0.81	1.01	1.42	0.55	0.42
SB1SH5	731	52	261.21	38.29	97.10	135.39	na	na	na	na	na	na
SB1SH9	390	46	102.50	6.29	41.36	47.65	14	0.80	1.62	3.65	3.14	1.32
SB1SH11	504	55	152.87	28.90	55.00	83.89	16	0.65	0.88	1.23	0.70	0.73
SB1SH13	398	34	116.98	12.53	27.16	39.69	14	0.86	1.08	2.16	1.90	1.06
SB1SH29	238	51	103.47	11.76	41.15	52.91	16	0.46	0.68	1.38	1.38	0.46
SB1SH32	235	35	138.43	10.79	37.75	48.54	16	0.67	1.21	1.21	1.28	0.41
SB1SH47	237	46	157.85	9.99	61.94	71.93	16	1.05	1.23	1.50	0.93	0.31
SB1SH48	264	44	94.26	11.03	30.08	41.11	16	1.04	1.03	1.02	1.05	0.37
BK9SH69	421	44	123.96	15.18	38.79	53.97	16	1.14	1.33	2.32	1.05	0.82
BK9SH70	1381	38	727.03	94.83	184.39	279.22	16	0.97	1.08	1.24	1.05	0.82
BK9SH71	548	43	304.63	55.67	74.22	129.89	16	0.76	0.80	1.16	1.10	0.93
Range	235-1381	22-62	88-727	2-115	27-184	35-282	14-21	0.46-1.38	0.68-1.47	0.58-3.65	0.32-3.14	0.31-1.32
Bhuban Fm												
KM1SH2	754	37	290.03	5.77	101.00	106.78	16	1.07	1.13	3.41	1.38	0.38
KM1SH3	357	61	132.38	38.21	42.31	80.52	na	na	na	na	na	na
KM1SH4	767	45	196.79	24.04	64.11	88.15	21	0.95	1.09	0.99	1.36	0.85
BG1SH5	243	52	86.87	9.50	35.70	45.20	16	0.94	0.99	2.11	1.08	0.27
BG1SH6	352	27	109.92	10.30	19.46	29.77	16	1.08	1.25	3.21	1.63	0.44
FN2SH7	239	32	82.26	3.10	22.93	26.03	16	1.06	1.11	1.95	0.98	0.39
FN2SH8	235	41	65.21	5.69	21.22	26.91	19	1.00	1.37	3.74	1.33	0.32
FN2SH9	396	39	98.96	14.70	23.52	38.21	19	0.99	1.33	2.50	0.99	0.32
T11SH52	1425	27	104.02	12.01	16.11	28.12	16	0.99	1.32	1.64	0.59	0.44
T11SH59	1778	55	197.56	46.77	62.00	108.78	16	1.11	1.27	2.76	2.26	0.30
T11SH61	846	28	59.57	3.30	13.19	16.49	16	0.88	1.29	1.22	1.26	0.47
T11SH62	1498	43	416.07	54.53	126.31	180.84	16	0.94	1.00	1.67	1.31	0.40
T11SH65	230	50	143.61	15.39	56.42	71.81	16	0.91	0.96	1.26	1.44	0.56
T11SH67	132	53	38.87	3.97	16.66	20.43	18	1.18	1.06	2.45	2.42	0.81
T11SH68	2814	30	461.31	49.23	89.85	139.07	16	0.98	1.02	1.55	1.19	0.91
Range	132-2814	27-61	60-461	3-54	13-126	16-139	16-21	0.88-1.18	0.96-1.37	0.99-3.41	0.59-2.42	0.27-0.91

Note: na = not analyzed.

4.1.3 Soluble extract and biomarker distributions

Aromatic hydrocarbon dominates over the aliphatic hydrocarbons in both of the analyzed formations. Measured aromatic hydrocarbon is 13-126 mg/g TOC in Bhuban Formation

and 27-184 mg/g TOC in Boka Bil Formation. Aliphatic fraction varies from 3 to 54 mg/g TOC in Bhuban and 2 to 115 mg/g TOC in Boka Bil. The measured total soluble hydrocarbon yields are in the range of 16-139 and 35-282 mg HC/g TOC in the analyzed shales. The total soluble extract ranges from 132-2814 ppm (Bhuban) and 235-1381 ppm (Boka Bil) in the analyzed samples. Besides, the high extract found in sample T11SH59 and T11SH68 possibly marks the presence of some migrated bitumen. It might have happened since this geological unit is now hosting and producing gas at this field.

GC and GCMS analyses are carried out for the aliphatic fractions of the studied shale samples. The TIC (total ion current), m/z 191 and m/z 217 chromatograms are used to gather data reported here. The identifications of the peaks of these traces are made from retention times and published available literatures. For example, Waples and Machihara (1991), Hossain et al. (2009) and Wang et al. (2011) are used for TIC; Ahmed et al. (2009), Kashirtsev et al. (2010) and Hakimi et al. (2011) for m/z 191 fragmentograms; Pearson and Alam (1993), Wan Hasiah (1999a) and Fabianska and Kruszewska (2003) for bicadinane and oleananes; and Abeed et al. (2011), Koeverden et al. (2011) and Sachse et al. (2012) for m/z 217 fragmentograms. Identity of these peaks and related other terms are described in Appendices B1 and B2.

4.1.3.1 GC: TIC (Total Ion Current)

In most of the analyzed samples, the odd carbon homologs dominate over the even carbon homologs. However, the even carbon homologs also dominate over the odd carbon homologs in n-alkane of some other samples (Appendix C4).

Table 4.1.6 . Hopane biomarker parameters (measured from m/z 191) of the analyzed shale samples (refer to Appendix B2).

Sample no.	Ts/Tm	C_{29}-hop/ C_{30}-hop	C_{30}-mor/ C_{30}-hop	C_{31} 22S/ (22S+22R)	C_{32} 22S/ (22S+22R)	Oleanane index	bc/C_{30}-hop
Boka Bil Fm							
RP4SH1	0.70	0.80	0.35	0.53	0.58	0.08	0.35
RP4SH2	0.75	1.35	0.29	0.41	0.52	0.06	0.65
PT5SH10	0.12	0.96	0.36	0.46	0.48	0.07	0.29
PT5SH13	0.73	0.77	0.05	0.56	0.65	0.11	0.03
PT5SH14	0.71	0.87	0.17	0.59	0.57	0.09	0.07
SB1SH3	1.24	1.05	0.22	0.47	0.43	0.05	0.52
SB1SH9	0.82	1.08	0.39	0.33	0.45	0.14	0.22
SB1SH11	0.43	1.48	0.32	0.52	0.44	0.18	0.29
SB1SH13	0.33	0.79	0.28	0.48	0.48	0.11	0.18
SB1SH29	1.29	0.28	0.15	0.43	0.50	0.17	0.03
SB1SH32	0.45	1.35	0.23	0.44	0.50	0.15	0.08
SB1SH47	1.86	0.30	0.13	0.60	0.60	0.18	0.04
SB1SH48	0.74	0.77	0.14	0.57	0.58	0.05	0.04
BK9SH69	0.34	1.21	0.70	0.50	0.44	0.12	0.05
BK9SH70	0.62	0.33	0.12	0.46	0.61	0.61	0.02
BK9SH71	1.15	0.73	0.14	0.58	0.57	0.14	0.08
Range	0.12-1.86	0.28-1.48	0.05-0.39	0.33-0.60	0.43-0.65	0.05-0.61	0.02-0.65
Bhuban Fm							
KM1SH2	0.68	0.34	0.14	0.51	0.52	0.33	0.05
KM1SH4	0.59	0.89	0.20	0.55	0.63	0.12	0.05
BG1SH5	0.57	0.83	0.15	0.58	0.61	0.05	0.03
BG1SH6	0.09	0.72	0.35	0.59	0.58	0.04	0.02
FN2SH7	0.82	0.26	0.09	0.47	0.49	0.11	0.04
FN2SH8	0.33	0.68	0.31	0.49	na	0.14	0.07
FN2SH9	0.29	0.54	0.37	0.48	0.47	0.07	0.11
T11SH52	0.69	0.51	0.19	0.49	0.47	0.22	0.06
T11SH59	0.38	1.08	0.39	0.33	na	0.14	0.04
T11SH61	0.53	0.30	0.16	0.46	0.47	0.17	0.05
T11SH62	0.79	0.27	0.15	0.47	0.49	0.18	0.04
T11SH65	0.60	0.37	0.44	0.60	0.43	0.21	0.06
T11SH67	0.14	0.48	0.15	0.55	0.63	0.17	0.09
T11SH68	0.87	0.32	0.18	0.54	0.59	0.20	0.04
Range	0.09-0.87	0.26-1.08	0.09-0.44	0.33-0.60	0.43-0.63	0.04-0.33	0.02-0.11

na = not analyzed.

Table 4.1.7. Sterane and diasterane biomarker parameters (measured from m/z 217) of the analyzed shale samples (refer to Appendix B2).

Sample no.	C_{27}-ster (%)	C_{28}-ster (%)	C_{29}-ster (%)	Ster-C_{27}/ ster-(C_{27}+C29)	Ster C_{29} 20S/ (20S+20R)	Ster C_{29} ββ/ (ββ+αα)	Diaste/ Sterane	Diaste 20S/ (20S+20R)	Sterane/ Hopane
Boka Bil Fm									
RP4SH1	50.51	14.14	35.35	0.59	0.20	0.35	0.37	0.60	0.83
RP4SH2	59.26	6.79	33.95	0.64	0.22	0.22	0.28	0.48	2.40
PT5SH10	26.23	9.29	64.48	0.29	0.23	0.40	0.26	0.51	1.09
PT5SH13	31.45	31.45	37.10	0.46	0.32	0.39	0.34	0.58	1.42
PT5SH14	34.25	33.15	32.60	0.51	0.38	0.48	0.34	0.65	1.15
SB1SH3	36.87	23.96	39.17	0.48	0.34	0.13	0.16	0.17	0.99
SB1SH9	20.59	17.65	61.76	0.25	na	0.23	na	na	0.87
SB1SH11	18.55	17.83	63.61	0.23	0.23	0.04	0.05	0.47	1.07
SB1SH13	23.53	21.41	55.06	0.30	0.03	0.29	0.04	0.33	1.07
SB1SH29	20.19	17.79	62.02	0.25	0.16	0.34	0.16	0.19	1.74
SB1SH32	33.46	20.30	46.24	0.42	0.07	0.34	0.09	0.39	1.41
SB1SH47	24.74	21.05	54.21	0.31	0.24	0.36	0.18	0.19	1.71
SB1SH48	32.24	19.18	48.57	0.40	0.22	0.41	0.15	0.56	1.08
BK9SH69	42.00	14.00	44.00	0.49	na	na	na	na	na
BK9SH70	27.09	19.62	53.28	0.34	0.07	0.32	0.39	0.46	1.62
BK9SH71	33.66	22.77	43.56	0.44	0.38	0.39	0.49	0.80	1.50
Range	19-59	7-33	33-62	0.23-0.64	0.03-0.38	0.04-0.48	0.04-0.49	0.17-0.80	0.83-2.40
Bhuban Fm									
KM1SH2	25.85	28.01	46.14	0.36	0.04	0.32	0.28	0.62	1.53
KM1SH4	33.33	31.01	35.66	0.48	0.37	0.40	0.27	0.58	1.03
BG1SH5	29.96	25.09	44.94	0.40	0.31	0.50	0.42	0.70	1.64
BG1SH6	23.56	17.28	59.16	0.28	0.24	0.29	0.13	0.55	1.97
FN2SH7	20.92	17.76	61.31	0.25	0.09	0.35	0.35	0.52	1.59
FN2SH8	23.58	16.04	60.38	0.28	na	na	na	na	na
FN2SH9	18.99	16.76	64.25	0.23	0.18	0.39	0.22	0.53	1.15
T11SH52	29.89	14.37	55.75	0.35	na	0.29	0.12	0.31	1.00
T11SH59	16.67	14.78	68.55	0.20	0.08	0.34	0.07	0.29	1.43
T11SH61	22.90	19.59	57.51	0.28	0.09	0.34	0.29	0.46	1.65
T11SH62	22.07	22.52	55.41	0.28	0.12	0.35	0.17	0.19	1.72
T11SH65	31.22	24.70	44.08	0.41	0.03	0.32	0.15	0.27	1.70
T11SH67	23.67	14.98	61.35	0.28	0.05	0.46	0.22	0.13	1.51
T11SH68	15.47	25.97	58.56	0.21	0.10	0.36	0.05	0.56	1.60
Range	15-33	14-31	36-69	0.20-0.48	0.03-0.37	0.29-0.50	0.05-0.42	0.13-0.70	1.00-1.97

na = not analyzed.

The pristane/phytane ratio is high to very high varying from 0.99 to 3.41 in Bhuban shales and 0.58 to 3.65 in Boka Bil shales. The unimodal distributions of n-alkanes from C_{10} to C_{35} with the maxima standing at C_{16} (mostly) or C_{18} are observed in the gas chromatograms

(TIC) of the analyzed Bhuban and Boka Bil shale samples. The calculated CPI^1 values are close to unity. CPI^1 is from 0.88 to 1.18 (CPI^2 0.96-1.37) in Bhuban shales and 0.68 to 1.47 (CPI^2 0.58-3.65) in Boka Bil shales (Table 4.1.5). Fig.4.1.7 and Appendix C5 display chromatograms of two representative immature samples of Boka Bil Formation. Fig.4.1.8 and Appendix C6 represent two mature samples of the same formation. Similarly, Fig.4.1.9 and Appendix C7 display chromatograms of two representative immature samples of Bhuban Formation. Fig.4.1.10 and Appendix C8 represent two mature samples of Bhuban.

4.1.3.2 GCMS: m/z 191 Fragmentogram

Abundant pentacyclic triterpanes (hopanes and moretanes) are dominated by C_{30}αβ-hopane in all the analyzed Bhuban and Boka Bil shale samples (Figs. 4.1.7, 4.1.8, 4.1.9 and 4.1.10). Homohopanes are lower in concentration but dominated by C_{31}-hopane in both of the formations. The R-isomers are dominant over the S-isomers among the homohopanes (C_{31} - C_{33}) of some analyzed Bhuban and Boka Bil shale samples (Figs.4.1.7B and 4.1.9B). It indicates that the samples are thermally immature for hydrocarbon generation. On the other hand, the S-isomers are dominant over the R-isomers in some other samples (Figs.4.1.8B and 4.1.10B). This again suggests the samples are thermally mature for hydrocarbon generation. A large amount of moretanes is also present in the studied samples. In general, αβ-hopanes are more prominent than the βα-hopanes (moretanes). Sterane profusions are generally low (Figs.4.1.7C, 4.1.8C, 4.1.9C and 4.1.10C) consistent with dominantly terrestrial input (c.f., Peters and Moldowan, 1993). The Ts/Tm ratio of the studied samples ranges from 0.09-0.87 in Bhuban and 0.12-1.86 in Boka Bil samples.

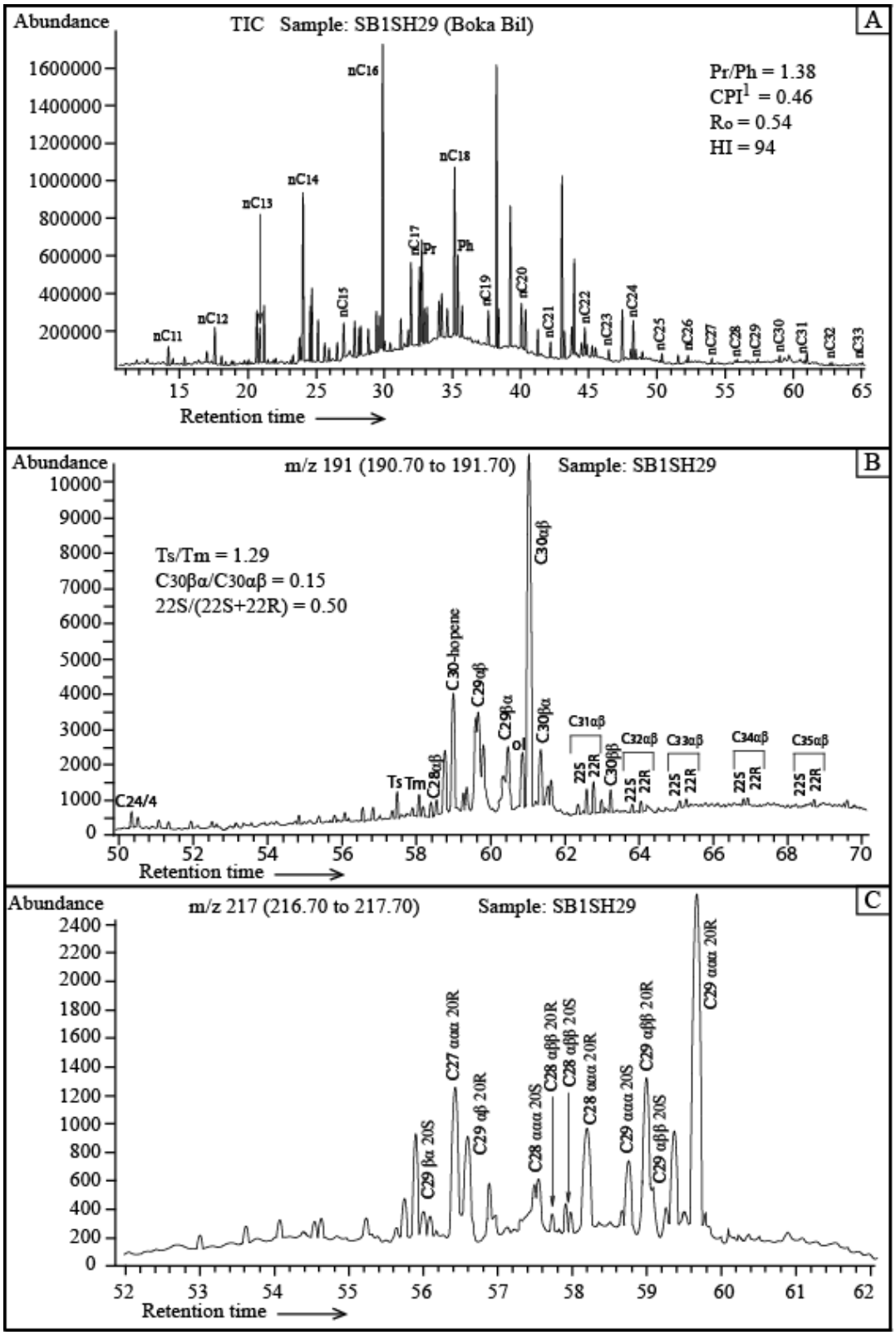

Fig.4.1.7. Gas chromatogram (TIC) and mass fragmentograms m/z 191 and m/z 217 of aliphatic fraction of a studied Boka Bil sample (SB1SH29). It represents immature oil window (peak i.d. in Appendix B2).

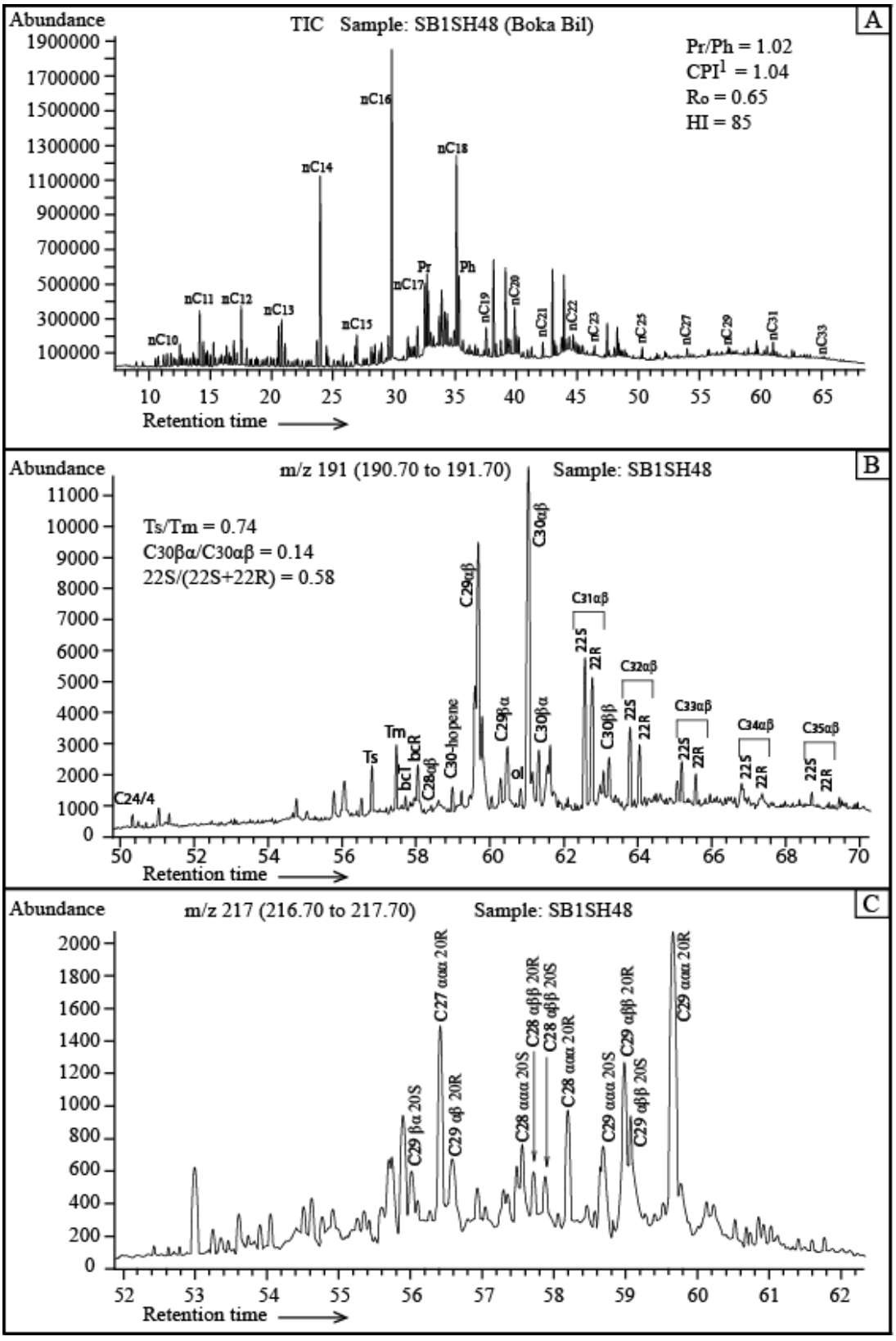

Fig.4.1.8. Gas chromatogram (TIC) and mass fragmentograms m/z 191 and m/z 217 of aliphatic fraction of a studied Boka Bil sample (SB1SH48). It represents mature oil window (peak i.d. in Appendix B2).

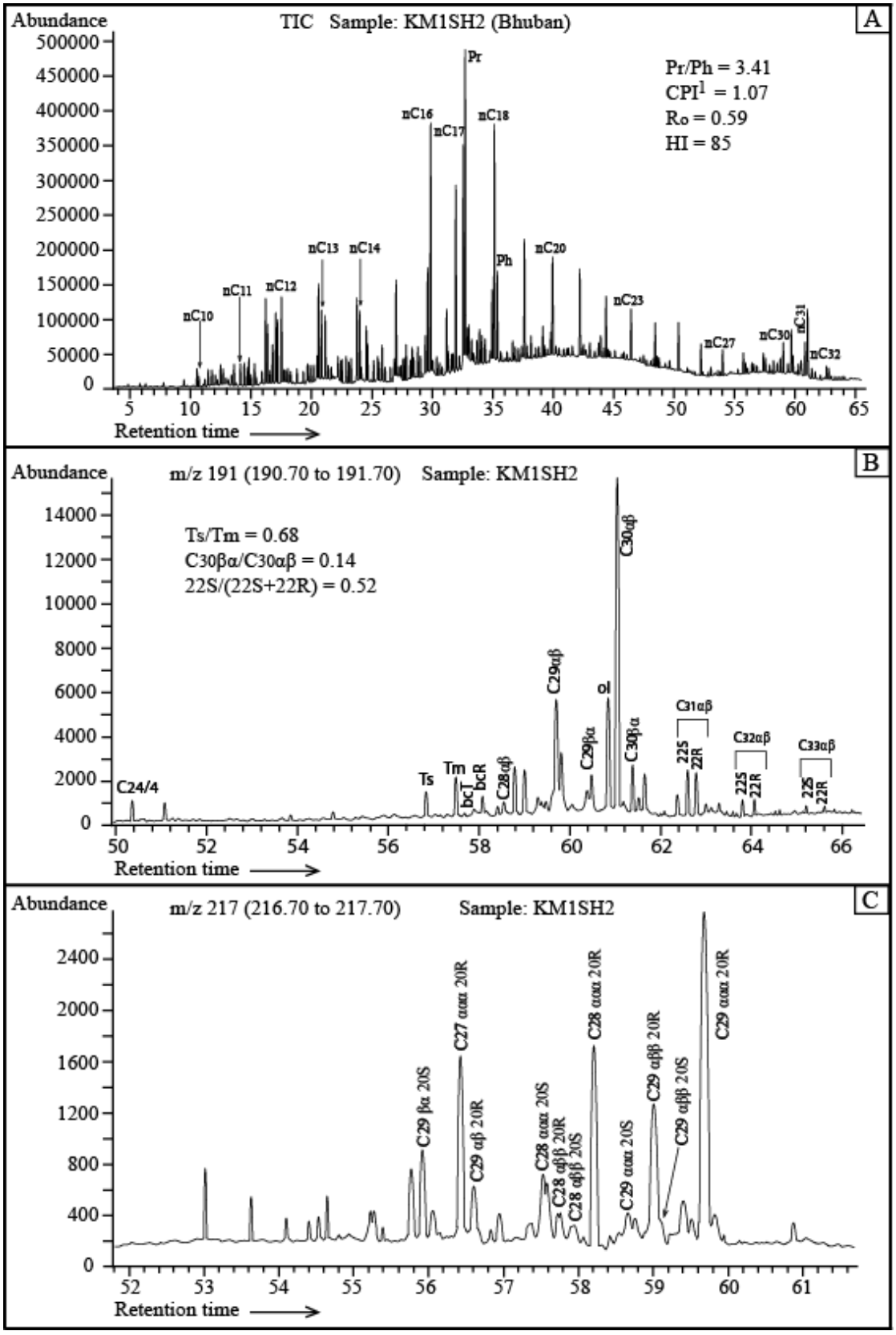

Fig.4.1.9. Gas chromatogram (TIC) and mass fragmentograms m/z 191 and m/z 217 of aliphatic fraction of a studied Bhuban sample (KM1SH2). It represents immature oil window (peak i.d. in Appendix B2).

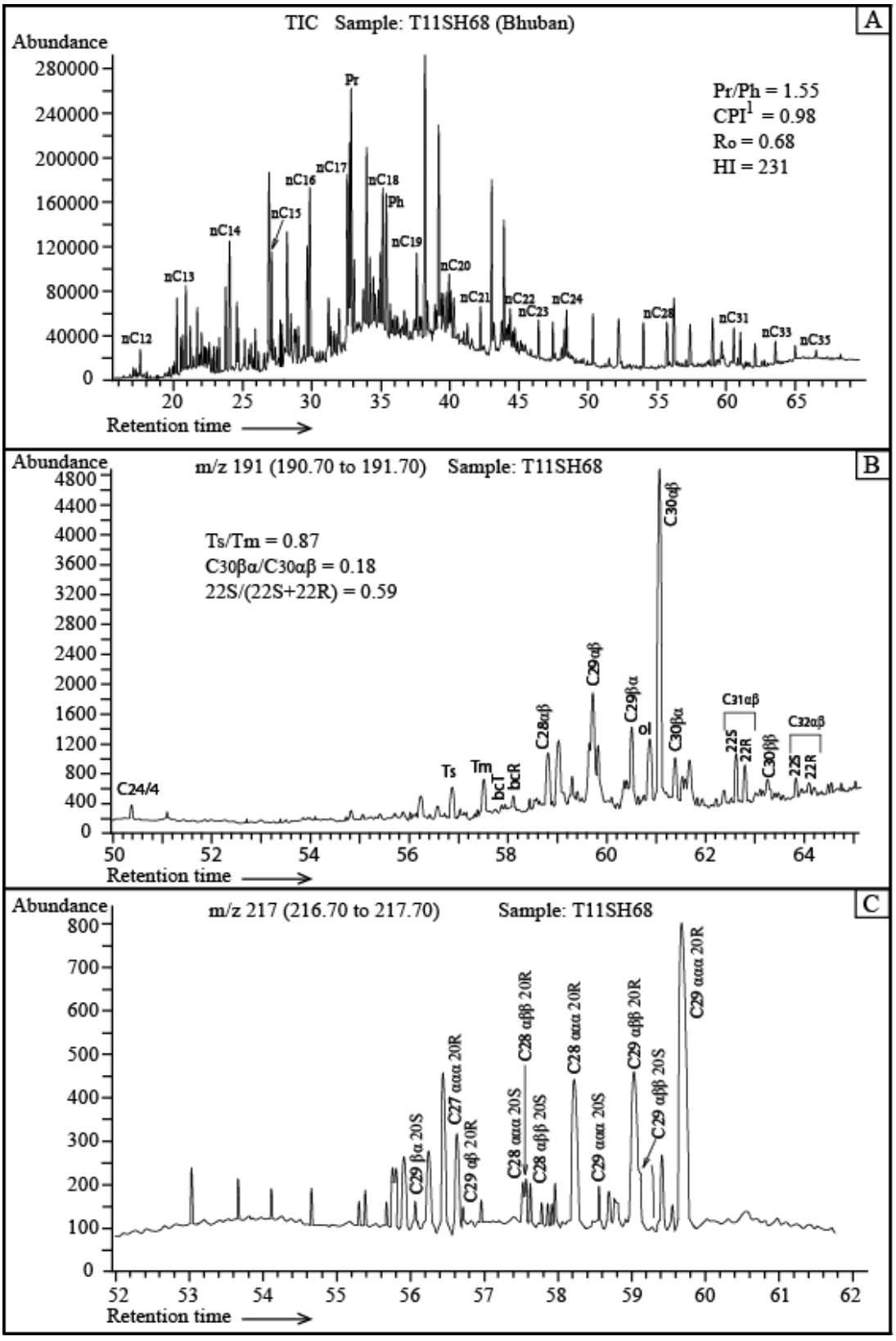

Fig.4.1.10. Gas chromatogram (TIC) and mass fragmentograms m/z 191 and m/z 217 of aliphatic fraction of a studied Bhuban sample (T11SH68). It represents mature oil window (peak i.d. in Appendix B2).

C_{30} moretane/C_{30} hopane and C_{32} 22S/(22S + 22R) range from 0.09 to 0.44 and 0.43 to 0.63, respectively, for the analyzed Bhuban Formation shales (Table 4.1.6). Similarly, C_{30} moretane/C_{30} hopane and C_{32} 22S/(22S + 22R) range from 0.05 to 0.36 and 0.43 to 0.65 respectively for the analyzed Boka Bil Formation shales. It is noted that the values of these features are very close to each other comparing with Bhuban and Boka Bil samples analyzed. Considerable abundances of 18α(H)-oleanane (higher plant marker) are found in all the studied samples. 18β(H)-oleanane is also identified in some of the analyzed samples. The calculated ol/C_{30}-hoapne (oleanane index) varies from 0.04 to 0.33 and 0.05 to 0.61 in the analyzed Bhuban and Boka Bil shales, respectively. Bicadinane (both T and R configurations) is identified in all the analyzed shale samples. The measured bc/C_{30}-hopane ranges from 0.02 to 0.11 (Bhuban) and 0.02 to 0.65 (Boka Bil). These values are plotted against the vertical depth profile (sample names shown here) of the study area (Appendix C9). The trend lines for both bc/C_{30}-hopane and ol/C_{30}-hopane values for Bhuban and Boka Bil formations do not show any definite agreement rather having inverse correlation each other. The trend line for bc/C_{30}-hopane shows better agreement with its data point where R^2= 0.3685 having negative gradient and it decreases with depth. On the other hand, the trend line for ol/C_{30}-hopane shows insignificant agreement among its data points irrespective of formation where the trend line shows positive gradient and R^2= 0.0065. It increases with depth profile.

4.1.3.3 GCMS: m/z 217 Fragmentogram

C_{29} sterane is the dominant component noted in the m/z 217 mass fragmentograms. These are dominated by regular steranes compared to diasteranes of the analyzed Bhuban and Boka Bil shale samples (Figs.4.1.7C, 4.1.8C, 4.1.9C and 4.1.10C and Appendices C5, C6, C7 and C8). The most commonly used sterane parameters include C_{29} 20S / (20S + 20R),

C_{29} ββ / (ββ + αα), sterane C_{27} / (C_{27}+C_{29}), diasteranes / steranes and diasterane 20S / (20S +20R). The values range from 0.03 to 0.37, 0.29 to 0.50, 0.20 to 0.48, 0.05 to 0.42 and 0.13 to 0.70, respectively, in the analyzed Bhuban shale samples. These parameters in the analyzed Boka Bil shale samples range from 0.03 to 0.38, 0.04-0.48, 0.23 to 0.64, 0.04-0.49 and 0.17-0.80, respectively (Table 4.1.7). The sterane abundance is very low compared to hopane compounds, marking the influence of mostly terrestrial organic matter (Huang and Meinschein, 1979; Peters et al., 2005).

4.1.4 Discussion

4.1.4.1 Thermal maturity

A thermally immature to early mature oil window was determined both for the examined Bhuban Formation and Boka Bil Formation shales, as shown by randomly measured mean vitrinite reflectance and T_{max} values. The measured mean vitrinite reflectance value ranges from 0.48 to 0.71 %R_o in the analyzed Bhuban shales and 0.48 to 0.70 %R_o in the analyzed Boka Bil shales. This implies the thermal maturity condition of the analyzed shale samples varies from immature to early mature for hydrocarbon generation (see Appendix B3 for standard parameters and their corresponding values) (Peters and Cassa, 1994). The T_{max} value obtained from SRA and RE ranges from 420 to 441 °C (Bhuban) and 420 to 440 °C (Boka Bil) indicates the analyzed Bhuban and Boka Bil shale samples are of thermally immature to early mature oil window, in good agreement with the interpretation made from vitrinite reflectance values (Farhaduzzaman et al., 2012d). The recorded production index (PI) value ranges from 0.11-0.40 in the analyzed Bhuban shales and 0.15-0.30 in Boka Bil shales, suggesting immature to early mature oil window conditions (Peters and Cassa, 1994).

The thermal maturity linked features of hopanes, steranes and diasteranes of the analyzed Bhuban and Boka Bil shales are mostly either at or close to their thermal equilibrium values. Commonly C_{31}- or C_{32}-homohopanes are used for calculations of the 22S/(22S+22R) ratio. This ratio rises from 0 to about 0.65 while 0.57 to 0.62 is the equilibrium range commonly observed during maturation (Seifert and Moldowan, 1986). The calculated ratio values are of 0.33-0.63 (Bhuban) and 0.33-0.65 (Boka Bil) for the studied shale samples falling within and outside the equilibrium range. Thus demonstrate the thermal maturity condition has reached partly, i.e., it represents immature to early mature oil window. For example, the analyzed Boka Bil shale sample SB1SH29 with the values of T_{max} 430 ˚C, vitrinite reflectance 0.54 $\%R_o$ and C_{32} 22S/(22S+22R) 0.50 demonstrate the sample is thermally immature. A similar immature thermogenic condition is also indicated by another Boka Bil sample PT5SH10 with the values of T_{max} 433 ˚C, vitrinite reflectance 0.57 $\%R_o$ and C_{32} 22S/(22S+22R) 0.48. But, the explored Boka Bil sample SB1SH48 with the values of T_{max} 440 ˚C, vitrinite reflectance 0.65 $\%R_o$ and C_{32} 22S/(22S+22R) 0.58 indicates the sample is thermally early mature for hydrocarbon generation. A similar early mature thermogenic condition is also suggested by another Boka Bil sample BK9SH71 with the values of T_{max} 437 ˚C, vitrinite reflectance 0.65 $\%R_o$ and C_{32} 22S/(22S+22R) 0.57. However, the analyzed Bhuban shale samples KM1SH2 and FN2SH7 correspond to immature oil window considering the maturity dependent factors (i.e., vitrinite reflectance, T_{max}, and biomarker ratio). Conversely, the analyzed Bhuban samples T11SH68 and BG1SH6 represent the early mature thermogenic condition for hydrocarbon generation following these evaluating parameters above. Mackenzie et al. (1980) reported the ratio of 17β(H),21α(H)-moretanes to their corresponding 17α(H),21β(H)-hopanes decreases with increasing thermal maturity from about 0.80 in immature bitumens to values of less than 0.15 in mature source rocks and in oils to a

minimum of 0.05. The calculated C_{30}-moretane/C_{30}-hopane ratio of the Bhuban and Boka Bil shales varies from 0.09 to 0.44 and 0.05 to 0.39, respectively. It matches the range of immature-mature thermal maturity condition. The cross-plot of ol/C_{30}-hoapne versus bc/C_{30}-hopane (Appendix C9) shows the bc/C_{30}-hopane generally decreases with depth whereas ol/C_{30}-hoapne increases with depth. This follows increased maturity of the analyzed samples with depth (e.g., Peters et al., 2005).

The calculated diasterane 20S / (20S + 20R) ratio of the studied shales varies from 0.13 to 0.70 (Bhuban) and 0.17 to 0.80 (Boka Bil). Mackenzie et al. (1980) stated the thermal equilibrium condition of the source rock might reach at the point of 0.60 for diasterane 20S / (20S + 20R). The calculated diasterane 20S / (20S + 20R) ratio of the analyzed Bhuban and Boka Bil samples again supports the range of immature to mature thermal condition as interpreted above. Nonetheless, the yellow-orange to orange-brown color corresponding to thermal alteration index (TAI) 2.5-2.8 of the identified spore under microscope (normal white reflected light) represents the immature to early mature oil window condition of the analyzed shale samples. The solid bitumen or bitumen stain is considered as 'free' or expelled hydrocarbon. This type of bitumen stain is observed in the analyzed shales under microscope. It also suggests the organic matter of the studied shales has partly expelled hydrocarbons in the related petroleum system of the Bengal Basin, Bangladesh.

4.1.4.2 Hydrocarbon generation potential

The cross-plot of T_{max} (°C) and production index (PI) shows that the organic matter of analyzed Bhuban and Boka Bil shale samples have already started to generate hydrocarbons (Powell, 1978; Farhaduzzaman et al., 2013h and 2013i) (Fig.4.1.11). It is also supported by the earlier interpretation based on vitrinite reflectance, TAI (2.5-2.8) and T_{max} values.

The measured SRA (or RE) T_{max} of the analyzed shale samples varies from 420 to 441 °C (Bhuban) and 420 to 440 °C (Boka Bil). The hydrocarbon generation usually starts at the maturity level of 435 °C (Peters and Cassa, 1994). The studied Bhuban and Boka Bil shales with low to fair TOC (Bhuban 0.14-1.42%; Boka Bil 0.14-0.57%), low to fair S2 values (Bhuban 0.13-3.76 mg HC/g TOC; Boka Bil 0.16-0.40 mg HC/g TOC), low to moderate total extract (Bhuban 132-2814 ppm; Boka Bil 235-1381 ppm), low to fair production index (Bhuban 0.11-0.40; Boka Bil 0.15-0.30), low to medium hydrocarbon yield (Bhuban 16-139 mg HC/g TOC; Boka Bil 35-282 mg HC/g TOC) and some liptinite macerals suggest poor to fair potential for hydrocarbon generation. The cross-plot of hydrocarbon yield (mg HC/g TOC) and hydrocarbon extract (%) corresponds to marginal to very good hydrocarbon potential of the analyzed Bhuban and Boka Bil shale samples (Fig.4.1.12). But this interpretation of high quality source potential is not supported by the other evidences. The mean vitrinite reflectance value ranges from 0.48 to 0.71 $\%R_o$ in the analyzed Bhuban shales and 0.48-0.70 $\%R_o$ in Boka Bil shales (equilibrium value is about 0.60) suggests that the organic matter of the analyzed Bhuban and Boka Bil samples have partly achieved the thermal maturity level for hydrocarbon generation. The dominancy of short chain n-alkanes (C_{16}-C_{20}) in the gas chromatogram (TIC) of both the Bhuban and Boka Bil Formations indicates the generation of gaseous hydrocarbon with some condensate. The liquid hydrocarbon potential in the analyzed shale samples is most likely due to the presence of liptinitic macerals (Farhaduzzaman et al., 2013j). The triangular diagram based on petrographic analyses (vitrinite-liptinite-inertinite) (Fig.4.1.13) indicates that the organic matter of the analyzed Bhuban and Boka Bil shale samples are suitable for gas generation. In fact, the entire petroleum discovery is natural gas with little amount of condensate and oil in the Bengal Basin, Bangladesh. This is in good agreement with the

present interpretation of hydrocarbon generation potential of the Bhuban and Boka Bil Formations.

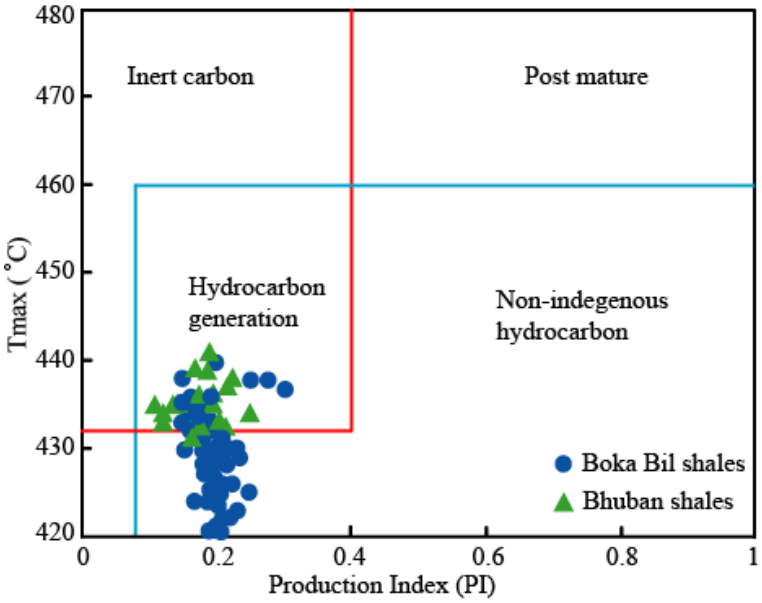

Fig.4.1.11. A cross-plot of T_{max} (˚C) and production index (PI). Both of the studied Bhuban and Boka Bil shale samples fall within and outside the hydrocarbon generation regime. But Bhuban shows relatively higher maturity (c.f., Powell, 1978).

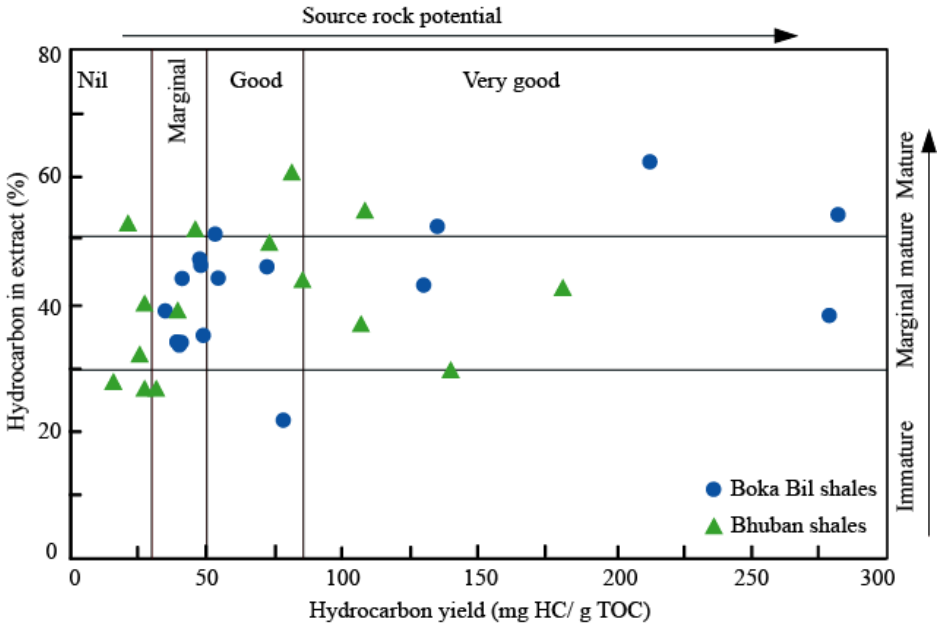

Fig.4.1.12. A cross-plot of HC yield and hydrocarbon in extract. The studied Bhuban and Boka Bil shale samples correspond mostly to marginal-good quality petroleum source rock potential with marginal to early mature thermogenic condition (e.g., Powell, 1978).

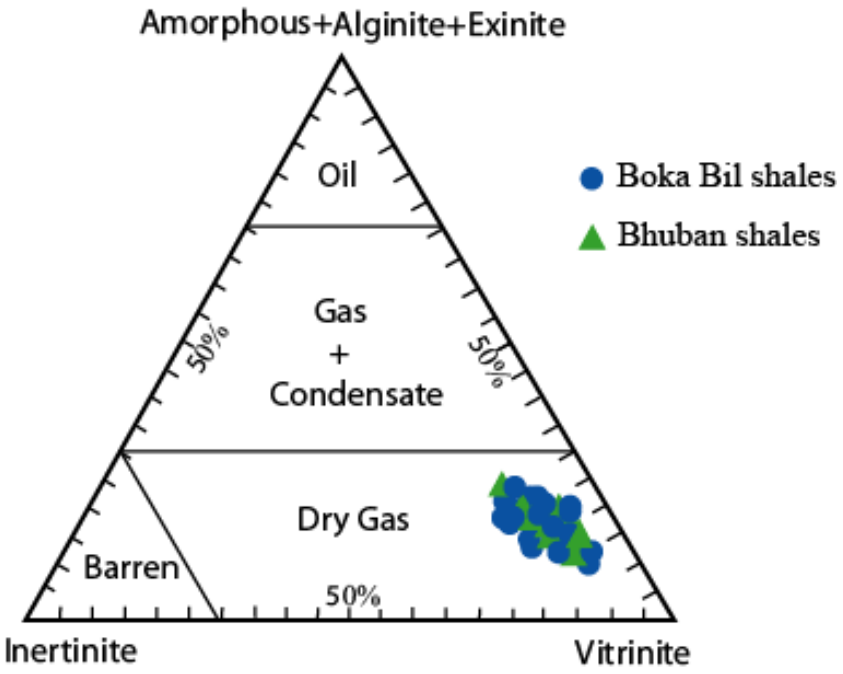

Fig.4.1.13. A triangular diagram from visual kerogen analysis (vol %). The analyzed Bhuban and Boka Bil shales represent the generation potential for dry gas (gas-prone) (adopted after Tissot and Welte, 1978).

4.1.4.3 Environment of deposition

The depositional environment of shale and its condition of deposition is often considered as very complex. The modeled steranes triangular plot (Fig.4.1.14) indicates that both of the analyzed Bhuban and Boka Bil shales deposited mostly in terrestrial environmental setting with some marine inputs (Huang and Meinschein, 1979). Diasteranes comparing with regular steranes depend on both lithology and maturity (Peters and Moldowan, 1993). They are, therefore, often used to distinguish carbonate facies (low diasteranes) from clastic facies (Waples and Machihara, 1991). The noticeable presence of diasteranes compared to steranes of the analyzed Bhuban and Boka Bil shale samples characteristically supports the clastic depositional facies.

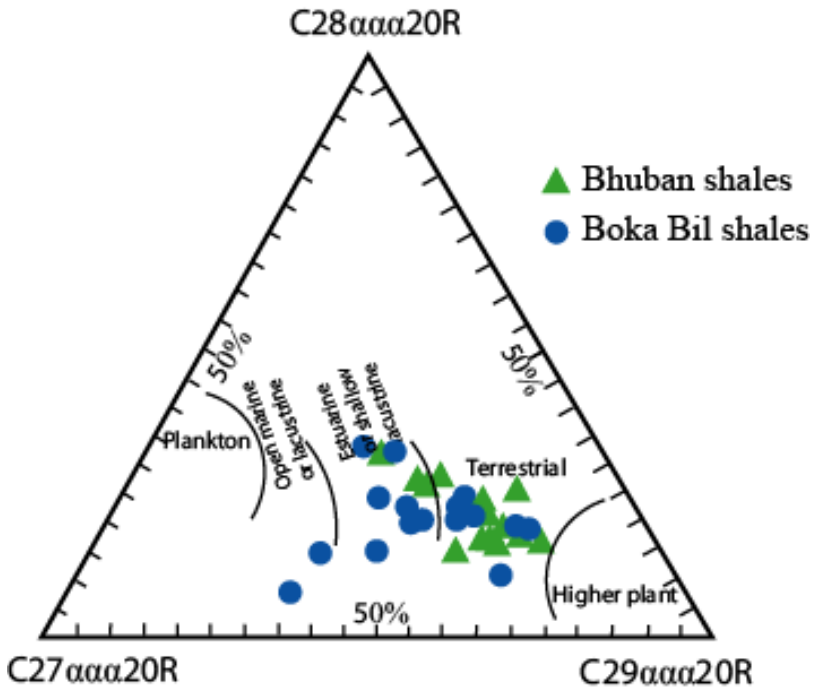

Fig.4.1.14. Relationship between sterane compositions, source input and depositional environment. Both of the analyzed Bhuban and Boka Bil Formation shales are dominated by terrestrial organic matter input. A minor contribution is from marine sources (e.g., Waples and Machihara, 1991).

The cross-plot of Pr/nC_{17} versus Ph/nC18 (Fig.4.1.15) based on the analyzed samples implies the source of the organic matter of Bhuban and Boka Bil shales is derived mainly from a terrestrial environment. The environment of deposition was an alternation of oxic (oxidation) to anoxic (reduction) conditions (Peters et al., 2005). The cross-plot of Pr/Ph versus $C_{27}/(C_{27}+C_{29})$ sterane from the present study (Bhuban and Boka Bil Formations) indicates mostly the terrestrial depositional environment with oxic-anoxic depositional condition (Waseda and Nishita, 1998) (Fig.4.1.16). The marine (pelagic) influence is also suggested by this diagram, in good agreement with the early interpretation above. The presence of cadalene, the diaromatic counterpart of cadinane identified in the analyzed PyGC pyrograms, represents another terrestrial marker compound. This is consistent with low thermal maturity as observed in the studied Bhuban and Boka Bil samples (Aarssen et al., 1992; Wan Hasiah, 1999a).

The presence of bicadinane in the gas chromatograms (m/z 191) of the analyzed Bhuban and Boka Bil samples also supports this terrestrial depositional setting as previously reported by Pearson and Alam (1993).

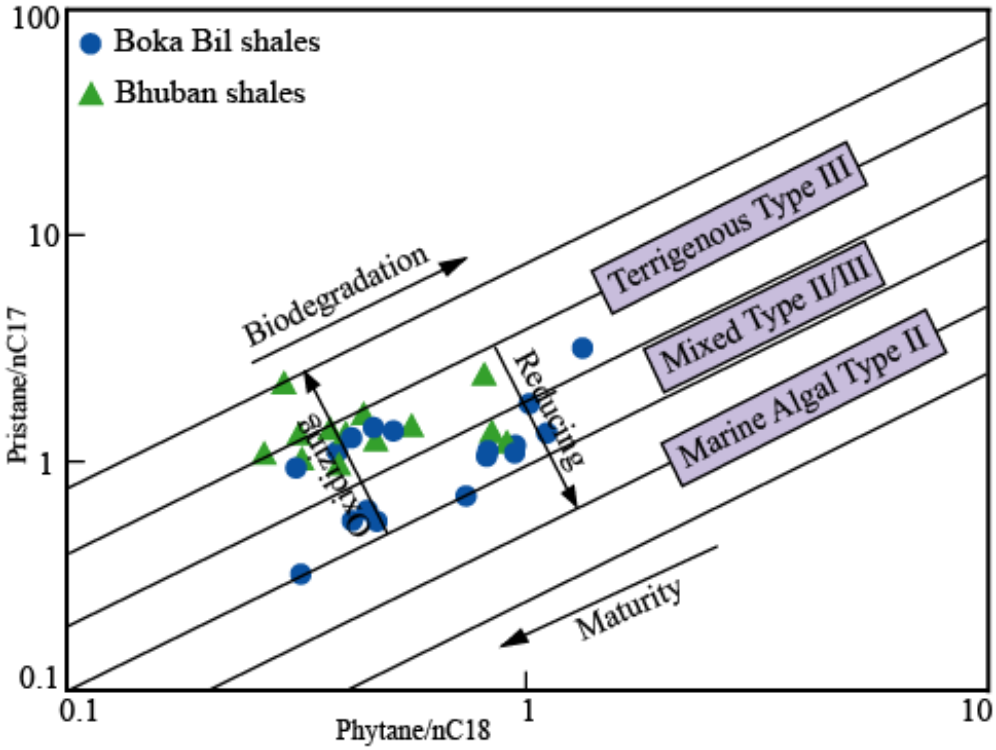

Fig.4.1.15. A plot of pristane/nC_{17} versus Phytane/nC_{18} for the examined samples infer oxicity and organic matter of the source rock depositional environment (e.g., Peters et al., 2005; Koeverden et al., 2011). The analyzed Bhuban and Boka Bil samples support the terrigenous Type III and mixed Type III/II source regions under oxic-anoxic condition.

The oxic condition of any terrestrial depositional environment has extensively been appraised by various authors considering the ratio of Pr/Ph (Brooks et al., 1969; Powell and McKirdy, 1973; Peters and Moldowan, 1993). They reported that pristane formation occurs in oxidizing environments (e.g., swampy peat bogs) whereas phytane occurs in reducing type environments. The source rocks with Pr/Ph ratio greater than one are more likely to have formed in an oxidizing environmental setting. However, there are some complexities in the mode of their formation.

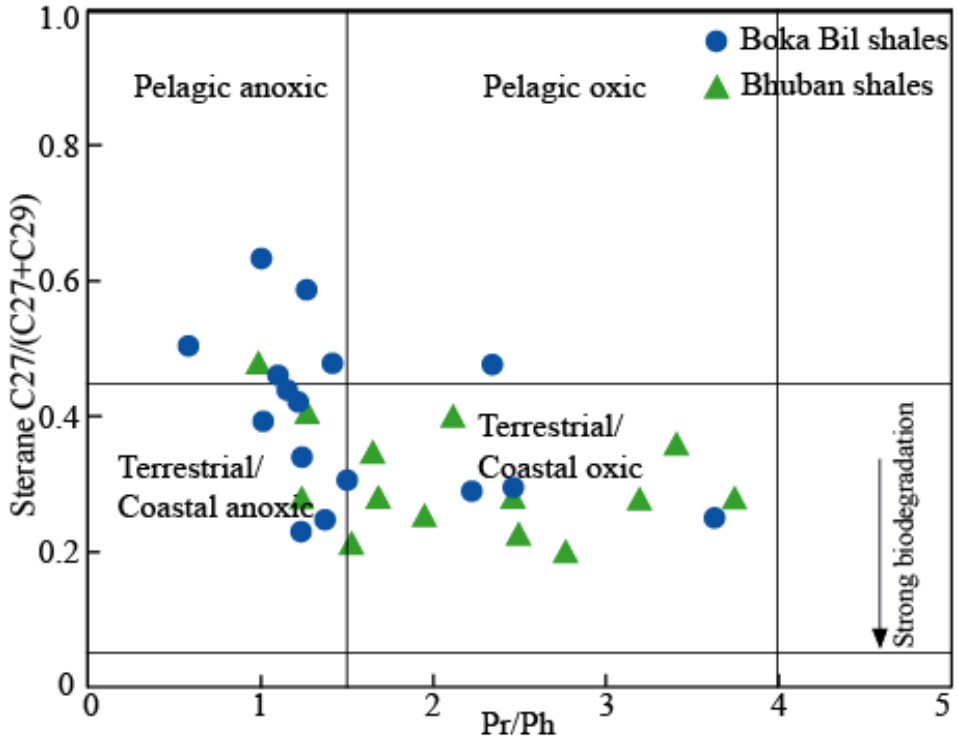

Fig.4.1.16. A cross-plot of Pr/Ph ratios and sterane $C_{27}/(C_{27}+C_{29})$ values related to deposition environment and source. Both of the analyzed Bhuban and Boka Bil shales suit terrestrial (oxic-anoxic) depositional setting and minor influence from pelagic source (c.f., Waseda and Nishita, 1998; Sawada, 2006; Hossain et al., 2009).

Peters and Moldowan (1993) argued that samples within the oil-generative window having high Pr/Ph ratios >3 indicate terrestrial organic matter under oxic conditions. Therefore, the Pr/Ph ratios of the analyzed shales, ranging from 0.99 to 3.41 (Bhuban Formation) and 0.58 to 3.65 (Boka Bil Formation), indicate terrestrial environment. And the condition of deposition was oxic. Nevertheless, the dominating C_{31}-homohopane and the large amounts of moretane of the explored Bhuban and Boka Bil shale samples also suggest the terrestrial environments as claimed by Waples and Mashihara (1991) and Peters and Moldowan (1993).

Mello et al. (1988), Barakat et al. (1997) and Huang and Pearson (1999) stated that the Ts/Tm value below one implies the lacustrine or marine environment and above one marks nonmarine or marine deltaic environment. The calculated Ts/Tm value of the analyzed Bhuban (0.09-0.87) and Boka Bil (0.12-1.86), however, supports the mixed (nonmarine to marine) depositional environment.

Berner and Raiswell (1984) discussed the source rocks with C/S ratio 0.5-5 represent marine environment while C/S ratio greater than 10 corresponds to nonmarine (fresh water or terrestrial) environment. The measured C/S ratio of the analyzed shale samples ranges from 4.2 to 128.6 (Bhuban Formation) and 2.4 to 53.3 (Boka Bil Formation). This indicates a mixed depositional environment, i.e., mostly terrestrial depositional settings with slight marine influenced sources. Sampei and Matsumoto (2001) used C/N ratio as an indicator for the organic matter found in the source rocks. They stated the C/N $\geq$15 implies the terrestrial vascular plants. The calculated C/N ratio of the analyzed shale samples varies from 0.6 to 13.3 (Bhuban Formation) and 0.8 to 4.2 (Boka Bil Formation) representing mixed depositional environmental sources (nonmarine to marine) for organic matter. So, in the source rocks containing less than 1% TOC, the inorganic nitrogen has influenced the ratio of C/N. It eventually has decreased the ratio values. This observation agrees with the observation previously reported by Sampei and Matsumoto (2001).

The current observation mentioned above suggests the organic matter derived mostly from terrestrial plants with minor influence from marine sources. The environment of deposition was an alternation of oxic to anoxic conditions. The terrestrial depositional environment is also supported by dominating vitrinite macerals and the high presence of woody fragments.

The marine influence is suggested by the presence of liptinite macerals (resinite, cutinite and liptodetrinite) and fluorescent amorphous materials under microscope. Detailed palynological study and isotopic analyses could be recommended for further clarification of its depositional type and geological settings.

4.1.4.4 Stratigraphic correlation

Most of the stratigraphic terms now used to describe the Tertiary successions of the Bengal Basin (Bangladesh) have been established in comparison to those of Lower or Upper Assam (India). Evan's (1932) classification of sediments is based almost only on lithologic characteristics and represents merely a local stratigraphy (Das Gupta, 1977). Because of lack of marker horizons (Khan and Muminullah, 1980), diachronism of formations and due to spatial changes in lithologies (which commonly occur in prograding delta sequences), it is impossible to lithologically correlate certain formations between different parts of a basin or even between two different basins as tried in the Bengal Basin (Bangladesh) in the past (Das Gupta, 1982; Reimann, 1993). The Tipam Sandstone, for instance, has a Miocene age in the Upper Assam Basin. This deltaic-fluviatile succession has a Pliocene age in the eastern portion of the Surma Trough (a sub-basin of the Bengal Basin), Bangladesh.

Surma Group has been divided into two formations: the lower Bhuban Formation and the upper Boka Bil Formation. Both the Bhuban and Boka Bil Formations show extensive lateral facies change as well as vertical variation in sand to shale ratio from place to place. This has made it difficult to correlate the units across the basin. Many workers have pointed out the subdivision of monotonous and repetitive sand-shale of Surma Group into Bhuban and Boka Bil Formations is often ambiguous without diagnostic criteria (Johnson and Alam, 1991; Imam, 2005).

Alam et al. (2003) reported the contact between the Bhuban and Boka Bil Formations or the internal units of these formations is difficult to recognize based on the Evan's (1932) scheme of lithostratigraphic correlation.

The findings of the current study from the geochemical and petrographical methods (e.g., organic matter quantity, quality and maturity, hydrocarbon generation potential, hydrocarbon yield, maceral analysis, elemental analysis and depositional environment) show there is no major difference between the studied shales of Bhuban and Boka Bil Formations, the Bengal Basin, Bangladesh (Farhaduzzaman et al., 2012b). For example, both Bhuban and Boka Bil shales correspond to similar properties which are shown in Appendix C10.

4.2 PETROLEUM SOURCE ROCK- PERMIAN COALS

4.2.1 Macroscopic Study of Coals

4.2.2 Microscopic Study of Coals

4.2.3 Organic Geochemical Study of Coals and Associated Sediments

Chapter 4.2.1 Macroscopic Study of Coals

A total of 27 coal samples are used for proximate and elemental analyses. Eleven samples form Barapukuria Coal Basin and 11 samples from Dighipara Coal Basin are used for the present purpose. An additional five bulk coal samples (collected from a stockpile of coal mine) are also analyzed for comparative assessment with the results obtained from core samples.

4.2.1.1 Coal seam characteristics

Six seams (Seam I, Seam II, Seam III, Seam IV, Seam V and Seam VI) are identified in the Barapukuria Basin (Armstrong, 1991). Seam VI is the thickest seam (average 36m) and apart from some thin impersistent bands of coal below, it is the basal coal seam in this Gondwana basin. It contains bulk of the Barapukuria coal resource (>90%). On the other hand, three seams (Seam A, Seam B and Seam C) are recognized in Dighipara Basin. The maximum cumulative coal thickness encountered in the Dighipara is 71m (Hasan and Islam, 2003). There is a close similarity of these coals with the Permian coals of Australia, South Africa and India (Armstrong, 1991; Akhtar, 2001; Farhaduzzaman et al., 2008). The sulfur content (%) of the coals from both of these Barapukuria and Dighipara basins is low. According to JMG results, it is 0.61% for Barapukuria coals and 0.66% for Dighipara coals. The calculated gross calorific value (GCV) is 5466-7032 (mean 6313) kcal/kg and 4815-7303 (mean 6382) kcal/kg for Barapukuria and Dighipara coals respectively.

The coals of Barapukuria and Dighipara are mainly banded dull to dull in nature as stated by the JORC Code (2004). The coals of Dighipara, on the other hand, show higher amounts of bright bands than those of Barapukuria. Banded bright and bright banded coals are not uncommon in the studied coal seams of the Barapukuria and Dighipara. The coal is highly

cleated. The cleats are generally irregular to planar and pyritic infill is common along the joint planes and cleats. Few photographs of the studied coals are shown in Fig.4.2.1.1.

4.2.1.2 Proximate analysis

The proximate analysis of coal can be reported on the basis of four ways as mentioned below (World Coal Institute, 2007):

- As received (ar)- includes total moisture (TM).
- Air dried (ad)- includes inherent moisture (IM) only.
- Dry basis (db)- excludes all moisture.
- Dry ash free (daf)- excludes all moisture and ash.

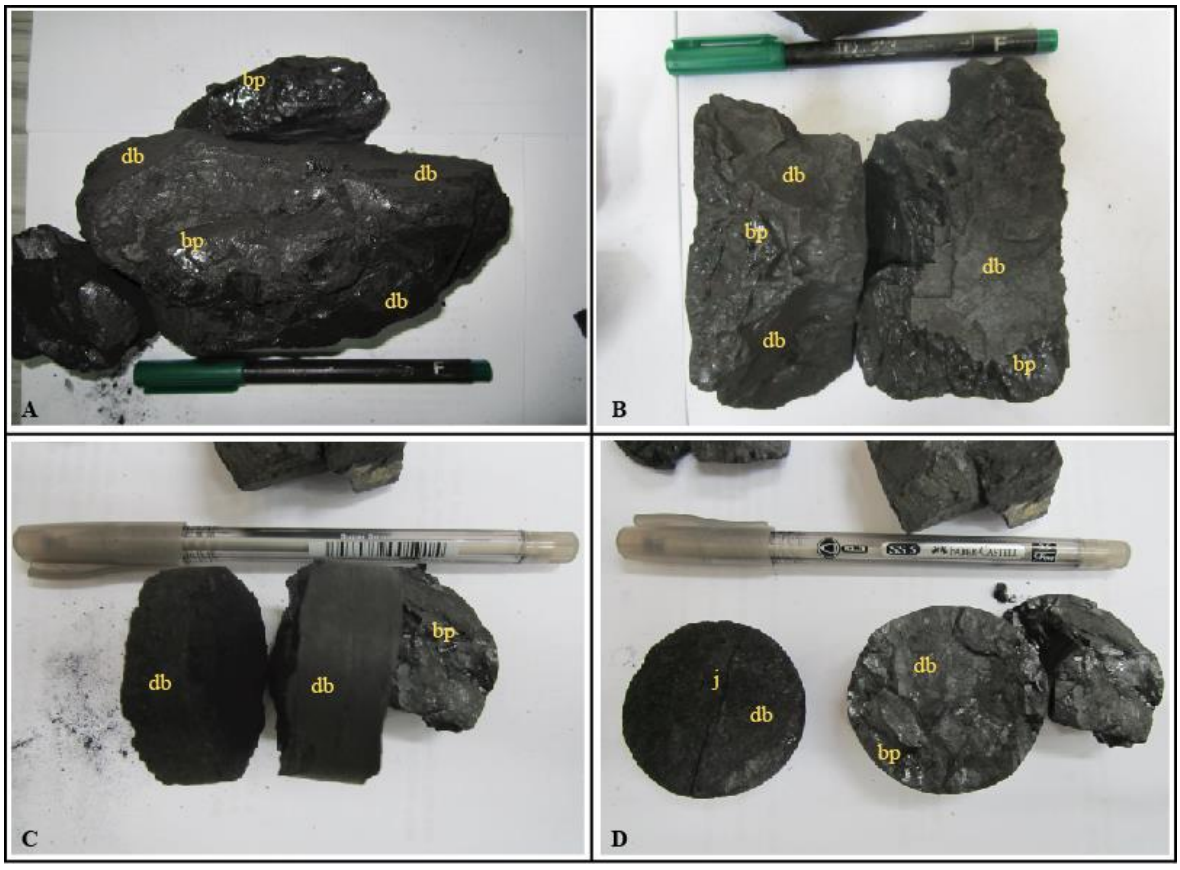

Fig.4.2.1.1. Photographs of coal samples collected from the Barapukuria and Dighipara basins. (A) and (B) are the bulk samples of Barapukuria Basin whereby (C) and (D) are the core samples of Dighipara Basin. The samples show different bands of coal, e.g., dull band (db) and bright parting (bp) along with a joint (j) in photograph D. This is a characteristic feature of a bituminous coal.

Table 4.2.1.1. The proximate analysis results (air dried, ad-basis) obtained from TG-DTA (ASTM D5800-96) method (UM Geology Lab; denoted by TGA) and ASTM D2013-07 (Geoscience Malaysia Lab; denoted by JMG) of the studied coal samples. Sulfur content (%) and gross calorific value (GCV, kcal/kg) are also added. 'Arm' denotes the results taken after Armstrong (1991).

Sample	Moisture %(TGA)	Moisture %(JMG)	Volatiles %(TGA)	Volatiles %(JMG)	Fixed C %(TGA)	Fixed C %(JMG)	Ash %(TGA)	Ash %(JMG)	Sulfur %(Arms)	Sulfur %(JMG)	GCV (Arms)	GCV (JMG)
Barapukria coal cores												
BPCL9	4.17	2.80	32.21	30.40	58.53	53.30	5.09	13.50	-	0.66	-	6404
BPCL12	3.26	2.90	22.66	30.40	54.94	49.20	19.14	17.50	-	0.59	-	5466
BPCL13	4.00	3.00	28.88	30.00	54.11	53.80	13.01	13.20	-	0.55	-	6439
BPCL15	3.67	2.90	25.54	31.70	56.79	58.70	14.00	6.70	-	0.78	-	7032
BPCL16	3.91	2.70	26.07	27.40	55.47	53.70	14.55	16.20	-	0.42	-	6235
BPCL17	3.25	2.00	27.16	28.10	48.05	44.70	21.54	25.20	-	0.46	-	5727
BPCL18	4.54	2.70	31.10	29.80	53.83	47.80	10.53	19.70	-	0.72	-	5929
BPCL24	3.96	3.90	32.10	31.80	49.84	55.40	14.10	8.90	-	0.61	-	6837
BPCL25	4.63	3.30	25.31	28.00	56.85	55.60	13.21	13.10	-	0.65	-	6437
BPCL27	4.31	2.70	25.19	29.00	52.61	56.40	17.89	11.90	-	0.58	-	6853
BPCL28	4.32	3.00	26.85	27.50	52.68	50.60	16.15	18.90	-	0.71	-	6087
Range	3-5	2-4	23-32	21-32	48-59	45-59	5-22	7-25	0.32-1.33	0.42-0.72	5669-6403	5466-7032
Mean	4	3	28	29	54	53	15	15	0.77	0.61	5806	6313
Dighipara coal cores												
DPCL30	4.47	3.00	30.19	32.30	58.35	59.00	6.99	5.70	-	0.61	-	7239
DPCL31	4.16	3.00	27.73	30.10	62.76	60.80	5.35	6.10	-	0.49	-	7249
DPCL32	4.45	3.20	31.14	33.50	59.36	56.00	5.05	7.30	-	0.88	-	7185
DPCL34	3.41	2.70	28.76	33.00	50.86	51.10	16.97	13.20	-	0.74	-	6658
DPCL35	5.11	2.90	29.86	30.10	59.27	59.20	5.76	7.80	-	1.14	-	7057
DPCL36	3.60	2.60	32.24	32.10	58.78	58.60	5.38	6.70	-	0.58	-	7303
DPCL37	2.44	2.00	25.55	23.80	22.89	47.70	22.95	26.50	-	0.41	-	4974
DPCL38	5.96	2.30	29.85	22.40	45.22	46.50	18.97	28.80	-	0.32	-	5353
DPCL39	5.51	4.60	27.92	26.10	62.28	56.30	4.29	13.00	-	0.63	-	6464
DPCL40	3.15	3.20	25.96	26.70	56.45	48.60	14.44	21.50	-	0.83	-	5909
DPCL44	2.56	2.00	25.78	22.60	45.52	48.20	26.14	27.20	-	0.61	-	4815
Range	2-6	2-5	26-32	23-34	45-62	48-61	4-26	6-29	-	0.32-1.14	-	4815-7303
Mean	4	3	29	28	55	54	12	15	-	0.66	-	6382
Barapukuria bulk coals												
BP6CL1	2.78	-	31.10	-	50.17	-	15.95	-	-	-	-	-
BP6CL2	2.94	-	28.90	-	52.97	-	15.19	-	-	-	-	-
BP6CL3	2.54	-	33.56	-	58.68	-	5.22	-	-	-	-	-
BP6CL4	2.16	-	31.13	-	60.11	-	6.60	-	-	-	-	-
BP6CL5	3.10	-	30.62	-	51.97	-	14.31	-	-	-	-	-
Range	2-3	-	29-34	-	50-60	-	5-16	-	-	-	-	-
Mean	3	-	31	-	55	-	12	-	-	-	-	-

The proximate analysis is carried out on air dried (ad) basis for the currently investigated coal samples. The results of proximate analysis (ad basis) including sulfur content (%) and gross calorific value (GCV, kcal/kg) of coals from the Barapukuria and Dighipara basins

are displayed in Table 4.2.1.1. Here the data taken from two laboratories such as University Malaya Geology Laboratory (denoted by TGA) and Minerals and Geoscience Department Malaysia (denoted by JMG) are compared. It finds a good similarity between these two results which has increased the confidence level of the data usage. The moisture, volatile matter, fixed carbon and ash are measured: 3-5%, 23-32%, 48-59% and 5-22% respectively for coal core samples of the Barapukuria Basin. These values are 2-6%, 26-32%, 45-62% and 4-26%, respectively for coal core samples of the Dighipara Basin. Bulk coal samples are also analyzed for comparative assessment with the core samples of the Barapukuria Basin. The values of moisture, volatile matter, fixed carbon and ash of the Barapukuria bulk samples are 2-3%, 29-34%, 50-60% and 5-16%, respectively. The arithmetic mean of carbon, hydrogen, nitrogen, sulfur and oxygen are defined (dry ash free- daf basis) 83%, 5.1%, 1.7%, 0.77% and 9.4%, respectively for Barapukuria (Armstrong, 1991).

The ash analysis (elemental concentration as oxides) of the Barapukuria coals has already been carried out by Armstrong (1991). But there is no work published on Dighipara coals and accordingly the elemental concentration (ppm, ad basis) of Dighipara coals has been measured (Table 4.2.1.2).

4.2.1.3 Discussion

The random mean vitrinite reflectance (%VR_r) of Barapukuria coal ranges from 0.72 to 0.78% while it ranges from 0.70 to 0.80% for Dighipara coals (details in chapter 4.2.3). Proximate analysis is one of the most important tools to investigate the geochemical properties of coal (World Coal Institute, 2007; Belkin et al., 2009). It can be used to establish the rank of coals and it provides the basis for buying and selling (ASTM D 3172-89).

Table 4.2.1.2. Ash yield (%, ad basis) and elemental concentration (ppm, ad basis) with Clarke values or world average (Valkovic, 1983; Ketris and Yudovich, 2009) of Dighipara Basin coals (Cr = Chromium, Ni= Nickel, Pb= Lead, Co= Cobalt, Cu= Copper, Fe= Iron, K= Potassium, Mg= Magnesium, Zn= Zinc, Ca= Calcium, Sr= Strontium, Cd= Cadmium).

Sample	Cr	Ni	Pb	Co	Cu	Fe	K	Mg	Zn	Ca	Sr	Cd	Ash
DPCL30	11	40	3	33	14	1756	205	51	28	3	2	7.84	6.99
DPCL31	77	19	3	15	11	943	70	15	16	5	3	1.52	5.35
DPCL32	31	22	2	12	20	730	402	50	30	3	1	1.76	5.05
DPCL34	26	23	8	21	24	1126	550	44	61	1	1	2.22	5.76
DPCL35	13	124	12	57	11	3065	142	95	22	54	18	1.68	5.38
DPCL36	13	9	2	3	27	540	204	50	42	4	1	2.04	22.95
DPCL37	59	38	1	7	31	4655	1598	551	92	26	1	2.68	18.97
DPCL38	44	46	15	12	41	12344	757	37	310	1	5	3.16	16.97
DPCL39	24	28	1	8	10	2193	65	113	64	2	2	2.12	4.29
DPCL40	44	50	20	12	43	1247	568	72	80	43	10	2.24	14.44
DPCL44	123	24	11	4	26	1777	1557	220	23	1	2	2.30	26.14
Mean	42	38	7	17	24	1852	556	118	70	13	4	2.69	12
Range	11-123	9-124	1-20	3-57	10-43	540-4655	65-1598	15-551	16-310	1-54	1-18	2-8	4-26
Clarke	17±1	17±2	9±0.7	6±0.2	16±1	10000	100	200	28±2	10000	100±7	0.2±0.04	--

Fig.4.2.1.2. The elemental concentration of the analyzed coal samples from the Dighipara Basin. Mostly all of the identified elements cross their Clarke values which point to the environmental hazards during combustion.

4.2.1.3.1 Moisture contents

Moisture is an important property of coal since all coals are mined wet. Groundwater and other extraneous moisture is known as adventitious moisture and is readily evaporated. Moisture held within the coal itself is known as inherent moisture (IM) and is analyzed quantitatively. According to results of TGA and JMG laboratories, the measured IM is low (2-6%).

4.2.1.3.2 Volatile matter

Volatile matter in coal refers to the components of coal (except for moisture) which are liberated at high temperature in the absence of air. This is usually a mixture of short and long chain hydrocarbons, aromatic hydrocarbons and some sulfur. The volatile matter is fairly high in both of the investigated basin coals. Measured volatile matter and ash content of Barapukuria coals are 28% and 14% (mean) while these are 29% and 12% (mean) for Dighipara coals (air dried basis; TGA laboratory). These mean values are 29% and 15% for Barapukuria and 28% and 15% for Dighipara coals following JMG laboratory respectively. These parameters are frequently used to classify the coal ranks and types (Stach et al., 1982; Singh and Singh, 1996). The coals of both basins are of similar high volatile bituminous B rank.

4.2.1.3.3 Ash yield

Ash content of coal is the non-combustible residue left after coal is burnt. It represents the bulk mineral matter after carbon, oxygen, sulfur and water are driven off during combustion. The ash content is low (4-26% TGA laboratory; 6-29% JMG laboratory) in the currently analyzed coal samples from both basins.

4.2.1.3.4 Fixed carbon

The fixed carbon content of the coal is the carbon found in the material which is left after volatile materials are driven off. This differs from the ultimate carbon content of the coal because some carbon is lost in hydrocarbons with the volatiles. Fixed carbon is used as an estimate of the amount of coke that will be yielded from a sample of coal. The high content of fixed carbon (48-60% TGA laboratory; 45-61% JMG laboratory) in the presently

analyzed coals indicates that these coals can partly be used to produce coke. This byproduct (coke) is an important fuel for the steel industries.

4.2.1.3.5 Elemental concentrations

A compositional analysis including major, minor and trace elements of coal is useful in the overall description of the coal quality (Finkelman, 1999). It is used to predict behavior of ashes and slags in combustion chamber (ASTM D 3682-87). The concentration of elements measured is correlated with coal Clarke values as well as themselves. 'Clarke' is the average content of a given chemical element in the Earth's crust and also in the hydrosphere (Ketris and Yudovich, 2009). Almost all of the identified elements exceed the coal Clarke values in the analyzed coal samples (Table 4.2.1.2 and Fig.4.2.1.2A-F). The toxicity of elements in coal and coal ashes and their environmental significance have been evaluated extensively by various authors (e.g., Swaine, 1990; Spears and Zheng, 1999; Goodarzi, 2002; Finkelman et al., 2002; Finkelman, 2004; Ren et al., 2004; Jorjani et al., 2008; Sia and Wan Hasiah, 2011; Dai et al., 2012). In general, the elements in coal can be divided into two broad groups namely (a) elements of prime environmental concern and (b) elements that could be of environmental interest (Swaine, 1990; Goodarzi, 2002). The first group includes Cr, Cd, Ni, Pb, As, F and Hg. The later includes Co, Cu, Zn, Mn, B, Be, Cl, Mp, Sb, Sn, Th, Ti, U and V.

The chromium (Cr) in the studied samples is fairly high (mean 42ppm) compared to the coal Clarke value (17±1ppm) (Fig.4.2.1.2A). Based on China coals, Ren et al (2004) stated that high concentration Cr could be one of the important causes of lung cancer. So it is one of the potentially hazardous elements in the studied coals. Mixed layer clay minerals, pyrite and hematite are considered as the host for Cr (Goodarzi, 2002). The nickel (Ni) content

(mean 38ppm) of the analyzed samples is high compared to the Clarke value (17±2ppm) (Fig.4.2.1.2A). Its origin is not well established (Swaine, 1990), but is thought to be occurred in millerite (Ni) and organic matter. Asthma, central nervous system effects, gastrointestinal effects, headache, neoplasia of lung and respiratory tract are some common health effects attributed to nickel exposure (Gupta, 1999).

Lead (Pb) is considered as both potentially hazardous element and regulated constituent as solid waste (Resources Conservation and Recovery Act RCRA, 1976). Chronic Pb poisoning often begins with vague symptoms in human health such as anorexia, muscle discomfort, malaise and headache as well as gastrointestinal effects (Gupta, 1999; Finkelman, 2004). The occurrence of Pb is most commonly associated with the minerals galena (PbS) (Swaine, 1990; Dai et al., 2006) and less commonly with clausthalite (PbSe) and crocoite ($PbCrO_4$) (Hower and Robertson, 2003; Sia and Wan Hasiah, 2011). Most of the samples showed low Pb concentration (mean 7ppm) (Fig.4.2.1.2B). Few samples show higher than the Clarke value (9±0.7ppm) and it could be a concern for environmental consideration. The copper (Cu) content (mean 24ppm) is much higher than the Clarke value (16±1ppm) (Fig.4.2.1.2B). It occurs in sulfur bearing minerals (e.g., chalcopyrite) and other clays and carbonates (Goodarzi, 2002). Gastrointestinal disorder is the main effect caused by high contents of copper (Gupta, 1999). It could be a hazardous element in the studied area during coal combustion.

The magnesium (Mg) concentration (mean 118ppm) of the analyzed coal is not too high falling below the world average (200ppm) (Fig.4.2.1.2C). It is related with clay minerals as well as the carbonates (Finkelman, 1994; Sia and Wan Hasiah, 2011). But hence it is consistent with association of clay minerals instead with carbonates.

To date there is no reported deleterious health or environmental impacts from zinc (Zn) emissions while utilizing the coal in coal-fired power plants (Swaine, 1990). The enrichment of Zn in coals is mostly related with the mineral sphalerite. Albeit mostly all of the samples show higher concentration than the Clarke value but hence the Zn is not a hazardous element (Fig.4.2.1.2C).

The cadmium (Cd) concentration is much higher (mean 2.69ppm) compared to the Clarke value (0.2±0.04) (Fig.4.2.1.2D). Cd occurs mostly as solid solution in sphalerite and pyrite. It also occurs in association with clays, carbonates and organic matter (Goodarzi, 2002; Dai et al., 2012). It is an extremely toxic element while exposed to the nature (HSE, 2003). Excessive amounts of Cd might cause many problems for kidney disease as well as fever, chest pain and eye-nose infections (Finkelman, 2004). Therefore, Cd is a potential hazardous element for the environmental concern during combustion of the analyzed coals. The strontium (Sr) concentration is lower than the Clarke value (Fig.4.2.1.2E) and it is not an environmental issue here.

The potassium (K) concentration of Dighipara coal is high (mean 556ppm) compared to the world average value (100ppm) (Fig.4.2.1.2F). The high concentration is possibly because of the enrichment of the mixed layer clays (Spears and Zheng, 1999; Sia and Wan Hasiah, 2011). It is not an environmental concern. The iron (Fe) concentration measured is very low (mean 1852ppm) compared to the world average (10000ppm) (Fig.4.2.1.2F). It can be combined inorganically (e.g., pyrite, marcasite, siderite and ankerite) or organically in coals. Microscopic observation showed that the Fe is associated with both syngenetic (Fig.4.2.1.3A) and epigenetic pyrites (Fig.4.2.1.3B). The presence of these kinds of pyrite

most frequently causes acid rain utilizing the coals (Hower and Bland, 1989). It is harmful for the environment, especially for the crops. The higher presence of Fe sometimes forms numerous pyrites (in association with sulfur) which would ultimately be a hazard for environments.

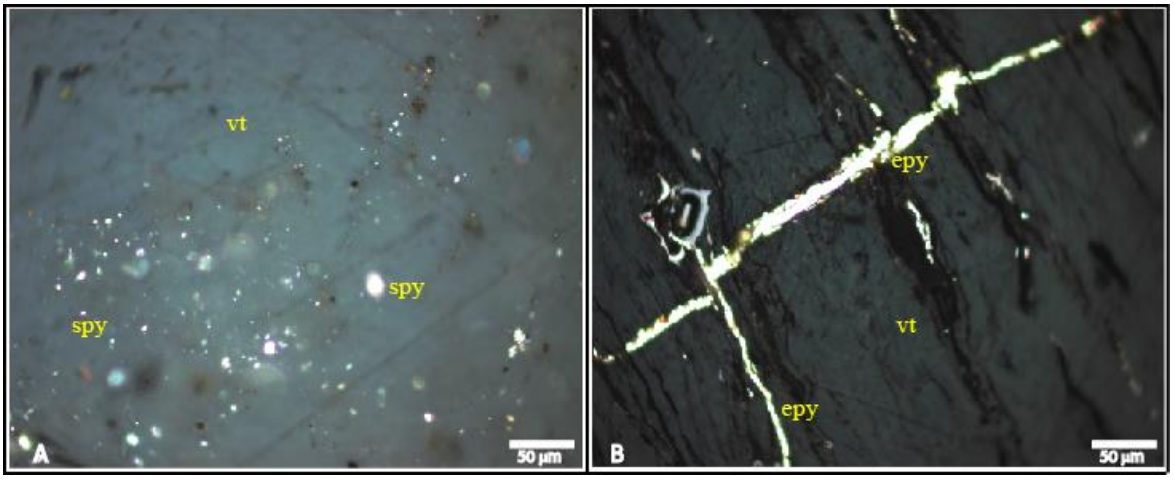

Fig.4.2.1.3. Photomicrograph shows iron and sulfur bearing mineral pyrite which is of syngenetic (spy, A) or epigenetic (epy, B) origin. It is associated with vitrinite macerals observed under microscope with normal reflected white light under oil immersion.

The cobalt (Co) concentration in the analyzed coal samples is much higher (mean 17ppm) than the Clarke value (6±0.2). Sulfide minerals or fine grained accessory sulfide in clays and organic matter in coal are the major source of cobalt (Goodarzi, 2002). Studies suggest that ingestion of an excessive amount of cobalt causes polycythemia and intercellular hypoxia. Chronic exposure to cobalt at higher concentrations produces goiter (Krishnan, 1995; Gupta 1999). Therefore, it is a hazardous element in the studied coals.

Chapter 4.2.2 Microscopic Study of Coals

The present study deals with two Permian coal deposits of the Barapukuria and Dighipara coal basins. These coal bearing basins are situated within the Rangpur Saddle area of Platform unit of the Bengal Basin, Northwest Bangladesh. The Gondwana Group contains the valuable coal in the Barapukuria and Dighipara coal basins. A total of 27 coal samples were analyzed for the current investigation. Among the total samples, 22 samples are collected from the cores and five samples from a stockpile of bulk coal dumped at the Barapukuria Coal Mine.

4.2.2.1 Macerals

The quantitative and qualitative analyses of macerals and associated minerals (vol.%) were carried out in the present study. The details of different macerals and mineral matter are summarized in Tables 4.2.2.1 and 4.2.2.2 and Appendix D1. The analyzed coal is rich in inertinite group macerals followed by vitrinite and liptinite group. Semifusinite, fusinite and inertodetrinite are the main constituents of the inertinite group. Collotelinite and collodetrinite are the dominant components of vitrinite group. Sporinite, cutinite and resinite are common macerals of the liptinite group.

4.2.2.1.1 Vitrinite group: All the macerals of vitrinite group (ICCP System 1994 (1998)) are observed in the analyzed coal samples. Of this maceral group (mean 31%, in total three sets of samples), telovitrinite (telinite-1% and collotelinite-18%) is the most dominant subgroup, followed by detrovitrinite (collodetrinite-9% and vitrodetrinite-2%) and gelovitrinite (gelinite-1% and corpogelinite-1%).

Telinite: Although telinite is rare, some large bands (100-300 μm width) are observed in the analyzed coal samples. The cell cavities and lumens are partially or completely filled with argillaceous mineral matters and other macerals such as corpogelinite, resinite, micrinite, clay minerals and carbonates. Telinite is characterized by its clear cellular structure and grey color in reflected white light (Photomicrograph 4.2.2.1A).

Table 4.2.2.1. A summary of maceral and mineral matter contents (vol. %) of the analyzed coal samples (22 cores and 5 bulks) of Barapukuria and Dighipara Basins. GI - TPI and GWI -VI values are also shown.

Maceral / Mineral matter	Bulk samples of Barapukuria Basin		Core samples of Barapukuria Basin		Core samples of Dighipara Basin	
	Range	Mean	Range	Mean	Range	Mean
Telinite	0.3-4.2	1.8	0.0-1.4	0.2	0.0-1.9	0.6
Collotelinite	16.6-23.0	20.1	5.6-26.7	15.2	1.8-36.1	18.2
Collodetrinite	5.6-10.8	8.0	4.8-23.2	11.0	0.8-14.4	7.8
Vitrodetrinite	1.4-2.4	2.0	0.1-6.6	2.5	0.9-2.6	2.7
Gelinite	0.6-0.7	0.5	0.0-1.4	0.5	0.0-1.4	0.6
Corpogelinite	0.2-1.2	0.7	0.0-0.9	0.4	0.0-1.9	0.4
Vitrinite group	**30.8-34.5**	**33.1**	**25.9-37.8**	**29.8**	**18.5-38.7**	**30.3**
Sporinite	10.6-15.6	12.8	5.4-21.5	14.6	9.5-21.7	13.9
Cutinite	2.2-5.1	3.6	2.0-11.3	4.0	2.0-5.3	3.4
Resinite	0.5-1.9	1.4	0.8-3.5	1.4	0.3-1.8	1.0
Bituminite	0.5-1.1	0.8	0.6-2.8	1.5	0.4-1.9	1.2
Fluorinite	0.9-1.7	1.4	0.0-7.4	1.0	0.1-1.3	0.5
Liptodetrinite	0.5-1.1	0.9	0.4-1.4	0.7	0.2-1.0	0.6
Exsudatinite	0.3-0.6	0.7	0.2-1.2	0.5	0.0-0.8	0.4
Liptinite group	**19.8-22.9**	**21.6**	**15.2-31.1**	**23.6**	**14.0-24.4**	**21.0**
Semifusinite	20.6-25.4	22.9	15.9-30.6	21.5	6.4-27.8	19.6
Fusinite	7.2-10.1	8.2	6.5-15.1	9.8	1.2-15.6	9.1
Inertodetrinite	3.8-5.7	4.8	3.1-10.1	6.9	1.8-13.5	7.4
Micrinite	0.3-1.2	0.6	0.1-1.6	0.8	0.4-2.5	1.5
Macrinite	0.4-3.4	1.4	0.5-1.6	1.1	0.2-2.7	1.2
Secretinite	0.5-1.4	1.4	0.2-1.6	0.9	0.0-3.2	0.9
Funginite	0.0-0.4	0.2	0.0-0.2	0.1	0.0-0.2	0.1
Inertinite group	**36.8-42.4**	**39.4**	**31.1-45.4**	**41.0**	**32.2-55.0**	**39.7**
Clay minerals	3.9-9.5	5.3	4.0-6.9	5.1	1.5-17.1	7.8
Pyrite-Quartz	0.2-1.5	0.6	0.1-1.3	0.5	0.2-2.3	1.1
Mineral matter	**3.2-11.0**	**5.9**	**3.5-7.1**	**5.6**	**2.2-18.4**	**8.9**
TPI	2.0-3.9	3.3	1.3-4.3	2.5	1.0-3.9	2.7
GI	0.9-1.0	1.0	0.7-1.1	0.8	0.5-1.2	0.9
VI	2.9-4.0	3.3	1.2-3.3	2.3	1.4-4.2	2.7
GWI	0.2-0.5	0.3	0.2-0.8	0.4	0.1-2.2	0.6

Collotelinite: Collotelinite is the most dominant maceral of the vitrinite group. It is characterized by a more or less homogeneous structureless appearance, which is most commonly found in the vitrain lithotype and, less commonly, in clarain. It is sometimes observed as a cement or impregnating material for the other associated macerals. A folded nature is also observed within this maceral. The color varies from light grey to moderately dark grey in reflected white light and occurs as both thick and thin bands (Photomicrograph 4.2.2.1B).

Table 4.2.2.2. A summary of maceral concentrations in mineral free basis (vol. %) of the analyzed coal samples (22 cores and 5 bulks) of Barapukuria and Dighipara Basins.

Maceral	Bulk samples of Barapukuria Basin		Core samples of Barapukuria Basin		Core samples of Dighipara Basin	
	Range	Mean	Range	Mean	Range	Mean
Telinite	0.3-4.7	1.8	0.0-1.4	0.2	0.0-1.9	0.6
Collotelinite	17.1-24.3	20.1	5.6-26.7	15.2	1.8-36.1	18.2
Collodetrinite	6.3-11.2	8.0	4.8-23.2	11.0	0.8-14.4	7.8
Vitrodetrinite	0.9-4.1	2.0	0.1-6.6	2.5	0.9-2.6	2.7
Gelinite	0.2-0.7	0.5	0.0-1.4	0.5	0.0-1.4	0.6
Corpogelinite	0.2-1.3	0.7	0.0-0.9	0.4	0.0-1.9	0.4
Vitrinite group	**33.9-36.5**	**33.1**	**27.3-40.6**	**29.8**	**22.7-41.3**	**33.8**
Sporinite	11.9-16.5	12.8	5.4-21.5	14.6	9.5-21.7	13.9
Cutinite	2.3-5.4	3.6	2.0-11.3	4.0	2.0-5.3	3.4
Resinite	0.5-2.2	1.4	0.8-3.5	1.4	0.3-1.8	1.0
Bituminite	0.5-1.2	0.8	0.6-2.8	1.5	0.4-1.9	1.2
Fluorinite	0.9-2.1	1.4	0.0-7.4	1.0	0.1-1.3	0.5
Liptodetrinite	0.5-1.2	0.9	0.4-1.4	0.7	0.2-1.0	0.6
Exsudatinite	0.3-1.3	0.7	0.2-1.2	0.5	0.0-0.8	0.4
Liptinite group	**21.0-24.2**	**21.6**	**16.3-33.3**	**23.6**	**15.1-29.5**	**22.6**
Semifusinite	23.1-26.8	22.9	15.9-30.6	21.5	6.4-27.8	19.6
Fusinite	7.5-10.7	8.2	6.5-15.1	9.8	1.2-15.6	9.1
Inertodetrinite	4.0-6.0	4.8	3.1-10.1	6.9	1.8-13.5	7.4
Micrinite	0.3-1.2	0.6	0.1-1.6	0.8	0.4-2.5	1.5
Macrinite	0.3-1.2	1.4	0.5-1.6	1.1	0.2-2.7	1.2
Secretinite	0.4-1.5	1.4	0.2-1.6	0.9	0.0-3.2	0.9
Funginite	0.5-2.2	0.2	0.0-0.2	0.1	0.0-0.2	0.1
Inertinite group	**40.2-43.8**	**39.4**	**33.3-47.7**	**41.0**	**37.2-57.2**	**39.7**

Table 4.2.2.3. A summary of concentrations of microlithotype and carbominerite (vol. %) of the analyzed coal samples (22 cores and 5 bulks) of Barapukuria and Dighipara Basins.

Microlithotype / Carbominerite	Bulk samples of Barapukuria Basin		Core samples of Barapukuria Basin		Core samples of Dighipara Basin	
	Range	Mean	Range	Mean	Range	Mean
Monomaceral						
Vitrite	1.3-12.9	6.6	0.2-19.4	4.5	0.0-21.0	5.6
Inertite	1.4-6.2	2.6	0.5-18.7	4.8	0.0-14.7	3.4
Fusite	0.4-2.2	0.9	0.0-4.9	1.5	0.0-2.6	1.0
Semifusite	3.8-11.8	6.7	0.9-17.7	6.6	0.0-14.6	3.7
Inertodetrite	0.0	0.0	0.0	0.1	0.0-0.1	0.0
Microite	0.0-0.4	0.1	0.0	0.0	0.0-1.1	0.4
Bimaceral						
Vitrinertite	1.2-14.4	6.8	1.0-12.5	8.1	0.2-19.0	4.7
Vitrinertite V	1.0-6.3	2.8	0.0-5.6	3.0	0.0-3.9	1.7
Vitrinertite I	0.2-9.5	3.4	0.0-4.9	3.5	0.0-5.3	2.1
Clarite	0.9-6.6	3.1	0.0-9.8	1.2	0.0-2.6	1.4
Clarite V	0.2-3.6	1.4	0.0-7.6	1.3	0.0-23.0	3.0
Clarite E	0.0-1.0	0.4	0.0-0.9	0.1	0.0-0.4	0.2
Durite	0.6-9.6	4.6	0.6-33.4	9.9	2.0-34.2	13.7
Durite E	0.0-0.8	0.2	0.0-5.8	1.3	0.0-12.8	3.1
Durite I	0.8-8.4	4.7	0.1-23.3	8.4	0.6-26.2	7.3
Trimaceral						
Clarodurite	14.8-29.5	21.6	2.5-34.3	21.2	4.0-29.0	21.8
Duroclarite	16.7-43.4	26.4	5.5-31.2	17.9	2.7-33.2	17.8
Carbargilite	4.8-9.2	7.0	3.0-10.9	5.7	1.0-16.9	7.7
Carbankerite	0.2-0.5	0.4	0.0-1.5	0.3	0.0-1.9	0.7
Carbopyrite	0.2-0.9	0.6	0.0-2.0	0.4	0.1-1.8	0.8

Vitrodetrinite: Vitrodetrinites are observed as isolated and small (less than 10µm) fragments of different shapes, surrounded by other non-vitrinitic macerals. Vitrodetrinite occurs more frequently in microlithotype vitrinertite and, less commonly, in durite (Photomicrograph 4.2.2.1C).

Collodetrinite: Collodetrinite is characterized by its mottled and amorphous vitrinitic groundmass that binds other different macerals and components. It is found in a small

number of places as material intruded within other macerals. It shows comparatively low reflectance. When observed parallel to bedding, it forms irregular patches (Photomicrograph 4.2.2.1D and 1E). The fluorescence nature of vitrinite is also observed in collodetrinite and collotelinite. It shows a dull yellow to yellowish brown fluorescence in ultraviolet light or reddish yellow when associated with sporinite groundmass. Collodetrinite is commonly found in clarite and, less commonly, in durite and vitrinertite.

Table 4.2.2.4. A summary of concentrations of microlithotypes in mineral free basis (vol. %) of the analyzed coal samples (22 cores and 5 bulks) of Barapukuria and Dighipara Basins.

Microlithotype	Bulk samples of Barapukuria Basin		Core samples of Barapukuria Basin		Core samples of Dighipara Basin	
	Range	Mean	Range	Mean	Range	Mean
Monomaceral						
Vitrite	1.4-14.1	7.2	0.2-20.6	4.8	0.0-21.6	6.2
Inertite	2.1-6.6	2.8	0.5-19.6	5.1	0.5-15.1	3.7
Fusite	0.4-2.3	0.9	0.0-5.2	1.6	0.0-2.8	1.1
Semifusite	4.2-12.9	7.3	1.0-19.1	7.1	0.8-6.4	4.1
Inertodetrite	0.0	0.0	0.0-1.0	0.1	0.0-0.1	0.0
Microite	0.0-0.4	0.1	0.0-0.1	0.0	0.0-1.9	0.4
Bimaceral						
Vitrinertite	1.3-15.3	7.4	1.1-16.5	8.7	0.2-20.7	5.2
Vitrinertite V	1.1-6.9	3.0	0.0-9.7	3.3	0.0-4.5	1.8
Vitrinertite I	0.2-10.4	3.6	0.0-10.2	3.7	0.0-8.1	2.3
Clarite	1.0-7.3	3.3	0.0-10.5	1.3	0.0-6.2	1.6
Clarite V	0.2-0.4	1.5	0.0-8.2	1.4	0.0-23.7	3.3
Clarite E	0.0-1.1	0.4	0.0-1.0	0.1	0.0-1.0	0.2
Durite	0.7-10.2	5.0	0.6-34.8	10.6	2.1-41.0	15.1
Durite E	0.0-0.9	0.2	0.0-6.3	1.4	0.0-15.3	3.4
Durite I	0.9-8.9	5.1	0.1-26.4	8.9	0.0-29.9	8.0
Trimaceral						
Clarodurite	16.2-31.4	23.5	2.8-36.4	22.6	4.1-38.9	24.0
Duroclarite	17.8-48.1	28.7	5.8-34.6	19.1	3.9-36.0	19.6

Gelinite: Gelinite is rare in the analyzed coal samples. It is observed as structureless infillings in the cracks and other voids of the semifusinites and fusinites (Photomicrograph 4.2.2.1E) and is, therefore, likely to be of secondary origin.

Corpogelinite: Corpogelinite has been found forming homogenous and discrete bodies of cell infillings, mainly incorporated in telocollinites. It is similar in color and reflectance to the surrounding telocollinite, but has a high relief (Photomicrograph 4.2.2.1F). It is not common in the analyzed samples.

4.2.2.1.2 Liptinite group

In the analyzed coal samples, the macerals of liptinite group are identified by their comparative darker color in reflected white light and different fluorescence nature in ultraviolet light. The structured liptinite macerals observed in the studied Permian coals are sporinite, cutinite, resinite and liptodetrinite while the unstructured liptinites include bituminite, fluorinite and exsudatinite. The most dominant sub-macerals of this group (mean 22%, in total three sets of samples) are sporinite (14%) and cutinite (4%), followed by resinite (1%), bituminite (1%), fluorinite (1%), liptodetrinite (1%) and exsudatinite (1%).

Sporinite: Sporinite is the most dominant maceral of the liptinite group. It occurs as elongated, flattened or disc-shaped, thread-like bodies that are parallel to the stratification. Both microsporinite (tenui and crassi) and megasporinite (tenui and crassi) have been found in the studied samples (Photomicrograph 4.2.2.2A and 2B). The interior of the spore is often recognized. Under white light, they appear darker (dark grey to brownish black) than the surrounding telocollinite, while under ultraviolet light they show reddish yellow to orange colors of moderate intensity. The megaspore is comparatively lower in concentration than the microspore. A sporangium consisting of numerous microspores has also been observed (Photomicrograph 4.2.2.2C). Some sporangia show a well-organized form whereas some do not have a definite form.

A particular colony of microspores has been identified in the studied samples (Photomicrograph 4.2.2.3A). Sporinite is common in microlithotypes of clarite and durite.

Cutinite: Cutinite is found as thin cylindrical bodies with serrated margins or a crenulated form. Megacutinite is common in these coals. Both tenui (thin-walled) and crassi (thick-walled) varieties are found. Cutinite is dark grey to black in color in reflected white light but shows a yellowish-orange to light brownish red color under ultraviolet light (Photomicrograph 4.2.2.3B and 3C). It is common in clarite bands.

Resinite: Resinite appears as a rounded, oval or spherical-shaped body and occurs as cell (cavity) fillings or isolated rounded to subrounded rod-like body. Clusters of resinite bodies have also been observed in the investigated coal samples (Photomicrograph 4.2.2.4A). They are dark grey to brown under reflected white light. In fluorescent light they show a wide range of color, mostly greenish-yellow to yellow, occasionally becoming orange and light brown in color. Resinite is frequently found in the microlithotype of clarite and, less commonly, in durite bands.

Liptodetrinite: Liptodetrinite embraces the fragmental parts and detrital remains of structured liptinite macerals produced due to degradation and crushing (Photomicrograph 4.2.2.4B).

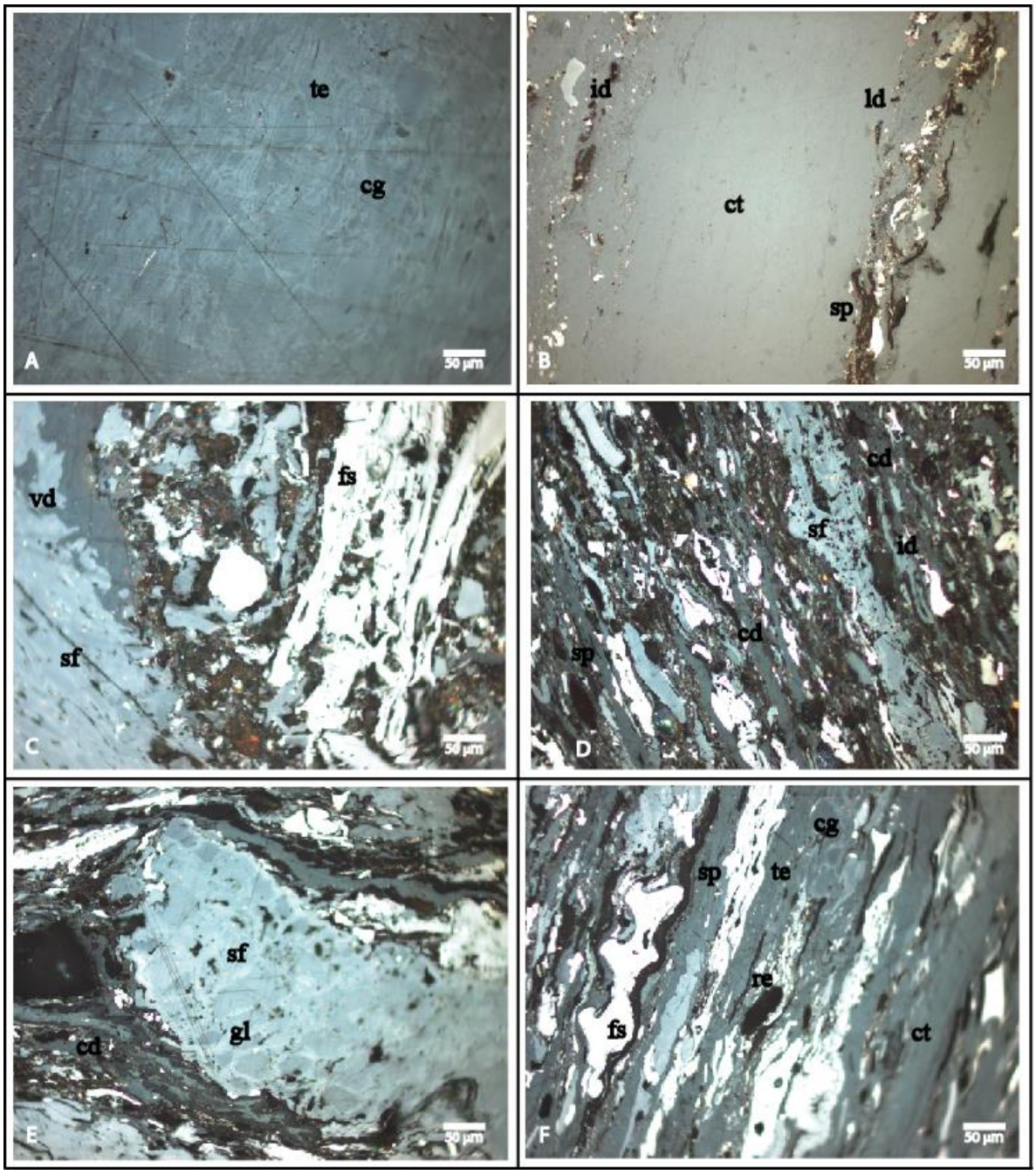

Photomicrograph 4.2.2.1. (A) Cell structure is clearly visible in moderate grey telinite (te). (B) Structureless collotelinite (ct). (C) Discrete small isolated vitrodetrinite (vd) is also observed in the analyzed samples. (D) Collodetrinite (cd) as vitrinitic ground mass binding other macerals (e.g., semifusinite-sf, inertodetrinite-id, liptodetrinite-ld and sporinite-sp). (E) Gelinite (gl) is found as cell fillings of semifusinite. (F) Corpogelinite (cg) is investigated as cell fillings of telinite [All photomicrographs are shown in normal reflected white light].

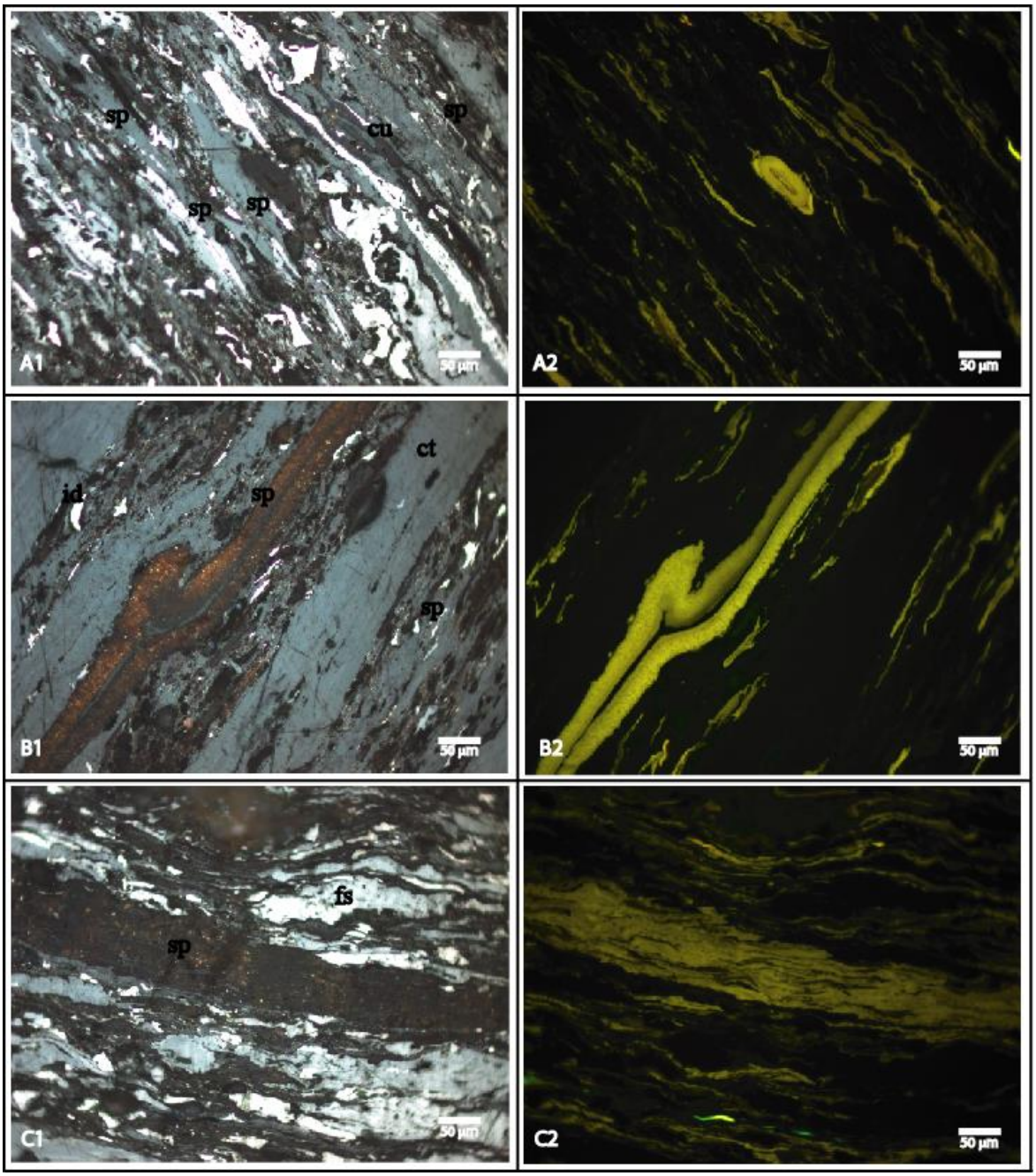

Photomicrograph 4.2.2.2. (A) Elongated to disc shaped micro-sporinite (sp). (B) Mega-sporinite; Both types show dark grey to brownish black color in reflected white light (A1 and B1). They fluoresce reddish-yellow to orange (A2 and B2) under ultraviolet light. Both thin-walled and thick-walled types are also identifiable. (C) Sporangium consisting of numerous microspores is frequently observed in the samples (C1 under reflected white light and C2 under ultraviolet light).

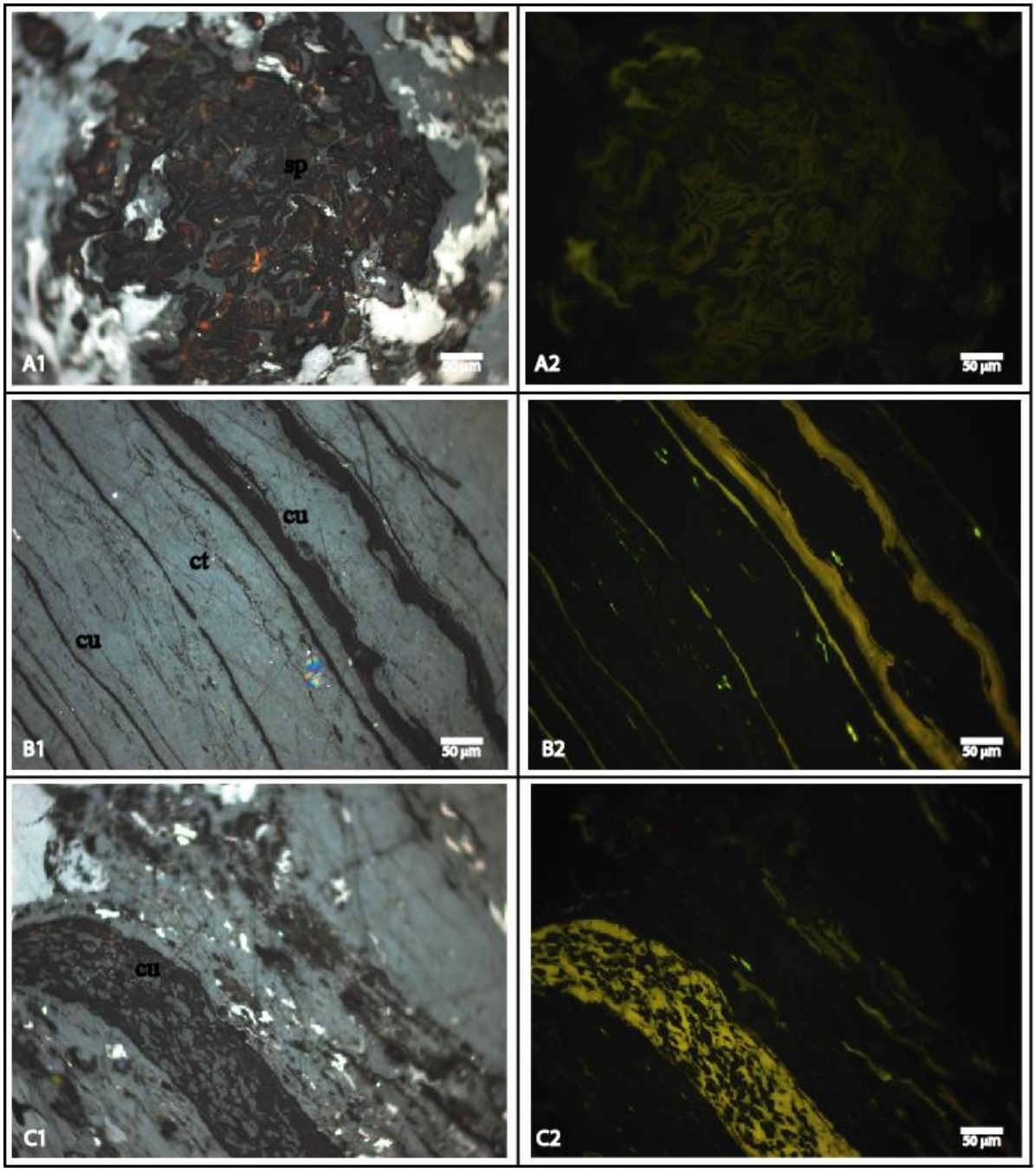

Photomicrograph 4.2.2.3. (A) Colony of microspores is observed whereby A1 shows under reflected white light and A2 shows under ultraviolet light. (B1) and (C1) Narrow banded to cylindrical micro-cutinite and mega-cutinite (cu) with serrated margins are dark grey to black in normal reflected white light. (B2) and (C2) Cutinite shows yellowish orange to light brownish red fluorescence under ultraviolet light. Both thin-walled (B) and thick-walled (B and C) cutinite are observed in the studied samples.

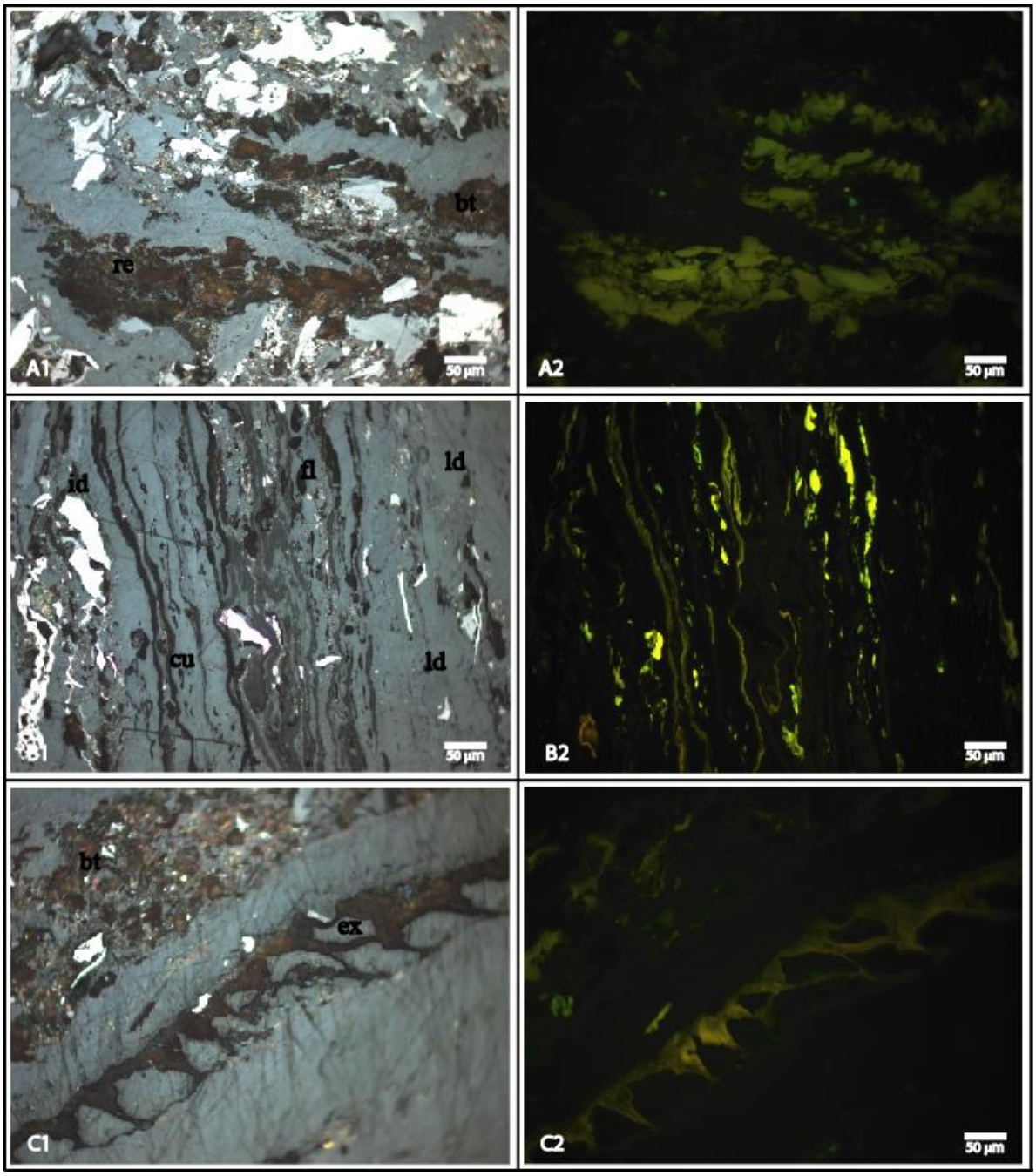

Photomicrograph 4.2.2.4. (A) Rounded to subrounded and oval shaped isolated and colonial resinite (re) dark grey to dark brown in reflected white light (A1). They show greenish-yellow to yellow fluorescence under ultraviolet light (A2). Lamellar formed bituminite (bt) shows dark brown color in reflected white light (A1). It fluoresces yellowish-brown under ultraviolet light. (B) Liptodetrinite (ld) is found as fragmental part of liptinite. B1 shows under reflected white light and B2 shows under ultraviolet light. Fluorinite (fl) is dark grey to dark brown in reflected white light (B1) while it shows brilliant yellow fluorescence occurred as oil droplets in ultraviolet light (B2). (C) Exsudatinite (ex), as cracks or empty cell filling secondary maceral, show dark brown color in reflected white light (C1). It fluoresces yellow to orange in ultraviolet light (C2). Lamellar bituminite (bt) is also observed here.

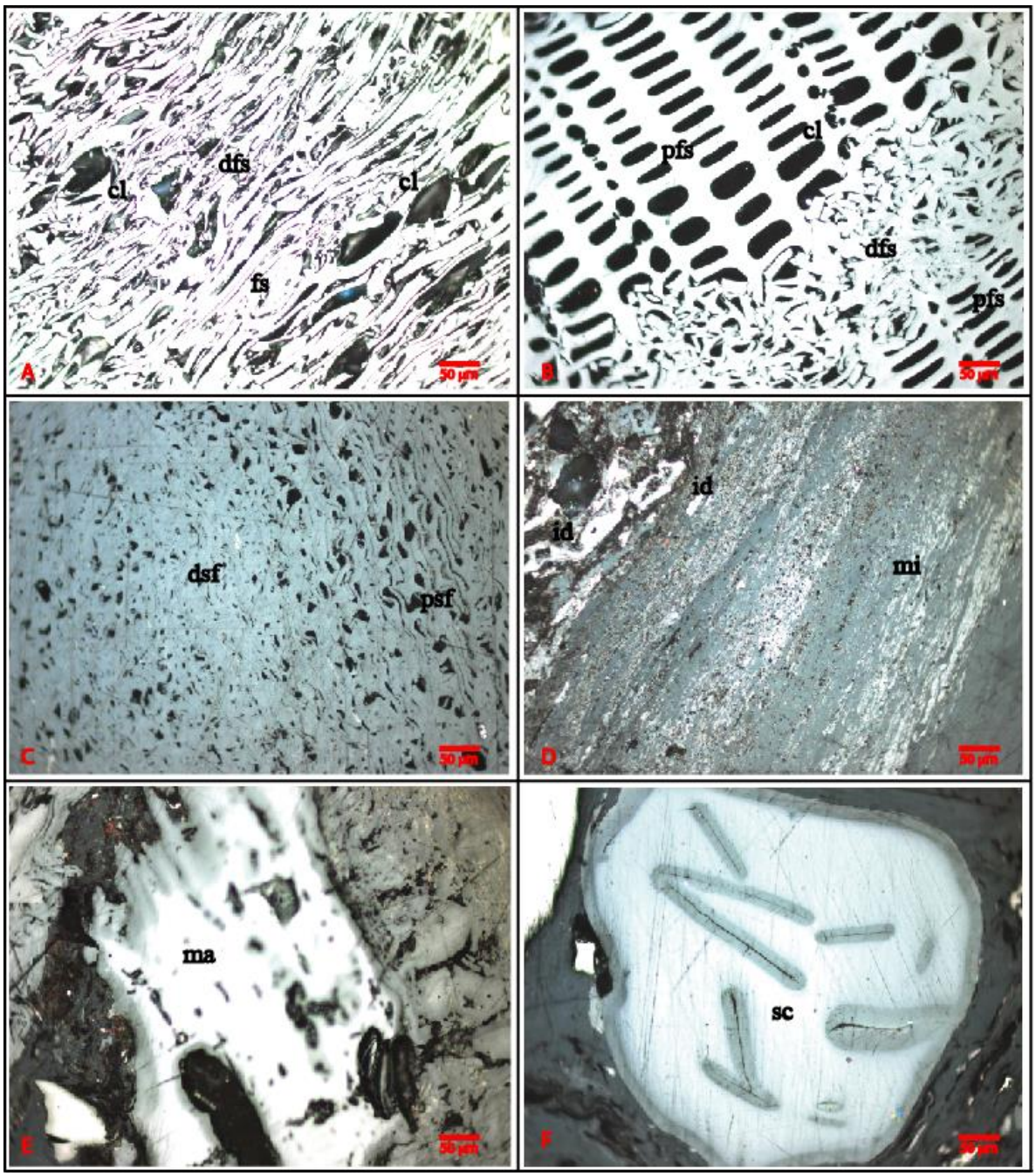

Photomicrograph 4.2.2.5. (A) White color degradofusinite (dfs) with poorly preserved cell structure in normal reflected white light and fusinite does not show any fluorescence under ultraviolet light. (B) White color pyrofusinite (pfs) with well-preserved cell structures contacted with degradofusinite. (C) Degradosemifusinite (dsf) and pyrosemifusinite (psf) show relatively lower reflectance than fusinite in normal reflected white light. (D) Inertodetrinite (id) is found as isolated fragment of fusinite; whitish color very fine grained aggregates (without any particular shape) are identified as micrinites. (E) Structureless macrinite (ma). (F) Oval shaped and rimmed with notches secretinite (sc) is observed in the samples [all photomicrographs are shown in normal reflected white light].

Fluorinite: Teichmüller (1974a) and Cook et al. (1981) have shown that fluorinite is formed from the oils and fats of higher plants. Teichmüller (1974a) differentiated fluorinite from resinite on the basis of its brilliant yellow fluorescence under ultraviolet light. In the studied coals, fluorinite occurs as cell fillings, and also as veins and lenses or oil droplets, which are characterized by a brilliant yellow color and very high intensity under ultraviolet light and dark brown color in reflected white light (Photomicrograph 4.2.2.4B).

Bituminite: Bituminite occurs as groundmass and lamellar forms (Singh and Singh, 1994). It may also be present as a solid bitumen. Bituminite commonly shows yellow to orange fluorescence (Photomicrograph 4.2.2.4C) and may at times show a brown fluorescence. Teichmüller (1974a and 1974b) and Singh and Singh (2004) demonstrate that bituminite is an amorphous liptinite maceral without a definite shape and that it occurs as finely dispersed lenses, streaks and, in places, as the groundmass of other liptinite macerals. Bituminite is considered to be a secondary maceral and therefore might be a secondary product derived from resinite and cutinite, with which it is more commonly associated in the studied coal samples.

Exsudatinite: Exsudatinite was first described by Teichmüller (1974b and 1974c). Its occurrence marks the first step in bituminization. It is genetically characterized as being an expelled hydrocarbon liberated from the lipid constituents of liptinites and perhydrous vitrinites or huminites. It occupies void ducts such as cracks, the empty cell lumens of fusinite and secretinite and bedding plane joints. In the studied coals, exsudatinite occurs as veins and has yellow to orange and red-brown colors with moderate to weak intensity under ultraviolet light (Photomicrograph 4.2.2.4C).

4.2.2.1.3 Inertinite group

Inertinite group macerals (mean 40%, in total three sets of samples) dominates both the Barapukuria and Dighipara coals when compared with the other maceral groups, vitrinite and liptinite. This group is characterized by its distinct higher reflectance in white light and absence of fluorescence in ultraviolet light when compared to the vitrinite and/or liptinite also associated with these coals. The macerals identified (ICCP System 1994 (2001)) are semifusinite, fusinite, inertodetrinite, micrinite, macrinite, secretinite and funginite. Semifusinite (21%), fusinite (9%) and inertodetrinite (6%) are the most common maceral subgroup of the macerals in this group, followed by micrinite, macrinite, secretinite and funginite.

Fusinite: The fusinite has a well-preserved cellular structure. The cell lumens are either empty or are filled mostly with mineral matter and, less commonly, with gelinite. They show a white to yellowish white color under reflected white light, with a very high relief. They show no fluorescence under UV light. Both degradofusinite and pyrofusinite are present but degradofusinite is more common (Photomicrograph 5A and 5B). Pyrofusinite shows a well-preserved cellular structure, a yellowish-white color and reflectance that is higher than that of degradofusinite, while degradofusinite is characterized by moderately well-preserved cellular structures with a white color and high reflectance. A ‘Bogen Structure’ is commonly observed in both types (Photomicrograph 4.2.2.5B). The folding nature of fusinite can also be observed in a few places. Sharp contacts have been observed between pyrofusinite and semifusinite, pyrofusinite and collotelinite, and pyrofusinite and degradofusinite. Fusinite is commonly found in microlithotype fusite and inertite, and less commonly, in durite.

Semifusinite: The most dominant maceral in the studied coal samples is semifusinite. It is identified by its reflectance, which is intermediate between the vitrinite and fusinite of the same coal sample. The cell cavities (lumens) are partially visible and smaller in size compared to those of fusinite. These cavities are found as being either empty or filled with other constituents, such as clay and resinite. Both pyro and degrade-semifusinite have been observed, but degradofusinite is the more dominant (Photomicrograph 4.2.2.5C). It is found mainly in microlithotype inertite (semifusite), followed by durite and clarodurite.

Inertodetrinite: Inertodetrinite can be identified as discrete small (<10µm) inertinite fragments in the studied samples. It is observed in high concentrations, which appear to have derived from fusinite and semifusinite macerals, and shows a white to yellowish-white color in reflected white light (Photomicrograph 4.2.2.5D). It is mostly observed in vitrinertite and durite bands.

Micrinite: Micrinite occurs as very fine (<2µm) rounded grains which are white to yellowish-grey in color in reflected white light (Photomicrograph 4.2.2.5D). Aggregates of micrinite with an indefinite outline are differentiated from macrinite by their granularity. It is common in microlithotype vitrite and is also found in both vitrinertite and durite. It is considered mainly to be the secondary relics of oil generation (Teichmüller, 1974c; Wan Hasiah, 2003).

Macrinite: Macrinite is found as an amorphous matrix (groundmass) or as discrete bodies showing no structure. The size ranges from 10 to 40 µm, commonly displaying an elongated shape, and it has a white to pale grey color in reflected white light. It is commonly found in durite (Photomicrograph 4.2.2.5E).

Secretinite: Secretinite is occasionally observed in the analyzed samples. It occurs as rounded to oval-shaped perforated bodies without any particular structure (Photomicrograph 4.2.2.5F). In a few cases, they show an oxidized rim of lower or higher reflectance and internal notches.

Funginite: Funginite is formed of single or multi-celled fungal spores, sclerotia, hyphae and mycelia (stromata, mycorrhiza), and other fungal remains. It is found very rarely in the analyzed coal samples.

4.2.2.1.4 Mineral matter

The mineral components are identified by their black appearance under reflected white light without any relief (with exception of quartz). A considerable amount of mineral matter (7 vol.%) is measured in the analyzed coal samples of both Barapukuria and Dighipara. Clay minerals (6%) are the dominant group with only minor amounts of carbonate, quartz and sulfide (pyrite). The minerals are mostly found as cell/cavity fillings of vitrinite, liptinite and inertinite bands (Photomicrograph 4.2.2.6A and 6B). Pyrite shows golden yellow color in reflected white light with distinct relief and these are identified both as framboids and cavity fillings (Photomicrograph 4.2.2.6C). Carbonate minerals are found as re-precipitated small irregular bodies or patches which show medium grey color in reflected white light with slight relief against vitrinite.

4.2.2.2 Microlithotypes

All the different microlithotypes in the analyzed coal samples are identified: Tables 4.2.2.3 and 4.2.2.4 and Appendix D2 show the concentration details. Trimaceral group members such as clarodurite (22%) and duroclarite (21%) (Photomicrograph 4.2.2.7A and 7B) are

found to be the most dominant maceral associations in the studied samples. Durite (9%) is the most dominant bimaceral group: durite I (Photomicrograph 4.2.2.7C) is present in higher amounts than durite E. Other bimaceral groups i.e., clarite (Photomicrograph 4.2.2.8A) and vitrinertite (Photomicrograph 4.2.2.8B) are also common in the samples.

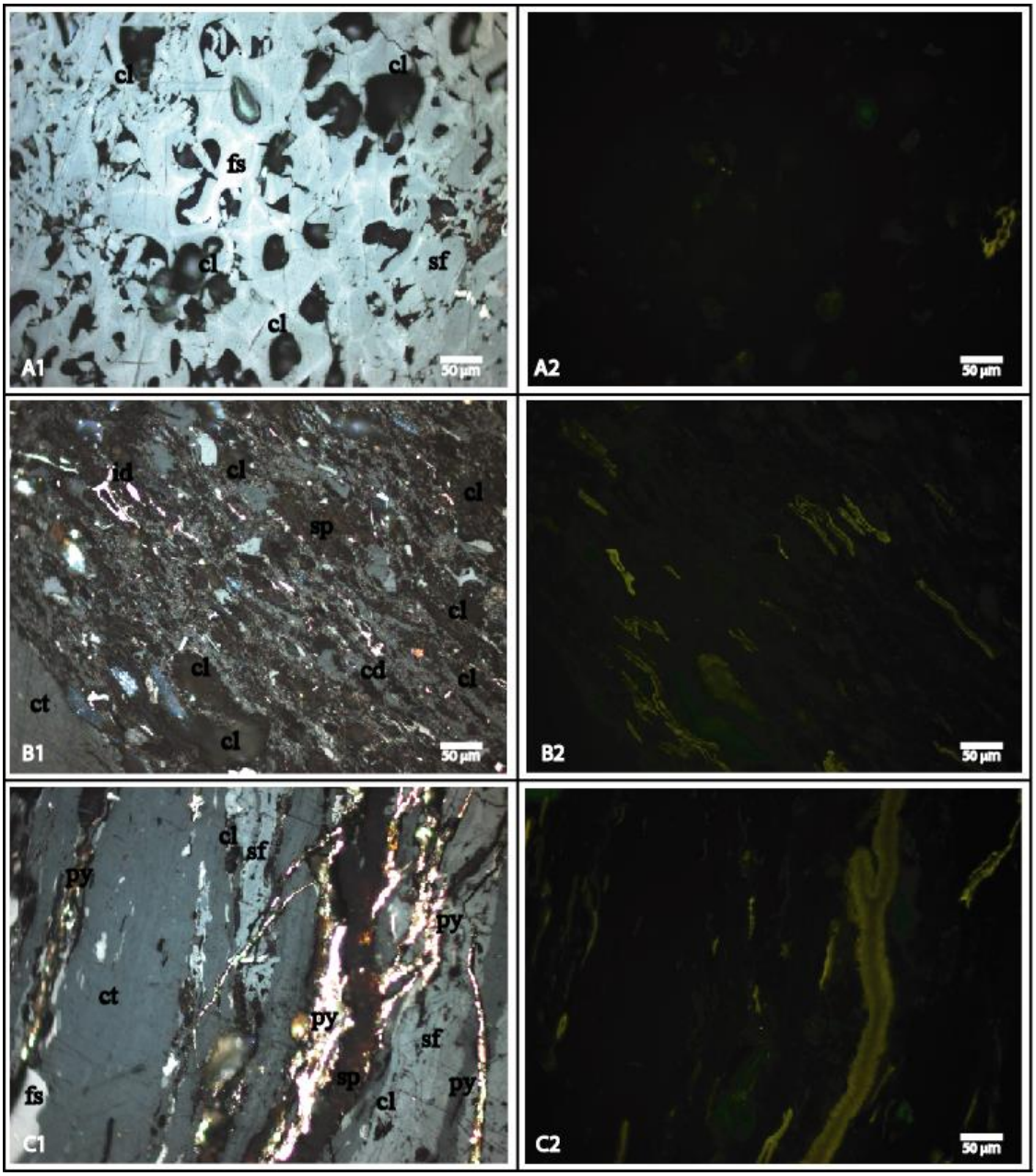

Photomicrograph 4.2.2.6. (A) Cell filling clay minerals (cl) show black color under reflected white light (A1). They don't show any fluorescence under UV light (A2). (B) Cavity filling clay minerals are black under white light (B1) and show no fluorescence (B2). (C) Cavity filling sulfide minerals, e.g., pyrite (py) occurs as golden yellow color under white light (C1). It does not show any fluorescence under ultraviolet light (C2).

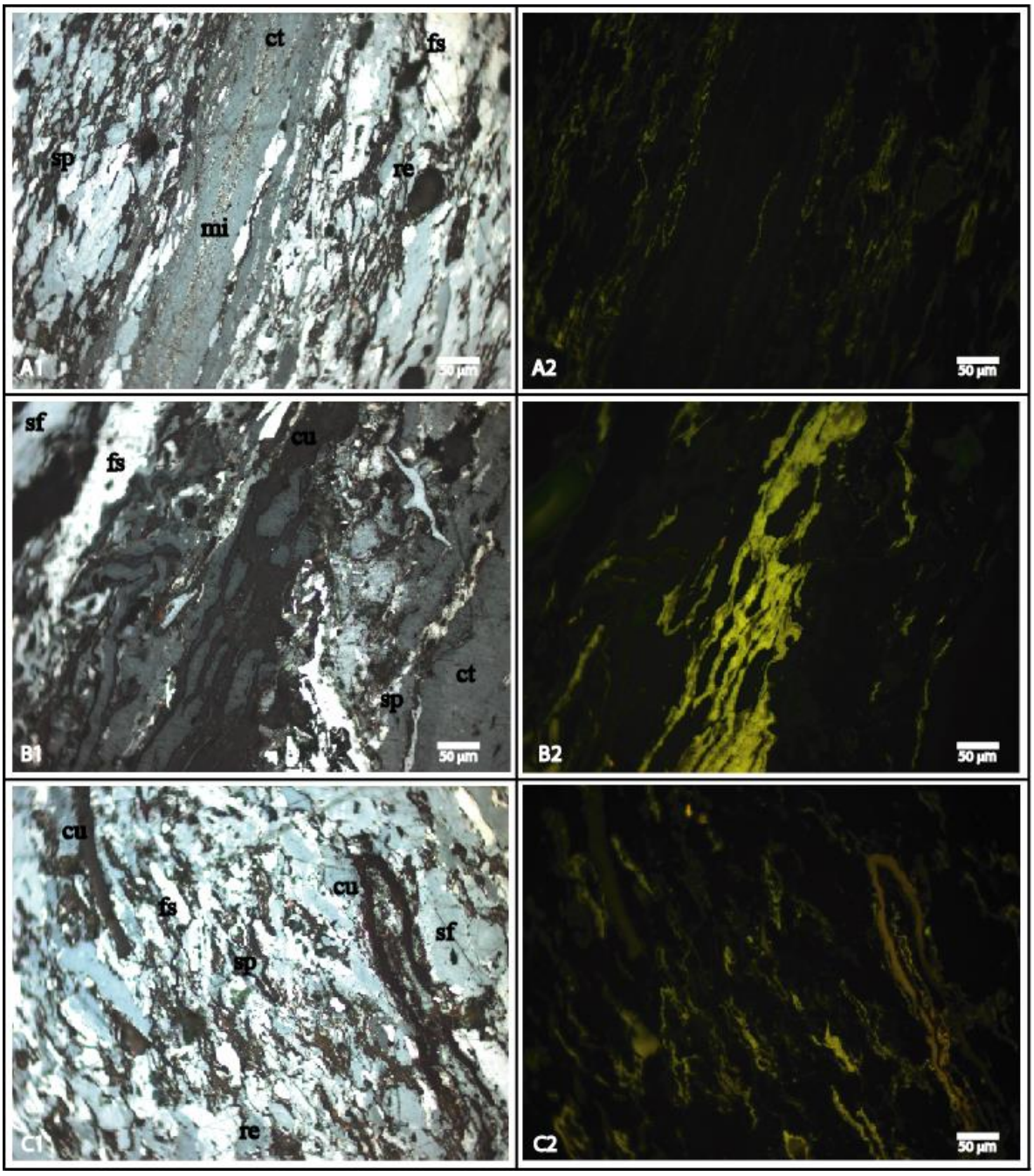

Photomicrograph 4.2.2.7. (A) The most dominantly observed trimaceral microlithotype is clarodurite- an association of inertinite (fs, mi), liptinite (cu, sp) and vitrinite (ct) macerals. (B) Another most commonly found trimaceral microlithotype is duroclarite- an association of vitrinite, liptinite and inertinite macerals. (C) Bimaceral microlithotype durite I which includes the inertinite and liptinite macerals with the dominancy of inertinite [Left photomicrographs A1, B1 and C1 are showed under reflected white light whereby the right ones A2, B2 and C2 are shown under ultraviolet light].

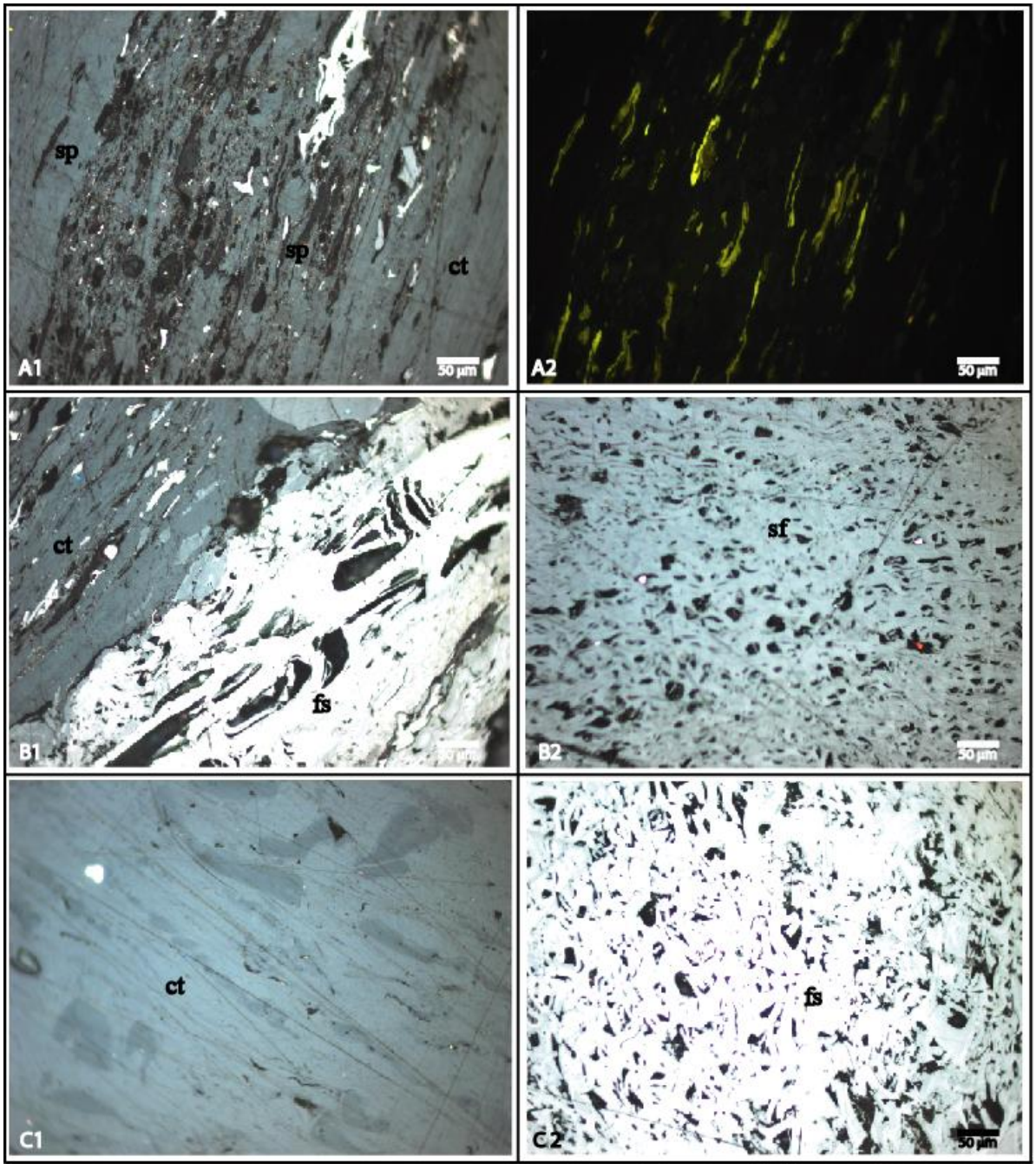

Photomicrograph 4.2.2.8. (A) Clarite is a bimaceral microlithotype including vitrinite (ct, cd) and liptinite (sp, cu) macerals. (B) Another bimaceral microlithotype is vitrinertite consisting of vitrinite and inertinite macerals. (C) Monomaceral microlithotypes semifusite. (D) Vitrite. (E) Fusite [Here only the photomicrography A2 is shown in ultraviolet light; all rest photomicrographs are taken under normal reflected white light].

Semifusite (6%) and vitrite (6%) are identified as the most common microlithotypes of the monomaceral group (Photomicrograph 4.2.2.8C and 8D). On the other hand, of the carbominerites, carbargillite (7%) is much more dominant than carbankerite (1%) and carbopyrite (1%).

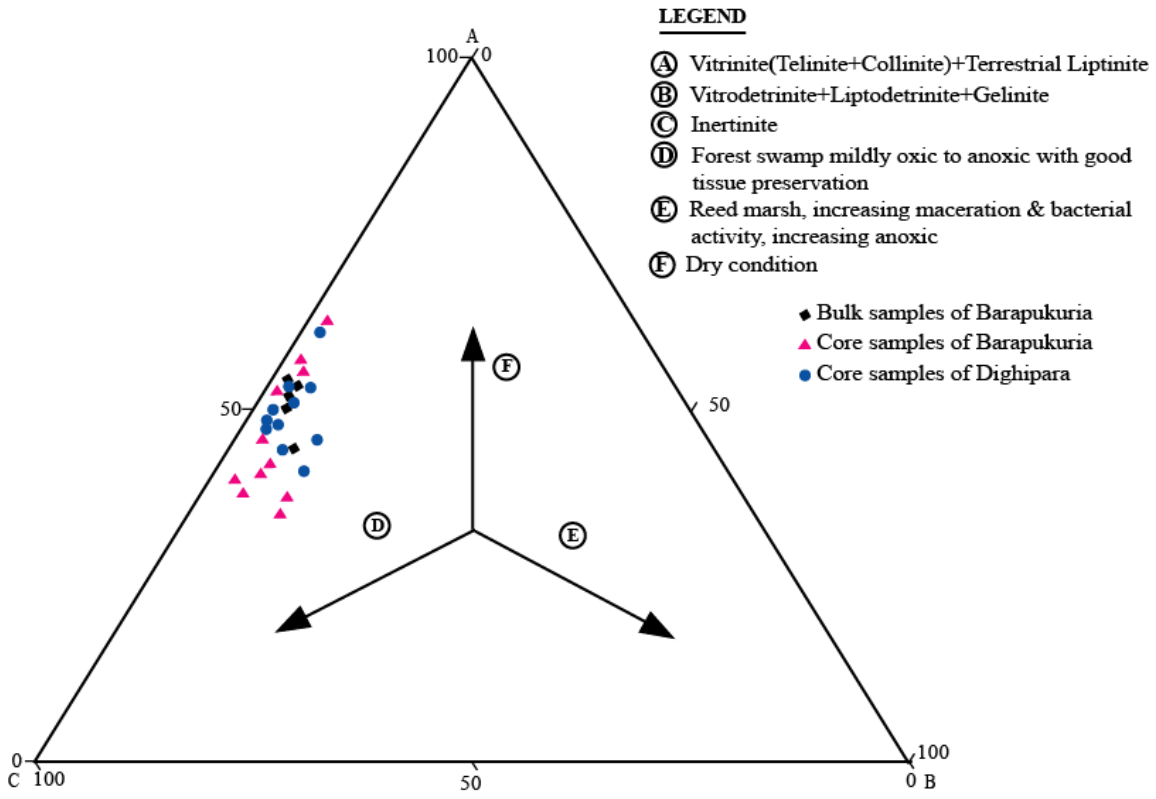

Fig.4.2.2.1. A triangular diagram illustrating peat-forming depositional environments based on maceral compositions. The studied samples represent forest swamp, mildly oxic to anoxic conditions, with good tissue preservation (adopted by Mukhopadhyay, 1986).

4.2.2.3 Discussion

4.2.2.3.1 Coal facies models

A number of facies models are in use based on maceral concentrations, maceral indices and maceral associations of the Permian coals studied in different parts of the world. Based on some of the more popular facies models, an initiative has been put in place to reconstruct the paleofacies and depositional conditions of the Permian coals of Bangladesh.

4.2.2.3.1.1 Mukhopadhyay (1986) facies model: This model uses macerals interpreting the depositional facies. The Permian Gondwana coals of the Barapukuria and Dighipara Basins are plotted and analyzed using this model (Fig.4.2.2.1), which indicates that these coals have originated from forest swamps under mildly oxic to anoxic conditions with good tissue preservation.

4.2.2.3.1.2 Singh and Singh (1996) facies model: Since the clastic mineral matter is directly related to water cover in the basin, due importance has been given to the mineral matter content; therefore both the macerals and mineral matter have been used in this facies model. The results for all of the coal samples studied (Fig.4.2.2.2) indicate that there were situations of alternation of oxic and anoxic moor conditions in the basin. This is attributed to fluctuating water cover in the basin.

4.2.2.3.1.3 Diessel (1986) facies model: The coal facies and condition of deposition is analyzed using a cross-plot according to Diessel (1986), based on two parameters, the Gelification Index (GI) and Tissue Preservation Index (TPI). The formulae of these two parameters are:

$$GI = \frac{\text{Vitrinite+Macrinite}}{\text{Semifusinite+Fusinite+Inertodetrinite}} \qquad TPI = \frac{\text{Telinite+Collotelinite+Semifusinite+Fusinite}}{\text{Collodetrinite+Macrinite+Inertodetrinite+Vitrodetrinite+Corpogelinite}}$$

The plots (Fig.4.2.2.3) suggest a high tree density in the terrestrial origin of these investigated coal samples, corresponding to a depositional environment of dry forest to piedmont plain conditions.

High values of both GI and TPI represent the wet conditions of peat development while low GI and TPI values correspond to dry conditions (Diessel, 1986). In the present study, the moderately high TPI and the considerable quantity of mineral matters are the indicators of intermittently dry forest swamps. The TPI values range from 1.0 to 4.3, suggesting a lateral increase in the rate of subsidence and depth of the basin.

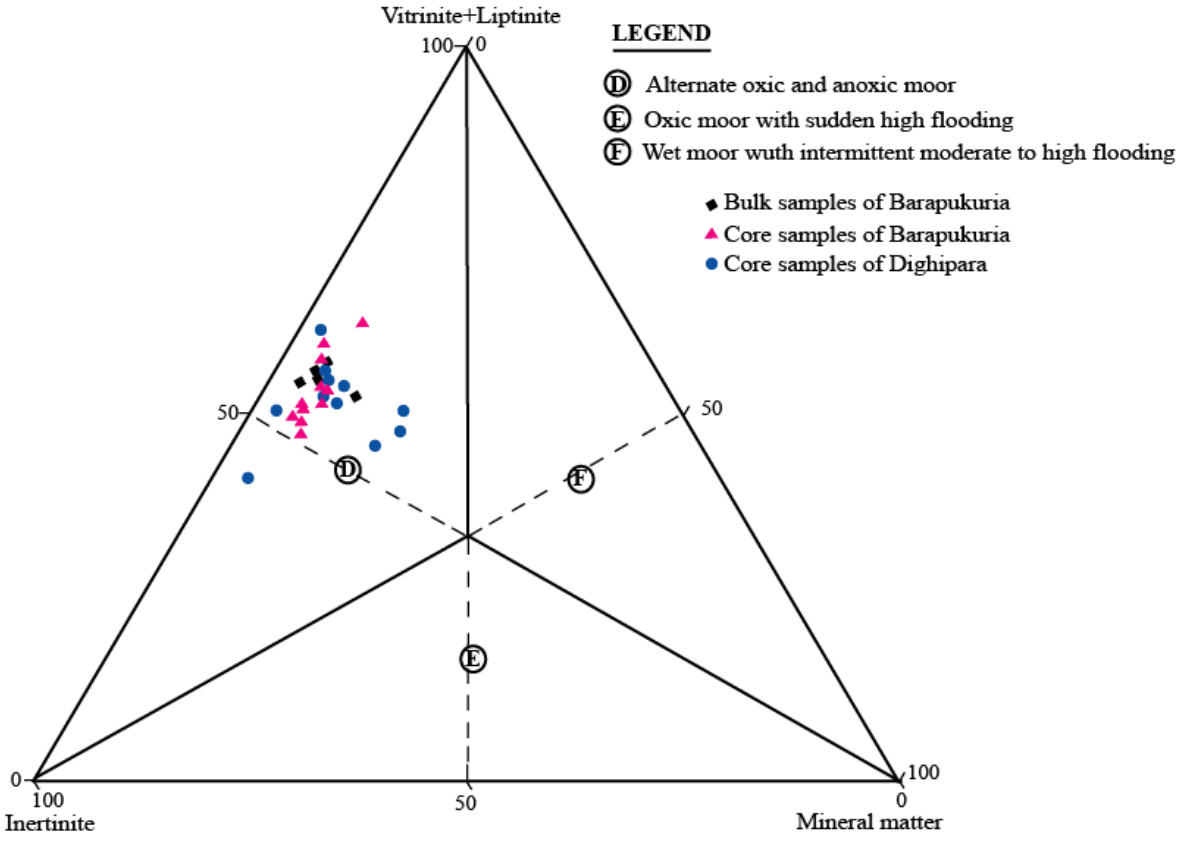

Fig.4.2.2.2. Environmental depositional conditions of the coals based on the composition of the macerals and mineral matter contents. The explored samples fall within an alternation of oxic-anoxic moor (c.f., Singh and Singh, 1996).

4.2.2.3.1.4 Calder et al. (1991) facies model: Water cover is an important condition for the deposition of the peat and coal in the swamp. In consideration of this, the Ground Water Index (GWI) and Vegetation Index (VI) have been calculated to identify the major peat mire paleoenvironments, that is, bog forest and swamp forest, together with the

hydrogeological conditions that would explain the ombotrophic, mesotrophic and rheotrophic mires. The following formulae are used for the current indices.

$$GWI = \frac{Gelinite+Corpogelinite+Clayminerals+Quartz+Vitrodetrinite}{Telinite+Collotelinite+Collodetrinite}$$

$$VI = \frac{Telinite+Collotelinite+Fusinite+Semifusinite+Funginite+Secretinite+Resinite}{Collodetrinite+Inertodetrinite+Alginite+Liptodetrinite+Cutinite}$$

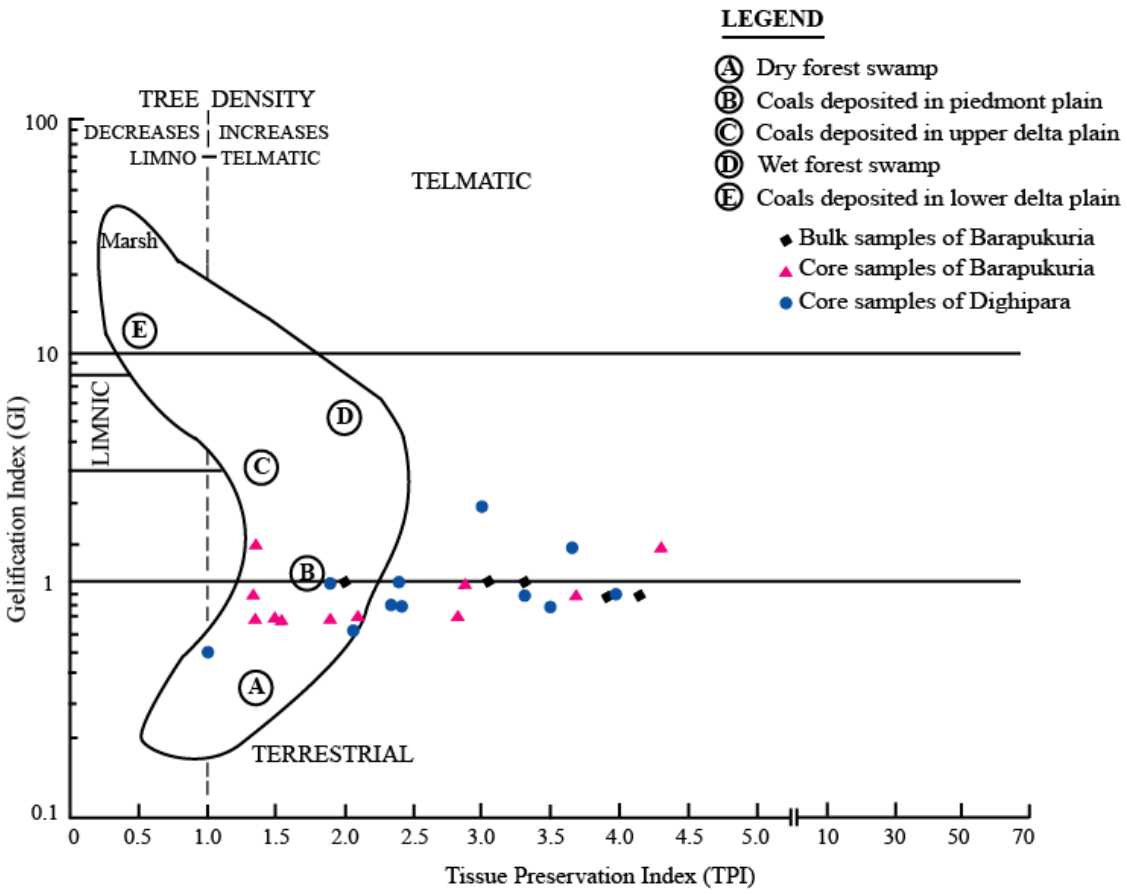

Fig.4.2.2.3. A cross-plot of the Gelification Index (GI) and Tissue Preservation Index (TPI) showing the depositional settings of the peat mires. The analyzed samples fall mostly within terrestrial dry forest swamp and piedmont plain (e.g., Diessel, 1986).

The low values of GWI (0.1 - 2.2) and moderate values of VI (1.2 - 4.2) indicate that the coals evolved under ombotrophic (incorporating very low nutrient levels for plant development) to mesotrophic (incorporating moderate nutrient levels for plant

development) hydrogeological conditions, containing herbaceous plants (Fig.4.2.2.4). It further supports the contention showed of the model of Singh and Singh (1996) that the water level frequently fluctuated (with a gradual lowering or raising) during the evolutional history of the peat of these Permian coal basins. This interpretation is also in agreement with the terrestrial dry forest to piedmont plain depositional condition (i.e., oxic-anoxic) suggested by the GI-TPI plot.

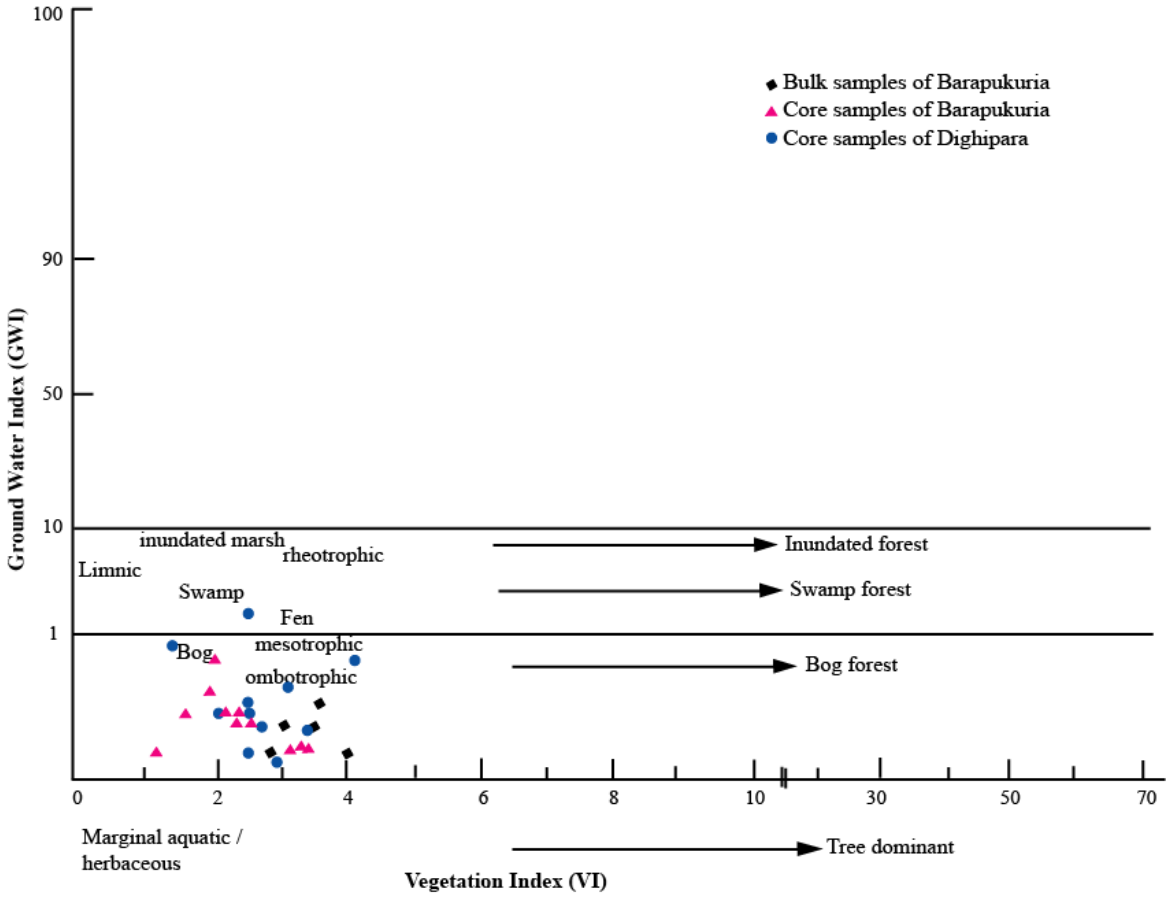

Fig.4.2.2.4 A cross-plot of the Ground Water Index (GWI) and Vegetation Index (VI) showing the palaeoenvironments of the coal mires. The studied samples also imply mostly bog forest environment and swamp forest (adopted by Calder et al., 1991).

4.2.2.3.1.5 Hacquebard and Donaldson (1969) facies model: The depth of water not only controls the various environments of the vegetation and the deposition of the peat mires,

but also affects the mode of preservation of the petrographic entities (Singh and Shukla, 2004). On this basis, Hacquebard and Donaldson (1969) constructed a double triangular facies diagram (later modified by Marchioni, 1980) using the microlithotypes (maceral associations) to interpret the coal facies and depositional conditions. The analyzed coal samples are plotted into this modified double triangle. The upper triangle represents relatively dry conditions (i.e., terrestrial and telmatic) and coals with lower than 20% of dull bands, while the lower triangle corresponds to subaquatic conditions (i.e., limnic and limno-telmatic) and coals with higher than 20% of dull bands. Since the analyzed Permian coals contain more than 20% of dull bands, they have essentially been in the lower triangle. The related four elements of the facies model are:

A = Sporoclarite+Duroclarite+Vitrinertoliptite

B = Fusitoclarite+Vitrinertite I+Fusite

C = Vitrite+Cuticoclarite+Vitrinertite V

D = Clarodurite+Durite+Macroite+Carbominerite

The plots in this facies model for the investigated coal samples suggest that the coals have evolved mostly in limno-telmatic zones containing floral assemblages associated with reed moor and with intermittent floods leading to the development of a forest moor facies (Fig.4.2.2.5). Hunt and Smyth (1989) have demonstrated that reed moor (swamps) are often associated with rising water tables (i.e., flooding), which is supported by the present interpretation based on the reconstructed models. However Teichmüller and Teichmüller (1982) and Singh and Shukla (2004) consider it can be difficult to separate telmatic (terrestrial) and limnic (subaquatic) facies in swamps due to the frequent of subaquatic sedimentation in the basin.

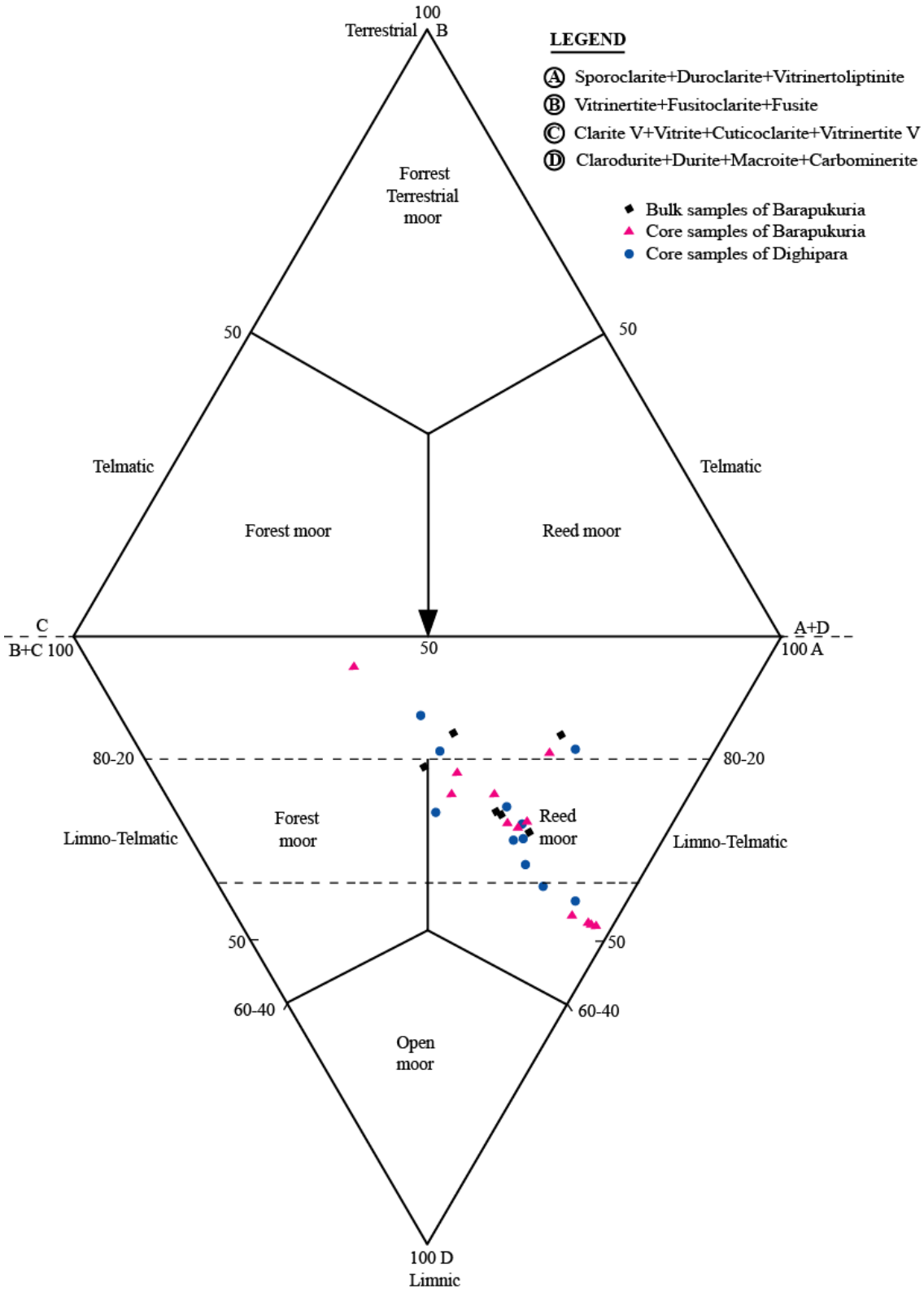

Fig.4.2.2.5. A double triangular diagram based on microlithotypes, illustrating the coal facies. The examined samples indicate a facies range from reed moor to forest moor (adopted by Hacquebard and Donaldson, 1969; Cited by Singh and Shukla, 2004).

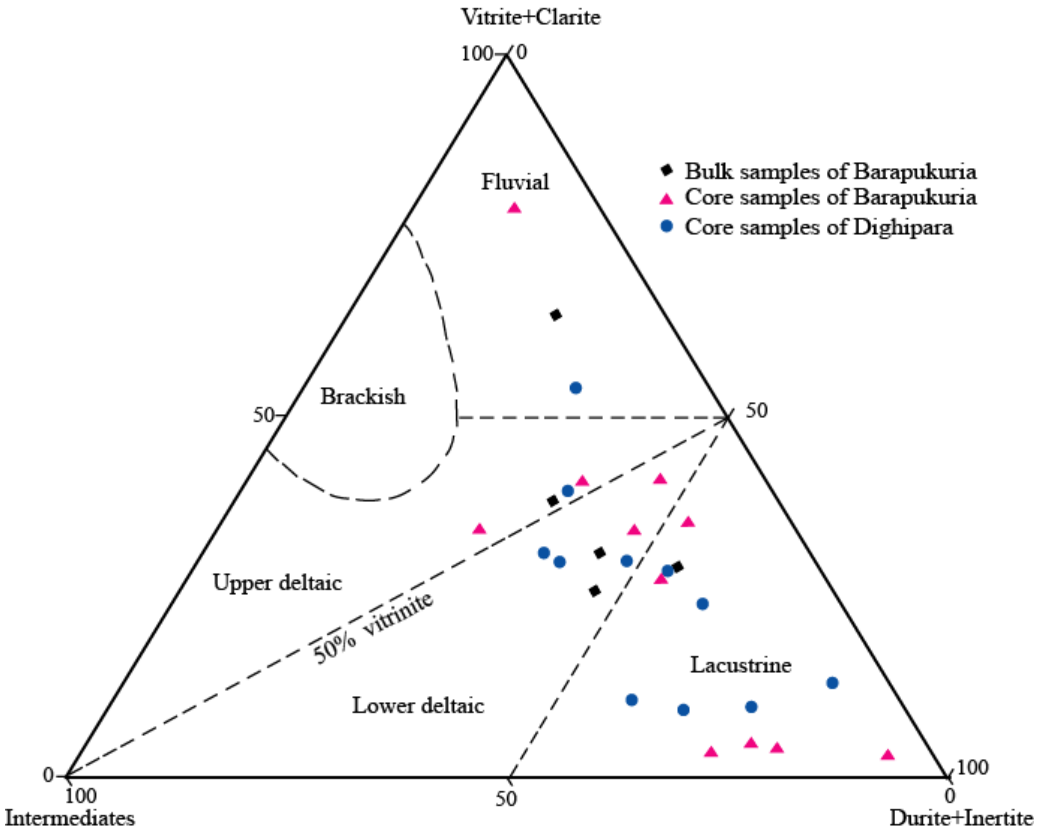

Fig.4.2.2.6. Coal depositional environments based on the composition of microlithotypes (free of mineral matter). The analyzed coal samples indicate deltaic-lacustrine-fluvial environments (e.g., Singh and Singh, 1996; Singh and Shukla, 2004; Smyth, 2009).

4.2.2.3.2 Depositional environment of the Barapukuria and Dighipara Basin coals

The Permian Gondwana sediments of the Barapukuria and Dighipara half-grabens (Bengal Basin) has been envisaged as derived from delta plain to fluvial (Alam et al., 2003; Islam and Hossain, 2006) based on the sedimentological analysis. Using organic geochemical parameters (in a biomarker study), Farhaduzzaman et al. (2011b and 2012a) proposed terrestrial oxic (dry) depositional conditions for the Permian coals. A predominantly delta-plain depositional environment and fluvial influenced lacustrine conditions have been visualized for the current study of the Permian coal samples, following the depositional model framed by Smyth (1984) and later cited by Singh and Shukla (2004) (Fig.4.2.2.6).

This interpretation is in fairly good agreement with the depositional scenario depicted by another depositional model constructed by Hunt (1982), where it suggests delta-plain (mainly upper delta) depositional conditions (Fig.4.2.2.7).

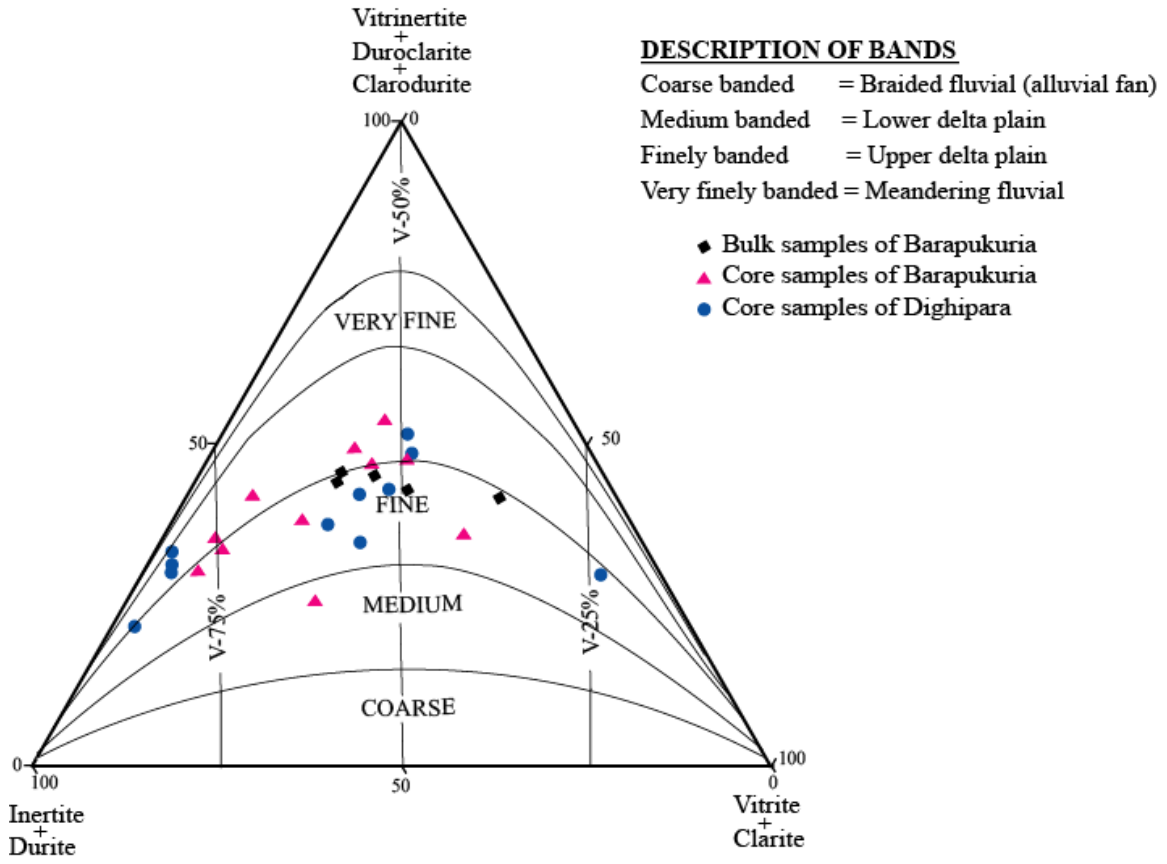

Fig.4.2.2.7. A triangular diagram based on microlithotypes, illustrating the depositional environments. The analyzed samples represent the upper delta plain (mostly) to lower delta plain deposits (adopted by Hunt, 1982).

The dominance of inertinite macerals and absence of alginite maceral is an additional evidence for a terrestrial oxic (dry) depositional environmental, which is in agreement with the interpretation made of Hunt and Smyth (1989). Teichmüller (1974a), Cook et al. (1981) and Sherwood and Cook (1986) state that bituminite is considered to comprise the decompositional products of higher plants under oxic and anoxic depositional conditions.

The presence of bituminite in the current analyzed samples therefore corresponds to alternating oxic and anoxic depositional conditions (with sudden floods), which are indicated by the facies models used (Mukhopadhyay, 1986; Singh and Singh, 1996). The studied basins are known to be shallow (Imam, 2005; Islam and Hayashi, 2008). This is indicated by the high concentrations of inertinite macerals found in them such as semifusinite, fusinite and inertodetrinite. The shallowness of the basins is also demonstrated by the moderate presence of mineral matter, which indicates there were frequent dry spells (i.e., alternating oxic and anoxic conditions) during the evolution of the basin. On the other hand, the higher concentration of vitrinitic macerals indicates the development of coals beneath deeper basins. A variation in the depth of these basins is also suggested by the TPI values, as is discussed in subsection 4.2.2.3.1.3. Using isotopic analysis, together with a petrographic study of the Permian Gondwana coals of India, Singh et al. (2012c) has shown that those coals were deposited under the alternating oxic-anoxic environmental conditions (i.e., dry-wet). The results of the current investigation are similar, in that the studied Permian coals of Bangladesh were also deposited under oxic-anoxic mixed conditions. The influence of dry conditions is supported by the presence of inertinite macerals (especially structured macerals) and of wet conditions by the presence of vitrinite macerals.

The petrographic analysis of coal is important to understand the palaeofacies and palaeodepositional conditions of the peat/mire (e.g., Teichmüller and Teichmüller, 1982; Holland et al., 1989; Mishra et al., 1990; Marchioni and Kalkreuth, 1991; Ratanasthien et al., 1999; Hower and Gayer, 2002; Singh and Shukla, 2004; Bechtel et al. 2004; Paul, 2005; Shaver et al., 2006; Singh et al., 2010a and 2010b; Dutta et al, 2011; Farhaduzzaman et al. 2011b; Singh et al., 2012a and 2012b).

An attempt has therefore been made to reconstruct the conditions of coal formation in the Barapukuria and Dighipara Basins on the basis of the maceral compositions and associations (microlithotypes) in the studied Permian coals. Facies and depositional conditions were investigated using petrography-based facies models, which have been used successfully in analyzing Permian Gondwana coals globally. Nevertheless, isotope analysis and a detail palynological study need to be carried out to investigate these coals further. The current investigation is consistent with the interpretations relating to Indian and Australian Permian coals.

A high concentration of inertinite and the low content of sulfide minerals (e.g., pyrite) is supported by the cross-plot of GI vs. TPI (terrestrial dry forest to piedmont plain depositional conditions) and GWI vs. VI (ombotrophic to mesotrophic hydrogeological conditions). As previously discussed, the terrestrial dry forest condition is known to be favorable for the development of more inertinite macerals in the coals, but is not congenial for sulfide mineralization. The dominance of structured inertinite macerals, such as fusinite and semifusinite, also indicate wild fire.

The variation of different maceral indices with a vertical depth pattern at the Barapukuria and Dighipara Basins is depicted in Fig.4.2.2.8. TPI, GI and VI values all increase with depth in both basins. However, the GWI value decreases with depth at Barapukuria but increases with depth at Dighipara. It indicates that a similar depositional condition prevailed at the time of deposition for both basins but that the groundwater level was fluctuating.

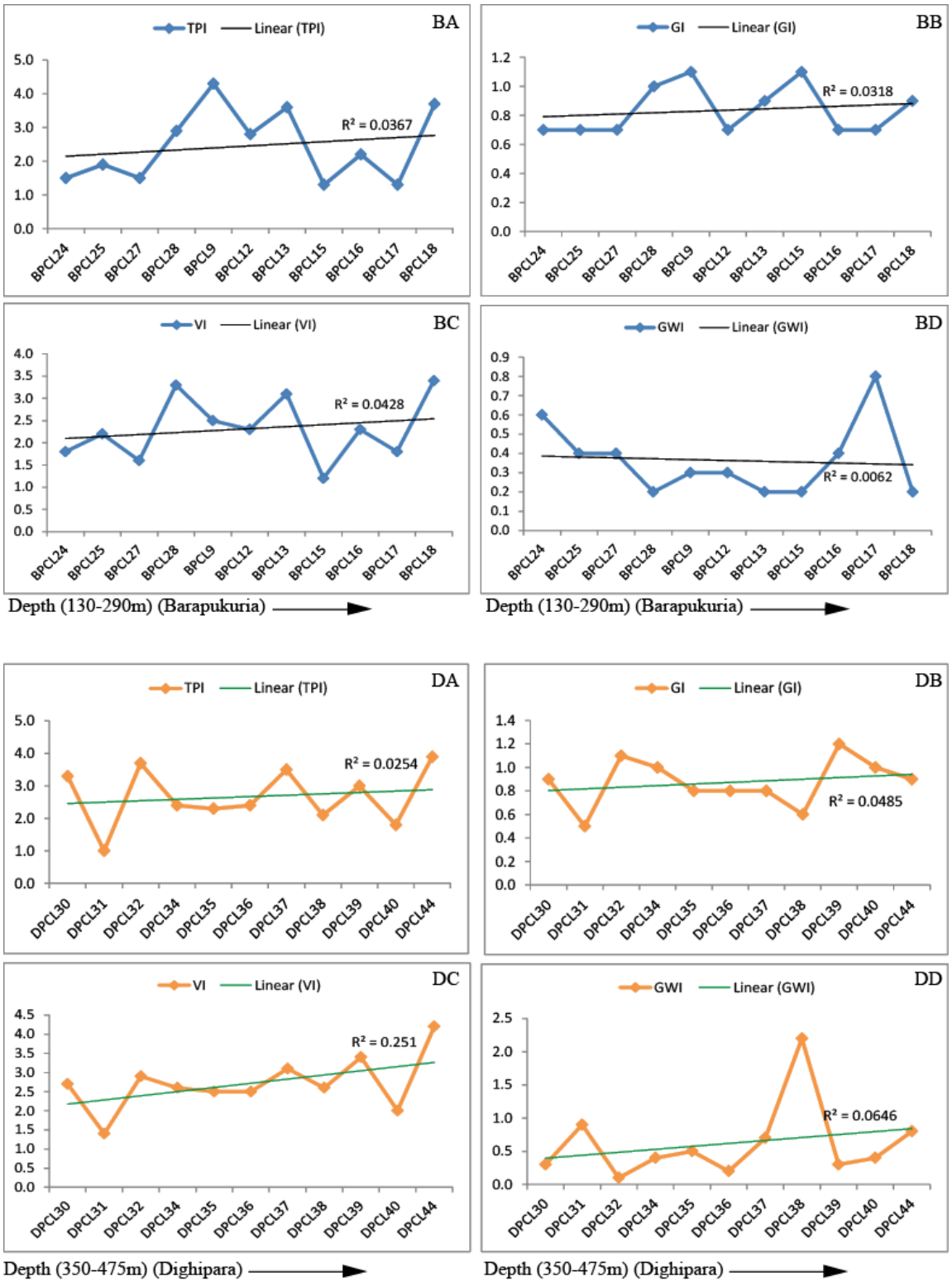

Fig.4.2.2.8. The variation of different maceral indices (TPI, GI, VI and GWI) with vertical depth patterns at the Barapukuria (BA, BB, BC and BD) and Dighipara (DA, DB, DC and DD). TPI, GI and VI values increase with depth in both basins. However, the GWI value decreases with depth at Barapukuria but increases with depth at Dighipara. It indicates that a similar depositional condition prevailed at the time of deposition for both basins, while the groundwater level is fluctuating.

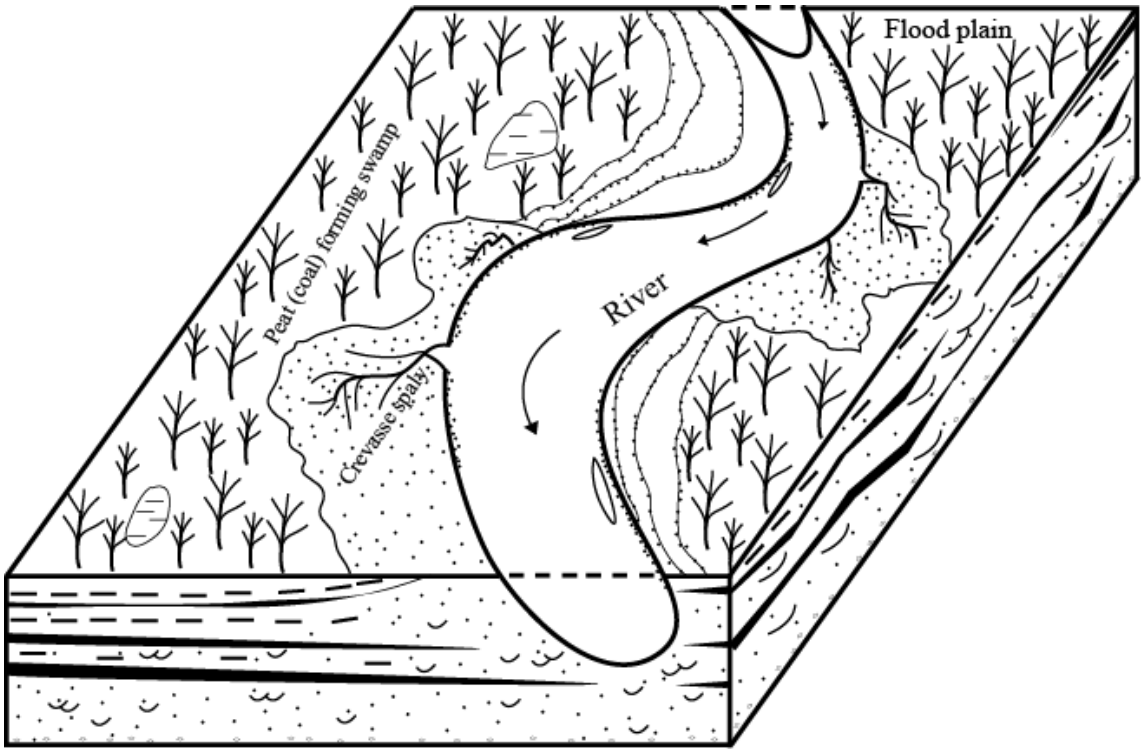

Fig.4.2.2.9. Schematic block diagram represents the palaeodepositional environments of the Permian Gondwana coal deposits of the Barapukuria and Dighipara Basins, NW Bangladesh (Farhaduzzaman et al., 2012a).

Casshap and Tewari (1987) and Islam and Hossain (2006) demonstrated that the Gondwana sediments were laid down by laterally migrating river channels. The protected mires/lakes that formed the coals evolved in the poorly drained flood plains and peat swamps, which were densely vegetated, due to the tropical humid climatic conditions. This contention substantiates the interpretations made by the present authors. The peat that formed these coals was deposited under mostly oxic but with alternating oxic-anoxic moor conditions that evolved through fluvial-controlled deltaic (mainly upper delta) to lacustrine deposits, with sudden and frequent high floods. In this regard, based on the present study and supporting data reported by previous workers, a mixed (oxic-anoxic) dominantly terrestrial depositional environmental setting as shown in Fig.4.2.2.9 is proposed for the Barapukuria and Dighipara coals.

Chapter 4.2.3 Organic Geochemical Study of Coals and Associated Sediments

The organic matter compared to inorganic mineral matter (MM) can be considered to distinguish petrographically three organic-rich rock types. These are coals (MM<20 vol.%), carbargillites (MM 20-60 vol.%) and mudstones (MM>60 vol.%). The proportion of the organic versus inorganic content is also reflected in the TOC content. The coals, carbargillites and mudstones have TOC>40 wt.%, between 40-20 wt.% and <20 wt.% respectively. The present study is carried out based on organic geochemical and organic petrological methods using 36 core samples. Five different drill holes were chosen from two different coal basins. An attempt is taken to characterize the organic facies of currently studied coals, carbargillites and mudstones of these basins. Biomarker analysis (TIC, m/z 191 and m/z 217 fragmentograms) and maceral composition (proportions and properties of vitrinite, liptinite and inertinite) distinguishes three different organic facies of the studied samples: coals, carbargillites (as defined by Mackowsky, 1982) and mudstones.

4.2.3.1 Source rock properties

A summary of vitrinite reflectance (%R_o) and other organic geochemical data of the analyzed samples obtained from SRA are shown in Table 4.2.3.1. Rock-Eval pyrolysis (RE) results of some selected samples are displayed in Appendix E1 for comparative evaluation. There is a good agreement between the results gained from SRA and those of RE, enabling high confidence in the SRA results. The recorded TOC value (wt.%) ranges 44-78 (coals), 19-39 (carbargillites) and 4-9 (mudstones). HI varies from 113 to 310 (coals), 243 to 381 (carbargillites) and 65 to 158 (mudstones) mg HC/g TOC. It shows noticeable variation which infers a mixture of kerogen types (III/II) (see Appendices B1 and B3 for definitions).

Table 4.2.3.1. Source Rock Analyzer (of Rock-Eval equivalent) parameters and vitrinite reflectane data of the analyzed samples- coal, carbargillite and mudstone (refer to Appendix B1).

Sample	Borehole	Depth (m)	TOC	Ro	Tmax	S1	S2	S3	HI	OI	PI
Coals											
BPCL9	DOB8	192	73.87	0.77	430.2	4.92	187.64	6.21	254	8	0.03
BPCL12	DOB8	207	47.45	0.78	433.2	1.31	147.04	0.81	310	2	0.01
BPCL13	DOB8	209	48.10	0.72	432.3	1.19	136.20	1.61	283	3	0.01
BPCL15	DOB8	214	64.24	0.73	430.1	3.41	92.03	3.86	143	6	0.04
BPCL16	DOB8	219	65.06	0.76	435.3	1.44	125.05	1.17	192	2	0.01
BPCL17	CSE7	278	73.71	0.75	435.6	0.96	141.47	5.53	192	8	0.01
BPCL18	CSE7	287	69.05	0.77	433.9	4.05	145.28	6.24	210	9	0.03
BPCL24	CSE9	134	54.70	0.77	432.7	1.92	130.95	1.27	239	2	0.01
BPCL25	CSE9	135	63.12	0.76	435.4	2.32	71.11	7.89	113	13	0.03
BPCL27	CSE9	167	78.10	0.77	429.8	2.27	175.26	2.25	224	3	0.01
BPCL28	CSE9	171	59.53	0.75	430.7	4.06	127.86	5.05	215	8	0.03
DPCL30	GDH60	358.14	75.39	0.70	433.8	6.04	130.36	2.96	173	4	0.04
DPCL31	GDH60	363.02	70.29	0.80	434.2	5.95	138.06	3.82	196	5	0.04
DPCL32	GDH60	368.81	73.73	0.73	434.7	3.15	136.26	4.94	185	7	0.02
DPCL34	GDH62	368.80	63.83	0.71	433.4	3.08	148.25	2.80	232	4	0.02
DPCL35	GDH62	396.85	66.71	0.79	431.9	2.68	150.41	3.85	225	6	0.02
DPCL36	GDH62	402.64	70.29	0.76	434.6	4.27	136.50	1.60	194	2	0.03
DPCL37	GDH62	403.56	73.73	0.71	432.9	4.02	133.23	3.84	181	5	0.03
DPCL38	GDH62	431.54	44.04	0.71	436.3	0.69	108.94	1.84	247	4	0.01
DPCL39	GDH62	436.78	58.87	0.72	438.1	1.80	138.34	2.00	235	3	0.01
DPCL40	GDH62	453.12	54.88	0.78	435.8	2.01	150.73	3.68	275	7	0.01
DPCL44	GDH62	469.15	63.07	0.73	436.7	0.88	115.92	6.03	184	10	0.01
Range		134-469	44-78	0.70-0.80	430-438	1-6	71-188	1-8	113-310	2-13	0.01-0.04
Carbargillites											
BPCR11	DOB8	198	24.87	0.78	431.3	1.78	76.44	0.58	307	2	0.02
BPCR14	DOB8	211	29.68	0.73	434.1	1.41	85.56	0.78	288	3	0.02
BPCR19	CSE7	290	18.94	0.71	434.2	0.04	65.34	2.43	345	13	0.01
BPCR23	CSE9	133	34.70	0.66	431.5	0.97	84.19	4.59	243	13	0.01
BPCR26	CSE9	153	38.81	0.72	429.6	1.88	106.56	4.64	275	12	0.02
BPCR29	CSE9	178	25.22	0.69	431.6	1.05	65.26	2.80	259	11	0.02
DPCR33	GDH60	395.63	24.96	0.77	437.2	2.21	81.18	2.74	325	11	0.03
DPCR41	GDH62	456.29	23.83	0.76	435.2	0.70	90.89	0.55	381	2	0.01
DPCR42	GDH62	459.64	38.14	0.81	434.4	1.84	99.20	1.56	260	4	0.02
DPCR43	GDH62	467.87	20.28	0.77	435.6	0.27	62.67	1.45	309	7	0.01
Range		133-468	19-39	0.66-0.81	430-437	0.1-2.2	63-107	1-5	243-381	2-13	0.01-0.03
Mudstones											
BPMT10	DOB8	196	4.37	0.80	430.8	0.06	6.83	0.18	156	4	0.01
BPMT20	CSE7	306	9.20	0.60	435.6	0.81	14.50	0.36	158	4	0.05
BPMT21	CSE7	307	5.06	0.76	438.1	0.08	3.48	0.88	76	17	0.02
BPMT22	CSE7	329	6.16	0.68	439.2	0.09	4.03	0.79	65	13	0.02
Range		196-329	4-9	0.60-0.80	431-439	0.1-0.8	4-15	0.2-0.9	65-158	4-17	0.01-0.05

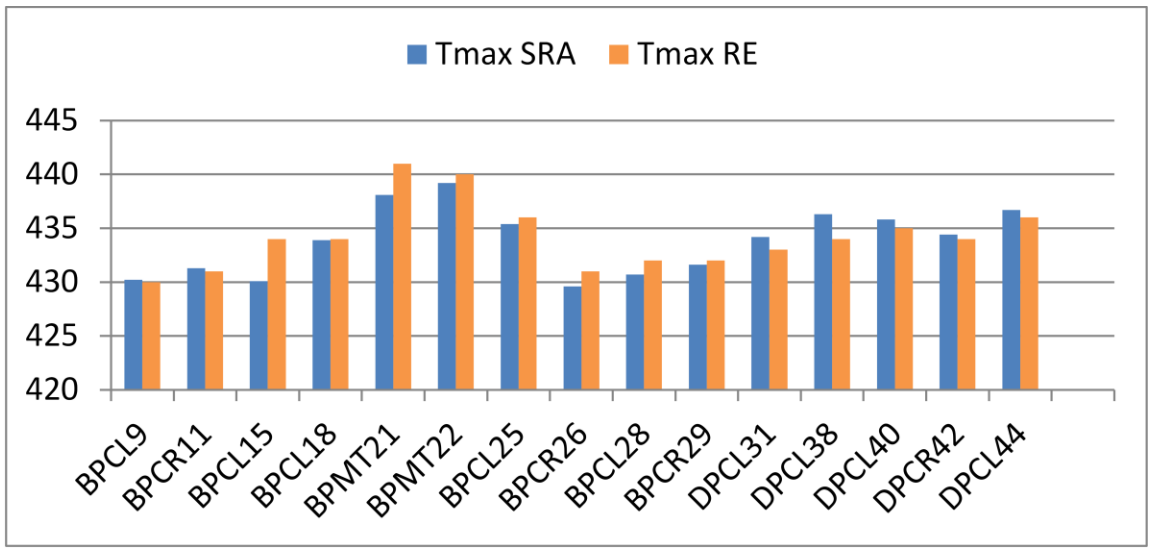

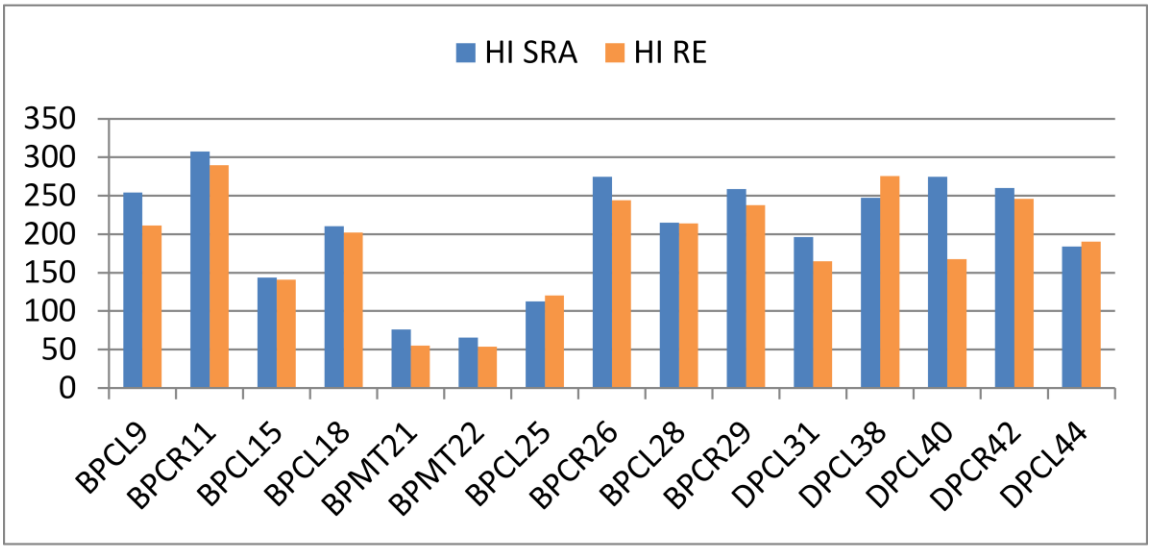

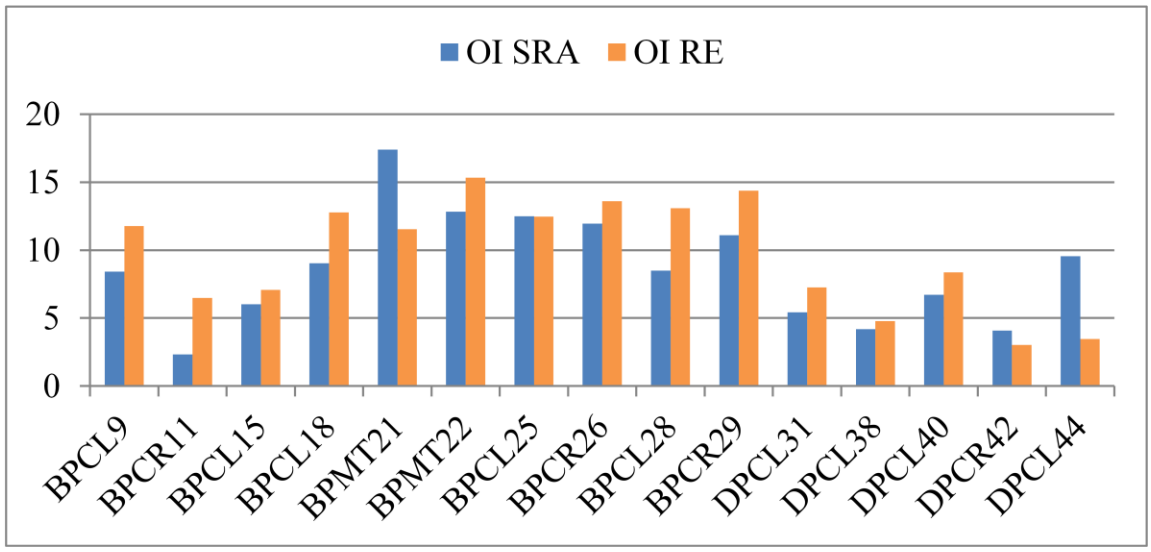

Fig.4.2.3.1. Pictorial comparison of T_{max}, HI and OI values found from two different methods SRA and RE. It shows a good agreement (see Appendix E1).

Peters (1986) showed the terrestrial organic matters (especially coals and coaly OM) of low maturity (%R_o less than 0.6%) produce large amounts of CO_2 during pyrolysis. Here OI values are consistent with the corresponding atomic O/C. But some mature coaly organic matter show unusually low OI with values lower than expected based on the atomic O/C. At higher levels of maturity, more pyrolytic oxygen releases as carbon monoxide which is not analyzed by SRA or Rock-Eval equipment. The recorded OI values of the currently analyzed samples are low. These can be caused by inadequate detection by the thermal conductivity detector (TCD) of CO generation during pyrolysis of this high maturity coaly organic matter as previously reported by Peters (1986), Hunt (1991) and Bordenave et al. (1993). It may also be related to different types of organic matter (Koeverden et al., 2011). T_{max} values are close to each other and range from 431 to 438 °C (coals), 430 to 437 °C (carbargillites) and 431 to 439 °C (mudstones). Based on the present analysis, a good quality source rock potential of the studied coal, carbargillite and mudstones is deduced following the classification adopted by Peters and Cassa (1994).

4.2.3.2 Macerals and kerogen type

A summary of the identified maceral composition viewed in the analyzed coal, carbargillite and mudstone samples are shown in Table 4.2.3.2. Inertinite (31-55 vol.%) is the dominant maceral followed by the vitrinite (19-39 vol.%) and liptinite (14-31 vol.%) group macerals with some inorganic mineral matter in the analyzed coal samples. Type III kerogen, represented by vitrinite, is the dominant maceral in carbargillites (19-35 vol.%) and mudstones (21-25 vol.%). Nearly equal amounts of liptinite (12-19 vol.% in carbargillites and 4-6 vol.% in mudstones) and inertinite (10-27 vol.% in carbargillites and 6-9 vol.% in mudstones) with large amounts of mineral matter are identified under microscope. Carbargillite samples show higher liptinite contents (range 21-34 vol.% and mean 27

vol.%, mineral free basis) than coal samples (range 15-33 vol.% and mean 24 vol.%, mineral free basis).

Table 4.2.3.2. A summary of maceral and mineral matter (MM) composition (vol.%) of the analyzed samples- coal, carbargillite and mudstone.

Sample	Vitrinite macerals	Liptinite macerals	Inertinite macerals	Mineral matter	Vitrinite macerals (MM free basis)	Liptinite macerals (MM free basis)	Inertinite macerals (MM free basis)
Coals							
BPCL9	31.2	31.1	31.1	6.6	33.4	33.3	33.3
BPCL12	25.9	25.2	43.9	5.0	27.3	26.5	46.2
BPCL13	34.8	19.1	40.2	5.9	37.0	20.3	42.7
BPCL15	37.8	15.2	40.2	6.8	40.6	16.3	43.1
BPCL16	27.4	20.0	45.8	6.8	29.4	21.5	49.1
BPCL17	26.6	22.4	45.0	6.0	28.3	23.8	47.9
BPCL18	30.5	29.2	36.8	3.5	31.6	30.3	38.1
BPCL24	28.5	23.5	40.9	7.1	30.7	25.3	44.0
BPCL25	26.8	23.0	45.4	4.8	28.2	24.2	47.7
BPCL27	27.3	24.0	43.7	5.0	28.7	25.3	46.0
BPCL28	31.0	26.8	38.0	4.2	32.4	28.0	39.7
DPCL30	31.2	24.4	38.8	5.6	33.1	25.8	41.1
DPCL31	23.8	17.4	55.0	3.8	24.7	18.1	57.2
DPCL32	38.7	22.7	36.4	2.2	39.6	23.2	37.2
DPCL34	36.7	17.9	38.8	6.6	39.3	19.2	41.5
DPCL35	30.9	20.5	39.4	9.2	34.0	22.6	43.4
DPCL36	28.5	22.0	46.9	2.6	29.3	22.6	48.2
DPCL37	27.8	18.0	37.8	16.4	33.3	21.5	45.2
DPCL38	23.5	24.1	34.0	18.4	28.8	29.5	41.7
DPCL39	38.3	14.0	40.5	7.2	41.3	15.1	43.6
DPCL40	31.2	22.6	37.4	8.8	34.2	24.8	41.0
DPCL44	28.2	22.0	32.2	17.6	34.2	26.7	39.1
Range	19-39	14-31	31-55	2-18	22-41	15-33	33-57
Carbargillites							
BPCR11	22.5	12.3	22.9	42.3	39.0	21.3	39.7
BPCR14	21.3	13.2	22.5	43.0	37.4	23.2	39.5
BPCR19	21.2	18.6	16.0	44.2	38.0	33.3	28.7
BPCR23	34.6	17.7	12.7	35.0	53.2	27.2	19.5
BPCR26	31.2	15.0	26.8	27.0	42.7	20.5	36.7
BPCR29	30.6	17.8	10.0	41.6	52.4	30.5	17.1
DPCR33	24.1	13.7	20.6	41.6	41.3	23.5	35.3
DPCR41	26.8	19.4	22.8	31.0	38.8	28.1	33.0
DPCR42	19.8	17.1	16.1	47.0	37.4	32.3	30.4
DPCR43	18.9	16.6	13.8	50.7	38.3	33.7	28.0
Range	19-35	12-19	10-27	27-54	37-53	21-34	17-40
Mudstones							
BPMT10	22.0	5.0	6.0	67.0	66.7	15.2	18.2
BPMT20	23.0	6.0	9.0	62.0	60.5	15.8	23.7
BPMT21	21.0	5.0	8.0	66.0	61.8	14.7	23.5
BPMT22	25.0	4.0	6.0	65.0	71.4	11.4	17.1
Range	21-25	4-6	6-9	62-67	61-71	11-16	17-24

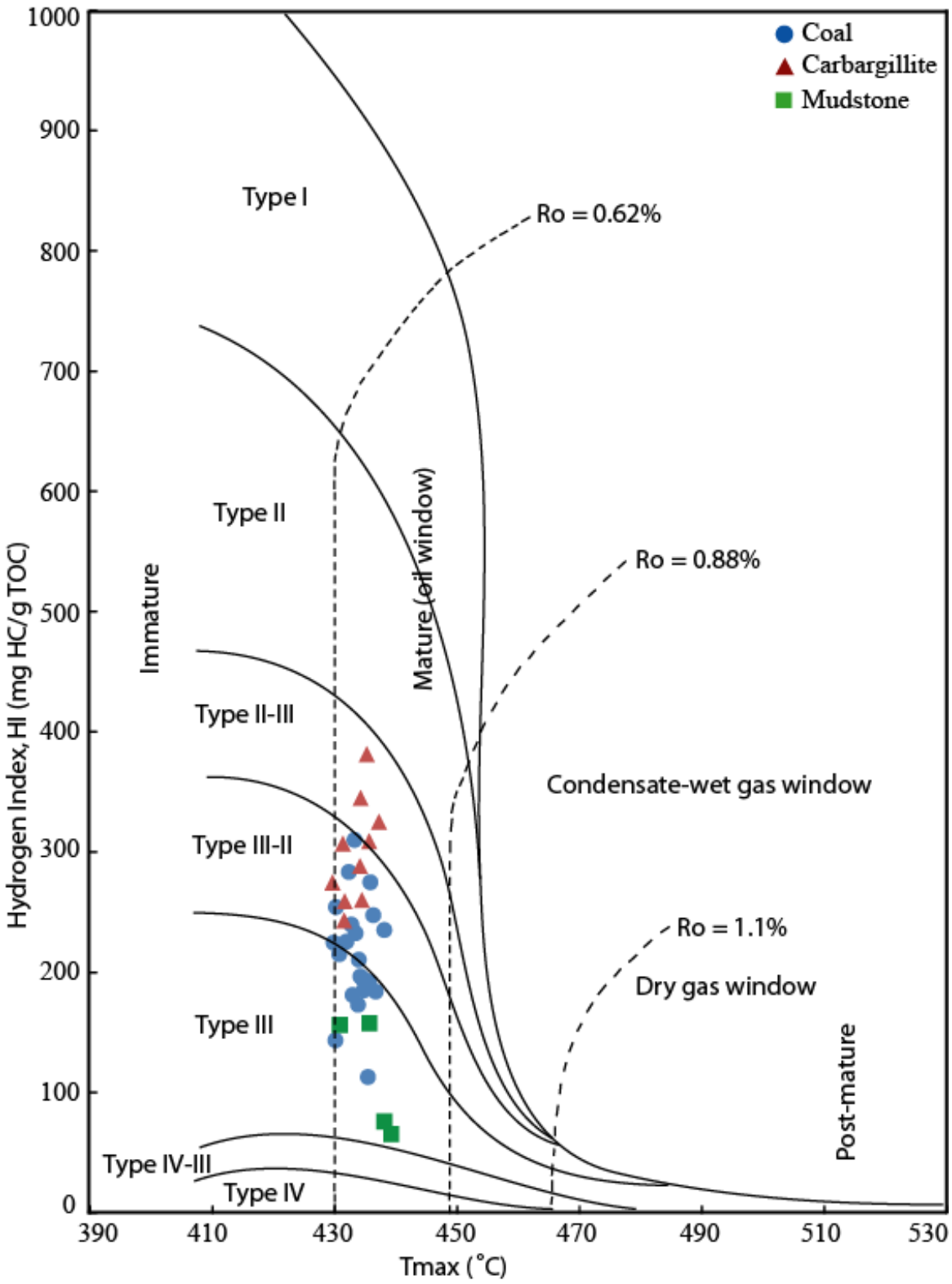

Fig.4.2.3.2. Organic facies distribution from HI versus T_{max} plot. The analyzed coals are dominated by Type III-II, carbargillites by Type II-III and mudstones by Type III organic matter. All the samples being early to mid-maturity thermal conditions (see Appendices B1 and B3 for definitions) (minor modification from Bjorøy et al., 1981; Davies and Nassichuk, 1988; Goodarzi et al., 1987; van Koeverden et al., 2011).

Significant amounts of Type II liptinite macerals are identified in all the studied samples. The carbargillite samples show higher concentration of these liptinite macerals. Important liptinite macerals include sporinite, cutinite, resinite, bituminite, fluorinite and exsudatinite (Table 4.2.3.2). The measured HI value of coals, carbargillites and mudstones varies in the ranges of 113-310, 243-381 and 65-158 mg HC/g TOC respectively. The higher value of HI in carbargillite is probably due to presence of more liptinite macerals. It suggests a higher oil and gas generation potential than the coals. A cross-plot of HI and T_{max} shows the coals match to Type III-II kerogen (dominantly III), carbargillites to Type II-III kerogen, and mudstone to Type III kerogen (Fig.4.2.3.2).

Dembicki (2009) stated that besides other geochemical data (e.g., Rock-Eval), PyGC provides a good solution to interpret kerogen mixtures. This shows the direct hint of hydrocarbon types that can be generated by the kerogen during maturation. The $>C_{15}$ fraction would be the least amount and $<C_{10}$ fraction would be the highest shown in the PyGC traces for the organic matter containing Type III kerogens. In case of Type I kerogens, it would be in reverse, i.e., highest $>C_{15}$ fraction and least $<C_{10}$ fraction. The intermediate one represents Type II kerogens (Giraud, 1970; Larter and Douglas, 1980; Dembicki et al., 1983; Dembicki, 2009). Following these discussions, the mixed kerogen fingerprints of mainly n-alkane/alkene doublets and aromatic compounds are displayed by the whole rock PyGC pyrograms of the analyzed coal, carbargillite and mudstone samples (Fig.4.2.3.3). These currently studied pyrograms show neither the typical signatures of Type II nor Type III. Instead, they show the intermediate signatures of these two. It is known that type III kerogen composes mainly of vitrinite macerals with large amounts of inertinites. Type II kerogen consist mainly of liptinite macerals with large amounts of vitrinite macerals.

The observed PyGC pyrograms of coal samples correspond to dominating inertinite macerals mixed with large amounts of vitrinite and liptinites, thus more likely representing 75% Type III and 25% Type II (Dembicki, 2009) (Fig.4.2.3.3A). Similarly, the PyGC pyrograms of carbargillite samples containing dominant vitrinite macerals with considerable amount of liptinites represent 50% Type II and 50% Type III (Fig.4.2.3.3B). The mudstone samples with dominant vitrinites correspond mostly to Type III kerogen (Fig.4.2.3.3C). The relative abundance of aliphatic to aromatic hydrocarbons may be quantified by the ratio of n-octene (C_8) to (m+p)-xylene. The calculated C_8/xylene ratio is low which ranges from 0.73 to 0.89. The analyzed samples show high profusion of aromatic hydrocarbons (for example, benzene, toluene and xylene) relative to n-alkanes/alkenes (i.e., low C_8/xylene ratio) in the pyrograms. It implies the higher input of humic materials in the source. The dominant inertinite macerals correspond to vascular higher plants, which represents the terrestrial environment of deposition.

4.2.3.3 Soluble extract and biomarker distributions

A summary of extractable organic matter (EOM) of the analyzed samples is shown in Table 4.2.3.3. The total amount of EOM is high in coal samples (13811-46529 ppm) compared to those of carbargillite (5182-24241 ppm) and mudstones (1704-2991 ppm). Hydrocarbon in extract (%) for all the three groups of samples is similar. Aromatic hydrocarbon fraction is higher than the aliphatic in all the analyzed samples. The values of calculated hydrocarbon yield (aromatic>aliphatic) are also close to one another. These are 17-34 mg EOM/g TOC in coal, 11-34 mg EOM/g TOC carbargillite and 20-23 mg EOM/g TOC mudstone samples. A significant amount of NSO is measured in all the samples.

The NSO fraction is higher than that of total hydrocarbons (aliphatic and aromatic) in most of the coal samples. It is higher than the aliphatic or aromatic in carbargillite or mudstone samples (Table 4.2.3.3).

Table 4.2.3.3. Soluble extract yield and alkane parameters of the studied coal, carbargillite and mudstones of the Barapukuria and Dighipara half-grabens, Bangladesh (refer to Appendix B1).

Sample no.	EOM (ppm of whole rock)		EOM (mg EOM/g TOC)					n-alkane parameters					
	Tot extr	HC in extract (%)	Tot extr	Alip	Aro	NSO	Total HC (yield)	n-alk max	CPI[1]	CPI[2]	Pr/Ph	Pr/nC17	Ph/nC18
Coals													
BPCL9	46529	42	62.99	7.20	19.28	36.51	26.48	25	1.35	1.56	4.87	5.85	0.59
BPCL15	29365	55	45.71	10.42	14.73	20.56	25.15	19	1.06	1.32	6.72	1.68	0.24
BPCL16	37953	58	58.34	11.09	22.48	24.76	33.57	18	1.13	1.40	7.67	2.30	0.26
BPCL24	21179	44	38.72	4.14	12.87	21.71	17.01	25	1.35	1.64	7.36	2.09	0.20
BPCL28	24095	48	40.47	7.05	12.44	20.99	19.49	19	1.25	1.57	5.64	2.22	0.28
DPCL31	30105	54	42.83	7.01	16.28	19.54	23.29	18	1.16	1.48	6.05	1.73	0.24
DPCL35	24855	58	37.26	8.04	13.46	15.76	21.50	23	1.33	1.69	9.33	1.49	0.13
DPCL38	13811	55	31.36	5.66	11.50	14.20	17.16	18	1.17	1.36	6.63	1.24	0.17
DPCL40	23257	47	42.38	5.00	15.12	22.26	20.12	19	1.20	1.43	6.65	2.89	0.33
DPCL44	17899	59	28.38	5.05	11.58	11.75	16.63	17	1.10	1.29	5.40	0.65	0.12
Range	13811-46529	44-59	28-63	4-11	12-22	12-37	17-34	17-25	1.1-1.4	1.3-1.7	5-9	0.7-5.9	0.1-0.6
Carbargillites													
BPCR11	10772	48	43.31	5.72	14.56	22.63	20.48	25	1.54	1.90	5.45	1.13	0.19
BPCR26	24241	54	62.46	13.94	20.08	28.44	34.02	19	1.23	1.25	6.63	3.15	0.35
BPCR29	5182	55	20.55	3.58	7.71	9.26	11.29	25	1.37	1.64	4.85	2.59	0.34
DPCR42	16992	57	44.55	10.73	14.85	18.97	25.58	25	1.46	1.93	4.00	0.42	0.09
Range	5182-24241	48-57	21-62	4-14	8-20	9-28	11-34	19-25	1.2-1.5	1.3-1.9	4-7	0.4-3.2	0.1-0.4
Mudstones													
BPMT21	1704	58	33.67	6.99	12.70	13.98	19.69	18	1.33	1.62	3.60	0.57	0.14
BPMT22	2991	48	48.55	10.02	13.71	25.21	23.34	18	1.27	1.43	5.90	1.42	0.21
Range	1704-2991	48-58	34-49	7-10	13-14	14-25	20-23	18	1.2-1.3	1.4-1.6	4-6	0.6-1.4	0.1-0.2

The aliphatic fractions of selected coal, carbargillite and mudstone samples are analyzed by GCMS. The peaks in GCMS are identified assuming mass spectra as well as comparing with published literature. For example, Philp (1985) and Pearson and Alam (1993) for TIC; Fabianska et al. (2003), Ahmed et al. (2009) and Kashirtsev et al. (2010) for m/z 191 fragmentograms; and Abeed et al. (2011), Koeverden et al. (2011) and Sachse et al. (2012) for m/z 217 fragmentograms.

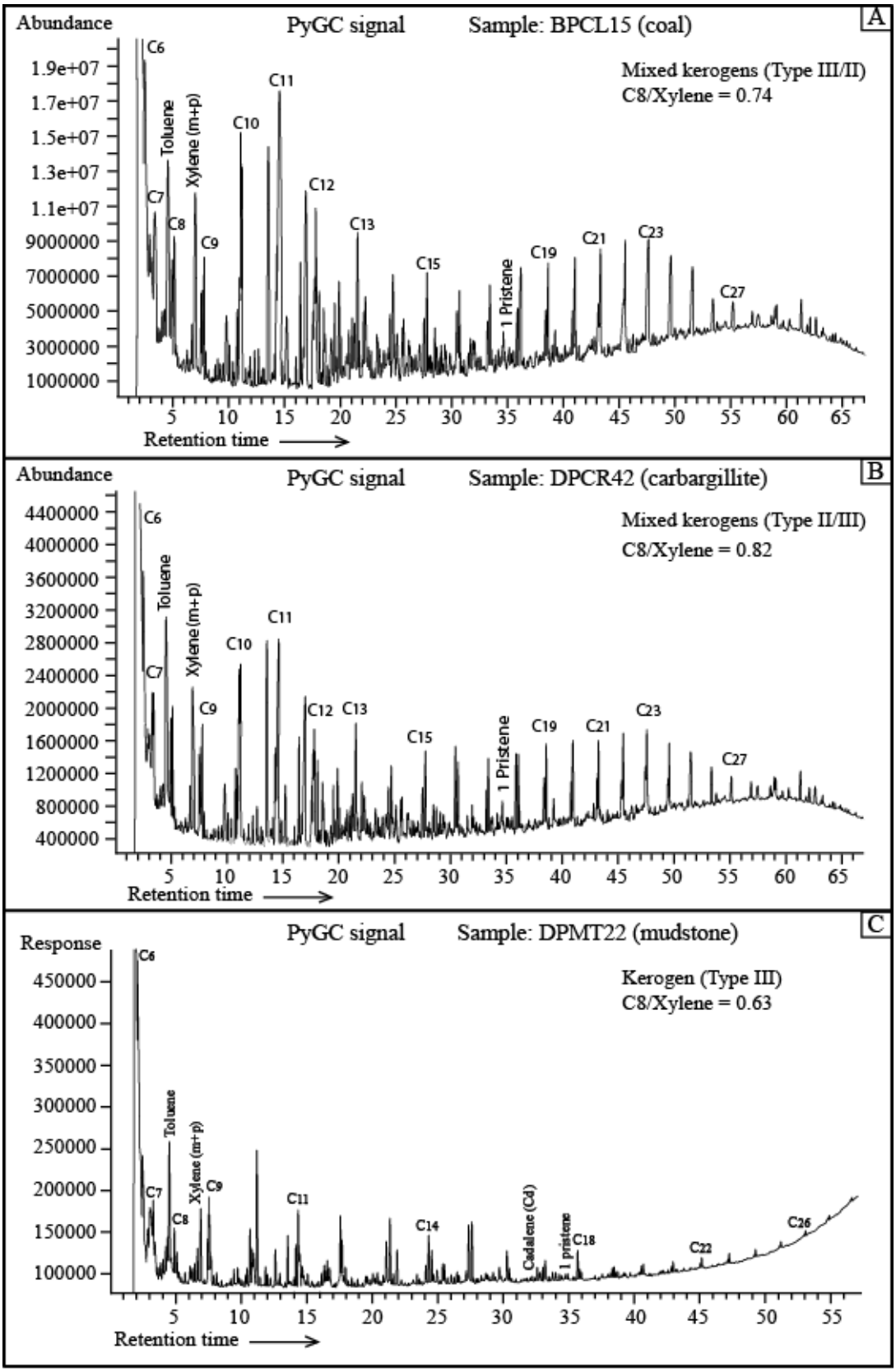

Fig.4.2.3.3. PyGC pyrograms of the analyzed coal, carbargillite and mudstone samples representing Type III/II (dominant Type III), Type II/III mixture and Type III kerogen respectively (c.f., Dembicki, 2009).

Table 4.2.3.4. Hopane biomarker parameters (measured from m/z 191) of the analyzed coal, carbargillite and mudstones (refer to Appendix B2).

Sample no.	Tm/Ts	C_{29}/C_{30}	C_{30}-mor/ C_{30}-hop	C_{31} 22S/ (22S+22R)	C_{32} 22S/ (22S+22R)	C_{35}-homo hopane index	Ster/Hop
Coals							
BPCL9	13.09	0.78	0.36	0.58	0.57	0.06	0.39
BPCL15	11.95	0.83	0.38	0.58	0.57	0.04	0.39
BPCL16	12.18	0.75	0.42	0.57	0.57	0.05	0.40
BPCL24	10.71	0.77	0.46	0.55	0.57	0.05	0.42
BPCL28	11.10	0.94	0.49	0.55	0.58	0.04	0.34
DPCL31	11.50	0.92	0.45	0.57	0.57	0.03	0.35
DPCL35	10.91	0.99	0.48	0.56	0.57	0.05	0.34
DPCL38	8.75	0.96	0.31	0.58	0.57	0.03	0.40
DPCL40	7.88	1.18	0.39	0.59	0.60	0.04	0.45
DPCL44	7.69	0.93	0.34	0.58	0.59	0.03	0.39
Range	8-13	0.8-1.2	0.3-0.5	0.55-0.59	0.57-0.60	0.03-0.06	0.3-0.4
Carbargillites							
BPCR11	8.17	0.83	0.32	0.57	0.57	0.04	0.46
BPCR26	11.98	0.75	0.41	0.58	0.57	0.04	0.42
BPCR29	10.12	0.85	0.53	0.56	0.59	0.05	0.41
BPCR42	5.26	0.89	0.37	0.61	0.59	0.05	0.49
Range	5-12	0.8-0.9	0.3-0.5	0.56-0.61	0.57-0.59	0.04-0.05	0.4-0.5
Mudstones							
BPMT21	6.33	0.82	0.31	0.57	0.59	0.03	0.22
BPMT22	20.67	0.96	0.45	0.60	0.59	0.04	0.35
Range	6-21	0.8-1.0	0.3-0.5	0.57-0.60	0.59	0.03-0.04	0.2-0.4

4.2.3.3.1 GC: TIC (Total Ion Current)

The TIC (total ion current- full scan), m/z 191 and m/z 217 chromatograms of the representative three samples (coal, carbargillite and mudstone) are shown in Figs.4.2.3.4, 4.2.3.5 and 4.2.3.6. A long range of n-alkanes ranging from nC_{10} to nC_{40} are identified in TIC fragmentograms of all the analyzed samples. These are dominated by medium to high molecular weight (nC_{16}-nC_{27}) n-alkanes (Figs.4.2.3.4A, 4.2.3.5A and 4.2.3.6A; Appendices E2 and E3).

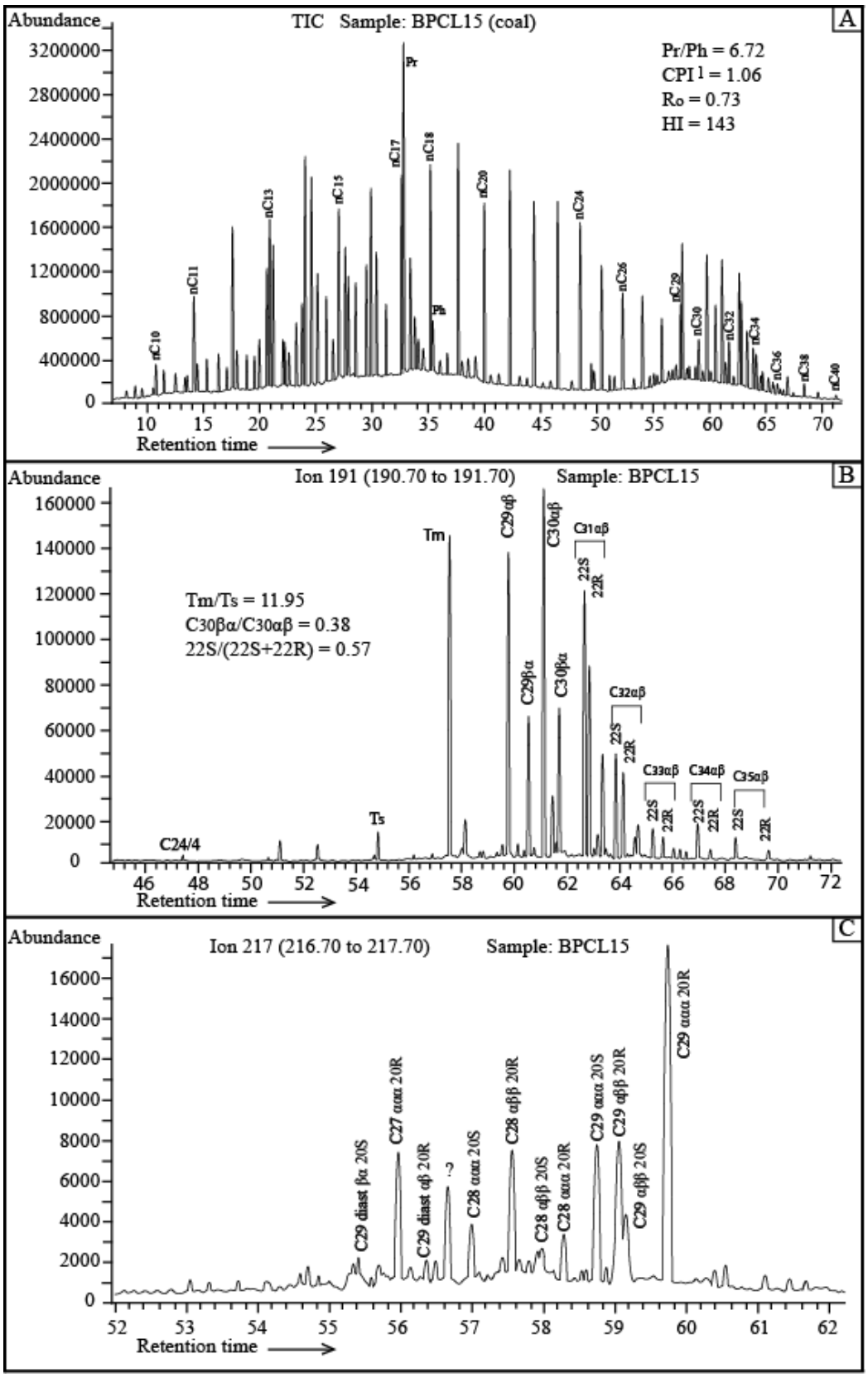

4.2.3.4. Gas chromatogram (TIC) and mass fragmentograms m/z 191 and m/z 217 of aliphatic fraction of a studied coal sample (BPCL15) of the Barapukuria Coal Basin (peak i.d. in Appendix B2).

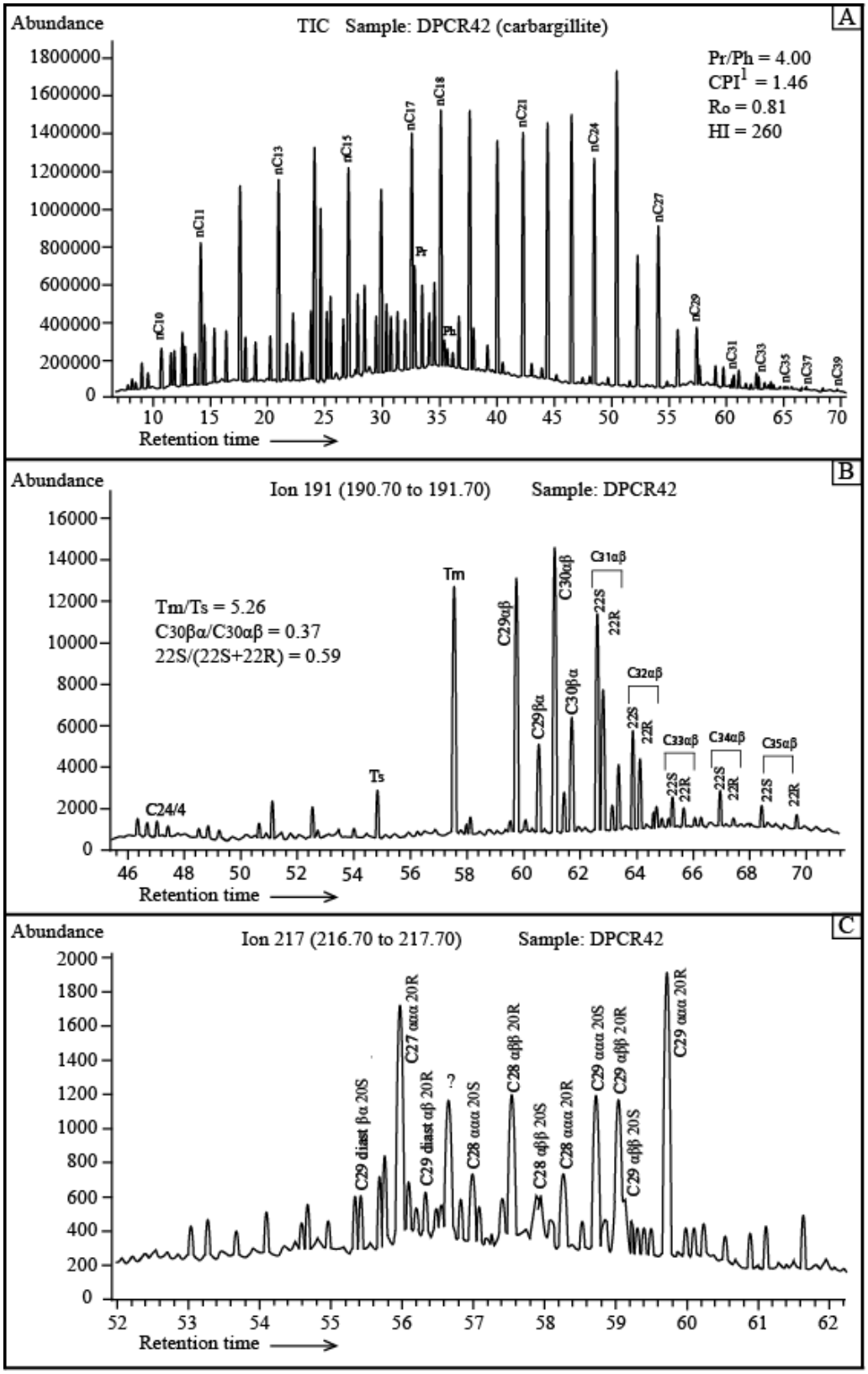

4.2.3.5. Gas chromatogram (TIC) and mass fragmentograms m/z 191 and m/z 217 of aliphatic fraction of a studied carbargillite sample (DPCR42) of the Dighipara Coal Basin (peak i.d. in Appendix B2).

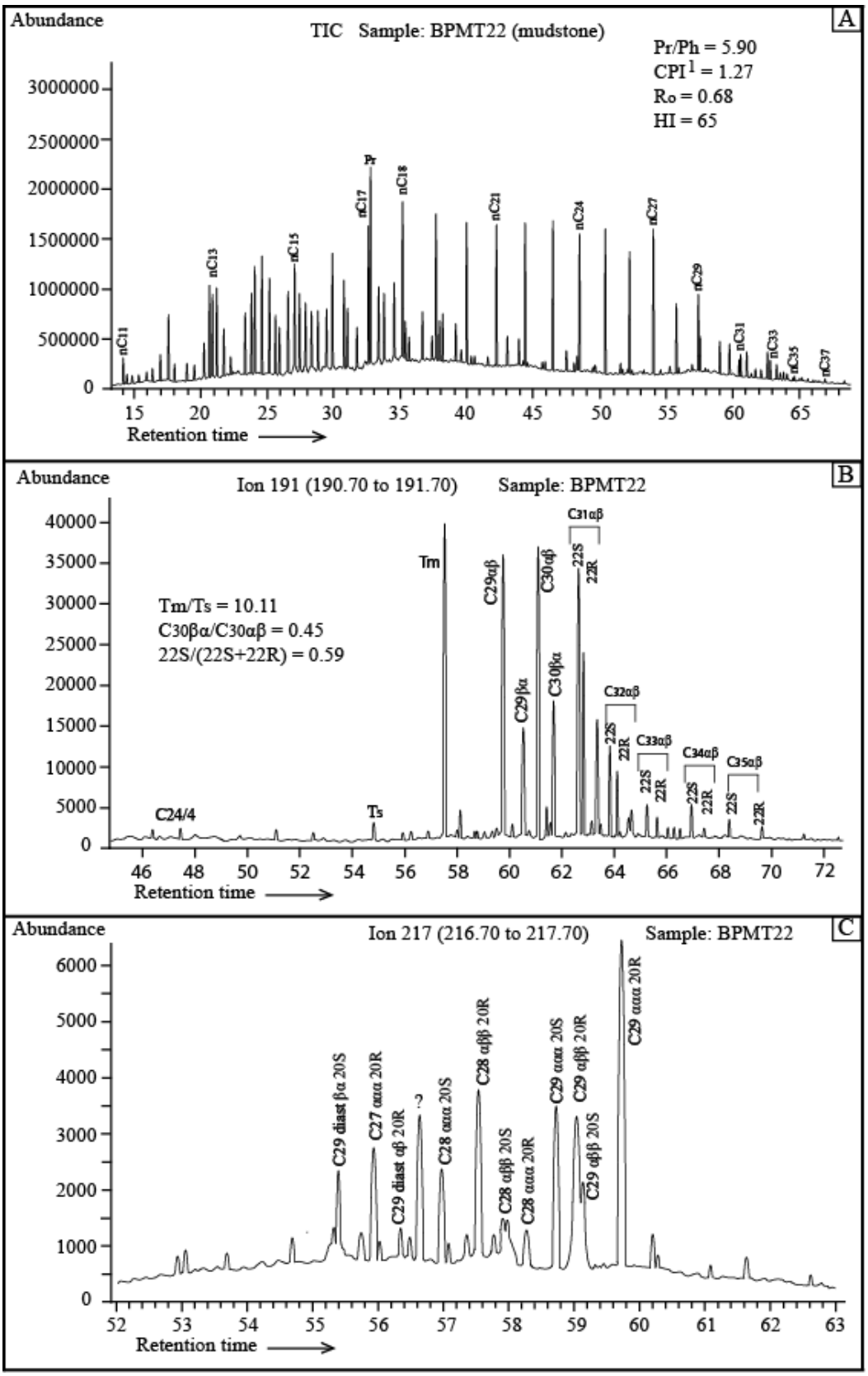

4.2.3.6. Gas chromatogram (TIC) and mass fragmentograms m/z 191 and m/z 217 of aliphatic fraction of a studied mudstone sample (BPMT22) of the Barapukuria Coal Basin (peak i.d. in Appendix B2).

The n-alkane maxima are found at nC_{18}-nC_{25} in coal and mudstone samples. It is mostly at nC_{25} in carbargillite samples, thus, representing more waxy appearance. The calculated peak height of pristane in all the analyzed samples is higher than that of nC_{17}. The peak height of phytane is lower than that of nC_{18}. The ratio of Pr/Ph is high (4-9) found in the analyzed coal, carbargillite and mudstone samples. Compared to carbargillites, the higher value of Pr/Ph in coal samples is likely because of strong terrestrial influence. The odd carbon-numbered n-alkanes are dominant over the even carbon-numbered members noted in TIC. Thus, CPI value is always higher than the unity.

4.2.3.3.2 GCMS: m/z 191 Fragmentogram

The m/z 191 mass chromatograms of the aliphatic hydrocarbon fractions are analyzed for all the three groups of sediments. They shows abundant pentacyclic triterpanes with trace amount of tetracyclic terpanes (Figs.4.2.3.4B, 4.2.3.5B and 4.2.3.6B; Appendices E2 and E3). Comparing the peak intensities, the pentacyclic triterpanes in coals are more abundant than those in mudstones or carbargillite (coal > mudstone > carbargillite). The $C_{30}\alpha\beta$-hopane is the dominant hopane. The $C_{31}\alpha\beta$-hopane is the most abundant compound among the homohopanes in all the three group of sediments analyzed. A large amount of $C_{30}\beta\alpha$-hopane and $C_{29}\beta\alpha$-hopane (moretanes) compared to their αβ-compounds is found in the analyzed samples. The Tm/Ts ratio of carbargillite samples is slightly lower than those of coal and mudstone samples (Table 4.2.3.4). The C_{35} homohopane index is very low (0.03-0.06) in all the analyzed samples.

Table 4.2.3.5. Sterane and diasterane biomarker parameters (measured from m/z 217) of the analyzed coal, carbargillite and mudstone samples (refer to Appendix B2).

Sample no.	C_{27}-ster (%)	C_{28}-ster (%)	C_{29}-ster (%)	Ster C_{29} 20S/ (20S+20R)	Ster C_{29} ββ/ (ββ+αα)	Diaste/ Sterane	Diaste 20S/ (20S+20R)
Coals							
BPCL9	22.63	6.84	70.53	0.34	0.26	0.05	0.58
BPCL15	25.13	9.05	65.83	0.31	0.30	0.07	0.60
BPCL16	25.67	9.78	64.55	0.23	0.32	0.08	0.60
BPCL24	23.81	7.74	68.45	0.28	0.29	0.05	0.61
BPCL28	21.88	9.38	68.75	0.31	0.27	0.05	0.61
DPCL31	27.80	8.29	63.90	0.26	0.32	0.09	0.64
DPCL35	16.22	10.81	72.97	0.24	0.26	0.03	0.60
DPCL38	26.83	9.27	63.90	0.42	0.28	0.05	0.61
DPCL40	24.08	7.33	68.59	0.41	0.27	0.05	0.60
DPCL44	34.07	8.89	57.04	0.41	0.32	0.09	0.60
Range	16-34	7-11	57-73	0.23-0.42	0.26-0.32	0.03-0.09	0.58-0.64
Carbargillites							
BPCR11	55.43	4.21	40.35	0.31	0.36	0.22	0.60
BPCR26	34.84	6.79	58.37	0.32	0.39	0.09	0.60
BPCR29	32.26	4.22	62.53	0.31	0.22	0.04	0.60
DPCR42	35.45	12.73	51.82	0.35	0.32	0.11	0.60
Range	32-55	4-13	40-63	0.31-0.35	0.22-0.39	0.04-0.22	0.60
Mudstones							
BPMT21	18.03	17.17	64.81	0.39	0.39	0.24	0.60
BPMT22	18.71	8.19	73.10	0.33	0.32	0.14	0.77
Range	18-19	8-17	65-73	0.33-0.39	0.32-0.39	0.14-0.24	0.60-0.77

4.2.3.3.3 GCMS: m/z 217 Fragmentogram

The m/z 217 fragmentograms show high relative abundance of C_{29} regular sterane than the C_{28} or C_{27} sterane in coal and mudstone samples (Figs.4.2.3.4C and 4.2.3.6C; Appendix E2). Near equal abundances of C_{27} and C_{29} regular steranes are found in the carbargillite samples (Figs.4.2.3.5C and Appendix E3). The comparative abundance (peak height) of diasterane is slightly higher in carbargillite and mudstone samples than those of coal

samples. The diasterane/sterane ratio varies from 0.03 to 0.09, 0.04 to 0.22 and 0.14 to 0.24 in the analyzed coal, carbargillite and mudstone samples respectively (Table 4.2.3.5). The calculated sterane/hopane ratios of the studied samples are close to one another. It varies from 0.2 to 0.5, which points out the hopane compounds are much higher compared with steranes.

4.2.3.4 Discussion

4.2.3.4.1 Thermal maturity of the organic matter

The measured mean vitrinite reflectance (%R_o) of coals and carbargillites is 0.70-0.80 and 0.66-0.81, respectively. Coal samples are of high volatile bituminous B rank (Stach et al., 1982), representing an early mature oil window. The %R_o varies from 0.60 to 0.76 (%R_o) in the mudstone samples, suggesting early to peak oil-window maturities following the classification adopted by Peters and Cassa (1994). T_{max} values of 429.8-438.1 ˚C for coals, 429.6-437.2 ˚C for carbargillites and 430.8-439.2 ˚C for mudstone samples likewise indicate early to peak maturities (see Appendix B3 for standard parameters and values) (Peters and Cassa, 1994; Petersen, 2002). However, the values of T_{max} and vitrinite reflectance are likely suppressed due to significant presence of liptinite with dominant Type III organic matter in the coal and carbargillite samples (c.f., Hunt, 1991; Hunt and Hennet, 1991; Snowdon, 1995; Petersen, 2006). However, following the maturity interpretation for coals by Petersen (2006), the organic matter in the studied coals marks immature to early mature oil window. A homohopanes ratio 22S/(22S+22R) (i.e., C_{31}- or C_{32}-homohopanes) of about 0.60 is considered to be an equilibrium value for oil window maturity. The calculated homohopanes ratio 22S/(22S+22R) (C_{31}- or C_{32}-homohopanes) of the analyzed samples ranges from 0.55 to 0.61, implying an immature to early thermal maturity stage.

The bimodal distribution of TIC fingerprints of the analyzed samples is in good agreement with this immaturity assessment. The samples' diasterane 20S/(20S+20R) ratios of 0.58-0.77 also support their immature to early maturity level for hydrocarbon generation (Peters and Moldowan, 1993). Other maturity related biomarker ratios such as moretane/hopane, C_{35} homohopane index, diasterane/sterane, sterane C_{29} 20S/(20S+20R) and sterane C_{29} ββ/(ββ+αα) do not show any substantial variation among the analyzed samples nor show correlation with the vitrinite reflectance data. The thermal maturity of the organic matter of any sediment governs, in part, the properties of organic matter and, therefore, can influence interpreting organic facies (Peters et al., 2005; Wan Hasiah, 1999a). Therefore, the biomarker fingerprints presented here are believed to have influenced by the facies difference, particularly source input and the depositional conditions of the organic matter. It is duly explained in the subsection 4.2.3.4.2 below.

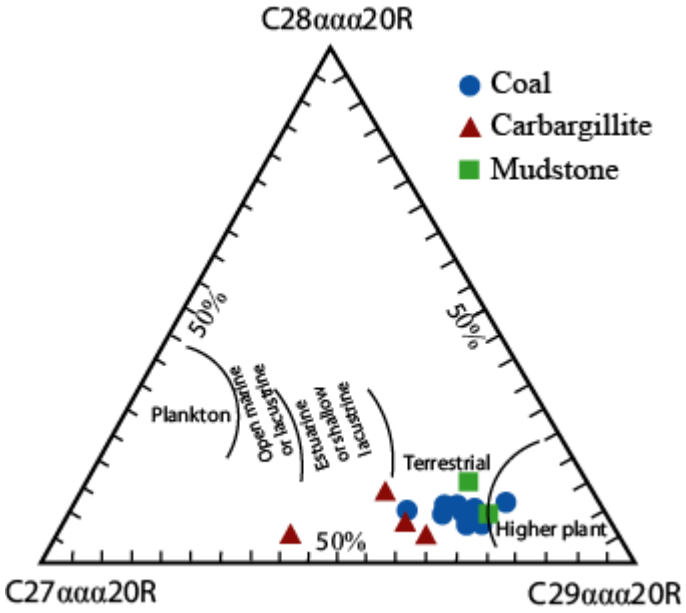

Fig.4.2.3.7. Organic facies related triangular diagram based on C_{27}, C_{28} and C_{29} regular sterane epimers. The analyzed coal samples correspond to mainly terrestrial organic matter with minor contribution from marine source. The carbargillite samples indicate mixed terrestrial and marine influenced sources and mudstones to terrestrial organic source (e.g., Waples and Machihara, 1991).

4.2.3.4.2 Organic facies characteristics

Biomarkers derive from biological precursor molecules in specific organisms. Each of these organisms lives only under specific conditions. So, it is logical to use biomarkers as indicators for both terrestrial and aquatic photosynthetic biota (Waples and Machihara, 1991). Steranes and triterpanes together can provide important clues about the organic facies. Huang and Meinschein (1979) and Pedersen et al. (2006) reported the relative proportions of C_{27}, C_{28} and C_{29} regular steranes (20R epimers) suggest valuable paleoenvironmental information. The dominant C_{29} corresponds to terrestrial facies and dominating C_{27} suggests marine depositional condition.

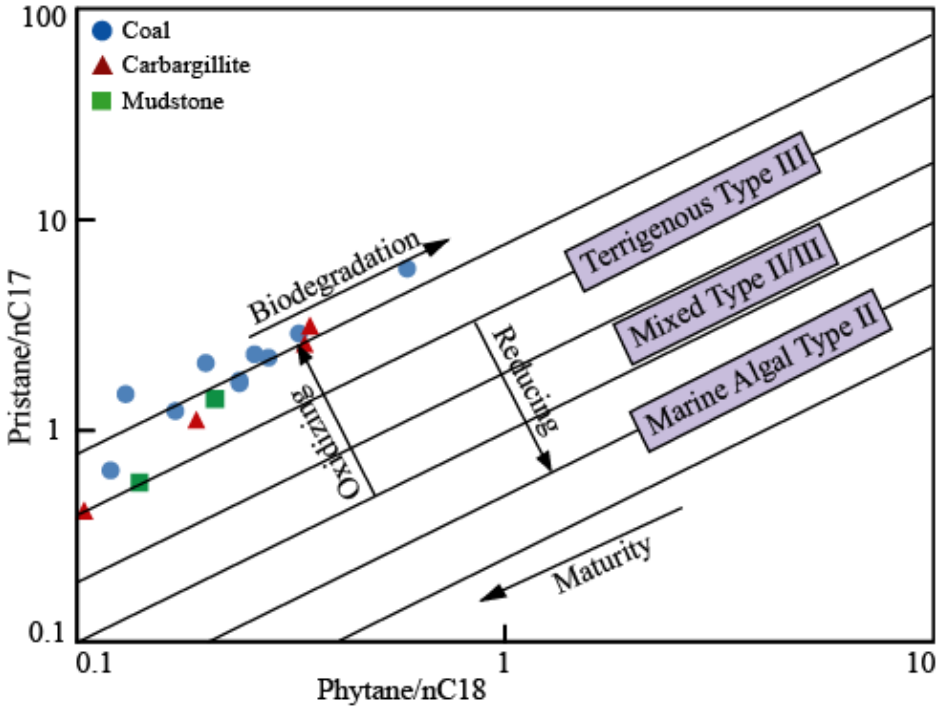

Fig.4.2.3.8. A cross-plot of pristane/nC_{17} versus phytane/nC_{18} for the currently explored coal, carbargillite and mudstone samples. It represents the sub-oxic depositional conditions with dominantly terrestrial organic matter (c.f., Peters et al., 2005).

The framed triangular plot based on the currently analyzed coal, carbargillite and mudstone samples showing dominant C_{29} sterane over C_{27} or C_{28} marks the predominating terrestrial organic facies within the depositional system (Fig.4.2.3.7).

However, the relative proportion of C_{27} of the carbargillite samples is higher than those of coals and mudstones. Thus, significant amount of marine organic matter would have present during the deposition of the Permian carbargillites (Figs.4.2.3.4C, 4.2.3.5C and 4.2.3.6C; Appendices E2 and E3; Fig.4.2.3.7). Petrographically, it is also supported by a higher presence of liptinitc macerals in carbargillites compared with coals and mudstones. The dominant terrestrial organic facies for the analyzed coal, carbargillite and mudstones are also shown by the cross-plot of Pr/nC_{17} versus Ph/nC_{18} (Fig.4.2.3.8). This points to an alternating oxic-anoxic depositional condition prevailed during that geological time. Powell and McKirdy (1973) and Philp (1985) reported the pristane forms in oxidizing condition and phytane in reducing environment. Therefore, the high value of Pr/Ph ratio (>3) shown by the analyzed samples also suggests the suboxic depositional condition of terrestrial environment. The dominated inertinite macerals provides further support to this condition during the deposition of these analyzed samples.

Brooks (1986) and Ramanampisoa et al. (1990) noted that high concentration of C_{29} hopane (C_{29}/C_{30}) indicates a terrestrial depositional facies. There is an overall high content of C_{29} hopane in all the analyzed samples, suggesting the dominant presence of terrestrial derived organic matter. The C_{29}/C_{30} ratios of the analyzed carbargillite samples show slightly lower values (0.8-0.9) compared to those of coals (0.8-1.2) and mudstones (0.8-0.1), also indicating that the coal and mudstone samples have stronger terrestrial organic inputs than the carbargillites. A minor contribution from marine derived facies is also suggested by the relatively lower value of C_{29}/C_{30} in some of the analyzed coal samples (BPCL9, BPCL24 and BPCL28).

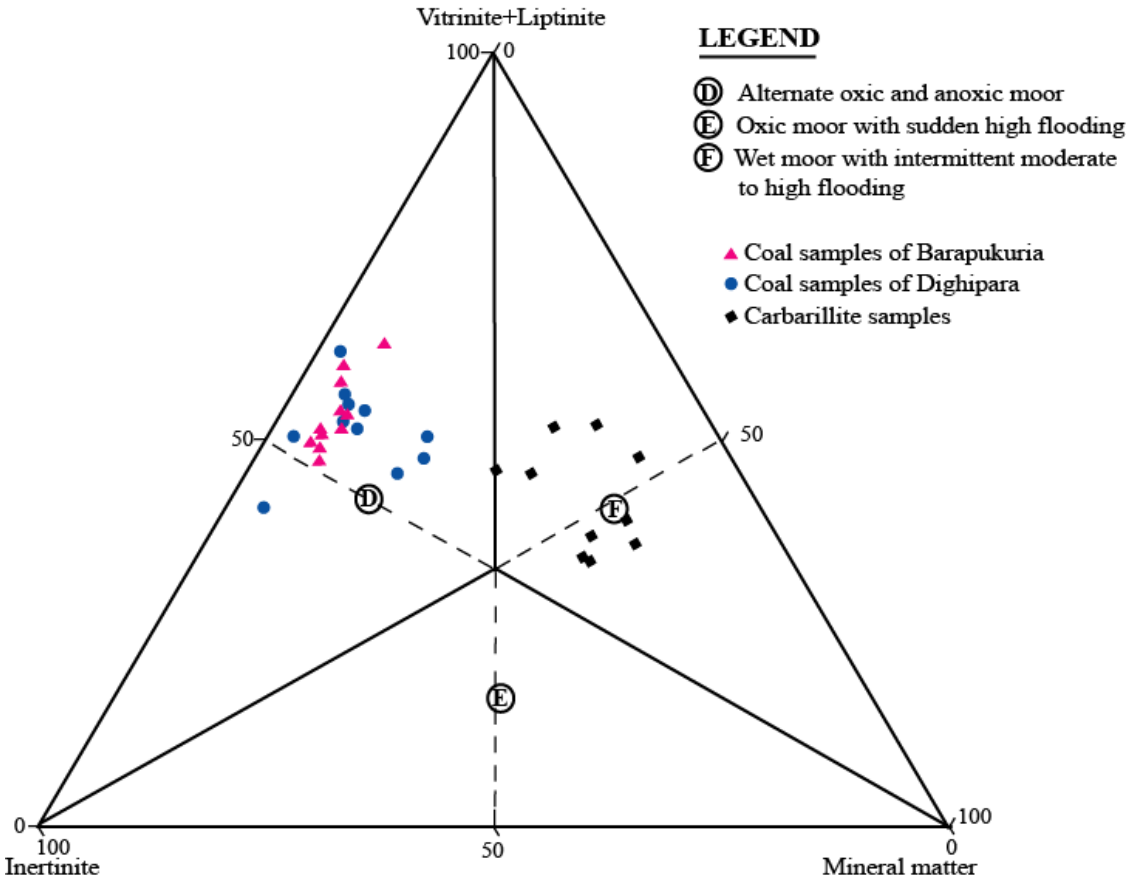

Fig.4.2.3.9. Environmental depositional conditions of coals and carbargillites based on the maceral and mineral matter contents (adopted by Singh and Singh, 1996). The analyzed coal samples fall within alternating oxic-anoxic swamp. The carbargillite samples fall within the wet swamp with intermittent and moderate to high flooding.

In the studied samples, there is a general decrease in peak heights of the homohopanes from C_{31} to C_{35} (C_{31}>C_{32}>C_{33}>C_{35}) (Figs. 4.2.3.4B, 4.2.3.5B and 4.2.3.6B). This, in turn, corresponds to terrestrial organic facies. The relative large amount of C_{34} hopane in the analyzed samples also agrees with the interpretation of strong terrestrial influence (Waples and Machihara, 1991). It is supported by low C_{35} homohopane indices (0.03-0.06) among the examined coal, carbargillite and mudstone samples (Peters et al., 2005). The high Tm/Ts ratio of the analyzed samples suggests a terrestrial sourced organic facies. But the Tm/Ts ratio of the carbargillite samples (5-12) is slightly lower than those of coals (8-13) and mudstones (6-21), supporting a mixed organic facies for the analyzed samples.

The coals and mudstones contain stronger terrestrial organic facies indicators than the carbargillites. The high value of Tm/Ts may indicate an oxic-anoxic depositional condition for the analyzed samples (Moldowan et al., 1986). The abundant moretane (moretane/hopane = 0.3-0.5) of the studied coal, carbargillite and mudstone samples is also consistent with the strong terrestrial organic facies (Connan et al., 1986). The presence of tetracyclic is a further support (Philp and Gilbert, 1986). Tissot and Welte (1984), Moldowan et al. (1986) and Clifton et al. (1990) reported that sterane/hopane ratio ≤ 1 typifies terrestrial organic facies. The measured very low sterane/hopane ratio of the analyzed samples points to dominating terrestrial higher plant and fungal material organic inputs. The higher value of sterane/hopane is found in the studied carbargillite samples (0.4-0.5) compared with coals (0.3-0.4) and mudstones (0.2-0.4). It again marks some contribution from different organic source inputs (possibly marine derived organic matter) compared to the dominantly terrestrial organic facies. Some of the coal samples (BPCL24, BPCL28 and DPCL40) with high value of sterane/hopane ratio also suggest a minor contribution from a marine influenced depositional environment. The dominantly terrestrial organic facies is further supported by the distributions of n-alkanes with the marked predominance of odd carbon-numbered homologs to even carbon-numbered homologs in n-alkanes. This is indicated by CPI^1 values of 1.06-1.54 and shown in Appendix E4.

The triangular plot from petrological data suggests an alternation of oxic to anoxic swamp for coal deposition (Fig.4.2.3.9), while the carbargillite matches to a wet swamp with intermittent to moderate high floods (Singh and Singh, 1996). The presence of micro and mega sporinite (both thin and thick walled), micro and mega cutinite (both thin and thick walled) and micro and mega resinite of the analyzed coal and carbargillite samples also support more than one organic input to the depositional system.

The cross-plot of HI versus T_{max} supports the assumption of a mixture of organic input within the analyzed coals that are dominated by terrestrial Type III-II kerogen. The carbargillites show a mixture of terrestrial and marine (Type II-III) kerogens and mudstones (Type III kerogen) are dominated by terrestrial organic facies. Such kerogen assemblages indicate that their deposition has taken place under oxic-anoxic condition. Here is a good agreement with the organic facies interpretation from biomarker characteristics as well as petrography. In addition, the dominancy of aromatic hydrocarbons in the extract of the analyzed coal, carbargillite and mudstone samples is in support of the strong terrestrial organic inputs to the depositional system during Permian time.

4.2.3.4.3 Hydrocarbon generation and expulsion

Over the last three decades, a long debate has been continuing among the scientists regarding the issue of generating and expelling hydrocarbon from coals. However, authors such as Snowdon and Powell (1982), Teichmüller and Durand (1983), Price and Barker (1985), Murchison (1987), Hunt (1991), Newman et al. (1997), Wan Hasiah (1997 and 2003), Petersen et al. (2000 and 2005) and Wilkins and George (2002) have published many papers in support of hydrocarbon generation and expulsion from coals. Now it is accepted the terrestrially derived organic matter from coal and coaly organic matter can generate commercial volumes of liquid hydrocarbon. The Kutei Basin of Indonesia (Thompson et al., 1985) and the Gippsland Basin of Australia (Thomas, 1982) are among the examples. However, generation is dependent on many different interrelated factors such as organic matter type, maturity, matrix property, depositional settings and coal age (Petersen and Nytoft, 2006). The liptinite macerals with perhydrous vitrinite in the coals are considered as the most important constituents for hydrocarbon generation as reported by these workers.

Hood et al. (1975) and Tissot and Welte (1984) reported the generation of hydrocarbon in most source rocks is considered to begin in the sub-bituminous A coal stage, which is equivalent to about 0.5 $\%R_o$. But the actual expulsion of hydrocarbons begins in the high volatile bituminous coal stage which is equivalent to 0.7 $\%R_o$ for Cenozoic coals (Wan Hasiah, 2003; Petersen, 2006). For Permian coals, Petersen (2006) proposed the expulsion threshold at a vitrinite reflectance of 0.85-0.90 $\%R_o$ or T_{max} of 440-445 °C. The coals analyzed here have $\%R_o$ of 0.70-0.80 and T_{max} of 430-438 ˚C and may, therefore, have generated and possibly expelled hydrocarbon. The considerable presence of liptinite macerals could have lowered the expulsion threshold in these coal samples. The vitrinite reflectance value of 0.6 ($\%R_o$) and T_{max} of 435 °C has been suggested as the start of oil window by Peters and Cassa (1994). Based on this interpretation, the analyzed mudstone and carbargillite samples holding $\%R_o$ of 0.60-0.81 and T_{max} of 430-439 °C have generated and possibly expelled hydrocarbons at their peak maturity stage.

The examined coal, carbargillite and mudstone samples with noticeable amounts of liptinite macerals would have generated and possibly expelled the hydrocarbon. Because these samples are registered in early to peak thermal maturity range based on $\%R_o$ of 0.60-0.81 and T_{max} of 430-439 ˚C (Farhaduzzaman et al., 2011a and 2012c). The presence of exsudatinite in the terrestrially derived samples analyzed is evidence of hydrocarbon generation (Teichmüller, 1974b). The exsudatinite within crack network appears to have developed in these samples and shows the liptinitic materials have already expelled their liquid hydrocarbon constituents to the carrier bed (Wan Hasiah, 1999b) (Photomicrograph 4.2.3.1A1 and A2).

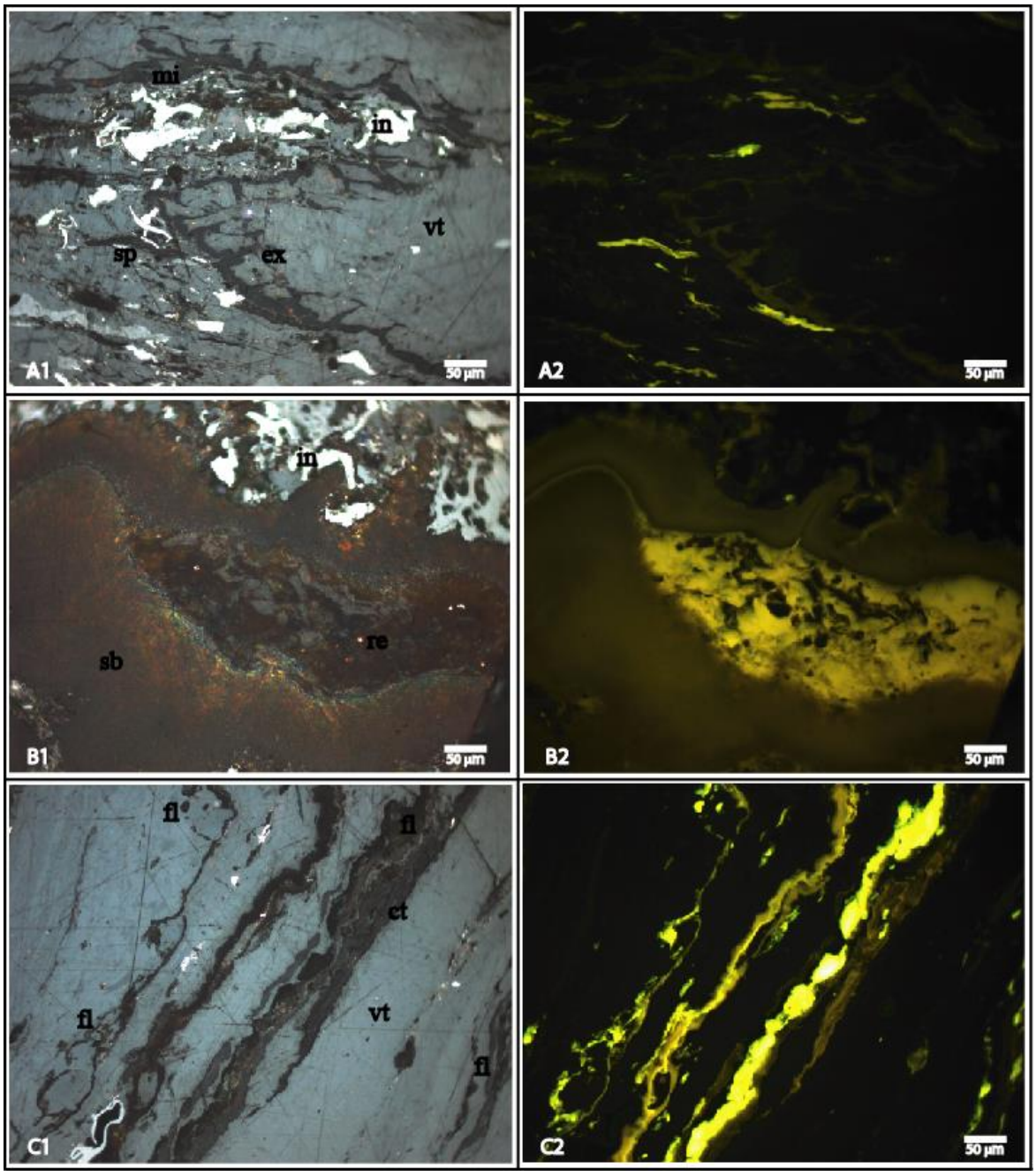

Photomicrograph 4.2.3.1. (A1) Low reflecting dark brown exsudatinite (ex) with crack network associated with vitrinite (vt), micrinite (mi), sporinite (sp) and inertinite (in) whereby this type of network is considered as probable conduits for hydrocarbon expulsion/migration as observed under reflected white light. (A2) Same view as A1 whereas the exsudatinite has expelled most of the liquid hydrocarbons therefore showing a dull brown fluorescence under ultraviolet light. (B1) Reddish brown indigenous solid bitumen (sb) which is considered as 'free' hydrocarbon observed under reflected white light, dark brown resinite (re) is also shown. (B2) Same view as B1 while solid bitumen shows dull brown fluorescence and resinite shows brownish yellow fluorescence under ultraviolet light (Caption continued next page).

Photomicrograph 4.2.3.1 (Caption continued). (C1) Dark brown color fluorinite (fl) both as dispersed and continuous form together with brown color cutinite (ct) and moderate grey vitrinite (vt) under normal reflected white light. (C2) Same view as C1 under ultraviolet light whereas the fluorinite shows brilliant yellow fluorescence and also occur as oil droplets and cutinite shows dull brown fluorescence (Note: Samples are studied under oil immersion objective whereby similar maceral types but different proportions are identified in all the coal, carbargillite and mudstone samples).

The indigenous solid bitumen found in the analyzed samples also suggests the generation and expulsion of hydrocarbon from these samples have occurred (Photomicrograph 4.2.3.1B1 and B2). The fluorinite is commonly considered to be free oils and these are observed as oil droplets in the studied samples under ultraviolet light excitation (Photomicrograph 4.2.3.1C1 and C2). Resinite, bituminite and cutinite macerals are the most significant liptinite to play important role in hydrocarbon generation (Teichmüller and Durand, 1983). The considerable amounts of resinite, bituminite and cutinite identified in the currently analyzed samples suggest good hydrocarbon (both liquid and gas) generation potential (Photomicrograph 4.2.3.2A1 and A2; B1 and B1; C1 and C2). Newman et al. (1997) reported that the fluorescent (perhydrous) vitrinite can also generate liquid hydrocarbons, for example, in the Gippsland Basin of Australia. It is observed in the presently analyzed samples (Photomicrograph 4.2.3.3A1 and A2). Micrinite is considered to be the residue of hydrocarbon generation (Teichmüller and Durand, 1983). The significant presence of micrinite (Photomicrograph 4.2.3.3B) in the analyzed samples suggests the organic matter has already expelled liquid hydrocarbons in the associated Gondwana Petroleum System.

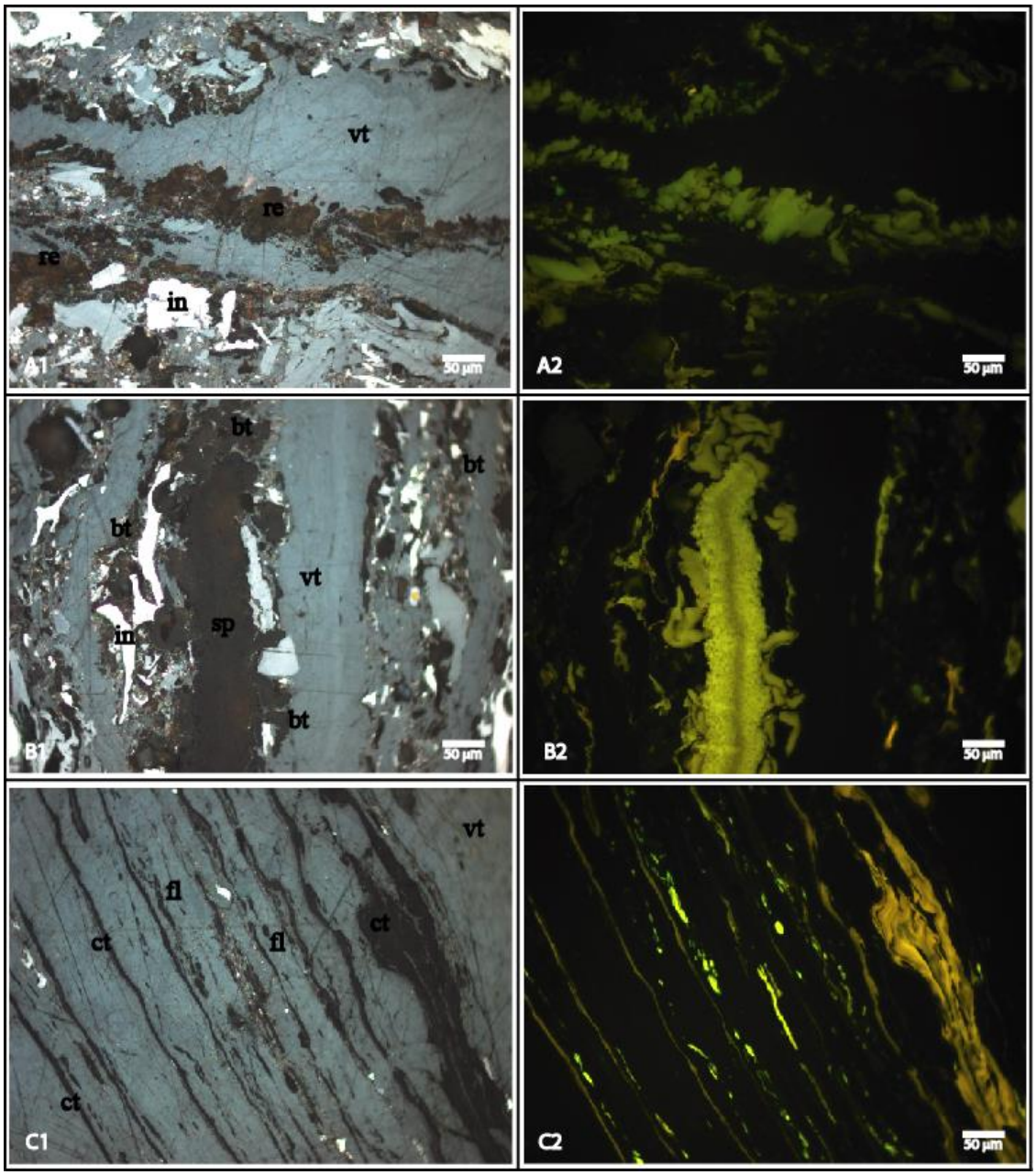

Photomicrograph 4.2.3.2. (A1) Brownish oval to rounded most oil-prone maceral resinite (re) associated with medium grey vitrinite (vt) under normal reflected white light. (A2) Same view as A1 under ultraviolet light whereas the resinite shows yellowish green fluorescence. (B1) Brownish megasporinite (sp) and another oil-prone structureless maceral bituminite (bt) associated with vitrinite (vt) and inertinite (in) under reflected white light. (B2) Same view as B1 under ultraviolet light whereas sporinite showing greenish yellow fluorescence and bituminite showing dull yellow fluorescence. (C1) Oil-prone brownish micro and mega cutinite (ct) associated with dark brown fluorinite (fl) and medium grey vitrinite (vt) under reflected white light. (C2) Same view as C1 under ultraviolet light whereby the cutinite fluoresces dull brown color and fluorinite fluoresces brilliant yellow in the form of oil droplets (Note: Samples are studied under oil immersion objective whereas similar maceral types but different proportions are identified in all the coal, carbargillite and mudstone samples).

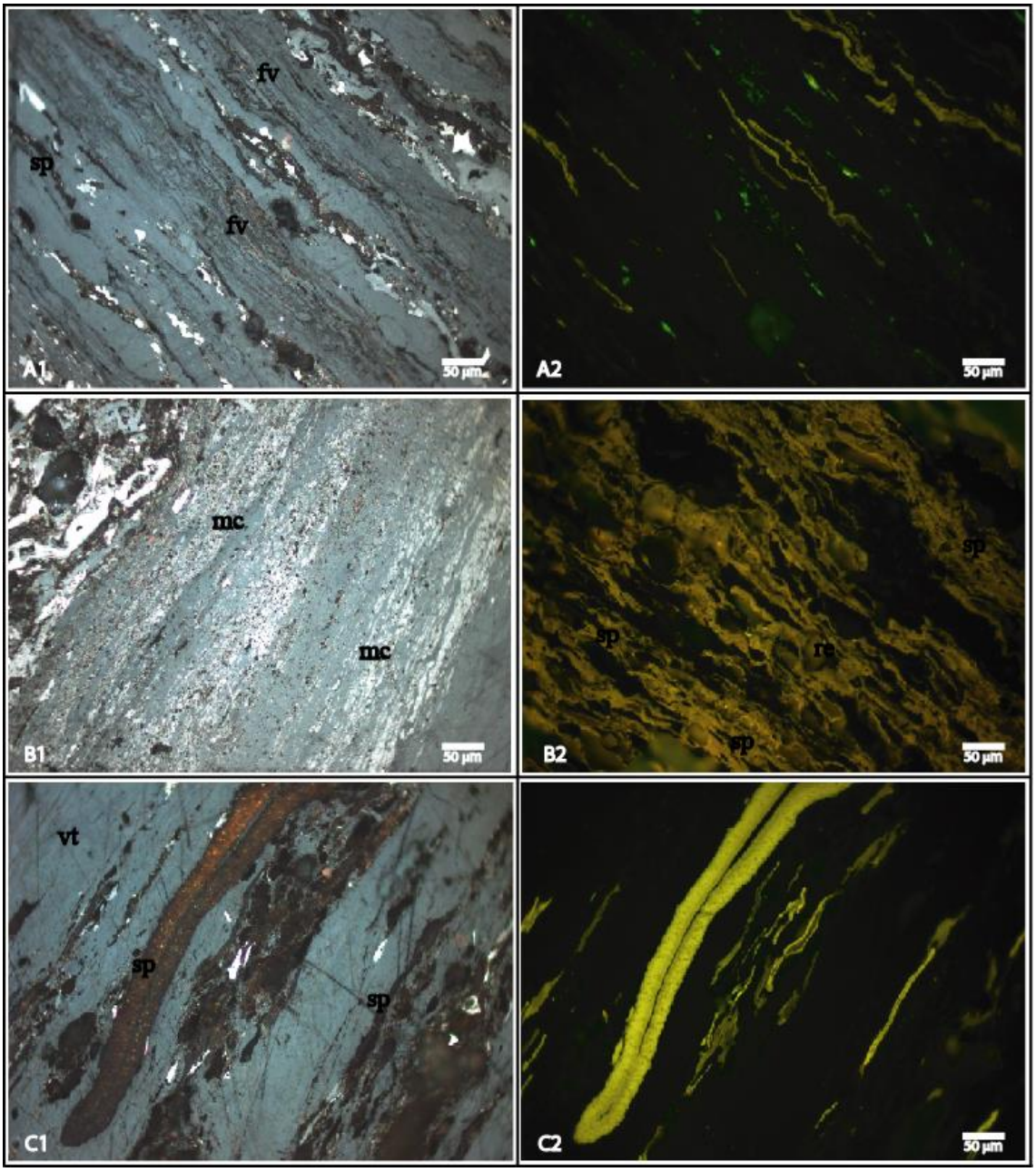

Photomicrograph 4.2.3.3. (A1) Light grey fluorescent vitrinite (fv) associated with darker grey vitrinite under normal reflected white light. (A2) Same view as A1 under ultraviolet light showing yellow cuticle and greenish yellow fluorescence haze which indicate the presence of generated hydrocarbon. (B) Whitish (B1) micrinite under normal reflected white light (B2- dark in UV light) and it is believed that these are the residual products formed after hydrocarbon expulsion from the hydrogen rich constituents. (C1) Reddish brown mega and micro sporinite (sp) associated with vitrinite (vt) under normal reflected white light. (C2) Same view as C1 under ultraviolet light and it shows intense yellow fluorescing megasporinite (Note: Samples are studied under oil immersion objective and similar maceral types but different proportions are identified in all the coal, carbargillite and mudstone samples).

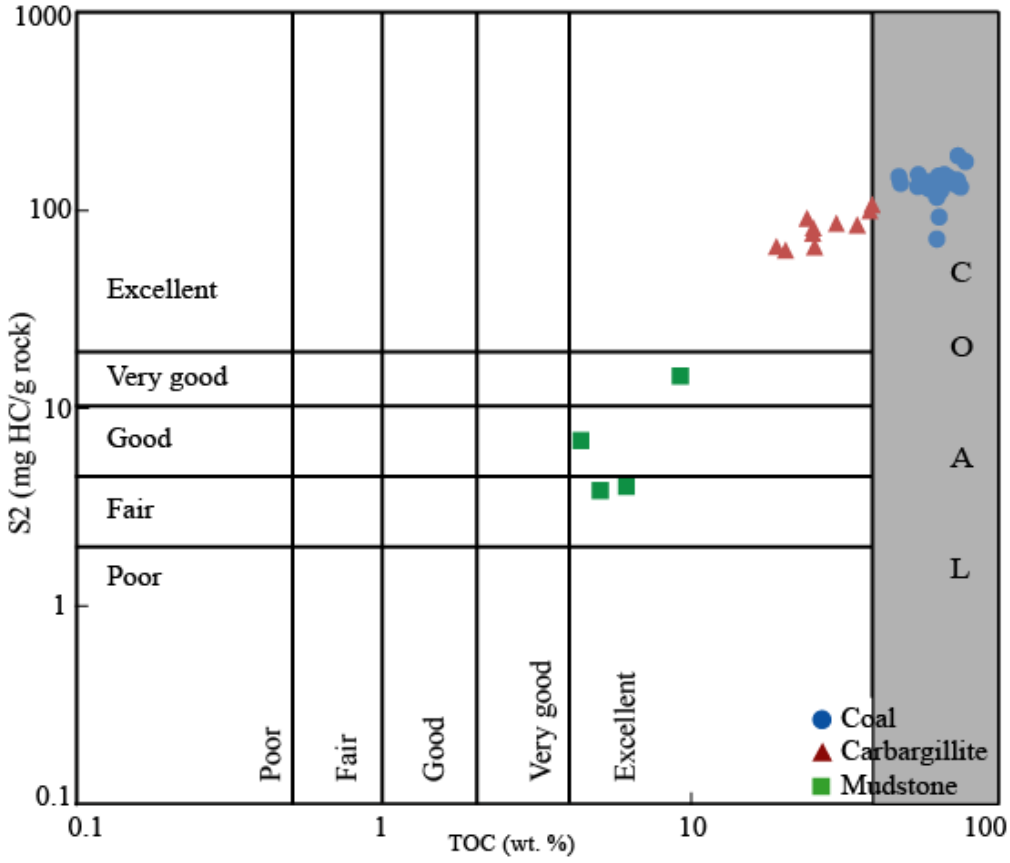

Fig.4.2.3.10. A cross-plot of TOC versus S2 in which all the analyzed samples fall within the range of fair to excellent hydrocarbon generation potential. Mudstone indicates the lowest potential and followed by carbargillite and coals (adopted by Peters and Cassa, 1994; Dembicki, 2009; cited by Farhaduzzaman, 2012a).

The relative higher content of liptinite macerals in the carbargillites compared with the coals and mudstones suggest the carbargillites and coals may possess some oil-generating potential, but they are predominantly gas-prone, while the mudstone samples are gas-prone. Peters and Cassa (1994) showed a source rock classification scheme ranging from poor (TOC <0.5%; S2 <2.5) to excellent (TOC >4%; S2 >20) based on Rock-Eval S2 and TOC contents. The measured TOC content of the analyzed samples are 44-78 wt.% (coal), 19-39 wt.% (carbargillite) and 4-9 wt.% (mudstone). The Rock-Eval S2 values are 71-188, 63-107 and 4-15 mg HC/g rock for the studied coal, carbargillite and mudstone samples, respectively.

An overall good hydrocarbon generation potential is estimated based on a cross-plot of TOC (wt.%) versus S2 (mg HC/g rock) for the analyzed samples. The coals and carbargillite are in the “excellent” category and mudstones are “fair-good” category source rocks (Fig.4.2.3.10). Although the coal and carbargillite samples are rich in inertinite, they also contain considerable amounts of liptinite macerals. Thus, they have petroleum source potential as reported by Powell et al. (1991) and Smyth (2009) for the Cooper Basin, Australia.

Frielingsdorf et al. (2008) mentioned the Permian Gondwana coal of northwest Bangladesh is the major petroleum source rock in the region, having already released up to 29% of its generation potential. It is also interesting to add the entire hydrocarbon discovery in the Bengal Basin, Bangladesh has consisted mainly of natural gas with minor oil (Imam, 2005). Therefore, this is in good agreement with the present hydrocarbon generation and expulsion potential of the analyzed samples.

4.3 PETROLEUM RESERVOIR ROCK- SANDSTONES

4.3.1 Petrography and Diagenesis of Sandstones

4.3.2 Petrophysical Study of the Well Rashidpur 4

CHAPTER 4.3.1 PETROGRAPHY AND DIAGENESIS OF SANDSTONES

The studied sandstone reservoir units belong to Miocene-Pliocene Surma Group in the Bengal Basin, Bangladesh (RPS Energy, 2009). The Surma Group sandstone deposited in deltaic to marine environment and, in general, has good porosity and permeability and this hosts all of the petroleum resources discovered so far in Bangladesh. A total of 33 core samples collected from eight different wells located in seven different gas/oil fields of Bangladesh are used for the current petrographic and diagenetic study. Here, the standard petrographic microscope, scanning electron microscope (SEM/FESEM) and XRD are used.

4.3.1.1 Sandstone texture and sorting

The investigated Surma Group sandstones are very fine to medium grained. The very fine grained to fine grained nature is observed especially for the sandstones of Kamta Filed. Predominantly subrounded to subangular grains are observed in the studied sandstone samples along with the common presence of rounded grains. The subangular nature is found especially among the smaller grains, whereby the larger grains show better rounded nature. The feldspar grains are observed mostly as subangular to even angular nature, especially in subfeldspathic arenite types. The examined grains are observed moderately well sorted to well sorted. The studied sandstones are mature in textural point of view (Folk, 1980).

4.3.1.2 Sandstone composition

Particle composition is a fundamental physical property of the sandstones and is the chief property used in their classification and provenance interpretation. Particle composition may also influence the economic importance of sandstones as hydrocarbons (oil and gas) reservoirs. It has a considerable contribution on the course of diagenesis in sandstones and,

thus, ultimately impacts the porosity and permeability of the particular sandstones (Boggs, 2009). Sand and silt size particles constitute the framework fraction of the analyzed sandstones. It also contains various amounts of matrix (material less than 0.03 mm) and cement present within the interstitial pore spaces among the framework grains.

Table 4.3.1.1. Petrographic results (%) of Surma Group reservoir sandstones of the Bengal Basin, Bangladesh.

Sample	Gas Filed	Well no.	Depth (m)	Grain size	Q			F		Mica		Ch	H	L			C	Matrix	Cement			TSP (%)
					Qm	Qp	Chert	K	P	Mus	Bio			Ls	Lm	Lv			Qc	Cc	Chc	
KM1ST1	Kamta	1	2839	VF-F	45.5	22	5.8	4.5	1.8	3.4	3.3	0.7	0.2	0.2	6.5	0.2	0.1	2.2	0.5	2.5	0.6	22
KM1ST2	Kamta	1	2840	VF-F	38.8	24.5	4.6	3.6	1.2	5.5	3.2	1.2	0	0.4	8.2	0.1	0	1.8	2.2	3.1	1.6	15
KM1ST3	Kamta	1	2842	VF-F	39.9	15.8	3.4	3.1	1.7	4.5	3.8	0.2	0	0.8	8.5	0.4	0.7	5.8	4.1	4.9	2.4	17
KM1ST4	Kamta	1	2958	VF-M	42.4	11.8	10.2	6.2	5.9	3.3	3.1	0	0	0.5	6.7	0.2	1.6	4.2	2.5	0.8	0.6	18
KM1ST5	Kamta	1	2961	VF-M	50.2	9.5	5.8	5.2	3.6	6.1	5.4	1	0.4	0	4.1	0.2	2.1	5.2	0.3	0.9	0	21
KM1ST6	Kamta	1	2962	VF-M	47.5	16.8	4.9	5	3.1	3.6	2.3	0.8	0.1	0.2	5.8	0.2	4.1	3.1	0.5	0.8	1.2	20
KM1ST7	Kamta	1	3021	VF-F	58.7	19.2	8.6	1.6	0.9	1.1	0.4	0.5	0	0.2	6.1	0	0	2.2	0.2	0	0.3	18
KM1ST8	Kamta	1	3022	VF-F	56.2	17.9	11	2.1	1.7	2.1	0.3	1.3	0	0	4.2	0.3	0.2	0.5	0.7	1.5	0	22
KM1ST9	Kamta	1	3025	VF-M	47.9	11.8	8.8	6.1	4.9	1.9	1.5	0.5	0	0	5.2	0.2	0	6.1	1.2	2.8	1.1	17
KM1ST10	Kamta	1	3377	VF-M	54.8	6.6	11.7	4.9	2.1	0.8	0.4	0.2	0	1.2	4.3	0.1	5.9	5.7	0.7	0.4	0.2	23
KM1ST11	Kamta	1	3379	VF-M	49.9	9.7	7.8	2.2	0.4	5.6	4.6	0.9	0.3	3.1	6.2	0.7	0	0.4	2.3	5.2	0.7	18
KM1ST12	Kamta	1	3380	VF-M	44.7	11.9	6.6	4.4	2.7	8.7	6.2	0.5	0	0.3	3.4	0.1	0.4	8.3	0.6	1.1	0.1	12
KT4ST1	Kailas Tila	4	3116.5	F-M	40.7	18.8	8.3	6.2	4.1	3.9	1.1	0.8	0	0.4	5.6	0.4	0	5.6	0.9	3.2	0	11
KT4ST2	Kailas Tila	4	3117.5	F-M	45.4	13.6	9.1	2.7	2.5	4.1	0.2	0.5	0	2.4	8.2	0.8	1.3	6.1	1.7	0.9	0.5	19
KT4ST3	Kailas Tila	4	3119.3	F-M	54.2	7.9	4.3	3.1	0.8	7.2	3.1	1.5	0	0	5.7	0.5	0.8	4.9	3.1	1.5	1.4	15
KT4ST4	Kailas Tila	4	3121	VF-M	56.2	5.5	3.8	5.1	0.5	6.9	5	0.8	0.1	0.1	6.2	0	0	5.2	2.2	1.6	0.8	18
KT4ST5	Kailas Tila	4	3262	F-M	37.8	11.9	7.2	5.4	3.2	7.2	4	0.7	0.4	2.1	5.9	0.3	0	8.4	4.1	0.5	0.9	10
KT5ST6	Kailas Tila	5	2398.5	VF-M	33.7	19.2	4.3	4.1	1.9	5.7	4.9	0.5	0	1.4	10.1	0.1	0.5	6.2	2.5	4.8	0.1	21
KT5ST7	Kailas Tila	5	2401.5	F-M	41.4	6.3	11.1	2.1	0.8	6.8	3.7	1.1	0	0	8.3	0.2	4.2	5.8	1.6	6.6	0	22
RP4ST8	Rashidpur	4	2670	F-M	34.9	18.8	5.9	4.6	1.6	8.2	4.1	0.9	0	0.5	6.9	0	3.4	6.2	0.8	3.2	0	23
RP4ST9	Rashidpur	4	2683	F-M	51.5	4.7	6.4	4.8	2.8	4.5	4.9	0	0	0.2	10.4	0.6	1.5	4.4	2.4	0.6	0.3	17
RP4ST10	Rashidpur	4	2715	F-M	55.4	13.6	4.9	1.9	0.5	2.9	1.6	0.2	0	2.8	8.8	0.2	0	2.7	3.7	0.8	0	20
RP4ST11	Rashidpur	4	2752	F-M	39.7	11.9	8.2	5.1	4.2	6.7	0.5	0.8	0.4	0	7.2	0.4	0	5.1	4.5	5.3	0	19
RP4ST12	Rashidpur	4	2757	VF-M	35.8	12.6	7.8	3.2	5.1	4.9	5.1	1.2	0	0.6	5.7	0	0	6.2	1.6	9.8	0.4	18
BG1ST17	Begumganj	1	3571.3	VF-M	56.2	5.7	4.2	2.8	2.5	6	2.5	0.2	0.2	0	9.2	0.1	3.7	2.7	0.8	3.2	0	10
BG1ST18	Begumganj	1	3577	F-M	48.9	19.7	5.1	5.2	0.9	1.5	1.5	0	0	0	8.8	0	1.5	5.3	0.9	0.7	0	14
BG1ST19	Begumganj	1	3578	VF-M	37.3	20.1	6.8	5.9	3.8	1.8	0.6	0.2	0	0.4	5.2	0.2	6.2	6.9	1.2	3.2	0.2	17
FN2ST20	Fenchuganj	2	3265	VF-M	51.2	6.8	4.9	3.2	0.5	7.6	1.2	0.8	0.3	4.2	6.1	0.2	0	5.1	2.6	0	5.3	17
FN2ST21	Fenchuganj	2	3620	F-M	44.4	11.9	5.2	5.9	4.1	6.8	5.9	0.6	0	1.5	4.8	0	1.8	4.6	0.4	0.9	1.2	13
SB1ST19	Shahbazpur	1	3404	F-M	38.9	20.2	7.7	6.1	2.6	1.9	1.5	0	0.2	0.2	7.2	0.3	0	5.8	1.9	5.5	0	20
SB1ST22	Shahbazpur	1	3409	F-M	54.7	7.5	5.9	3.8	1.7	4.9	0.5	0.4	0	3.2	8.3	0.2	0.2	6.2	0.4	2	0.1	16
T11ST23	Titas	11	2699	F-M	51.4	10	7.1	4.8	4.1	1.5	0.4	0.2	0	0.4	10.5	0	0	4.5	3.2	1.7	0.2	19
T11ST27	Titas	11	2784	F-M	49.8	19.6	8.3	4.3	1.4	3.1	1.1	0.7	0.1	0	7.7	0.3	0.1	2.1	0.9	0	0.5	20
Range	7 fields	8 wells	2398-3620	VF-M	33.7-58.7	4.7-24.5	3.4-11.7	1.6-6.3	0.4-5.9	0.8-8.7	0.2-6.2	0-1.5	0-0.4	0-4.2	3.4-10.5	0-0.8	0-6.2	0.2-8.4	0.2-4.5	0-9.8	0-5.3	10-23

(Note: Q= quartz, Qm= monocrystalline quartz, Qp= polycrystalline quartz, F= feldspar, K= potash feldspar, P= plagioclase feldspar, H= heavy minerals, C= detrital carbonate, Mus= muscovite, Bio= biotite, Ch= chlorite, L= labile lithic grains, Ls= sedimentary lithics, Lm= metamorphic lithics, Lv= volcanic lithics, Qc= quartz cement, Cc= carbonate cement, Chc= chlorite cement, F= fine, VF= very fine, M= medium, TSP= thin section porosity).

Authigenic minerals that replace some framework grains, matrix or cement are also observed in the studied thin sections of sandstones. The empty pore spaces (porosity), both connected and unconnected, are also found under microscope. The compositional description of the investigated Surma Group sandstones is added below.

Framework grains

The studied Surma Group sandstones are composed of a variety of major detrital minerals and rock fragments (labile lithic grains) together with some accessory minerals (Table 4.3.1.1). Detrital constituents are defined as those derived by mechanical and chemical disintegration of a parent rock. The observed detrital constituents are terrigenous siliciclastic particles that are generated through the process of weathering, explosive volcanism and sediment transport from parent rocks located outside the depositional basin. Accordingly, the framework grains of the analyzed sandstone samples are composed of predominantly of quartz (76-91%) and nearly equal amounts of feldspar (3-14%) and rock fragments (5-16). Several other detrital minerals such as chlorite, muscovite, biotite, calcite and heavy minerals are also found in lesser amounts of the investigated samples.

Quartz (Q): The principal silica crystalline mineral identified in the studied sandstones is the quartz. It is distinguished optically by its grey interference color and low birefringence along with uniaxial positive sign (Photomicrograph 4.3.1.1A). Many quartz grains display undulatory extinction, which is a pattern of sweeping extinction as the microscope stage is rotated (Photomicrograph 4.3.1.1A). Basu et al. (1975) differentiated undulatory quartz with extinction angle higher than 5 degrees while others are nonundulatory quartz. The bubbles or mineral inclusions are found in many of the analyzed quartz grains. The bubbles are also known as vacuoles seemed to filled with liquid, liquid and gas or gas alone. These bubbles are randomly distributed throughout the quartz grains in most cases (Photomicrograph 4.3.1.1A). However Folk (1980) stated that the quartz crowded with bubbles to the point that it appears milky in reflected light is probably derived from hydrothermal veins.

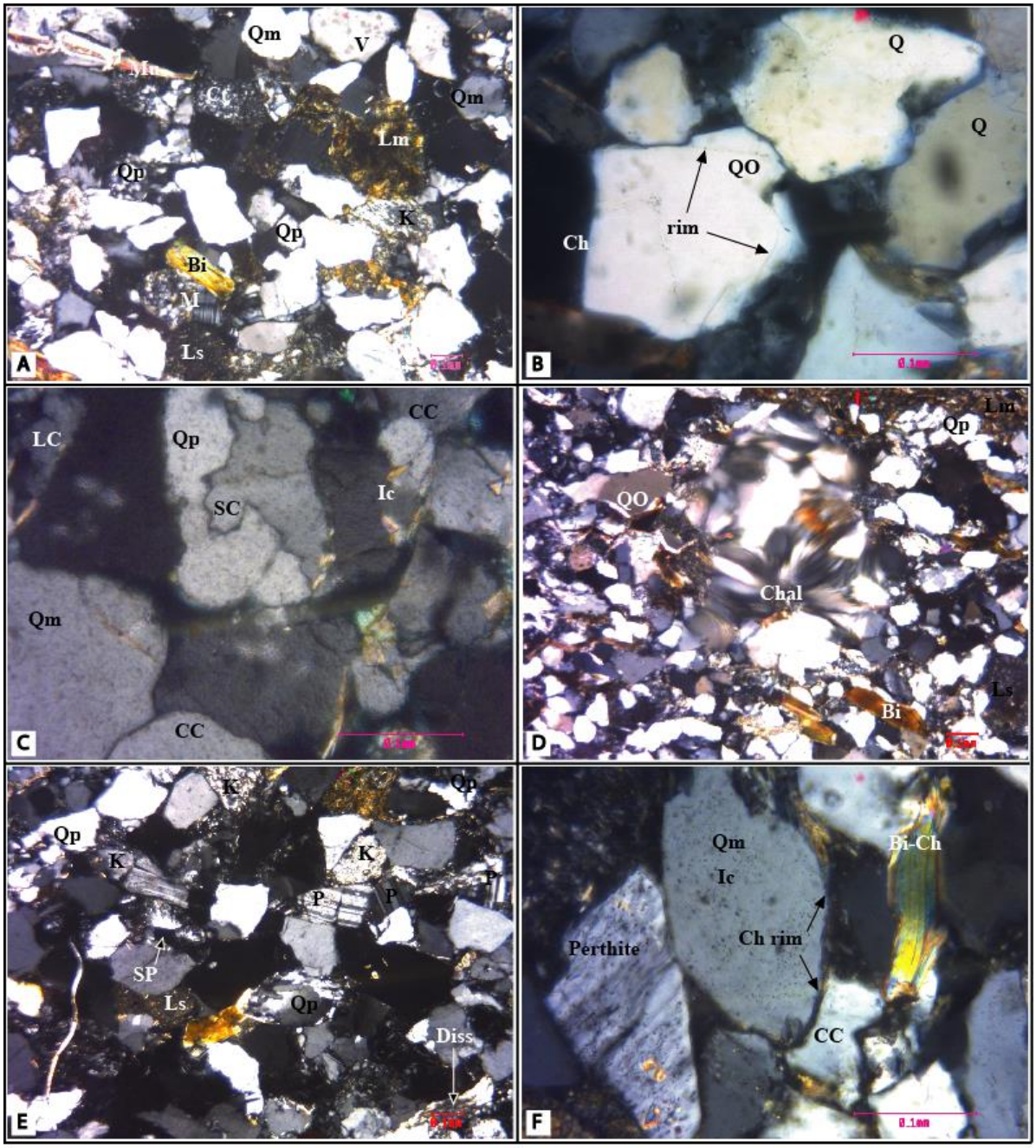

Note: Thin sections under crossed nicols.

Photomicrograph 4.3.1.1. (A) The most abundant both kinds of quartz (Qm and Qp) show grey interference color in association with chert (Ct) consisting of numerous microquartz grains. Several quartz grains (dark grey) show undulatory extinction and few show vacuoles (V). Microcline (M) shows cross-hatched twining attached with brownish mica (Bi). Other commonly found sedimentary rock fragment (Ls) and metamorphic rock fragments (Lm), depth 3025m at Kamta well-1 (KM1ST9. (B) Rounded quartz grain shows overgrowth separated by its thin clay rim 'dust line'. Dark green chlorite cement (Ch) also observed between grains, depth 3379m at Kamta well-1 (KM1ST11). (C) Different kinds of grain contacts between quartz grains- long contact (LC) correspond relatively to early stage of diagenesis whereby concavo-convex (CC) and suture contacts (SC) represent intermediate stage of diagenesis. Mica inclusions (Ic) also shown, depth 3578m at Begumganj well-1 (BG1ST19) (Continued).

Photomicrograph 4.3.1.1 (Continued). (D) Fibrous variety of quartz, chalcedony (Chal), rarely found. Quartz overgrowth (QO) also showed, depth 2670m at Rashidpur well-4 (RP4ST8). (E) Plagioclase feldspar (P) identified by its albite twining. Altered alkali feldspar (K) and its dissolution (Diss) also shown. Mold as secondary porosity (SP) also found, depth 2401.5m at Kailas Tila well-5 (KT5ST7). (F) Perthitic texture distinguished by patchy intergrowth of albite into the orthoclase. Dark green chlorite (Ch) cement rims the quartz grain. Brownish biotite is altering to greenish chlorite (Bi-Ch), depth 2699m at Titas well-11 (T11ST23).

Thus, the presence of sparse vacuoles in quartz appears to have no provenance significance. Tiny mineral inclusions are common in quartz; including micas, chlorite, zircon, apatite and rutile although it is very difficult to identify these minerals using the ordinary petrographic microscope. Smaller quartz grains of the studied samples are relatively subangular to subrounded, whereas, many of the larger grains are rounded in shape. Silica overgrowths are observed onto the original surfaces of these rounded quartz grains in the presence of open pore space. The original grain outline is commonly revealed by the presence of small specks of hematite, clay or other mineral rim 'dust line' (Photomicrograph 4.3.1.1B). However, all these overgrowths are not marked by this kind of clay rim and, in fact, it is more clearly identified by scanning electron microscopy (described in the next section).

Monocrystalline quartz occurs preferentially as sand-size individual crystals in the analyzed samples. Polycrystalline quartz, also known as composite quartz, is very common in the studied sandstone thin sections. It is actually made up of aggregates of two or more quartz crystals (Photomicrograph 4.3.1.1C). The individual crystals within a polycrystalline grain are equant or elongate in shape, fine grained or coarse grained and even same size or variable in size. The observed grain contacts or crystal boundaries are straight, concavo-convex and sutured to various degrees (Photomicrograph 4.3.1.1C).

The fibrous variety of quartz, chalcedony, is also found in the studied sandstones although it is very rare because of its unstable nature on weathering (Photomicrograph 4.3.1.1D).

Quartz is the most stable, dominant and widespread constituent in the sandstones. It is thought to have generated from felsic plutonic rocks. The older sedimentary rocks also contribute to its content in sandstones (Folk, 1980).

Feldspar (F): Feldspar and rock fragments are identified almost in equal abundances after quartz in the analyzed samples (Table 4.3.1.1). They can be divided into two main groups: alkali feldspars (potassium feldspars) and plagioclase feldspars. Both of the groups are well preserved in the studied Surma Group sandstone samples. The content of plagioclase feldspar (0.4-5.9%) is almost equal to those of alkali feldspars (1.6-6.3%). Orthoclase and microcline are the most abundant members identified in the alkali feldspar group of the samples under microscope. Albite is the most dominant and easily identifiable member of the plagioclase group.

Untwined orthoclase appears very similar with quartz in thin section and it is a bit difficult to identify properly. However, orthoclase is distinguished by its relatively lower birefringence than quartz and apparent cleavage faces (Photomicrograph 4.3.1.1E). It is cloudy or pale brownish color (because of alteration) in plane polarized (PPL) view while the quartz is usually clear and unaltered. The twined microcline is easy to recognize in thin section owing to the common presence of its distinctive ‘grid’ or ‘cross-hatch’ twining with the two sets of twin lamellae approximately at right angles to each other (Photomicrograph 4.3.1.1A).

Alkali feldspars are thought to have derived particularly from alkali and acid igneous rocks and are especially abundant in syenites, granites, granodiorites and their volcanic equivalents. They occur also in pegmatites and acid and intermediate composition metamorphic rocks such as gneisses (Boggs, 2009).

Most of the plagioclase feldspars are easily identified by their characteristic albite twining with lamellae that are straight and parallel to each other (Photomicrograph 4.3.1.1E). Both twined-untwined and zoned-unzoned plagioclases are observed in the samples analyzed. Perthitic intergrowths are observed frequently in the studied samples. Perthitic intergrowth is microcline or orthoclase characterized by patchy intergrowths of albite in the form of small strings, lamellae, blebs, films or irregular veinlets (Photomicrograph 4.3.1.1F).

The principal source for detrital plagioclase is probably basic and intermediate lavas where it occurs as phenocrysts. It may also be derived from basic intrusive rocks and is a very common constituent of many metamorphic rocks where its composition is related to the metamorphic grade of the host rock (Boggs, 2009).

Coarse micas: The principal coarse micas identified as detrital grains in the analyzed Surma Group sandstones include muscovite and biotite. Folk (1980) stated that muscovite is chemically more stable than biotite and accordingly the content of muscovite (0.8-8.7%) is slightly higher than that of biotite (0.2-6.2%) in the analyzed sandstones (Table 4.3.1.1). Another detrital grain chlorite is not uncommon in the studied samples although it is in lesser amounts. The micas are distinguished from other associated minerals by their typical platy or flaky habit (Photomicrographs 4.3.1.1F and 4.3.1.2A). Rounded micas are rare and they are commonly deposited with their flattened dimension parallel to the bedding.

The bending of mica flakes is also found in the studied samples (Photomicrograph 4.3.1.2A). Muscovite is colorless in thin section. Biotite is observed as yellow, brown or green in color and can be leached pale yellow or almost colorless in some cases. Muscovite does not show any pleochroism whereas biotite shows strong pleochroism along with the parallel extinction. Both muscovite and biotite are found with moderately high birefringence in second order reds, blues and greens. Chlorites are characterized by their green color and pleochroism in the studied these sections. They are distinguished from the associated minerals by anomalous interference colors, particularly in blues. The transformation from biotite to green chlorite is frequently found in the studied sandstone samples (Photomicrograph 4.3.1.2A). The identified detrital chlorite is common in all of the studied sandstone samples although its content is very low (trace to1.5%).

Boggs (2009) suggested that the micas and chlorite are derived primarily from metamorphic rocks but biotite occurs also in basic intrusive and volcanic rocks and in granites. Muscovite occurs in granites and pegmatites as well.

Rock fragments (L): Rock fragments, also known as labile lithic grains, are detrital particles made up of two or more mineral grains. The abundance of rock fragments depends on several factors such as grain size, lithology and source area provenance etc (Dickinson, 1985; Boggs, 2009). For example, sandstone with coarse grains contains higher amount of rock fragments than those with finer grains. Almost all kinds of rock fragments are observed in the investigated thin section of the Surma Group sandstones. Nonetheless, the content of metamorphic rock fragments (3.4-10.5%) is higher than that of sedimentary (trace to 4.2%) or volcanic (trace to 0.8%) rock fragments in the analyzed samples.

The most common igneous rock fragment is volcanic rock fragments with porphyritic and aphanitic texture. The lathwork grains (volcanic rock fragments) are recognized by the plagioclase laths forming intergranular and insertal (triangular patches of interstitial glass between feldspar laths) texture (Photomicrograph 4.3.1.2B). It is derived mainly from basaltic lavas. Metamorphic rock fragments are characterized by the schistose, semischistose or slaty fabric resulting from preferred orientation of recrystallized mineral grains (Photomicrograph 4.3.1.2C). The higher presence of quartz and mica indicates the metasedimentary rock fragment. Metamorphic rock fragments include schist, phyllite, slate and quartzite with foliated fabric. Shale, siltstone and chert with fragmental or microgranular texture are the most commonly found sedimentary rock fragments although cherts are included in the polycrystalline quartz (Photomicrographs 4.3.1.2.C and 4.3.1.1E). Chert is distinguished by the microgranular texture composed entirely of quartz (Photomicrograph 4.3.1.2C).

The rock fragments are derived from the ancient parent rocks that have yet to weather away to individual mineral grains. It could be any fine-grained or coarse-grained igneous, metamorphic or sedimentary rock (Boggs, 2009).

4.3.1.3 Sandstone classification

The sandstones can broadly be divided into two groups: siliciclastic (mainly of terrigenous origin) and nonsiliciclastic (mainly carbonates and evaporates). The present research deals with the siliciclastic sandstones of Bengal Basin. As noted above, the framework grains of the studied sandstones are dominated by quartz, feldspar and rock fragments (labile lithic gains).

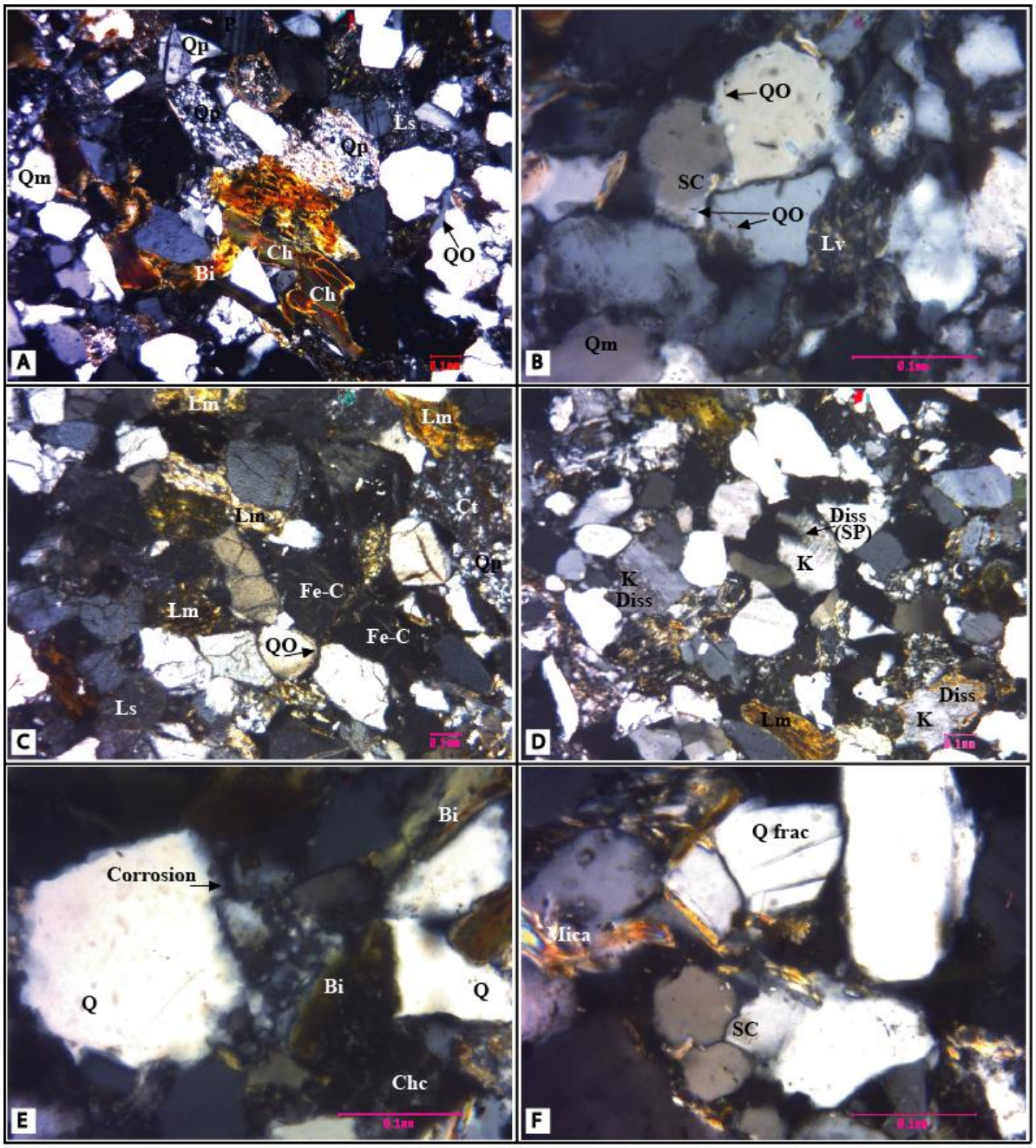

Note: Thin sections under crossed nicols.

Photomicrograph 4.3.1.2. (A) The brownish coarse mica biotite (Bi) which is bended (compaction effect) because of diagenesis and altered (transformation) to greenish clay chlorite (Ch). Quartz overgrowth (QO) (cementation) is also shown, depth 3265m at Fenchuganj well-2 (FN2ST20). (B) Moderate stage diagenetic components quartz overgrowth (QO) and suture contact (SC) associated with volcanic lithic grain (Lv), depth 3404m at Shahbazpur well-1 (SB1ST19). (C) Framework grain metamorphic rock fragment schist or mica schist (Lm), sedimentary rock fragment shale or siltstone (Ls) and chert (Ct) in association with diagenetic constituent quartz overgrowth (QO) and dark brownish blocky Fe-carbonate (Fe-C) cement, depth 2757m at Rashidpur well-4 (RP4ST12). (D) Potash feldspar dissolution (Diss) creates secondary porosity (SP) which enhanced the porosity and permeability, depth 3262m at Kailas Tila well-4 (KT4ST5) (Continued).

Photomicrograph 4.3.1.2 (Continued). (E) Corrosion of quartz grain occurred due to digenesis. Brownish coarse mica biotite (Bi) that also altered to dark greenish chlorite (Ch), depth 3380m at Kamta well-1 (KM1ST12). (F) Quartz grains fractured because of compaction effect at moderate stage diagenesis which is also corresponded by suture grain contact (SC) and mica bending, depth 3577m at Begumganj well-1 (BG1ST18).

Some other minerals are also measured in lesser quantities. Accordingly, they are ignored for the classification scheme although there are some difficulties in this type of straightforward classification (Folk, 1980; Friedman and Sanders, 1978; Pettijohn et al., 1987; Boggs, 2009).

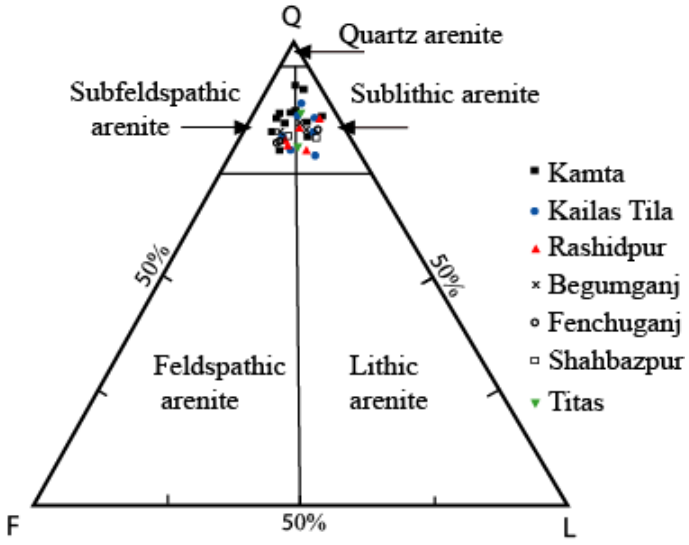

Fig.4.3.1.1 A tri-plot of the modal composition of the studied Surma Group sandstones of the Bengal Basin, Bangladesh. The sandstones place within the sublithic arenite to subfeldspathic arenite class (adopted by Folk, 1980).

There are two types of classification: genetic classification, in which the rocks putatively convey the information about their origin, and descriptive classification, which deals with observable properties of rocks without regard to their origin. Hence, the later descriptive classification scheme established by Folk (1980) is used for the current study. The sublithic arenite to subfeldspathic arenite type sandstone is identified based on the petrographic data obtained from the Surma Group sandstones (Fig.4.3.1.1). Lithic arenite contains less than 90% quartz (including chert and quartzite) and unstable rock fragments in excess of

feldspars. On the other hand, lower than 90% quartz and feldspar higher than rock fragments correspond to feldspathic arenite (also known as arkose). Since the content of lithic grains or feldspar is less than 25% together with 75-90% quartz in the studied sandstones, the samples correspond to sublithic arenite to subfeldspathic arenite, respectively followed by Folk (1980). In addition, this interpretation for Surma Group sandstone is also supported early by Imam and Shaw (1985, 1987), Islam (2009, 2010) and Rahman and McCann (2012).

4.3.1.4 Diagenetic constituents

In the broad sense, diagenesis is the process that modifies the sediment after its deposition. The petrographic study of any sandstone normally focuses on the palaeodepositional environment. But recently the postdepositional changes or the diagenesis have become very significant for better understanding the reservoir sandstones, especially when it becomes economically important as a host for oil or gas. Diagenesis plays an important role in the modification and development of reservoir porosity (Bashari, 1998). It may either decrease the porosity as a result of cementation-compaction or increase in porosity owing to solution processes (Folk, 1980; Boggs, 2009). Therefore, to avoid erroneous interpretations or costly errors in economic evaluations, the following diagenetic observations that would have affected the studied siliciclastic sandstones are highlighted.

4.3.1.4.1 Quartz cements

The process of precipitating silica cement in sandstones during diagenesis involves three important factors such as silica sources, timing of cementation and mechanisms of silica precipitation. The most commonly found silica cement is in the form of quartz overgrowth although its content is very low (0.2 to 4.5%) in the studied Tertiary sandstones (Table

4.3.1.1). They are identified as the syntaxial overgrowths on preexisting quartz grains which are, in fact, the optical continuity with the detrital quartz nuclei. In many cases, the authigenic quartz overgrowths are easily distinguished due to the outlines ‘dust line’ of the original detrital quartz grains in thin sections. They are identified out by a line of very tiny iron oxide particles, clay particles or bubbles, although in some cases it is not possible to distinguish with a standard petrographic microscope (Photomicrographs 4.3.1.1B; 4.3.1.2A; 4.3.1.2.B and 4.3.1.2C). SEM is very useful to characterize these overgrowth features. It is found as euhedral crystal faces in partially filled cavities or irregular overgrowth boundaries in filled cavities (Photomicrograph 4.3.1.3A). The local occurrence of pyramid shaped quartz overgrowth is recognized under SEM or FESEM and it occupies the open spaces (Al-Gailani and Ala, 1984). SEM study reveals that, in some cases due to the barrier of chlorite rim, the incomplete development of quartz overgrowth is also observed. The quartz overgrowth sometimes encloses the pore throats between the detrital grains which ultimately reduces the reservoir porosity (Photomicrograph 4.3.1.3B).

4.3.1.4.2 Clay mineral authigenesis

Authigenic minerals are formed in place within sediments either shortly after deposition or during burial and diagenesis. These minerals can occur as cements or crystallize in pore space as new minerals that do not act as cements or form by replacement of original detrital grains. However, the diagenetic changes that affect clay minerals include alteration of nonclay-mineral precursor minerals; comprising the transformation of feldspars and volcanic glass to produce clay minerals, alteration of one kind of clay minerals to another and precipitation of clay minerals into pore spaces where no obvious precursor mineral is present (Boggs, 2009).

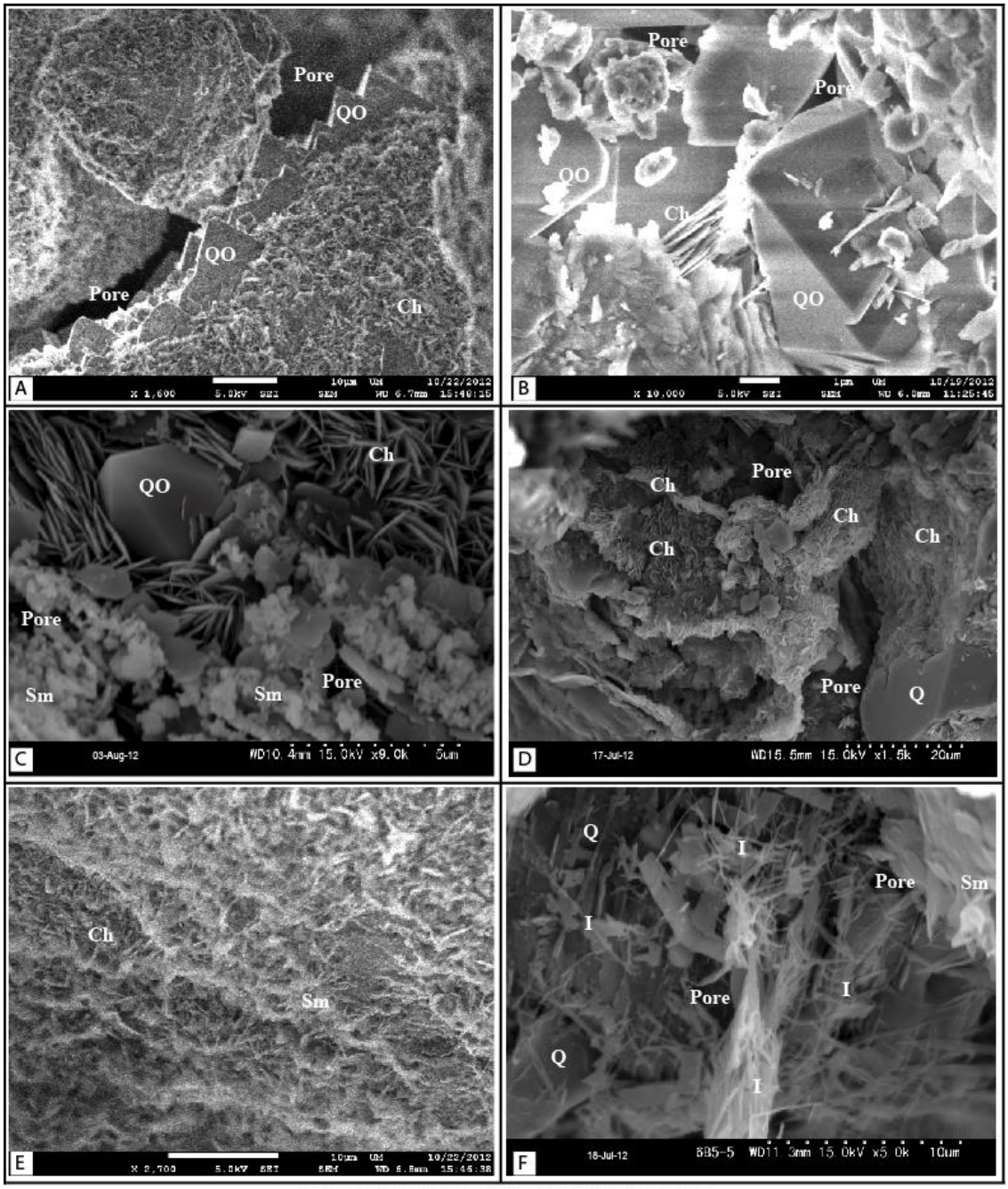

Note: Scanning electron micrographs of reservoir sandstones.

Photomicrograph 4.3.1.3. (A) Pore-lining authigenic quartz overgrowths (QO) show irregular boundaries partially filled the cavities, depth 2699m at Titas well-11 (T11ST23). (B) Pore-filling pyramidal shaped quartz overgrowths associated with chlorite (Ch) stack, depth 3409m at Shahbazpur well-1 (SB1ST22). (C) Clusters of pore-filling euhedral and pseudohexagonal chlorite crystals associated with quartz overgrowth and smectite (Sm), depth 3578m at Begumganj well-1 (BG1ST19). (D) Pore-filling and pore-bridging euhedral chlorite platelets which dramatically reduced the permeability, depth 3380m at Kamta well-1 (KM1ST12). (E) Frequently found mixed layer chlorite and webby smectite, depth 3620m at Fenchuganj well-2 (FN2ST21). (F) The filamentous illite (I) coating the detrital grain surfaces associated with crenulated morphology smectite, depth 3119.3m at Kailas Tila well-4 (KT4ST3). Quartz overgrowths and smectite-chlorite are formed during intermediate stage of diagenesis.

The most important clay cement identified in the analyzed Surma Group sandstone samples is chlorite, ranging from trace to 5.3%. XRD results show the highest relative abundance of chlorite compared to other related clay minerals in the studied samples (Figs.4.3.1.2A and 4.3.1.2B). In thin section, the authigenic chlorite cement forms thin and uniform green rims around the detrital grains (Photomicrograph 4.3.1.1F). Under the SEM, the chlorite is identified by the typical euhedral and pseudohexagonal crystals or platelets that are arranged in different forms and pattern such as rosette pattern, fan shaped, cluster pattern and face-to-face stacked pattern (Photomicrographs 4.3.1.3C and 4.3.1.3D). It is found either as individual crystal or composite crystal or mixed layer clay partly filling the pores in the studied sandstones (Photomicrograph 4.3.1.3E). Other important observed authigenic clay minerals include illite, smectite, kaolinite and mixed layer illite-smectite.

In the Surma Group sandstone samples, the illite is characterized by its filamentous habit under SEM (Photomicrograph 4.3.1.3F). But it looks brownish in thin section which, in sometimes, makes thin ‘dust line’ separating the detrital quartz grain from its authigenic growths. It is found as pore-lining as well as pore-bridging which could act as permeability barriers for fluid (especially hydrocarbons) movement. Sometimes the thin ribbons form a mat-like feature lining the pore coating the detrital grain surfaces (Photomicrograph 4.3.1.4A). Even the development of illite helps to preserve porosity by covering potential quartz nucleation sites, thus inhibiting quartz growth and cementation.

Smectite is distinguished by the highly crenulated, thin, webby and flaky morphology partly coating the detrital quartz grains (Photomicrograph 4.3.1.4B). In few specimens, the chlorite-smectite mixed with blocky kaolinite books is also observed in the samples under SEM (Photomicrograph 4.3.1.4C).

The mixed layer clay of filamentous illite and webby smectite is fairly common in the samples analyzed. The pore-bridging smectite is rarely found in the studied samples (Photomicrograph 4.3.1.4D).

In thin section, dark brown patches of kaolinite partly filling the pores between detrital quartz and carbonate grains are identified in the samples. It occurs as face-to-face stacks of pseudohexagonal plates or books (typical morphology) partly filling the pore spaces under SEM (Photomicrographs 4.3.1.4E and 4.3.1.4F). Locally developed vermicular kaolinite is also found the samples.

4.3.1.4.3 Carbonate cements

Both precipitation and dissolution of carbonate minerals can take place during diagenesis until the chemical equilibrium is established. The carbonate cements identified in the analyzed samples are both ferroan calcite (siderite) and nonferroan pure calcite together with some dolomite that range from trace to 9.8% are observed in the samples as well. The Fe-calcite is also identified by its blocky habits under SEM (Photomicrograph 4.3.1.5B). The considerable presence of blocky carbonate cements significantly reduce the porosity of the reservoir sandstones analyzed.

4.3.1.4.4 Feldspar authigenesis

A small amount of feldspar overgrowth is seen in the studied samples. The overgrowths are identified either as rimmed K-feldspar authigenesis over the original plagioclase detrital grains or as blocky euhedral to irregular faced K-feldspar over the original clean detrital plagioclases (Photomicrographs 4.3.1.5C and 4.3.1.5D).

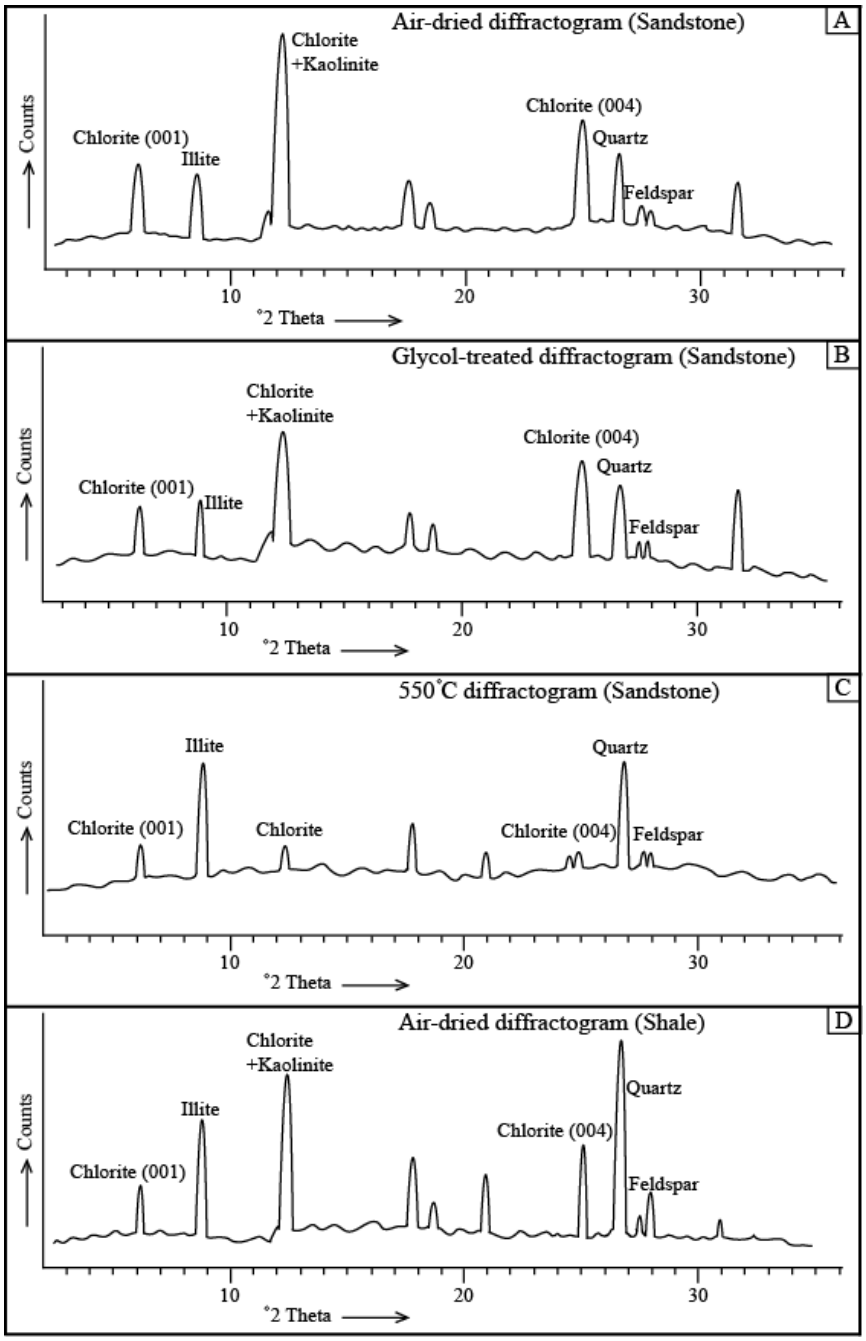

Fig.4.3.1.2. XRD analysis of clay minerals identified in the analyzed reservoir sandstones and interlayered shales. (A) Non-treated air-dried diffractogram of sandstone samples. (B) Glycol saturated diffractogram of sandstone samples. It shows relative high abundance of clay mineral chlorite compared to others. Both air-dried and glycol-treated diffractograms show the similar responses due to the absence of smectite swelling clay. (C) 550 °C heated diffractogram of sandstone sample and hence the kaolinite peak is disappeared remained a small peak for chlorite. (D) Non-treated air-dried diffractogram of the interlayered shale sample is also shown which indicates the similar clay responses compared to those found in sandstone sample (A and B). It suggests the similar genetic origin for the clay minerals found both in sandstones and shales (e.g., Moore and Reynolds, 1979).

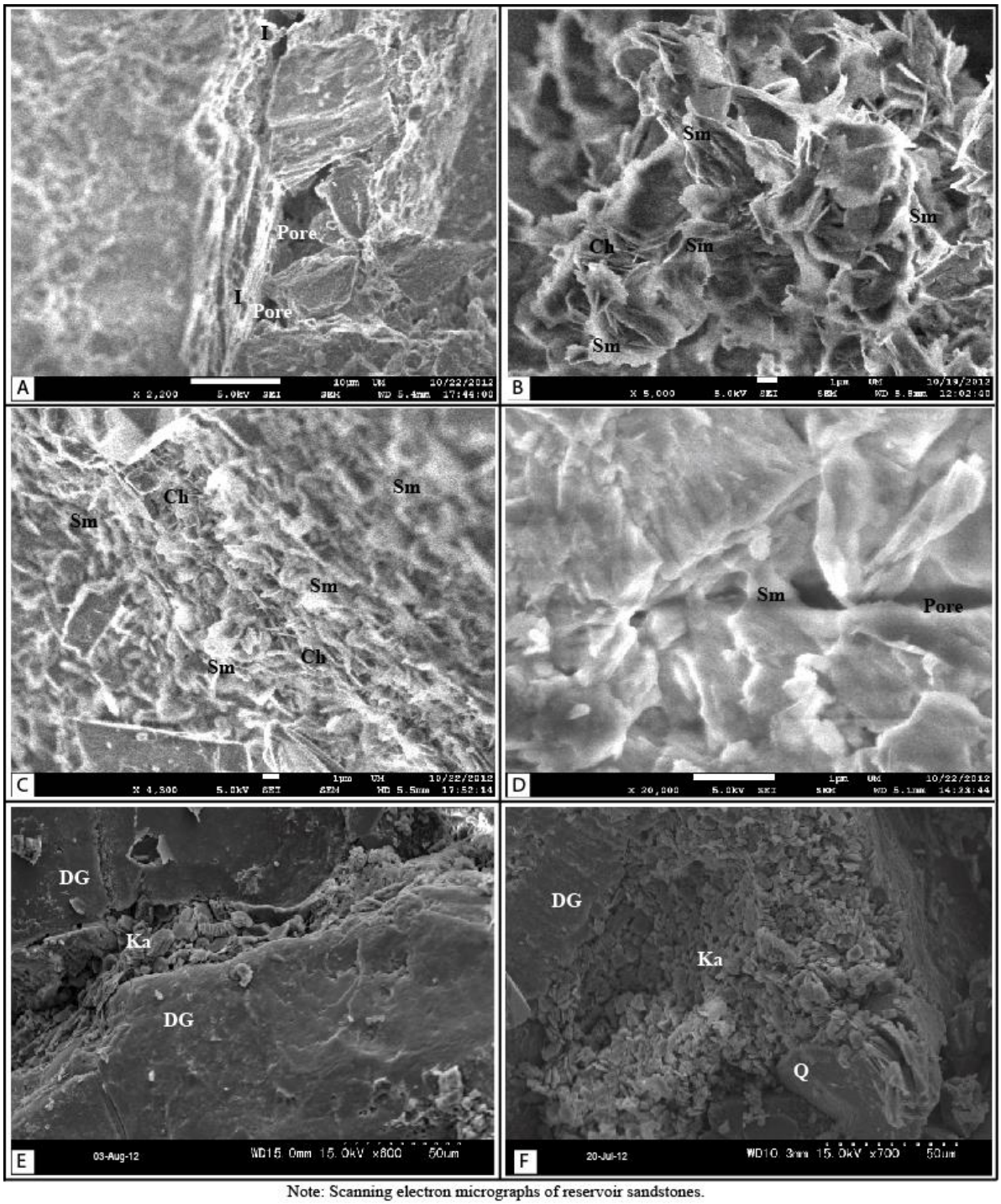

Note: Scanning electron micrographs of reservoir sandstones.

Photomicrograph 4.3.1.4. (A) The illite (I) thin ribbons formed a mat-like feature lining the pore coating the detrital grain surface. Pore-bridging illite is also shown and it reduced the porosity-permeability, depth 3377m at Kamta well-1 (KM1ST10). (B) Typical webby and crenulated morphology smectite (Sm), depth 3404m at Shahbazpur well-1 (SB1ST19). (C) Mixed layer webby smectite and euhedral pseudohexagonal chlorite (Ch), depth 2752m at Rashidpur well- (RP4ST11). (D) Pore-bridging smectite that reduced the porosity and permeability, depth 3578m at Begumganj well-1 (BG1ST19). (E) and (F) Kaolinite books (face-to-face stacks of pseudohexagonal plates) partly occluded the pore throats. It is altered from detrital feldspars during early diagenetic stage, depth 2398.5m at Kailas Tila well-5 (KT5ST6).

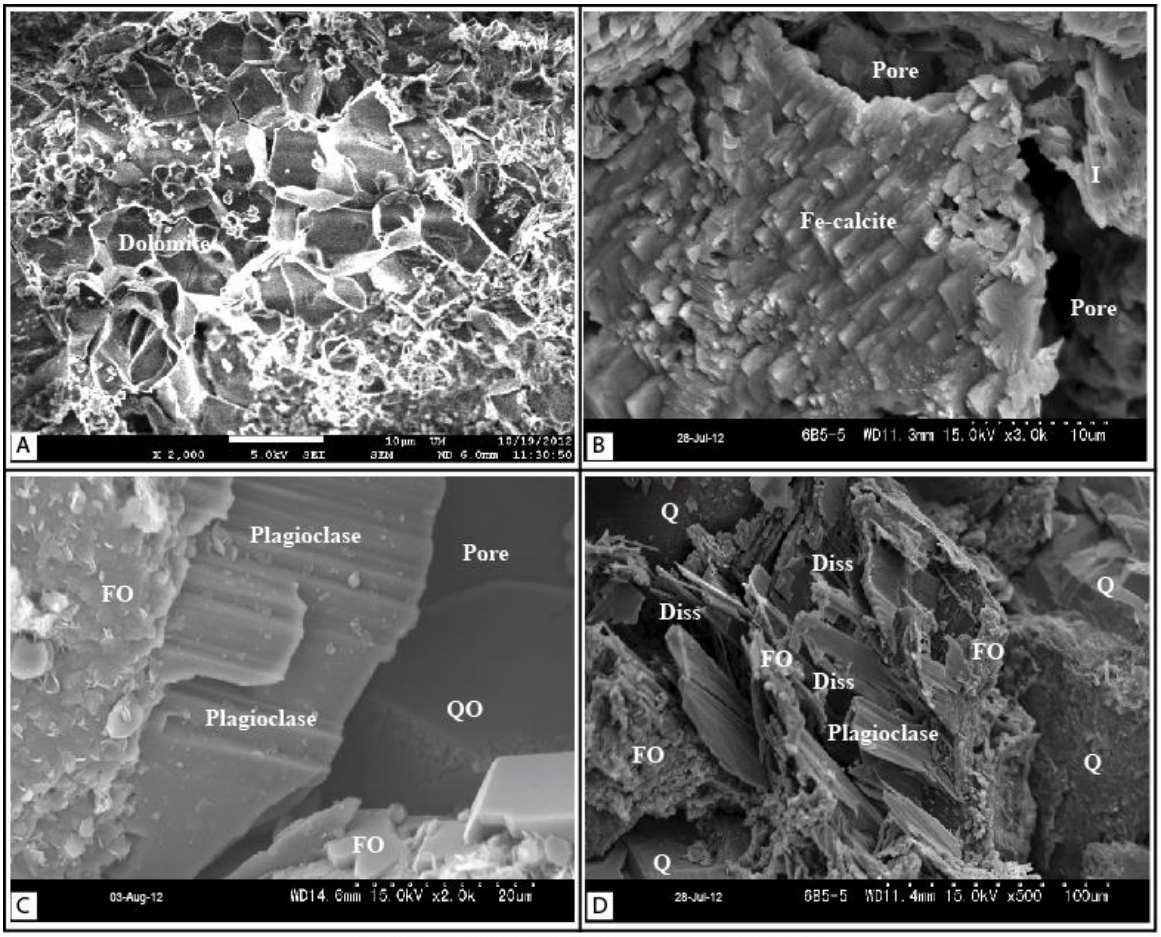

Note: Scanning electron micrographs of reservoir sandstones.

Photomicrograph 4.3.1.5. (A) Rhombic morphology dolomite surrounded by other detrital grains, depth 2840m at Kamta well-1 (KM1ST2). (B) A mosaic of blocky habit Fe-calcites precipitated in pores associated with filamentous illite which occluded the pores, depth 2757m at Rashidpur well-4 (RP4ST12). (C) K-feldspar overgrowth (FO) developed on the original clean detrital plagioclases, depth 3136.5m at Kailas Tila well-4 (KT4ST1). (D) Rimmed K-feldspar authigenesis (FO) over the original plagioclase feldspars. Dissolution (Diss) resulted the secondary porosity during diagenesis, depth 2784m at Titas well-11 (T11ST27).

Dolomite is found in the samples as clusters of small rhombic crystals under SEM (Photomicrograph 4.3.1.5A). The Fe-calcite (and pure calcite) cement is recognized easily by pore filling mosaic of fine crystals (blocky habit), although single large crystals are not uncommon in the analyzed thin sections (Photomicrograph 4.3.1.2C). The distribution is rather patchy and displacive locally, although some uniform pore filling large area is also

covered occasionally by calcite cement. This single crystal is even so large to surround the detrital grain producing the poikilotopic texture.

4.3.1.4.5 Dissolution and replacement

The replacement involves dissolution of one mineral and essentially simultaneous precipitation of another mineral in its place. It occurs as a partial or complete dissolution-replacement event in the samples analyzed (Photomicrograph 4.3.1.2D). Several kinds of minerals are observed as dissolved and, subsequently, either partially or fully replaced in the analyzed siliciclastic sandstones. The most commonly found are albitization whereby the albite plagioclase replaces the K-feldspar or calcic plagioclase types and chloritization where the chlorite replaces the biotite (Photomicrograph 4.3.1.1F). The replacement of clay matrix by carbonate minerals is also identified. Even the dissolution of detrital quartz as a result of corrosion is recognized in few cases under the microscope (Photomicrograph 4.3.1.2E).

4.3.1.5 Compaction and grain packing

Compaction is the decrease of sediment volume and concomitant shrinking of porosity as a result of grain rearrangement and other processes caused by sediment load and tectonic forces. The compaction signatures of diagenesis of the investigated samples are recognized by the estimation of grain packing, ductile grains, primary porosity and grain fractures. The grain packing, in turn, involves the presence of various grain contacts and grain deformation. The five different types of grain contacts defined by Taylor (1950) such as floating, tangential (point-point), long (straight), concavo-convex (embayed) and sutured (serrated) are observed in the studied siliciclastic sandstone thin sections (Photomicrograph 4.3.1.1C and 4.3.1.2.F). The floating and tangential contacts are less common than

concavo-convex and suture contacts. Nonetheless, the bending of flexible grains such as mica flakes, deformation of ductile grains and the fractured grains are the visual evidence of the compaction (Photomicrograph 4.3.1.2.F).

4.3.1.6 Discussion and reservoir implications

Cementation involves the reduction of reservoir porosity and permeability. It was already stated that the development of silica cement (quartz overgrowth) during diagenesis is a function of the silica source, timing and mechanisms. The multiple source of quartz is explained by many workers (Folk, 1980; Boggs, 2009). Pressure solution of quartz grains at points of contact and various mineral reactions that release silica appear to be the most reasonable source of silica cement (quartz overgrowth) in the analyzed siliciclastic sandstones at intermediate and deeper depths (Boggs, 2009). The major phase of quartz cementation (overgrowth) in the studied samples most likely occurs at temperatures of 50-75 ºC at shallow burial depths as noted by Blatt (1979) and Dutton and Diggs (1990). Minor quartz cementation would also continue to greater depths and a temperature of 200 ºC. Following the model proposed by Leder and Park (1986), the most probable mechanism of quartz cementation in the sandstones involves with the basin-wide circulation of silica-supersaturated fluids driven by thermal convection or hydrostatic head. Cooling of pore waters offers another reasonable explanation for late-stage quartz cementation locally at moderate depths. The observed straight and long contacts of individual quartz grains correspond to the early stage of diagenesis whereas the concavo-convex and suture contacts represent comparatively later stage of diagenesis (Estupiñan et al., 2010).

Clay mineral diagenesis is influenced by temperature and chemical reactions that affect the composition of the pore-water (Pittman, 1979). It is also associated with a time factor, for

example, the chlorite and illite are statistically increased with time (Garrels and Mackenzie, 1971; Blatt et al., 1980). This interpretation is supported by the comparative higher presence of chlorite and illite in the studied siliciclastic sandstones (Figs.4.3.1.2A, 4.3.1.2B and 4.3.1.2C). In fact, a range of diagenetic stages is suggested in the analyzed sandstones. For example, the presence of kaolinite (feldspar transformation) corresponds to the early stage of diagenesis whereby the smectite-chlorite (clay transformation) represents the moderate stage of diagenesis (SEM Photomicrographs) (Bjorlykke, 1983; Lee et al., 1989). The identified kaolinite is possibly formed from the feldspar transformation since it is found mostly overlying the feldspar grains under SEM. The chlorite could be of a number of origins (Worden and Morad, 2009; Al-Juboury et al., 2010), but in the analyzed sandstone the most possible mechanism of chlorite precipitation is either the direct replacement from detrital biotite or precursor clay transformation (from smectite to chlorite) or direct precipitation from pore water (Zhang et al., 2012). The chlorite is frequently found in association with altered biotite (Farhaduzzaman et al., 2013k). The similar clay mineral composition (chlorite-smectite-illite) is also found in the interlayered shale lamina which is considered as the major source of clay minerals in the studied sandstones (Figs.4.3.1.2A and 4.3.1.2D). The overall peak intensity in shale samples is comparatively higher than those in sandstone samples. It occurs possibly because of the relative higher concentration of those clay minerals in interlayered shales than those in reservoir sandstones. The pore-lining chlorite (SEM) acts as the barrier of local development of quartz cement which preserves the porosity and permeability. It is encouraging for petroleum geologists affecting positively on hydrocarbons flow (Al-Ramadan et al., 2004; Rahman and McCann, 2012). The identified dominant illite-smectite mixed layer clay would generate at comparatively intermediate diagenetic stage (mesogenesis) at temperature of 100-200 ºC whereby the dominant smectite is at 55-100 ºC

(Bjorlykke, 1983; Lee et al., 1989). This mixed diagenetic stage is also consistent with the interpretation based on silica cement (quartz overgrowth).

The range of the diagenetic regime is reflected by the presence of microcrystalline to coarse crystalline, patchy to blocky, isolated stringers of carbonate cements in the pores. The observed patchy distribution of the calcite cement reflects initial partial removal of more evenly distributed cement at the early stage of diagenesis subsequently followed by complete carbonate precipitation during comparatively later stage of diagenesis and burial (Photomicrographs 4.3.1.2C, 4.3.1.5C and 4.3.1.5D). In cementation process, the bicarbonate ions are supplied by organic matter reactions. A source of calcium must also be available to form calcite cements. Dolomite precipitation further requires a source of magnesium and on iron source is essential for Fe-calcite (siderite and ankerite) cements. Many authors stated that a steady contribution of both cations and anions must be continued in pore water for carbonate cementation (Berner, 1980; Morad et al., 1990, Boggs, 2009). In the studied Surma Group sandstone samples, it is possible that the mixing of marine-nonmarine sources (with parallel oxidation and sulfate reduction) contributes to carbonate cementation at the early stage of diagenesis (Curtis and Coleman, 1986). The dissolution of skeletal grains of the sandstones furnishes the bicarbonate, calcium and magnesium ions in the pore water. The organic matter fermentation (methanogenesis) and sulfate reduction would also contribute to these ions. The additional Fe, Ca and Mg are supplied from the dissolution of ferromagnesian minerals, calcium feldspar and smectite. This hypothesis is also applicable for organic rich shales interbedded with the studied sandstones and, in fact, it is more appropriate for the succession consisting of alternating sandstone and shale like the currently studied group (Morad et al., 1990). They proposed that the temperature of 120-160 ºC is suitable for Fe-carbonate cementation, however, if the sources are available.

Using oxygen isotope study Rahman and McCann (2012) suggested this type of mixing source (nonmarine-marine) for carbonate cementation in the same succession. However Imam and Shaw (1985) and Islam (2009) emphasized on the skeletal dissolution for carbonate cements in the sandstones.

The decementation and destruction of framework grains increases the porosity as a result of the development of secondary porosity in the analyzed Surma Group sandstones (Photomicrographs 4.3.1.2D and 4.3.1.5D) (Folk, 1980; Reed et al., 1993; Boggs, 2009). Moreover, it is not always the true case as a result of the incongruent dissolution whereby the K-feldspar is replaced by kaolinite (kaolinization) with little and no increase in porosity. The reprecipitated silica overgrowth as a result of pressure solution reduces the porosity.

The replacement process, like dissolution, affects the porosity evolution of the studied sandstones during diagenesis. The principal causes include alteration of feldspar (albitization and kaolinization) and micas to clay minerals (chloritization) with concomitant increase in volume (Photomicrograph 4.3.1.1F). It appears to plug the pore space which ultimately reduces its porosity and permeability. In addition, the complete dissolution-replacement of framework grains also provides the misleading interpretation of the provenance analysis (although currently it is not discussed in detail) (Morad and Aldahan, 1987).

Wolf and Chilingarian (1976) stated that the compatibility of sandstone is a function of grain size, sorting, shape, orientation, composition, matrix content and cements. As a result of grain rearrangements, the mechanical compaction considered to be the dominant process in the initial stage of diagenesis up to 1.5 km in the studied siliciclastic sandstones. It is

determined by the presence of long contacts (Photomicrograph 4.3.1.1F). Subsequently, in deeper part and at the later stage, the diagenesis is dominated by chemical compaction while the additional mechanical compaction is indicated by mica bending, fractured quartz and concavo-convex and suture contacts (Photomicrograph 4.3.1.2A) (Schmidt and McDonald, 1979). At the intermediate stage of diagenesis; the chemical compaction is marked by dissolution and replacement (Photomicrograph 4.3.1.2D). The well sorted sandstone samples look less compacted while diagenesis followed by less porosity reduction than those with moderately sorted samples followed by greater porosity reduction (Houseknecht, 1987). The observed long and concavo-convex contacts would develop either during diagenesis (as a result of deformation or solution) or deposition (dependent on grain shapes). The suture contacts are thought to have been generated as a result of dissolution (pressure solution) during comparatively later stage of diagenesis in the sandstones (Taylor, 1950; Hoholick et al., 1982). A summary of digenetic events and their respective comparative stages are shown in Fig.4.3.1.3.

4.3.1.6.1 Implications to reservoir porosity and permeability

Porosity in sandstones is the aggregate total of all the openings or interstices in a rock framework and within grains. It could be either primary porosity that is created during deposition or secondary porosity that is formed during diagenesis (Worden and Burley, 2003). In the petroleum aspect, the interconnected pores (effective porosity) is the most important element for reservoir evaluation. The permeability of any sandstone is its property to permit the passage of fluids (e.g., petroleum) through these interconnected pores. Both porosity and permeability are the controlling parameters for the movement of petroleum in the reservoir.

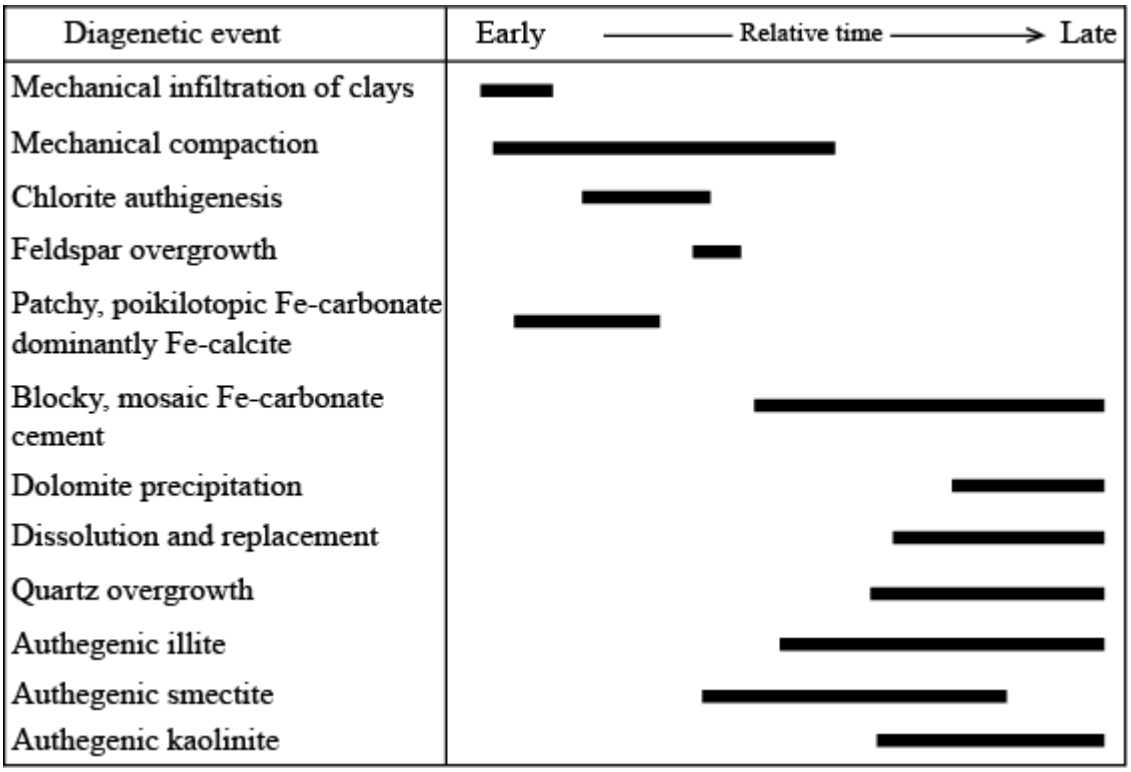

Fig.4.3.1.3. Paragenetic sequence of the important diagenetic events observed in the studied Surma Group sandstone reservoirs, the Bengal Basin, Bangladesh.

The measured total thin section porosity of the studied Surma Group siliciclastic sandstones ranges from 10 to 23% with an average of 18% and it is mostly primary porosity developed during its deposition. The well connected pores (permeable), including intergranular porosity (dominant) and solution porosity, are observed in many of the analyzed samples. Imam (2005), Islam (2009) and Rahman and McCann (2012) measured the average porosity of the Surma Group sandstone as 18-20%. The porosity values calculated for the current investigation is very consistent with the earlier interpretations. In the present analysis, comparatively less sorted samples show lower porosity (e.g., RP4ST12 = 12%) than that found in well sorted samples (e.g., T11ST27= 20%). Similarly relatively deeper samples show lower porosity value (e.g., BG1ST8= 14%) than that measured in shallower samples (e.g., T11ST27= 20%), although it is always not true in the analyzed samples.

Hence, the mechanical compaction (as a result of sediment load) is the controlling factor affecting the porosities of the samples with burial depth and time. Grain rearrangement and reorientation significantly reduces the primary porosity in the sandstones. The overall porosity of the investigated Tertiary sandstones samples decreased with depth (Fig.4.3.1.4). At deeper depths, few samples shows high porosity compared to relatively shallower samples. Porosity occurs due to the development of secondary porosity (e.g. dissolution) during intermediate diagenetic stage. Nonetheless, at shallow depths, few samples show low porosity compared to deeper samples (Fig.4.3.1.4). The early diagenetic constituents (e.g., patchy carbonate cements) is considered for this porosity reduction at these shallow depths. The cementation plays important role here to reduce the porosity and permeability in the sandstones analyzed. The pore-filling blocky Fe-calcite cement, pore lining authigenic clays (chlorite-illite-smectite) and quartz overgrowths decreases the porosity and permeability. In very few cases, the pore-bridging mixed layer clay (illite-smectite) plays the most significant role to deteriorate its reservoir quality through the reduction of permeability (SEM photomicrographs). The reservoir permeability is not significantly affected by the diagenetic constituents.

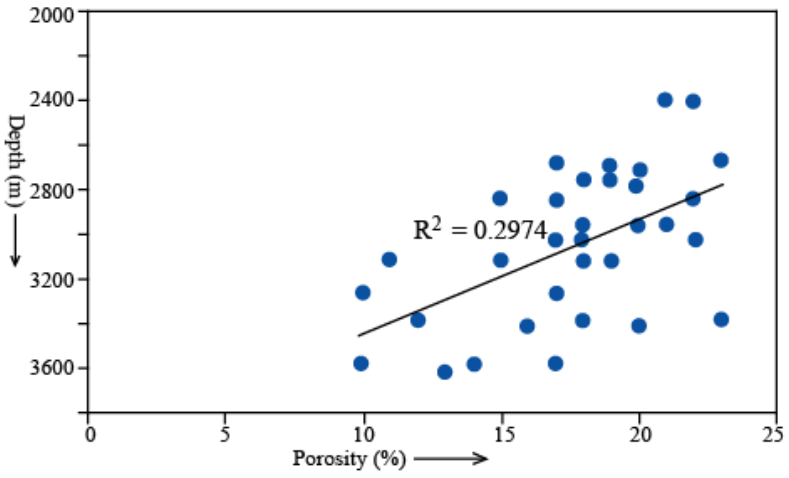

Fig.4.3.1.4. A cross-plot of porosity and depth observed in the Tertiary reservoir sandstones of the Bengal Basin, Bangladesh. It shows the overall porosity decreases with depth.

The secondary porosity observed in the studied samples developed because of the dissolution of carbonate cements, feldspars and other unstable constituents during diagenesis (Photomicrographs 4.3.1.2D and 4.3.1.5D). It increases the total porosity of the reservoir sandstone although its amount is not too high compared to the primary porosity. This type of secondary porosity is observed mostly in moderate to deeper parts of the reservoir. Nevertheless, the dissolution followed by subsequent replacement again reduces its porosity. The quantitative measurement of permeability was not carried out in the present petrographic study, but it is measured in petrophysical study chapter (4.3.2). Permeability was measured for the Surma Group sandstone by a few workers, for example, 100-400 millidarcy by Imam (2005). On the basis of discussion above, the analyzed sandstone can be ranked as good to excellent petroleum reservoir which is also supported by Imam and Hussain (2002), Islam (2009) and Rahman and McCann (2012).

Chapter 4.3.2 Petrophysical Study of the Well Rashidpur 4

Petrophysical log interpretation is one of the most useful and important tools to characterize the reservoir properties (Asquith and Gibson, 1982). Petrophysical study involves the analysis of different parameters of reservoirs including lithology, volume of shale, porosity, water saturation, hydrocarbon saturation, permeability, hydrocarbon moveability and pore geometry by using appropriate well log data. It provides the unique opportunity to observe the relationship between porosity and saturation (Sakurai et al., 2002). Reliable evaluation of hydrocarbon resources in shaly clastic reservoir rocks is an important task. The determination of reservoir quality and formation evaluation processes largely depends on quantitative evaluation of petrophysical properties. Nawab and Islam (2005) estimated shale volume in the Miocene succession for selected gas fields of Bangladesh using gamma ray and porosity logs. But in Bangladesh, the petrophysical analysis concerning shaly sandstone has been performed in limited extent, for example, Islam et al. (2006, 2007 and 2009) and Islam (2010). In this regard, this study attempts to analyze the petrophysical properties of shaly sand gas reservoir encountered in the well Rashidpur 4 (RP4) of Rasidpur Gas Field, the Bengal Basin, Bangladesh. The Neogene sandstones in the studied well were also analyzed.

4.3.2.1 Data analysis and interpretation

Well log data helps to identify permeable zones; productive zones for hydrocarbon with depth and thickness; and the interfaces of oil, gas or water of a particular reservoir. Permeable zones may contain either hydrocarbons or water or both. The permeable zones have been identified with the help of GR, SP, resistivity, neutron, density and sonic log responses. Permeable beds are delineated by SP deflection from shale base line. Very low

gamma value and low caliper readings in uncaved borehole condition confirm the permeable zones. High resistivity value also indicates permeable zones. Hydrocarbons do not conduct electrical current but saline water highly conducts electrical current. Naturally water bearing permeable zones show low resistivity values compared to hydrocarbon bearing zones. On the other hand, high SP value and low gamma value suggests hydrocarbon bearing permeable zones (Asquith and Gibson, 1982). Very low bulk density and neutron porosity compared to water bearing sandstone and a negative separation between density and neutron responses are also the indicators of hydrocarbon bearing zones (Fertl, 1987). In this study, 20 permeable zones have been identified from the composite log analysis of 1464 m (1310-2774 m) thickness of the well RP4. Among these permeable zones, four zones have been identified as hydrocarbon bearing and the remaining are water bearing (Table 4.3.2.1).

4.3.2.2 Identification of hydrocarbon bearing zones

Hydrocarbon bearing zones can be identified with the combined use of GR, SP, resistivity (RILD and RSFL), neutron, density and sonic log responses. In identified hydrocarbon bearing zones, gamma ray log shows low response and SP log shows high value and it deflects from the shale base line (Figs. 4.3.2.1, 4.3.2.3, 4.3.2.5 and 4.3.2.7). For this purpose, resistivity logs are the best option to detect hydrocarbon bearing zones. The resistivity log response in the hydrocarbon bearing zones is very high. Normally, in hydrocarbon bearing zones deep resistivity log (RILD) value is higher than the shallow resistivity log (MSFL). High deflection of neutron and density log with sharp decrease of porosity and density indicate gaseous hydrocarbon. In all of the identified four hydrocarbon bearing zones, some shales are interbedded with the reservoir sandstone, affecting the

reservoir properties. The log depth of 1310-2774m is analyzed for the present study. However, the depth range of 1447-2731 m covers the identified four hydrocarbon bearing zones (cumulative thickness 168 m) in the Miocene sandstone reservoir of the well RP4.

Table 4.3.2.1. Permeable zones identified from the log based petrophysical analysis of the well Rashidpur 4, the Bengal Basin, Bangladesh.

Depth range (m)	Thickness (m)	Remarks
1374-1402	28	Water bearing
1447-1522	**75**	**Hydrocarbon bearing**
1534-1550	16	Water bearing
1555-1565	10	Water bearing
1575-1595	20	Water bearing
1635-1670	35	Water bearing
1718-1740	22	Water bearing
1760-1780	20	Water bearing
1795-1805	10	Water bearing
1855-1885	30	Water bearing
1930-1960	30	Water bearing
1962-1985	23	Water bearing
2060-2090	30	Water bearing
2180-2190	10	Water bearing
2215-2225	10	Water bearing
2314-2335	21	Water bearing
2337-2350	**13**	**Hydrocarbon bearing**
2405-2440	35	Water bearing
2466-2483	**17**	**Hydrocarbon bearing**
2668-2731	**63**	**Hydrocarbon bearing**

Note: Total log analyzed (1310-2774)= 1464m; Gas bearing gross thickness= 168m

4.3.2.3 Shale distribution

Generally, shale evaluation includes the determination of shale parameters as well as its volume and types. The determination of shale parameters often depends on the experience of log analyst since these parameters vary with different geological factors.

Volume of shale in the hydrocarbon bearing zones of the reservoir sandstones of the studied well has been calculated using Schlumberger (1975) and Dresser Atlas (1979) formulas. The average shale volume of the identified hydrocarbon bearing zones of the well RP4 is 20% (Table 4.3.2.2). Zone 3 contains the lowest and Zone 1 contains the highest volume of shale. Waxman and Smits (1968) suggested that CEC value > 0.2 indicate smectite or illite, whereas CEC value < 0.2 indicates kaolinite or chlorite. In the present study, CEC values are found ≈ 0.2 which indicates mixed types of clay (i.e., chlorite, illite and kaolinite) throughout the Surma Group reservoir intervals of the Bengal Basin, Bangladesh.

4.3.2.4 Porosity (φ) distribution

Porosity of rock is a fraction of void space compared to its total volume. The determination of porosity is a very important step for calculating fluid saturation in reservoir evaluation (Ruhovets, 1990). Neutron and density logs have been used to calculate porosity distribution for the current study. The porosity values of the individual zone are graphically represented in Figs. 4.3.2.2, 4.3.2.4, 4.3.2.6 and 4.3.2.8. The estimated porosity of the hydrocarbon zones of the Neogene sequence ranges from 7% to 36%, with an average porosity of 21% (Table 4.3.2.2). The calculated porosity data is independent without having any control by any other means.

4.3.2.5 Water saturation (S_w) distribution

Water saturation of the currently investigated hydrocarbon bearing zones in the studied well has not been used for Archie's (1942) formula. Because this formula is valid for clean sandstone and the values are grately affected by incursion of shale and porosity.

Therefore, three most popular formula have been used those were proposed by Simandoux (1963), Fertl (1975) and Schlumberger (1975). The calculated values of water saturation using these formulas are graphically represented in Figs. 4.3.2.2, 4.3.2.4, 4.3.2.6 and 4.3.2.8. Finally, the average value of the water saturation calculated from these three different formulas have been considered for further calculation. The calculated average water saturation values of the four hydrocarbon bearing zones 1-4 in the well RP4 are 20%, 35%, 39% and 14% (Table 4.3.2.2).

Table 4.3.2.2. Log based petrophysical analysis results of 4 hydrocarbon (HC) bearing zones identified in well Rashidpur 4 of Bengal Basin, Bangladesh [Vsh = shale volume; phi = porosity; Sw= water saturation (%) whereas Sc- Schlumberger (1975), Ft= Fertl (1975), Sd= Simandoux (1963); Sh= hydrocarbon saturation (%); Sw/Sxo= moveability; BVW= bulk volume of water; K= permeability (mD) whereas Wy- Wyllie and Rose (1950), Ct- Coates and Dumanoir (1973)]

Gas Zone (depth, m)	Thick (m)	Vsh (%) average range	ϕ (%) average range	Sw (Sc) average range	Sw (Ft) average range	Sw (Sd) average range	Sw (avrg) average range	Sh (Sc) average range	Sh (Ft) average range	Sh (Sd) average range	Sh (avrg) average range	Sw/Sxo average range	BVW average range	K (Wy) average range	K (Ct) average range	K (avrg) average range
Zone 1 (1447-1522)	75	36	19	19	15	26	20	81	85	74	80	0.1	0.04	22	87	54
		6-60	10-27	11-43	6-40	13-75	10-53	57-89	60-94	25-87	47-90	0.1-0.4	0.02-0.05	1-27	1-526	1-306
Zone 2 (2337-2350)	13	14	19	33	35	36	35	67	65	64	65	0.2	0.07	3	62	33
		0-58	15-22	28-43	23-45	32-45	30-44	57-72	55-77	55-68	56-70	0.1-0.2	0.05-0.07	1-6	1-19	4-63
Zone 3 (2466-2483)	17	11	19	38	39	41	39	62	61	59	61	0.1	0.07	4	51	28
		0-40	7-24	29-69	31-65	30-84	30-73	31-71	35-69	16-70	27-70	0.1-0.2	0.05-0.08	1-11	1-157	1-84
Zone 4 (2668-2731)	63	18	28	14	13	16	14	86	87	84	86	0.2	0.04	253	357	305
		3-61	13-36	9-28	7-27	9-39	9-32	72-91	73-93	61-91	68-91	0.1-0.4	0.02-0.06	2-850	1-820	1-735
Gross value	168	20	21	26	26	30	27	74	75	70	73	0.2	0.06	71	139	105

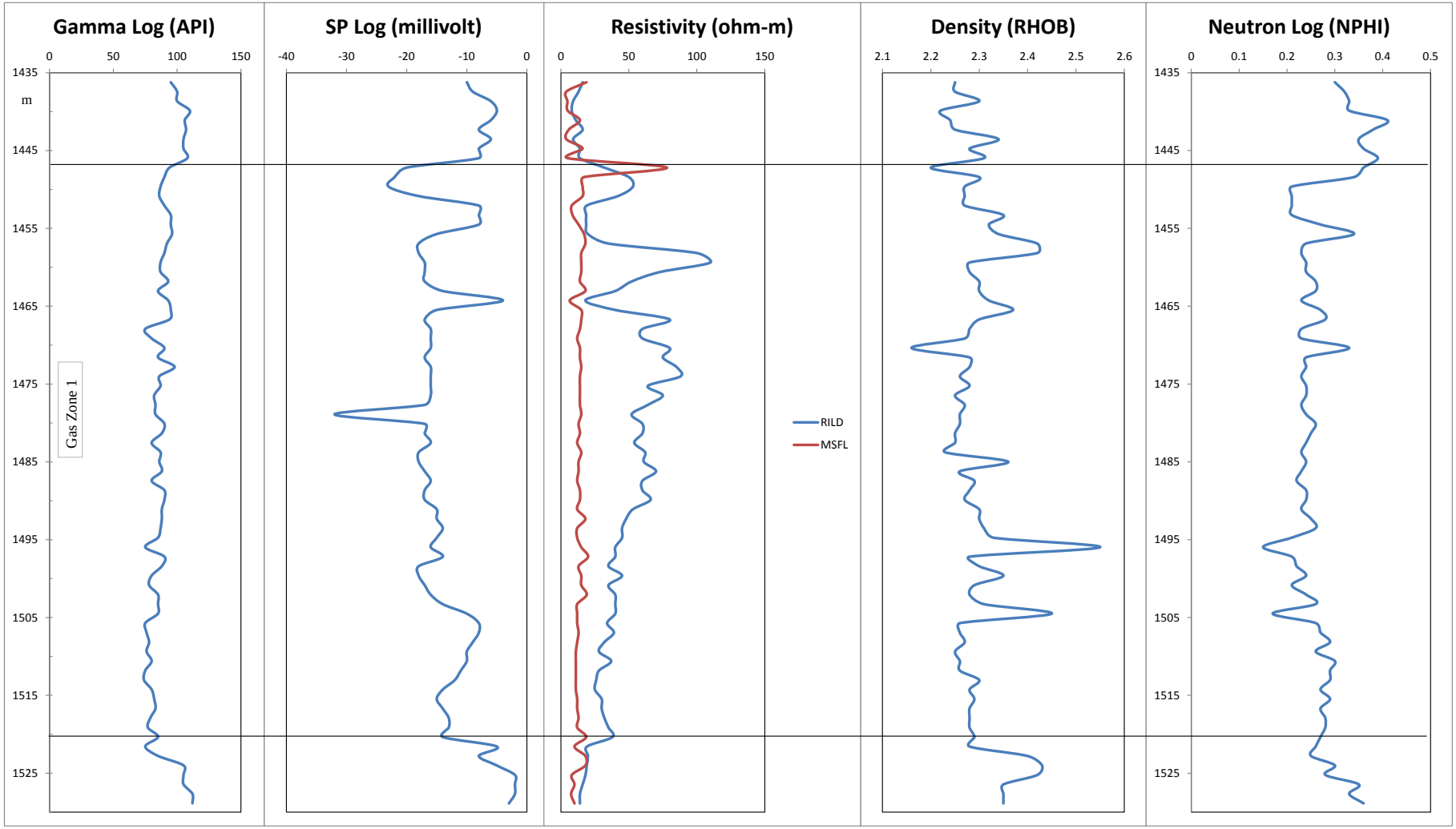

Fig.4.3.2.1. Composite log responses of the hydrocarbon bearing Zone 1 (1447-1522 m) identified in Surma Group of well Rashidpur 4, the Bengal Basin, Bangladesh.

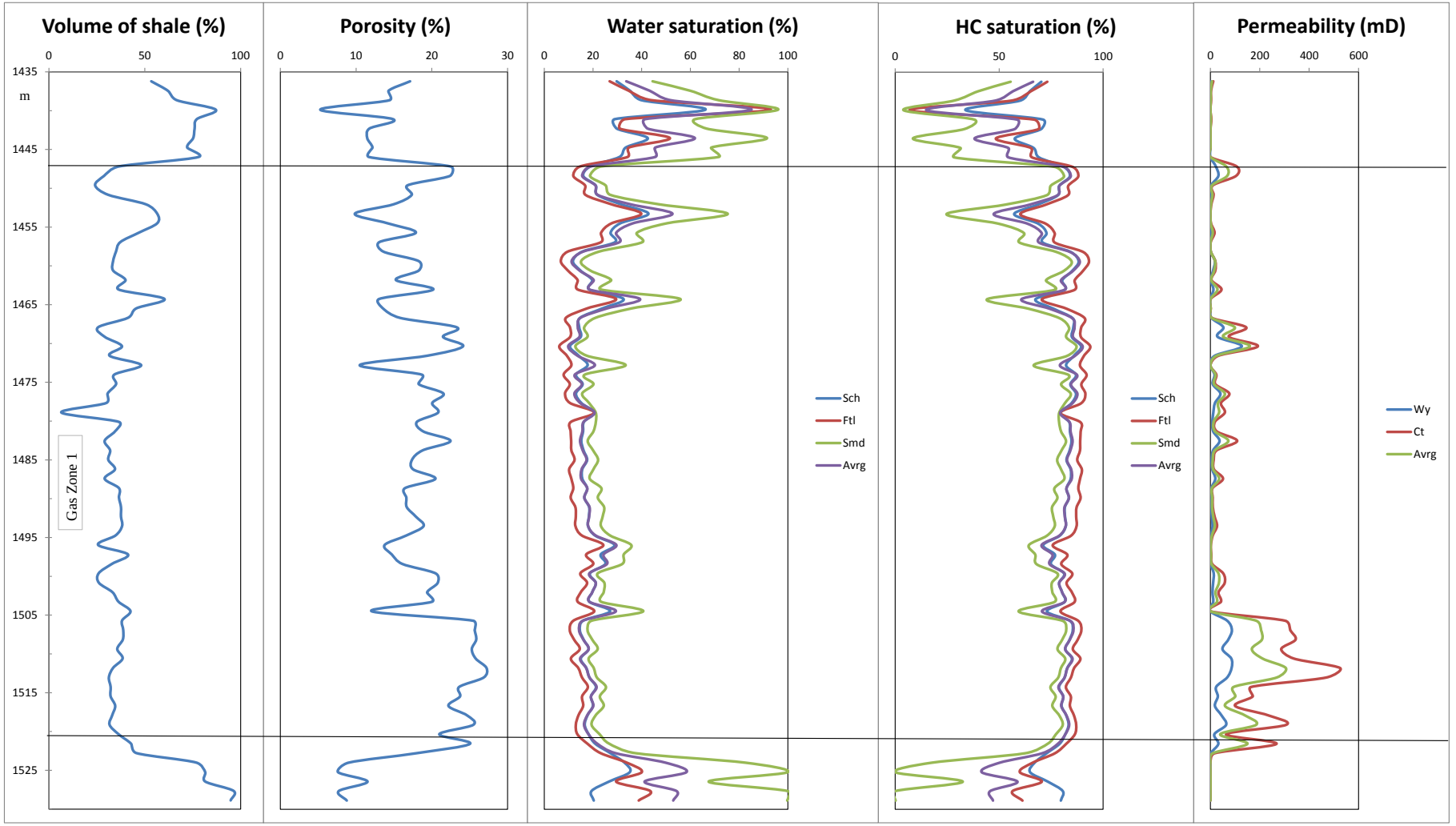

Fig.4.3.2.2. Graphical presentation of the petrophysical parameters of the hydrocarbon bearing Zone 1 (1447-1522 m) identified in Surma Group of well Rashidpur 4, the Bengal Basin, Bangladesh.

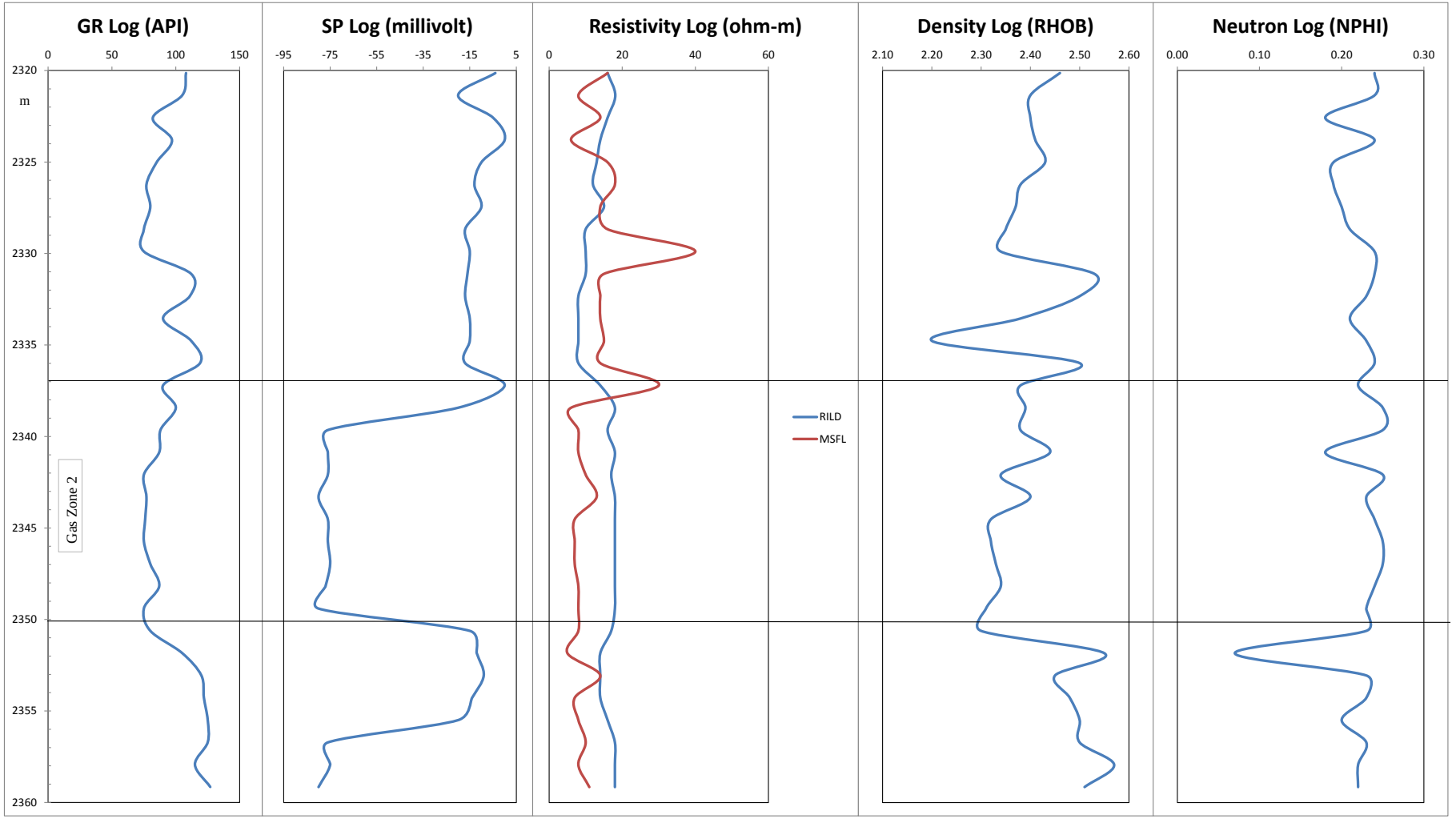

Fig.4.3.2.3. Composite log responses of the hydrocarbon bearing Zone 2 (2337-2350 m) identified in Surma Group of well Rashidpur 4, the Bengal Basin, Bangladesh.

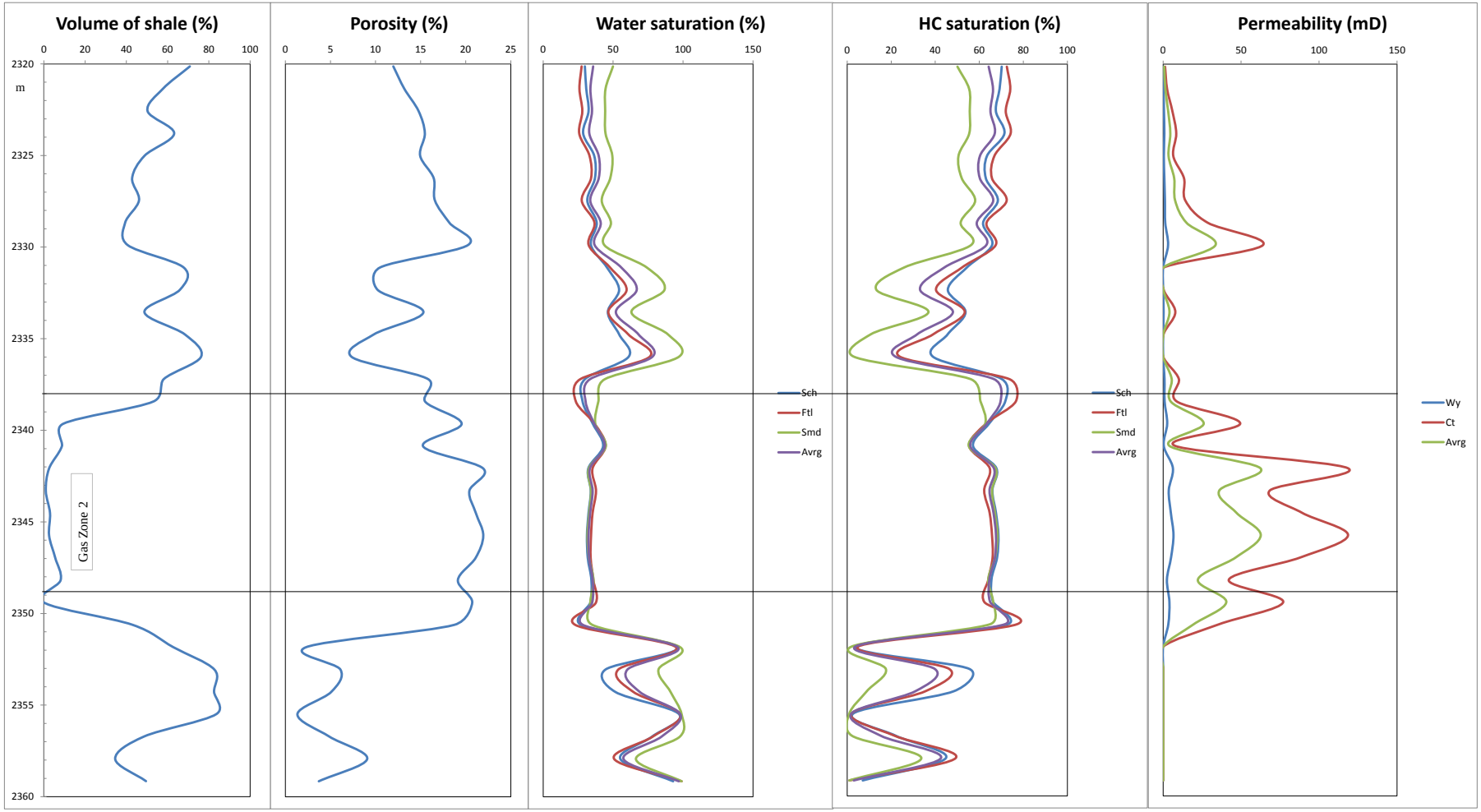

Fig.4.3.2.4. Graphical presentation of the petrophysical parameters of the hydrocarbon bearing Zone 2 (2337-2350 m) identified in Surma Group of well Rashidpur 4, the Bengal Basin, Bangladesh.

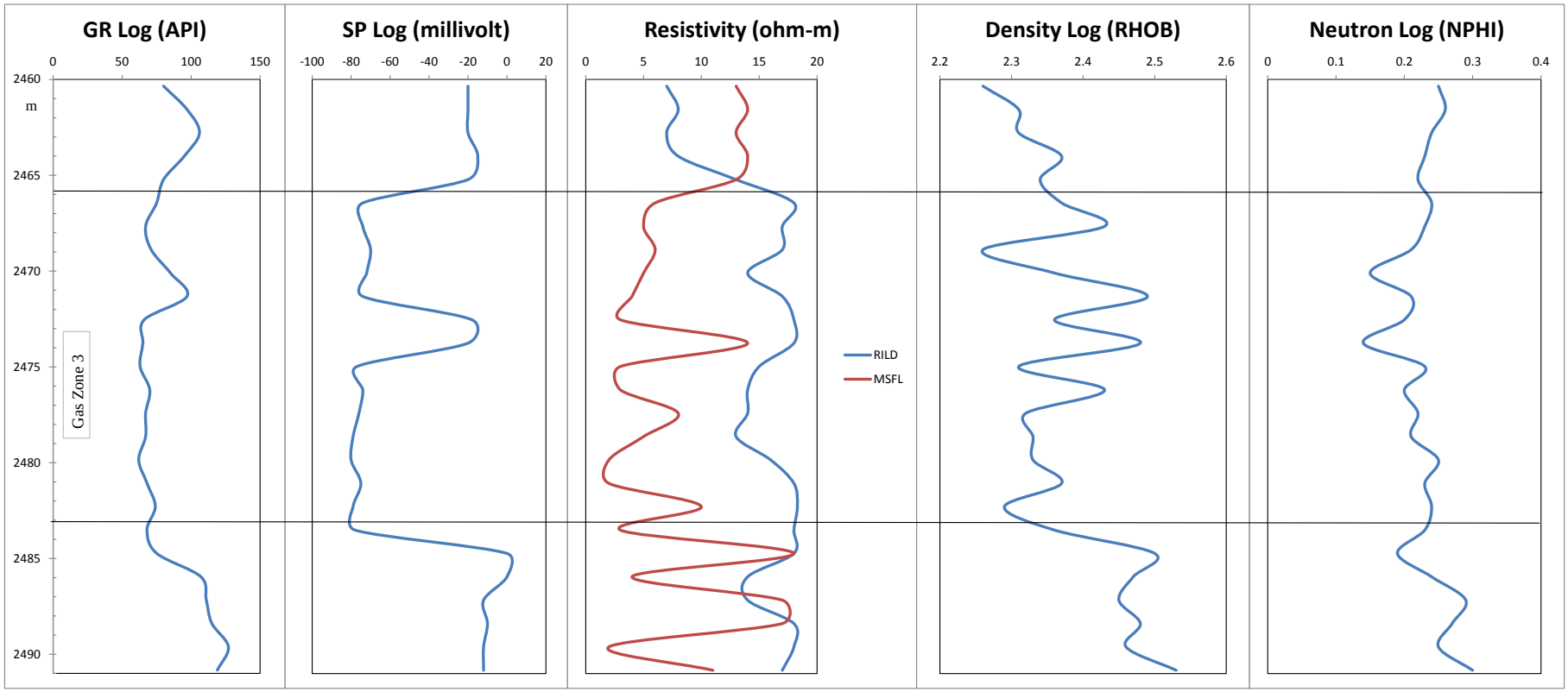

Fig.4.3.2.5. Composite log responses of the hydrocarbon bearing Zone 3 (2466-2483 m) identified in Surma Group of well Rashidpur 4, the Bengal Basin, Bangladesh.

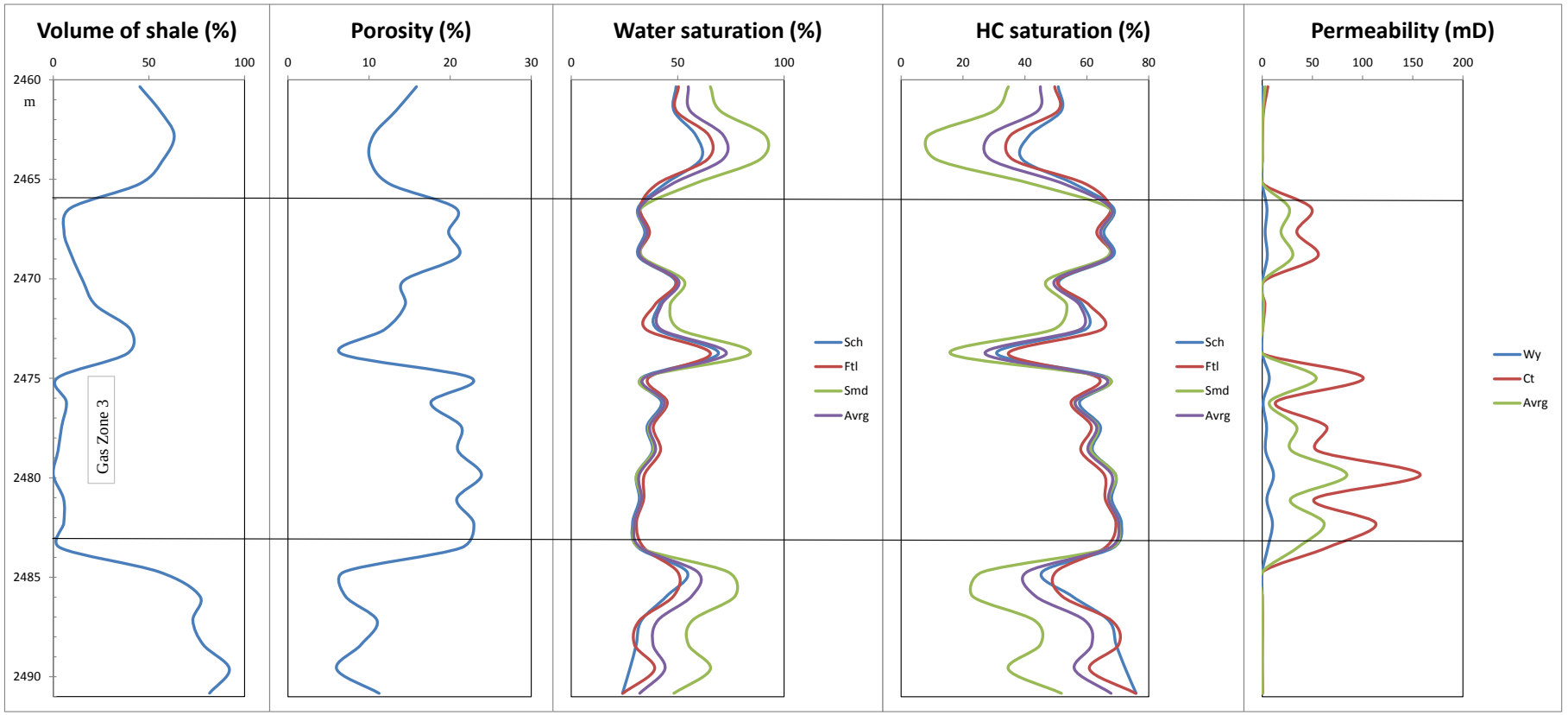

Fig.4.3.2.6. Graphical presentation of the petrophysical parameters of the hydrocarbon bearing Zone 3 (2466-2483 m) identified in Surma Group of well Rashidpur 4, the Bengal Basin, Bangladesh.

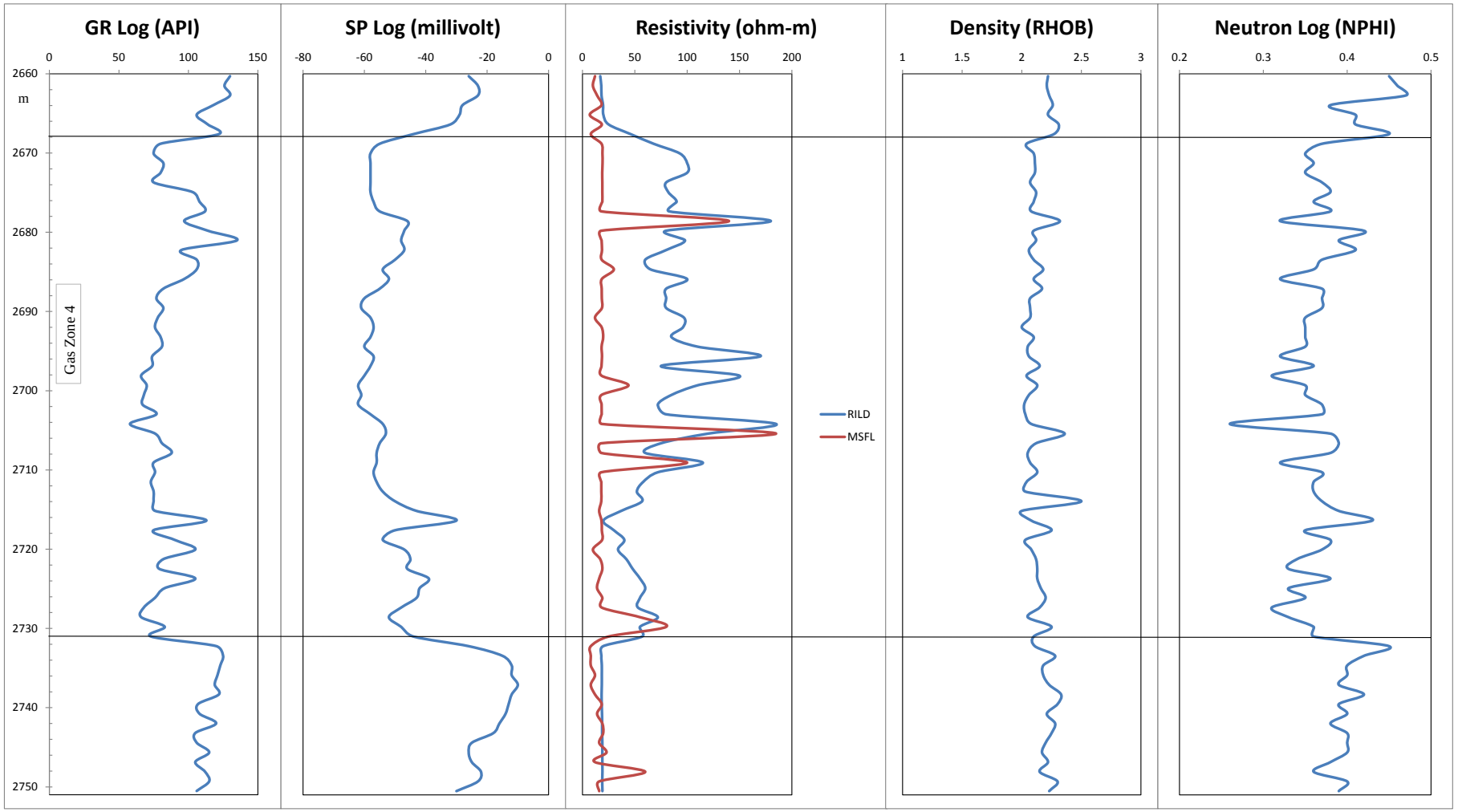

Fig.4.3.2.7. Composite log responses of the hydrocarbon bearing Zone 4 (2668-2731 m) identified in Surma Group of well Rashidpur 4, the Bengal Basin, Bangladesh.

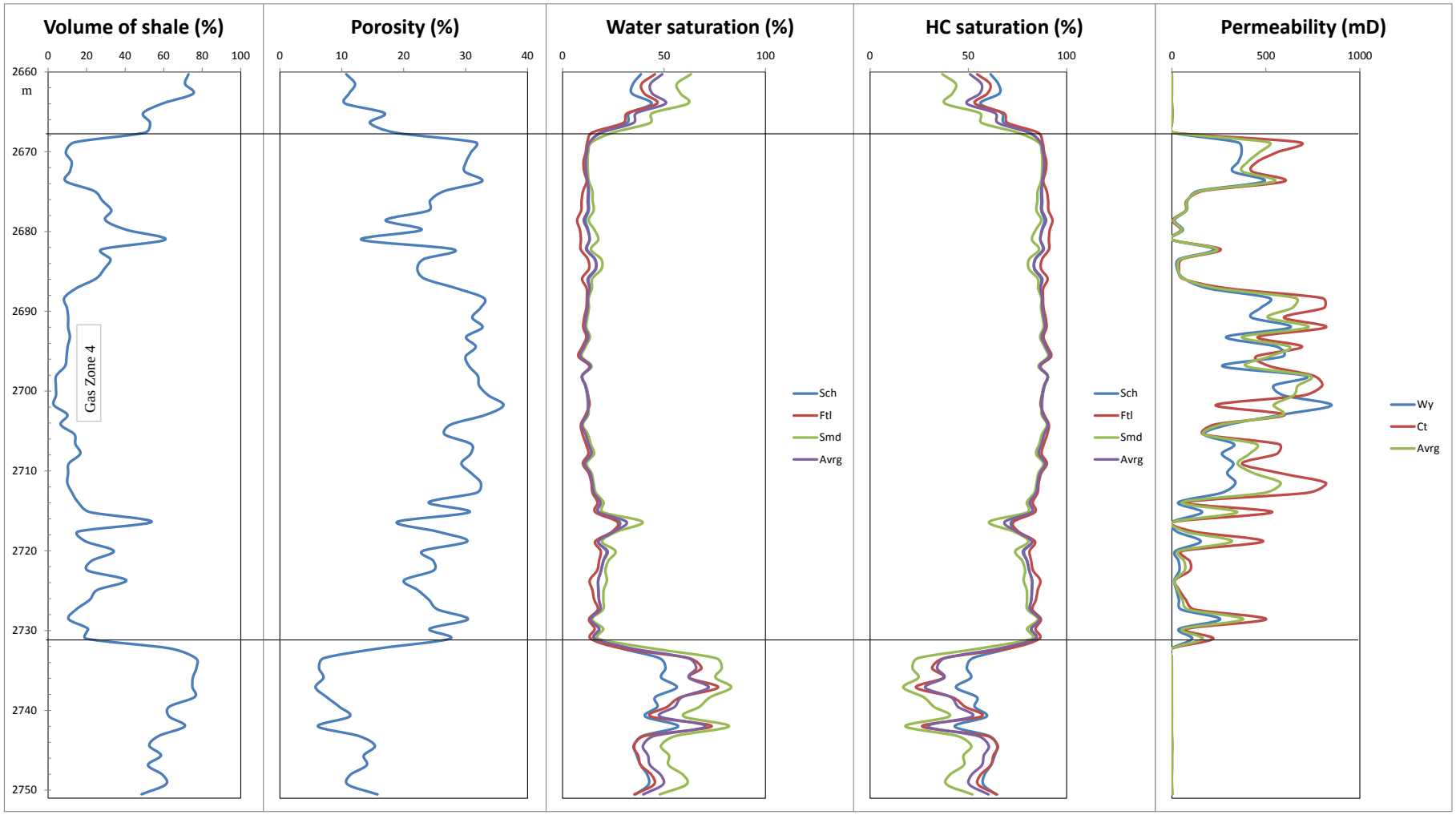

Fig.4.3.2.8. Graphical presentation of the petrophysical parameters of the hydrocarbon bearing Zone 4 (2668-2731 m) identified in Surma Group of well Rashidpur 4, the Bengal Basin, Bangladesh.

4.3.2.6 Hydrocarbon saturation (S_h) distribution

Hydrocarbon saturation of a reservoir is determined by subtracting water saturation from the value of total saturation which is 1 (one). The permeable zone having more than 60% hydrocarbon saturation (S_h) value is commonly treated as a hydrocarbon bearing zone (Asquith and Gibson, 1982). Following all three commonly used formulas, S_h values of all hydrocarbon bearing zones are greater than 60% (Figs. 4.3.2.2, 4.3.2.4, 4.3.2.6 and 4.3.2.8). Sometimes, the presence of shale in the Miocene reservoir sandstones decreases the content of S_h. In case of water saturation calculation, Schlumberger's (1975) formula has been found better suited among these three formulas (c.f., Islam et al., 2006 and 2013; Islam, 2010). The calculated average values of hydrocarbon saturation of the zones 1-4 of the studied well RP4 are 80%, 65%, 61% and 86%. Based on hydrocarbon saturation, the zones can be ranked as Zone 4 > Zone 1> Zone 2> Zone 3.

4.3.2.7 Permeability (K) distribution

Permeability is an indicator of the ability of a rock to transmit fluids. Permeability (K) values of hydrocarbon bearing zones in the studied wells have been calculated using Coates and Dumanoir (1973) formula. The results are shown in Table 4.3.2.2. The average permeability values of the gas zones 1-4 of the investigated reservoir sandstones are 54, 33, 28 and 305 mD respectively. Considering its average permeability, Zone 4 has the greatest potential. All values calculated here indicate that the identified hydrocarbon bearing zones are commonly good to very good reservoirs according to the generalized observation made by Asquith and Gibson (1982).

4.3.2.8 Hydrocarbon moveability index (S_w/S_{xo})

Hydrocarbon moveability index is the ratio between water saturation of uninvaded zone (S_w) to the water saturation of flushed zone (S_{xo}). If the ratio of S_w and S_{xo} is ≥ 1, then the hydrocarbon would not move toward the well bore. If this ratio is less than 0.7 (for sandstone), the hydrocarbon is considered to be moveable (Schlumberger, 1972). From the calculated results (Table 4.3.2.2), it can be inferred that the hydrocarbons of the selected zones in the studied well RP4 are moveable because all movability index values are less than 0.7.

4.3.2.9 Bulk volume of water (BVW)

Bulk volume of water is the product of formation's water saturation and its porosity. It is important to know BVW whether the formation is at irreducible water saturation or not. When the value of BVW is constant or close to constant with some minor scattering, it indicates the homogenous formation having as close to irreducible water saturation. If the BVW ranges from 0.035 to 0.07, the grain size of the rock succession is fine to very fine grained sandstone (Fertl and Vercellino, 1978). The BVW values of the hydrocarbon bearing zones in the studied well have been calculated using Morris and Biggs (1967) formula. The calculated bulk volume of water is nearly constant with some minor scattering in the hydrocarbon bearing zones, indicating that the reservoir rock consists mainly of fine to medium grained sandstone.

4.3.2.10 Discussion

Porosity and permeability are the two most important parameters which can be determined directly or indirectly from well log analysis (Asquith and Gibson, 1982).

These characteristics of rock are affected in many ways during logging measurements. There are many variables and techniques to minimize the adverse down hole effects and drawbacks of some computation procedures. However, none of them is unique. For example, a, m and n are three parameters (constants) termed as the tortuosity, cementation and saturation exponents. These parameters differ from rock to rock and basin to basin. In the Bengal Basin, there are no prescribed values of these parameters. In this study, the values of these parameters have been used in a generalized fashion and considered as 0.62, 2.15 and 2 respectively. These values might also affect the overall calculations. Neutron, density and sonic log readings have been used to determine the porosity. Porosity measurements from density logs require matrix density. Most postulated matrix density for sandstone is 2.7 cc/gm (Schlumberger, 1972). Core derived density values from this study range from 2.1 to 2.6 gm/cc. The constant value of matrix density might also affect the porosity calculation from density log. The computation processes needs some correction due to shale effect on the log data because the studied reservoirs consist of more than 10% shale. If the effects of shale on the porosity measurement are not duly minimized, then the measurement might lead to deviation from the correct values.

There is no known tool that can measure permeability without any error. Core derived permeability is often calculated based on empirical rather than measured studies. Well logs can predict relative indications of permeability, which are usually termed "permeability index" and are qualitative rather than quantitative. The quality of the index hinges on the quality of the data (Brock, 1986). The hardest parameter to pin down is that of the irreducible water saturation (S_{wirr}). Log derived permeability formulas are only valid for estimating permeability in formation with irreducible water saturation (Schlumberger, 1977).

The product of water saturation (S_w) and porosity (ø) is known as bulk volume of water (BVW). If values for BVW across the reservoir interval are constant or very close to constant, then the hydrocarbon production from the reservoir should be water free. Hence, the saturated water in the uninvaded zone will not move due to capillary pressure existing between the sediment grains (Morris and Biggs, 1967). Nevertheless, it is always difficult to find a reservoir at irreducible water saturation state due to heterogeneities in the reservoir properties. The present study also suffers from this difficulty. In the shaly sand calculation, the shale parameters within the reservoir were translated from the neighboring shale zone, which may not be same in all cases.

In this study, petrography (thin section) based average porosity ranges from 17% to 23% having an average value of 19%. On the other hand, log derived average porosity is 7-36%, while the average is 21%. There is a slight increase of porosity values in case of log analysis. Among other core samples, only five selected sandstone samples of RP4 were chosen for petrographic (thin section) analysis. Here, comparatively shale free sandy samples are considered for measurement. Relatively clean sandstone provides high permeability and comparatively high porosity. Due to larger pore radius, core samples exhibit high permeability and porosity; and due to shale effects, log measurements exhibit significant increase in porosity and a decrease in permeability. Four gas zones from the well RP4 consist of 168 m thick gas sands. So huge data points, even from thinly laminated shaly horizons, are accompanied by comparatively less shaly sandy horizon increase the log porosity and decrease the log permeability. The heterogeneity of the studied reservoirs might responsible for down grading the log permeability values.

There are many examples from petroleum basins around the world showing that Petroleum reservoir rocks may range from 0.1 to 1000 or more millidarcies (mD). The quality of a reservoir as determined by permeability (in mD) may be judged as poor if K<1, fair if 1<K<10, moderate if 10<K<50, good if 50<K<250 and very good if K>250 (Tiab and Donaldson, 1996). The average permeability measured for the gas zones ranges from 28 to 306 mD. In this regard, permeability values of all reservoir intervals of the well Rashidpur 4 indicate good to very good quality reservoirs (Table 4.3.2.2). Porosity, hydrocarbon saturation and movability index values of the selected hydrocarbon zones of the studied well indicate good to very good reservoir conditions in the Bengal Basin. This interpretation is also supported by Imam (2005), Islam (2009, 2010) and Rahman and McCann (2012). The identified zone 4 (2668-2731 m) has the best potential as a hydrocarbon bearing zone in terms of its porosity and it is also supported by other parameters such as hydrocarbon saturation and permeability. The studied clays within the reservoir sandstone samples are mixed types (i.e., chlorite, illite and kaolinite) throughout the Surma Group, which is consistent with the interpretation made with the help of XRD and microscopic study (see section 4.3.1). This is also supported by Imam and Shaw (1987), Islam (2009, 2010) and Rahman and McCann (2012). However, the study assumes that the anomaly in log based measurements may be because of the inherent problems of different formulas, e.g., selection of saturation and permeability formulas and constraints related to values of different constants.

CHAPTER 5: CONCLUSIONS AND RECOMMENDATIONS

5.1 Shale

Based on geochemical and petrographical characteristics of the analyzed shale samples the following salient findings are drawn:

- Both Bhuban and Boka Bil shales of Bengal Basin possess poor to fair quality source potential for hydrocarbon generation. The organic matter, comprising a mixture of Type III/II kerogens, cross-plots of TOC versus S_2, PI versus T_{max} and hydrocarbon yield versus hydrocarbon in extract supports this hydrocarbon potential. The dominancy of aromatic compounds and n-alkane/alkene doublets in the PyGC pyrograms agree with each other regarding this poor to fair hydrocarbon potential of the studied shale samples.

- The examined Bhuban and Boka Bil shale samples were found to be thermally immature to early mature oil window for hydrocarbon generation based on the mean vitrinite reflectance and T_{max} values. The production index, TAI value and the biomarker values of 22S / (22S + 22R) hopane, moretane/hopane ratio and sterane parameters also support this level of thermal maturity.

- The biomarker parameters, such as very low to low Ts/Tm ratio, moderate Pr/Ph ratio, alternating dominance of odd over even and even over odd homologs in n-alkanes, high abundance of C_{29} regular steranes and medium to high C/S ratio, support the concept that the organic matter of the analyzed shales derived from land plants of terrestrial environmental settings with minor contribution from marine

sources. The depositional condition is considered here an alternation of oxic to anoxic. The marine influence is detected in the analyzed shale samples by the presence of liptodetrinite, resinite and other fluorescing amorphous materials under microscope.

- The present study affirms that the Bhuban and Boka Bil formations exhibit similar geochemical and petrological characteristic. The similar environmental setting and depositional condition are also noticed.

5.2 Coal

On the basis of macroscopic, microscopic and organic geochemical study of the Permian coals, the following salient features are stated:

- The coal seams are very thick with a maximum cumulative thickness of 71m. The nature of coal is dull to banded dull. The coal is low ash, low sulfur, high volatile bituminous B. It also has coking properties. Chemical composition (especially Cr, Cd, Pb, Co and Ni) directs the environmental hazards for coal combustion.

- Inertinite is the most dominant maceral group of the analyzed Gondwana coals of both the Barapukuria and Dighipara basins. Semifusinite, fusinite and inertodetrinite are the principal macerals of the inertinite group. Vitrinite is the second predominant group of the studied macerals. Collotelinite, collodetrinite and vitrodetrinite are the most commonly found vitrinite group maceral in these coals.

Sporinite, cutinite and resinite comprises the major constituents of the liptinitic macerals. Trimacerite (e.g., clarodurite and duroclarite) is identified as the dominant microlithotype of the investigated coal samples, followed by bimacerite and monomacerite with considerable carbominerites. Durite, vitrinertite and clarite are the most common bimaceral microlithotypes in the studied samples. Vitrite and semifusite are the most dominant monomaceral group.

- The analyzed different facies models suggest mostly the forest swamps with mixed palaeodepositional conditions. Alternating oxic to anoxic conditions under terrestrial environments with recurrent flooding were inferred for deposition. The studied Permian coals evolved in limno-telmatic zones under fluvio-lacustrine conditions with development of upper delta to lower delta plain conditions close to fresh water lake areas, as demonstrated by the composition of the microlithotypes in the models. The cross-plot of TPI versus GI suggests a terrestrial origin with increased tree density within the depositional system. GWI versus VI cross-plot implies the herbaceous plant-dominated ombotrophic to mesotrophic hydrogeological conditions. The pictorial presentation of maceral indices with depth also supports the fluctuating palaeodepositional environment.

- The organic geochemical and organic petrological approaches applied here are able to differentiate the organic facies in the analyzed coal, carbargillite and mudstone samples. The organic facies parameters including high C_{29}/C_{30}, Tm/Ts, CPI values, sterane/hopane and predominance of aromatic hydrocarbons over aliphatic

hydrocarbons are strongly associated with the source facies input. The coals are dominantly terrestrial with minor contribution from marine influenced sources.

The carbargillites are mixture of terrestrial marine influenced sources and mudstones being terrestrial with no marine derived organic input. This interpretation is also supported by the relative proportions of regular steranes, cross-plot of HI versus T_{max} and maceral analysis. Another cross-plot of Pr/nC_{17} versus Ph/nC_{18} indicates the suboxic depositional conditions for the organic matter related with the studied coal, carbargillite and mudstone samples. These are also supported by the high Tm/Ts ratios, very high Pr/Ph values and the predominance of inertinite macerals.

- Fair to excellent hydrocarbon generation potential is estimated for the analyzed samples. The carbargillites possess reasonably good potential for both oil and gas. It is followed by coals (mainly gas with minor oil) and mudstones (gas only). The considerable presence of liptinite macerals (cutinite, liptodetrinite, resinite, bituminite and sporinite) along with fluorescing vitrinite are believed to play important roles in hydrocarbon generation. All of the studied samples were found to be thermally mature. The common presence of exsudatinite, fluorinite, solid bitumen and micrinite suggests the analyzed coal, carbargillite and mudstone samples have already expelled hydrocarbons in the associated Gondwana Petroleum System.

5.3 Sandstone

- The principal framework grains identified in the analyzed siliciclastic Surma Group sandstones include quartz, feldspar and lithic grains. The studied sandstones are classified as sublithic arenite to subfeldspathic arenite.

- The observed most important diagenetic constituents include quartz cement (overgrowth), authigenic clays, carbonate cements and dissolution-replacement together with the compaction. The measured average thin section porosity is 18% though it is mostly of primary origin. The primary porosity is controlled chiefly by textural maturity as a function of grain size, sorting and fabric during burial. A range of diagenetic stages early to intermediate is estimated on the basis of several distinguishing properties such as compaction effects, alterations, cements and clay mineral authigenesis.

- The dissolution of unstable grains and cements increases the porosity (secondary). Thus, it enhances the permeability and reservoir quality. The precipitation of cements (quartz overgrowth, carbonate, clays) greatly influences the porosity reduction. SEM revealed that the pore-bridging authigenic constituents (illite-smectite) tend to plug the pore throats. This can reduce the permeability drastically, although it is very rare. The pores and its passage throats are distributed more or less consistently in the samples analyzed. The studied Surma Group sandstone is characterized as good to excellent petroleum reservoir.

- Among twenty permeable zones of the well RP4, four potential gas zones were identified with a gross cumulative thickness is 168 m. The study measured the log derived petrophysical parameters including shale volume, porosity, water saturation, hydrocarbon saturation, permeability, moveability index and bulk volume of water. These are (gross average) 20%, 21%, 27%, 73%, 105mD, 0.2 and 0.06, respectively. The log derived porosity slightly exceeds thin section porosity. The study reveals that all of the four gas zones possess good to very good quality reservoirs in the well Rashidpur 4 of the Bengal Basin, Bangladesh, a conclusion also supported by the interpretation based on petrography. Nonetheless, zone 4 is considered the best potential for hydrocarbon generation and production of the well Rashidpur 4.

5.4 Recommendations for future work

The present research covers some of the important essential petroleum system elements of Bengal Basin, Bangladesh. The following are recommended for future study.

- Detailed palynological analysis would add the important information on the palynofacies, biostratigraphy and depositional environments.
- Isotopic (O, H and C) study could supplement the present output on source and maturity of organic matter.
- A study on source-oil correlation and oil-oil correlation is strongly advised.
- Detail seismic study is recommended for better understanding of the basin as well as the petroleum reservoir.

- Samples from the deeper part of the basin could be required to envisage the source rock coverage with more accuracy. Accordingly, deeper (up to 6 km) drilling is advised.
- Cathodoluminescence study is required for getting information on fracture network, polycrystallinity of quartz, grain boundary nature, cements, microstructure, growth zoning, deformation features, fluid flow, alteration features and diagenetic events as well.
- Insitu measurements of core porosity and permeability of the reservoir sandstones.
- Usage of different geological software (e.g., PetroMod, BasinMod, IP, Techlog, Petrel, etc.) for basin modeling, reservoir characterization and petroleum system analysis for supplementing the current study.

APPENDICES

International Journal of Coal Geology 90–91 (2012) 162–179

Contents lists available at SciVerse ScienceDirect

International Journal of Coal Geology

journal homepage: www.elsevier.com/locate/ijcoalgeo

Depositional environment and hydrocarbon source potential of the Permian Gondwana coals from the Barapukuria Basin, Northwest Bangladesh

Appendix: A1
[IF=2.70; Q1]

Md. Farhaduzzaman [a,*], Wan Hasiah Abdullah [a,1], Md. Aminul Islam [b,2]

[a] Department of Geology, Faculty of Science, University of Malaya, 50603 Kuala Lumpur, Malaysia
[b] Department of Petroleum Geoscience, Faculty of Science, Universiti Brunei Darussalam, Gadong BE1410, Brunei

ARTICLE INFO

Article history:
Received 20 June 2011
Received in revised form 10 December 2011
Accepted 15 December 2011
Available online 29 December 2011

Keywords:
Gondwana coal
Depositional environment
Hydrocarbon potential
Biomarker
Thermal maturity
Kerogen type

ABSTRACT

Barapukuria Coal Basin is situated in Dinajpur district of the northwestern part of Bangladesh. A total of eight coal samples have been collected from two different locations of the basin and analyzed using organic geochemical and organic petrological methods.

The extracted organic matter of the studied samples is a mixture of Type-III and Type-II kerogen as evaluated by the source rock analyzer (SRA) and PyGC pyrograms. The measured total organic carbon (TOC) ranges from 61 to 74 wt. % and the recovered extractable organic matter (EOM) varies from 27,561 to 41,389 ppm. These results suggest that the coals are ranked as good quality source rock. The hydrocarbon yield has been calculated which is also high and it ranges from 12,192 to 20,799 ppm. The organic matter is thermally mature for hydrocarbon generation considering their T_{max} and measured mean vitrinite reflectance values of 431 to 435 °C and 0.72 to 0.81%Ro respectively. The hopane 22S/(22S + 22R), moretane/hopane ratio and sterane parameters are also in support of these thermal maturity assessment.

The maceral composition is dominated by the inertinite group with significant amounts of vitrinite and liptinite. The more dominant odd carbon numbered n-alkanes, high Pr/Ph ratio (4–8), high Tm/Ts ratio (13–18), predominant sterane C_{29} (i.e., $C_{29} > C_{28} > C_{27}$) and Pr/nC_{17} – Ph/nC_{18} values, GI vs TPI cross-plot and dominance of inertinite macerals group clearly demonstrate that the organic matter has been derived from terrestrial inputs and the condition of deposition was oxic (i.e., dry forest swamp) which was also supported by the absence of alginite. It is most likely that the coals were deposited within a peat-swamp flood basin environmental setting.

© 2011 Elsevier B.V. All rights reserved.

1. Introduction

The aim of the present study is to interpret the depositional environment of the Permian Gondwana coals of the Barapukuria basin on the basis of biomarker distributions together with other organic geochemical and organic petrological methods. So far no record of working detail on depositional environment considering the organic geochemical and organic petrological approach have been published on the Permian Gondwana coals of Bangladesh although there are few publications on Gondwana coals of Bangladesh. Bostick et al. (1991) discussed on petrography of the Barapukuria coal. Akhtar and Kosanke (2000) published on Palynology of Permian Gondwana coals of Barapukuria. Shamsuddin et al. (2001) discussed on the source rock potentiality of Gondwana coals of Bangladesh as a partial study on Petroleum Systems of Bangladesh. Islam and Kamruzaman (2006) studied on inorganic geochemistry and techno-environmental issues related to mining and uses of Barapukuria coal of Bangladesh. Islam and Hossain (2006) worked on the lithofacies and Embedded Markov Chain analysis of Gondwana sequence of Barapukuria coal basin, Bangladesh. Farhaduzzaman et al. (2008) published on properties (e.g., moisture, ash, volatile matter, fixed carbon, calorific value, sulfur, etc.) of Gondwana coals of Bangladesh. Islam and Hayashi (2008) published on geology and coal bed methane resource potential of the Gondwana Barapukuria coal basin, Dinajpur, Bangladesh. Frielingsdorf et al. (2008) presented a paper on tectonic subsidence modeling and hydrocarbon potential from a structural point of view based on the wells located in the Northwest Bangladesh considering thermal and maturity modeling. The depositional environment is the focus of the present study emphasizing the biomarker characteristics of the Permian coals of Barapukuria and this study will certainly add further important information to the understanding of the condition of depositional settings related to the coals of the Bengal basin.

* Corresponding author. Tel.: +60 149248160; fax: +60 379675149.
E-mail addresses: farhad.geo@siswa.um.edu.my, farhadgeo@gmail.com (M. Farhaduzzaman), wanhasia@um.edu.my (W.H. Abdullah), aminul_gm_ru@yahoo.com, aminul.islam@ubd.edu.bn (M.A. Islam).
[1] Tel.: +60 379674232; fax: +60 379675149.
[2] Tel.: +673 2463001x1371; fax: +673 2463051.

0166-5162/$ – see front matter © 2011 Elsevier B.V. All rights reserved.
doi:10.1016/j.coal.2011.12.006

Appendix: A2
[IF=1.01; Q2]

SOURCE ROCK POTENTIAL OF ORGANIC-RICH SHALES IN THE TERTIARY BHUBAN AND BOKA BIL FORMATIONS, BENGAL BASIN, BANGLADESH

Md. Farhaduzzaman[1*], Wan Hasiah Abdullah[1], Md. Aminul Islam[2] and M. J. Pearson[3]

Sandstones in the Miocene Bhuban and Lower Pliocene Boka Bil Formations contain all of the hydrocarbons so far discovered in the Bengal Basin, Bangladesh. Organic-rich shale intervals in these formations have source rock potential and are the focus of the present study which is based on an analysis of 36 core samples from wells in eight gasfields in the eastern Bengal Basin. Kerogen facies and thermal maturity of these shales were studied using standard organic geochemical and organic petrographic techniques.

Organic matter is dominated by Type III kerogen with lesser amounts of Type II. TOC is 0.16-0.90 wt % (Bhuban Formation) and 0.15-0.55 wt % (Boka Bil Formation) and extractable organic matter (EOM) is 132-2814 ppm and 235-1458 ppm, respectively. The hydrogen index is 20-181 mg HC/g TOC in the Bhuban shales and 35-282 mg HC/ g TOC in the Boka Bil shales. Vitrinite was the dominant maceral group observed followed by liptinite and inertinite. Gas chromatographic parameters including the C/S ratio, n-alkane CPI, Pr/Ph ratio, hopane Ts/Tm ratio and sterane distribution suggest that the organic matter in both formations is mainly derived from terrestrial sources deposited in conditions which alternated between oxic and sub-oxic. The geochemical and petrographic results suggest that the shales analysed can be ranked as poor to fair gas-prone source rocks. The maturity of the samples varies, and vitrinite reflectance ranges from 0.48 to 0.76 %VR_r. Geochemical parameters support a maturity range from just pre- oil window to mid- oil window.

INTRODUCTION

The Bengal Basin covers on- and offshore Bangladesh and extends into the Indian states of West Bengal to the west and Tripura to the east (Fig.1A). The basin is bordered to the west by the Precambrian Indian shield, to the north by the Shillong Massif and to the east by the frontal fold-belt of the Indo-Burmese Range. To the south it extends for some distance into the Bay of Bengal (Fig.1A). The deltas of three major river systems (Ganges, Brahmaputra (Jamuna) and Meghna) pass into the Bengal Fan whose frontal lobes extend about 3000 km south of the coast line (Curray and Moore, 1974).

[1] Department of Geology, Faculty of Science, University of Malaya, 50603 Kuala Lumpur, Malaysia.
[2] Department of Petroleum Geoscience, Faculty of Science, Universiti Brunei Darussalam, Gadong BE1410, Brunei.
[3]Department of Geology and Petroleum Geology, University of Aberdeen, King's College, Aberdeen, AB24 3UE.
*Corresponding author, email: farhadgeo@gmail.com, farhad.geo@siswa.um.edu.my

Key words: Bhuban Formation, Boka Bil Formation, Miocene, Pliocene, organic petrology, source rocks, thermal maturity, hopane, sterane, Bengal Basin, Bangladesh.

© 2012 The Authors. Journal of Petroleum Geology © 2012 Scientific Press Ltd

Journal of Asian Earth Sciences 64 (2013) 272–287

Appendix: A3
IF = 2.24; Q1

Contents lists available at SciVerse ScienceDirect

Journal of Asian Earth Sciences

journal homepage: www.elsevier.com/locate/jseaes

Petrographic characteristics and palaeoenvironment of the Permian coal resources of the Barapukuria and Dighipara Basins, Bangladesh

Md. Farhaduzzaman [a,*], Wan Hasiah Abdullah [a,1], Md. Aminul Islam [b,2]

[a] Department of Geology, Faculty of Science, University of Malaya, 50603 Kuala Lumpur, Malaysia
[b] Department of Petroleum Geoscience, Faculty of Science, Universiti Brunei Darussalam, Gadong BE1410, Brunei

ARTICLE INFO

Article history:
Received 24 March 2012
Received in revised form 13 December 2012
Accepted 15 December 2012
Available online 5 January 2013

Keywords:
Gondwana coal
Macerals
Microlithotypes
Facies model
Paleofacies evolution
Palaeoenvironment

ABSTRACT

Twenty-seven coal samples from the Barapukuria and Dighipara Coal Basins of Bangladesh were analysed for their maceral content, petrographic characteristics and vitrinite reflectance. The most predominant maceral was the inertinite group (mean 40%), followed by vitrinite (mean 31%) and liptinite (mean 22%), with considerable amounts of mineral matter (mean 7%). Semifusinite, fusinite and inertodetrinite were the most common macerals of the inertinite group. Collotelinite, collodetrinite and vitrodetrinite were the most frequently found macerals of the vitrinite group, while sporinite and cutinite were the most common in the liptinite group. Clay minerals occurred in higher concentrations than other minerals. The measured vitrinite reflectance values (%R_o) ranged from 0.71 to 0.80, indicating a high volatile bituminous B ranking.

Facies modelling using maceral composition and maceral indices suggested an environment of forest swamps with alternating oxic–anoxic depositional conditions. Microlithotype-dependent depositional modelling indicated evolution in limno-telmatic zones under fluvio-lacustrine control, accompanied by the development of upper to lower deltaic plain conditions. A terrestrial origin with dry forest to piedmont plain conditions was suggested by the Gelification Index (GI) and Tissue Preservation Index (TPI). The lateral variation of the measured TPI values indicated an increase in the rate of basin subsidence. A cross-plot of the Ground Water Index (GWI) vs. the Vegetation Index (VI) suggested mires under ombotrophic to mesotrophic hydrogeological conditions containing herbaceous plants.

© 2012 Elsevier Ltd. All rights reserved.

1. Introduction

The Gondwana succession of the Bengal Basin (Bangladesh) is very important because of its preserved coal deposits. To date, it has been estimated to contain 3 billion tons of coal resources (Farhaduzzaman et al., 2008). The coal deposits of these two basins occur at shallow depths (Imam, 2005). Petrography is an important method, commonly used to evaluate the facies and palaeoenvironmental interpretation, that is used worldwide by numerous researchers and for various geological ages (e.g., Amijaya et al., 2006; Daulay and Cook, 1988; Hower et al., 2008; Jasper et al., 2010; Kalkreuth et al., 1999; Querol et al., 2001; Singh and Singh, 2004; Toprak, 2009; Wan Hasiah, 2003; Wan Hasiah and Abolins, 1998).

No systematic work has as yet been carried out on the Permian Gondwana coals of Bangladesh. Published studies have covered: the petrography of the Barapukuria coal using the new analytical technique of reflectance scanning (Bostick et al., 1991); the palynomorphs of the Permian Gondwana coals of Barapukuria (Akhtar and Kosanke, 2000); the potential source rock of the Gondwana coals of Bangladesh (Shamsuddin et al., 2001); a study of the Barapukuria coal, focussing on the geochemistry and techno-environmental issues related to mining (Islam and Kamruzaman, 2006); an analysis of the lithofacies and cyclicity of the Gondwana succession of the Barapukuria Basin, Bangladesh (Islam and Hossain, 2006); the methane resource potential of the coal beds of the Gondwana Barapukuria Basin, Bangladesh (Islam and Hayashi, 2008); the proximate analysis and coal rank of the Gondwana coals of Bangladesh (Farhaduzzaman et al., 2008); and tectonic subsidence modelling based on the Gondwana coals from the Kuchma, Singra and Hazipur wells of Bangladesh (Frielingsdorf et al., 2008). The present paper evaluates the palaeofacies and palaeodepositional environment on the basis of the petrographic characteristics of the Permian coal deposits of Bangladesh.

* Corresponding author. Tel.: +60 149248160; fax: +60 379675149.
E-mail addresses: farhad.geo@siswa.um.edu.my, farhadgeo@gmail.com (Md. Farhaduzzaman), wanhasia@um.edu.my (W.H. Abdullah), aminul_gm_ru@yahoo.com, aminul.islam@ubd.edu.bn (Md.A. Islam).
[1] Tel.: +60 379674232; fax: +60 379675149.
[2] Tel.: +673 2463001x1371; fax: +673 2463051.

1367-9120/$ - see front matter © 2012 Elsevier Ltd. All rights reserved.
http://dx.doi.org/10.1016/j.jseaes.2012.12.017

www.jpg.co.uk

Journal of Petroleum Geology, Vol. 36(2), April 2013, pp 117 - 138

Appendix: A4
[IF=1.01; Q2]

ORGANIC FACIES VARIATIONS AND HYDROCARBON GENERATION POTENTIAL OF PERMIAN GONDWANA GROUP COALS AND ASSOCIATED SEDIMENTS, BARAPUKURIA AND DIGHIPARA BASINS, NW BANGLADESH

Md. Farhaduzzaman[1]*, Wan Hasiah Abdullah[1], Md. Aminul Islam[2] and M. J. Pearson[3]

In the Barapukuria and Dighipara coal basins, NW Bangladesh, the Basement Complex is overlain by the coal-bearing Permian Gondwana Group. In the present study, 36 core samples collected from five boreholes in these two basins were analysed using organic geochemical and organic petrological methods. Based on the results of biomarker analyses (TIC, m/z 191 and m/z 217 fragmentograms) and maceral composition (proportions of vitrinite, liptinite, inertinite), three organic facies were identified: coals, carbargillites and mudstones. Together with other evidence, cross-plots of HI versus T_{max} and Pr/nC_{17} versus Ph/nC_{18} indicate that the coals, as expected, were dominated by terrestrial organic matter (OM). The carbargillites contained a mixture of terrestrial and probable Type II aquatic OM, and the mudstones contained mostly terrestrial OM. Accordingly the coals, carbargillites and mudstones are interpreted to have been deposited in swamp-dominated environments in a delta-plain setting which was subject, in the case of carbargillites, to periodic flooding. Suboxic conditions were indicated by very high Pr/Ph ratios and a high content of inertinite macerals.

All the samples analysed were immature or early mature for hydrocarbon generation, as indicated by mean vitrinite reflectance (%R_o) of 0.60-0.81%, Rock-Eval T_{max} of 430-439°C, and biomarker ratios (hopane C_{32} 22S/(22S+22R)) of 0.57-0.60. Carbargillites showed potential for both liquid and gaseous hydrocarbon generation; coals were mainly gas-prone with minor liquid hydrocarbon potential; and mudstones were dominantly gas-prone. The oil-prone nature of the samples was attributed to the presence of resinite, cutinite, bituminite and fluorescent vitrinite. The presence of exsudatinite within crack networks, solid bitumen and oil droplets as well as bituminite at early oil-window maturities suggests that the organic matter may have expelled some hydrocarbons.

[1] Dept. of Geology, Faculty of Science, University of Malaya, 50603 Kuala Lumpur, Malaysia.
[2] Dept. of Petroleum Geoscience, Faculty of Science, Universiti Brunei Darussalam, Gadong BE1410, Brunei.
[3] Dept of Geology and Petroleum Geology, University of Aberdeen, King's College, Aberdeen, AB24 3UE.
* Corresponding author, email: farhad.geo@siswa.um.edu.my; farhadgeo@gmail.com

INTRODUCTION

In the Bengal Basin, Bangladesh (Fig. 1), all of the hydrocarbon discoveries so far made (gas = 28.42 TCF GIIP; oil = 137 million barrels STOIIP) are

Key words: Coal, carbargillite, mudstone, Barapukuria Basin, Dighipara Basin, source rocks, Bengal Basin, Bangladesh, Permian, Gondwana Group.

© 2013 The Authors. Journal of Petroleum Geology © 2013 Scientific Press Ltd

Appendix: A5 (accepted)
[IF=0.59; Q4]

Farhaduzzaman Farhad <farhadgeo@gmail.com>

JGSI: Your manuscript entitled HYDROCARBON SOURCE POTENTIAL AND DEPOSITIONAL ENVIRONMENT OF THE SURMA GROUP SHALES OF BENGAL BASIN, BANGLADESH

4 messages

B. Mahabaleswar <editorjournalgsi@gmail.com> Fri, May 18, 2012 at 3:09 PM
To: "Md. Farhaduzzaman" <farhadgeo@gmail.com>

Ref.: Ms. No. JGSI-D-12-00123R1
HYDROCARBON SOURCE POTENTIAL AND DEPOSITIONAL ENVIRONMENT OF THE SURMA GROUP SHALES OF BENGAL BASIN, BANGLADESH
Journal of the Geological Society of India

Dear Mr. Farhaduzzaman,

I am pleased to tell you that your work has now been accepted for publication in Journal of the Geological Society of India.

It was accepted on 18 May 2012.

Thank you for submitting your work to this journal.

With kind regards

B. Mahabaleswar
Editor-in-Chief *
Journal of the Geological Society of India

Reviewer #1: Page 10 - line 10- values for sulfur should be upto first decimal
Abstract- merge last two paragraphs, too many paragraphs in the abstract does not look good.

—

Farhaduzzaman <farhadgeo@gmail.com> Fri, May 18, 2012 at 4:04 PM
To: Aminul Islam <aminul.islam@ubd.edu.bn>

Dear Sir

Our paper has already been accepted in JGSI as you will see the message below.

Sincerely yours
Farhad
[Quoted text hidden]
--
Md. Farhaduzzaman
PhD Student (Petroleum Geology)
Department of Geology, Faculty of Science
University of Malaya, 50603 Kuala Lumpur, Malaysia.
E-mail: farhad.geo@siswa.um.edu.my

Geosciences Journal

Petrography and diagenesis of the Tertiary Surma Group reservoir sandstones, Bengal Basin, Bangladesh

--Manuscript Draft--

Manuscript Number:	GEOJ-D-13-00050
Full Title:	Petrography and diagenesis of the Tertiary Surma Group reservoir sandstones, Bengal Basin, Bangladesh
Article Type:	Article
Corresponding Author:	Md. Farhaduzzaman University of Malaya Kuala Lumpur, MALAYSIA
Corresponding Author Secondary Information:	
Corresponding Author's Institution:	University of Malaya
Corresponding Author's Secondary Institution:	
First Author:	Md. Farhaduzzaman
First Author Secondary Information:	
Order of Authors:	Md. Farhaduzzaman
	Md. Aminul Islam, PhD
	Wan Hasiah Abdullah, PhD
Order of Authors Secondary Information:	
Abstract:	The aim of the present research was to evaluate the petrographic characteristics of the Tertiary Surma Group sandstone reservoirs. The diagenetic constituents, processes and their impacts on reservoir quality were evaluated. A total of 33 core samples collected from 8 different wells located in 7 different gas/oil fields of Bangladesh were used for the current petrographic and diagenetic study. The standard petrographic microscope, scanning electron microscope (SEM/FESEM) and XRD were used in the current study. The framework grains, mineralogy, matrix, pore properties and cements were identified and counted properly. The framework grains were in accordance to dominance quartz (76-91%), rock fragments (5-16%) and feldspar (3-14%). The identified important diagenetic components were quartz cements, authigenic clays, carbonate cements and dissolution. The early to intermediate stage of diagenetic realm was estimated in the studied samples based on diagenetic events, e.g., mechanical compaction, chloritization, carbonate precipitation, dissolution, quartz overgrowth and authigenesis of clays. The reservoir quality was not much affected by the effects of diagenesis. However it was controlled mostly by the mechanical compaction including its grain size, sorting and fabric. In addition the authigenic cements (quartz, clays and carbonate) slightly modified its porosity and permeability status during diagenesis. The measured average thin section porosity and its permeability suggested good to excellent reservoir quality for hydrocarbon accumulation and production.
Suggested Reviewers:	Md. Sultanul Islam, PhD Professor, University of Rajshahi, Bangladesh sultal_ul_islam@yahoo.com A good expert.
	Badrul Imam, PhD Professor, University of Dhaka, Bangladesh badrulimam@yahoo.com Pioneer sedimentary geologist.
	M. P. Singh, PhD Professor, Banaras Hindu University mpsingh02@yahoo.co.in

Appendix: A6 (under review)
IF = 0.62; Q4

Powered by Editorial Manager® and Preprint Manager® from Aries Systems Corporation

Journal of the Geological Society of India

LOG BASED PETROPHYSICAL ANALYSIS OF MIO-PLIOCENE SANDSTONE RESERVOIR ENCOUNTERED IN WELL RASHIDPUR 4, BENGAL BASIN, BANGLADESH

--Manuscript Draft--

Manuscript Number:	JGSI-D-13-00142
Full Title:	LOG BASED PETROPHYSICAL ANALYSIS OF MIO-PLIOCENE SANDSTONE RESERVOIR ENCOUNTERED IN WELL RASHIDPUR 4, BENGAL BASIN, BANGLADESH
Article Type:	Research Article
Corresponding Author:	Md. Farhaduzzaman, PhD University of Malaya Kuala Lumpur, Selangor MALAYSIA
Corresponding Author Secondary Information:	
Corresponding Author's Institution:	University of Malaya
Corresponding Author's Secondary Institution:	
First Author:	Md. Aminul Islam, PhD
First Author Secondary Information:	
Order of Authors:	Md. Aminul Islam, PhD
	Md. Farhaduzzaman, PhD
	Wan Hasiah Abdullah, PhD
	Joyanta Dutta, MSc
Order of Authors Secondary Information:	
Abstract:	Rashidpur is located in the northeastern part of Bangladesh. It is surrounded three sides by India and one small part by Myanmar. Gamma-ray, spontaneous potential, density, neutron, resistivity, caliper, temperature and sonic logs are used to analyze petrophysical parameters of the well Rashidpur 4, Bangladesh. Quantitative measurements of different factors such as shale volume, porosity, permeability, water saturation, hydrocarbon saturation and bulk volume of water are carried out using well logs. Petrographic and XRD results based on several core samples are also compared with log-derived parameters. Twenty permeable zones are identified whereby four are hydrocarbon bearing in the studied Mio-Pliocene reservoir sandstones. Measured shale volume ranges from 11% to 38% and porosity is 19% - 28%. However, log-derived porosity is slightly higher than the thin section porosity. Water saturation of the interested zones varies from 14-38%, 13-39% and 16-41% measured from Schlumberger, Fertl and Simandoux formula respectively. Conversely, hydrocarbon saturation of the examined hydrocarbon zones ranges from 62-86%, 61-83% and 59-84% respectively. In the analyzed zones, the permeability values are calculated as 28-305 mD. Good to very good quality hydrocarbon reservoir is appraised for the studied four zones based on the petrophysical parameters, petrographic observation and XRD analysis. Nonetheless, Zone 4 is the best quality reservoir for hydrocarbon.
Suggested Reviewers:	Delwar Hossain, PhD Professor, Jahangirnagar University, Dhaka bdh2judgs@yahoo.com He is an experienced Petrophysicist based on Bengal Basin.
	M. P. Singh, PhD Professor, Banaras Hindu University, India mpsingh02@yahoo.co.in Prof. Singh is an excellent academician who have a vast research experience.

Appendix: A7 (under review)
IF = 0.59; Q4

Powered by Editorial Manager® and ProduXion Manager® from Aries Systems Corporation

Farhaduzzaman Farhad <farhadgeo@gmail.com>

Appendix: A8 (under review)
IF = 0.27; Q3

[Sains Malaysiana] Submission Acknowledgement

1 message

R. Abd-Shukor <jsm@ukm.my> Mon, Jun 10, 2013 at 3:28 PM
To: Mr Md Farhaduzzaman <farhadgeo@gmail.com>

Mr Md Farhaduzzaman:

Thank you for submitting the manuscript, "Petroleum Source Rock Properties of the Neogene Bhuban Shales, Bengal Basin, Bangladesh" to Sains Malaysiana. With the online journal management system that we are using, you will be able to track its progress through the editorial process by logging in to the journal web site:

Manuscript URL: http://ejournal.ukm.my/jsm/author/submission/3274
Username: farhad

If you have any questions, please contact me. Thank you for considering this journal as a venue for your work.

R. Abd-Shukor
Sains Malaysiana

Sains Malaysiana
http://202.185.40.102/ojs/index.php/jsm

Gmail by Google

Farhaduzzaman Farhad <farhadgeo@gmail.com>

Appendix: A9 (under review)
Scopus-cited

Acknowledgement (Malaysian Journal of Science)

1 message

Editorial Assistant, Malaysian Journal of Science <mjs_um2009@yahoo.com> Fri, Jun 21, 2013 at 4:59 PM
Reply-To: "Editorial Assistant, Malaysian Journal of Science" <mjs_um2009@yahoo.com>
To: Farhaduzzaman <farhadgeo@gmail.com>
Cc: "wanhasia@um.edu.my" <wanhasia@um.edu.my>, "DR.P.Agamuthu" <agamuthu@um.edu.my>

Dear **Dr Wan Hasiah,**
MALAYSIAN JOURNAL OF SCIENCE

This is to acknowledge receipt of your team's manuscript, entitled:

" ORGANIC GEOCHEMICAL AND PETROLOGICAL EVALUATION OF THE EARLY PLIOCENE BOKA BIL SHALES OF THE BENGAL BASIN, BANGLADESH "

The manuscript has been filed with the manuscript number **025/2013/B.**

Please use this reference numbers in all future correspondence with the Secretariat.

the decision of requesting the services of the experts provided is at the sole discretion of the Editor-in-Chief or Associate Editor.

Thank you for considering the *Malaysian Journal of Science*.

Yours Sincerely,

Professor Dr. P. Agamuthu
Editor – In – Chief
Malaysian Journal of Science
Faculty of Science
University of Malaya
50603 Kuala Lumpur

Appendix B1: Some definitions and measurement terms used in the literature.

Term	Description
TOC	Total Organic Carbon (wt.%).
S1	Free or thermally extractable HCs (mg HC/g Rock).
S2	HCs generated by pyrolytic degradation of kerogen (i.e., hydrolysable HCs) (mg HC/g Rock).
S3	CO2 generated from low temperature (upto 390 °C) pyrolysis (mg CO2/g Rock).
Tmax	Maximum temperature at top of S2 peak (°C) during Rock-Eval (RE) pyrolysis.
HCs	Hydrocarbons.
PP	Petroleum Potential (i.e. Genetic Potential): S1+S2 (mg HC/g Rock).
PI	Production Index (i.e. Transformation Ratio): {S1/ (S1 + S2)}.
HI	Hydrogen Index: (S2/TOC)*100 (mg HC/g TOC).
OI	Oxygen Index: (S3/TOC)*100 (mg CO2/g TOC).
EOM	Extractable Organic Matter (Bitumen).
Ro	Mesured random vitrinite reflectance (VRr) (%).
Tot extr	Total extract.
Alip /Arom	Aliphatic / Aromatic.
NSO	Polar compounds (e.g., N, S, O etc).
nC15, ...	Normal alkane with 15 carbon numbers, ...
C15, ...	Normal alkene with 15 carbon numbers, ...
Pr/Ph	Pristane / Phytane.
CPI 1	Carbon Preference Index (Peters and Moldowan, 1993): 2(C23+C25+C27+C29)/[C22+2(C24+C26+C28)+C30]
CPI 2	Carbon Preference Index (Peters and Moldowan, 1993): 1/2*[(C25+C27+C29+C31+C33)/ (C26+C28+C30+C32+C34) + (C25+C27+C29+C31+C33)/(C24+C26+C28+C30+C32)]
hop / mor	Hopane / Moretane
ster /diaste	Sterane / Diasterane
Type I kerogen	Highly oil-prone organc matter showing RE pyrolysis HI over 600 mg HC/g TOC when thermally immature; cotains algal and bacterial input dominated by amorphous liptinite macerals; typically in lacustrine settings (Tissot and Welte, 1984; Peters and Cassa, 1994).
Type II kerogen	Oil-prone organic matter showing RE pyrolysis HI in the range of 600-300 mg HC/g TOC when thermally immature; contains algal and bacterial organic matter dominated by liptinite macerals, such as exinite and sporinite; typically in marine settings (Tissot and Welte, 1984; Peters and Cassa, 1994).
Type III kerogen	Gas-prone organic matter showing RE pyrolysis HI in the range of 200-50 mg HC/g TOC when thermally immature; contains higher plant organic matter dominated by vitrinite macerals; typically in paralic marine settings (Tissot and Welte, 1984; Peters and Cassa, 1994).
Type IV kerogen	Inert organic matter showing RE pyrolysis HI below 50 mg HC/g TOC in immature rocks; contains contained organic matter which has been recycled or extensively oxidized during deposition (Tissot and Welte, 1984; Peters and Cassa, 1994).
Kerogen	Insolubale (in organic solvents) particulate organic matter comprised of various macerals. It originates from componenets of plants, animals and bacteria that are preserved in sedimentary rocks. Kerogen (precursor of petroleum) can be isolated from rock by extracting bitumen with solvents and removing the rock matrix with HCL and HF acids. Soluble portion is know as bitumen (Tissot and Welte, 1984).

Appendix B2: Peak assignments for alkane HCs in the gas chromatograms of the aliphatic fractions (i) in the m/z 191 mass fragmentogram and (ii) m/z 217 mass fragmentogram.

	Peak identity	Compound	Carbon no.
(i) Fragmentogram m/z 191	Ts	18α(H),22,29,30-trisnorneohopane	27
	Ts*	Rearranged Ts	27
	Tm	17α(H),22,29,30-trisnorhopane	27
	C28αβ	17α(H),29,30-bisnorhopane	28
	C29αβ	17α(H),21β(H)-norhopane	29
	C29Ts	18α(H),30-norneohopane	29
	C29βα	17β(H),21α(H)-hopane (moretane)	29
	C30αβ	17α(H),21β(H)-hopane	30
	C30βα	17β(H),21α(H)-hopane (moretane)	30
	C31αβ	17α(H),21β(H)-homohopane (22S & 22R)	31
	C31αβ 22S	17α(H),21β(H)-homohopane (22S)	31
	C31αβ 22R	17α(H),21β(H)-homohopane (22R)	31
	C32αβ	17α(H),21β(H)-homohopane (22S & 22R)	32
	C33αβ	17α(H),21β(H)-homohopane (22S & 22R)	33
	C34αβ	17α(H),21β(H)-homohopane (22S & 22R)	34
	C35αβ	17α(H),21β(H)-homohopane (22S & 22R)	35
(ii) Fragmentogram m/z 217	C27ααα 20S	5α(H),14α(H),17α(H)-cholestane (20S) (sterane)	27
	C27αββ 20R	5α(H), 14β(H),17β(H)-cholestane (20R) (sterane)	27
	C27αββ 20S	5α(H), 14β(H),17β(H)-cholestane (20S) (sterane)	27
	C27ααα 20R	5α(H),14α(H),17α(H)-cholestane (20R) (sterane)	27
	C28ααα 20S	24-methyl-5α(H),14α(H),17α(H)-cholestane (20S) (sterane)	28
	C28αββ 20R	24-methyl-5α(H),14β(H),17β(H)-cholestane (20R) (sterane)	28
	C28αββ 20S	24-methyl-5α(H),14β(H),17β(H)-cholestane (20S) (sterane)	28
	C28ααα 20R	24-methyl-5α(H),14α(H),17α(H)-cholestane (20R) (sterane)	28
	C29ααα 20S	24-ethyl-5α(H),14α(H),17α(H)-cholestane (20S) (sterane)	29
	C29αββ 20R	24-ethyl-5α(H),14β(H),17β(H)-cholestane (20R) (sterane)	29
	C29αββ 20S	24-ethyl-5α(H),14β(H),17β(H)-cholestane (20S) (sterane)	29
	C29ααα 20R	24-ethyl-5α(H),14α(H),17α(H)-cholestane (20R) (sterane)	29
	C29βα 20S	24-ethyl-13β(H),17α(H)-diacholestane (20S) (diasterane)	29
	C29αβ 20R	24-ethyl-13α(H),17β(H)-diacholestane (20R) (diasterane)	29

Appendix B3: Some important standard parameters used for petroleum source rock screening in the thesis.

Table 1. (a) Generative potential (quantity) of immature source rock; (b) Keorogen type and expelled products (quality); (c) Thermal maturity (Peters and Cassa, 1994; Peters et al., 2005).

(a) Potential (quantity)	TOC (wt.%)	Rock-Eval (mg HC/g rock) S1	S2	Bitumen (ppm)	Hydrocarbons (ppm)
Poor	< 0.5	< 0.5	< 2.5	< 500	< 300
Fair	0.5 - 1	0.5 - 1	2.5 - 5	500 - 1000	300 - 600
Good	1 - 2	1 - 2	5 - 10	1000 - 2000	600 - 1200
Very good	2 - 4	2 - 4	10 - 20	2000 - 4000	1200 - 2400
Excellent	> 4	> 4	> 20	> 4000	> 2400

(b) Kerogen (quality)	Hydrogen index (mg HC/g TOC)	S2 / S3	Atomic H/C	Main product at peak maturity
Type I	> 600	> 15	> 1.5	Oil
Type II	600 - 300	15 - 10	1.5 - 1.2	Oil
Type II / III	300 - 200	10 - 5	1.2 - 1	Oil / Gas
Type III	200 - 50	5 - 1	1 - 0.7	Gas
Type IV	< 50	< 1	< 0.7	None

(c)	Maturation			Generation		
Maturity	R_o (%)	T_{max} (°C)	TAI	Bitumen (mg/g rock)	Bitumen/TOC*	Production index {S1/(S1+S2)}
Immature	0.20 - 0.60	< 435	1.5 - 2.6	< 50	< 0.05	< 0.10
Mature early	0.60 - 0.65	435 - 445	2.6 - 2.7	50 - 100	0.05 - 0.10	0.10 - 0.15
Mature peak	0.65 - 0.90	445 - 450	2.7 - 2.9	150 - 250	0.15 - 0.25	0.25 - 0.40
Mature late	0.90 - 1.35	450 - 470	2.9 - 3.3	-	-	> 0.40
Post mature	> 1.35	> 470	> 3.3	-	-	-

* Many gas-prone coals have high bitumen yields like those of oil-prone samples, but extract yields normalized to TOC are low (less than 30 mg HC / g TOC). Bitumen / TOC ratios 0.25 indicate contamination, migrated oil, or artifacts caused by ratios of small, inaccurate numbers; Please see Appendix: B1 for symbol explanations.

Table 2. Approximate relationship between thermal alteration index (TAI), vitrinite reflectance (R_o %) and spore color (Jones and Edison, 1978; Peters et al., 2005).

TAI	1.5	2.3	2.5	2.8	3.0	3.5	3.6	3.7	3.8	3.9	4.0
Spore color	Pale yellow		Yellow orange	Orange brown	Reddish brown		Dark brown		Dark brownish-black		Black
R_o (%)	0.2	0.4	0.5	0.8	1.0	1.5	1.7	2.0	2.7	3.4	4.0

Appendix C1: TOC (wt.%) of both Boka Bil and Bhuban shales plotted with vertical depth profile (m) of the study area. It shows that the TOC increases with overall depth increasing irrespective of any particular wells.

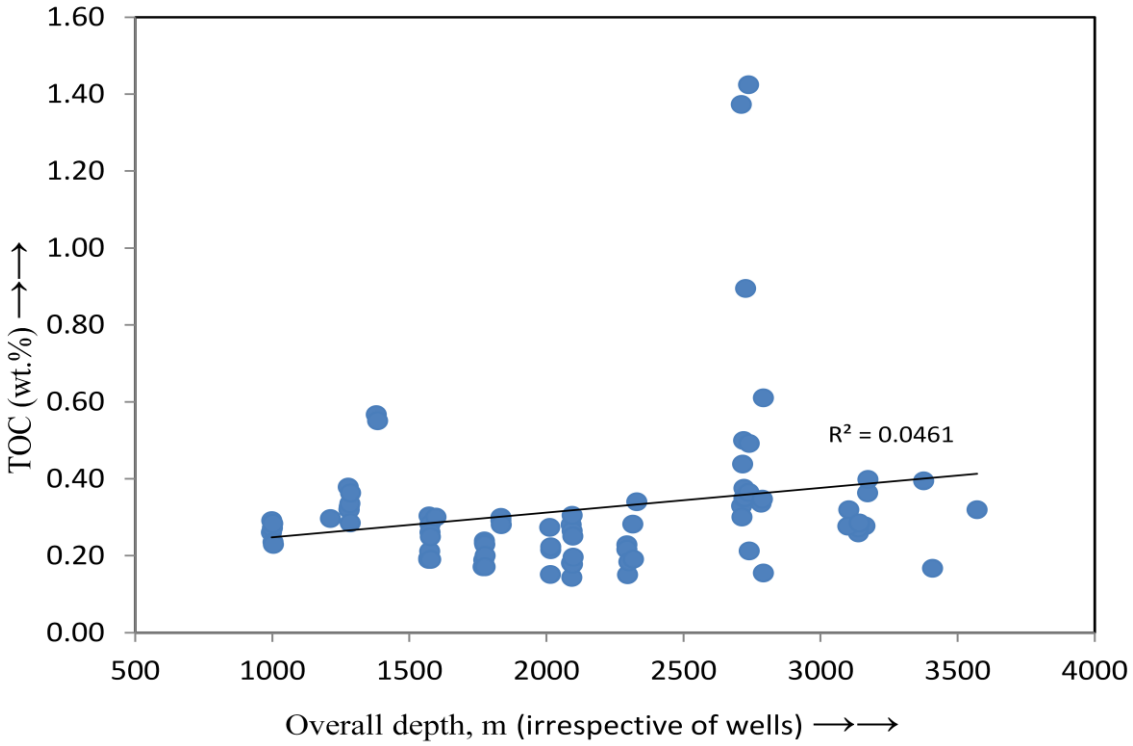

Appendix C2: Modified van Krevelen diagram (HI versus OI) shows that the analyzed both Bhuban and Boka Bil samples consist of a mixture of Type III and II kerogens (see Appendices B1 and B3 for definitions).

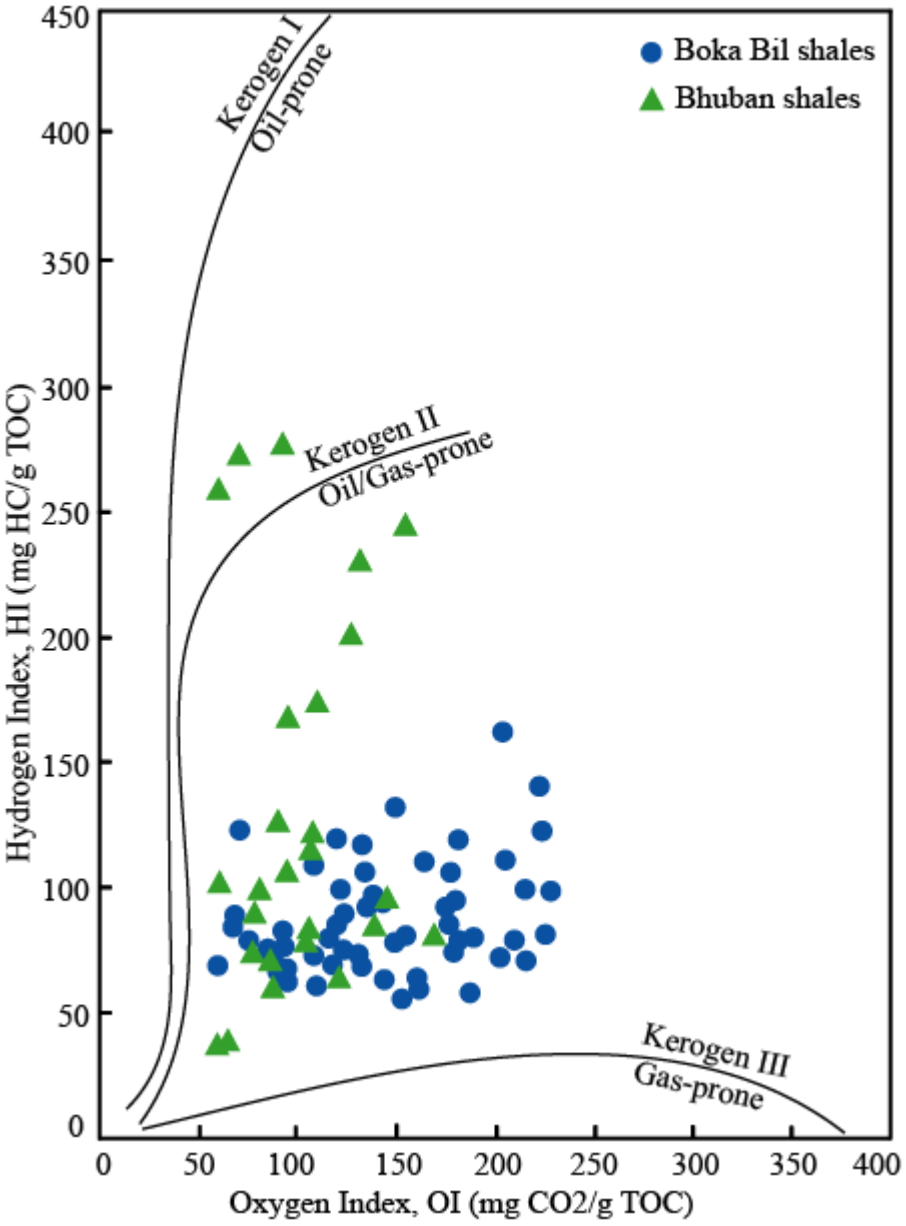

Appendix C3: PyGC pyrograms of Boka Bil and Bhuban shales (PT5SH14 and KM1SH4) display a mixed kerogen of Types III and II.

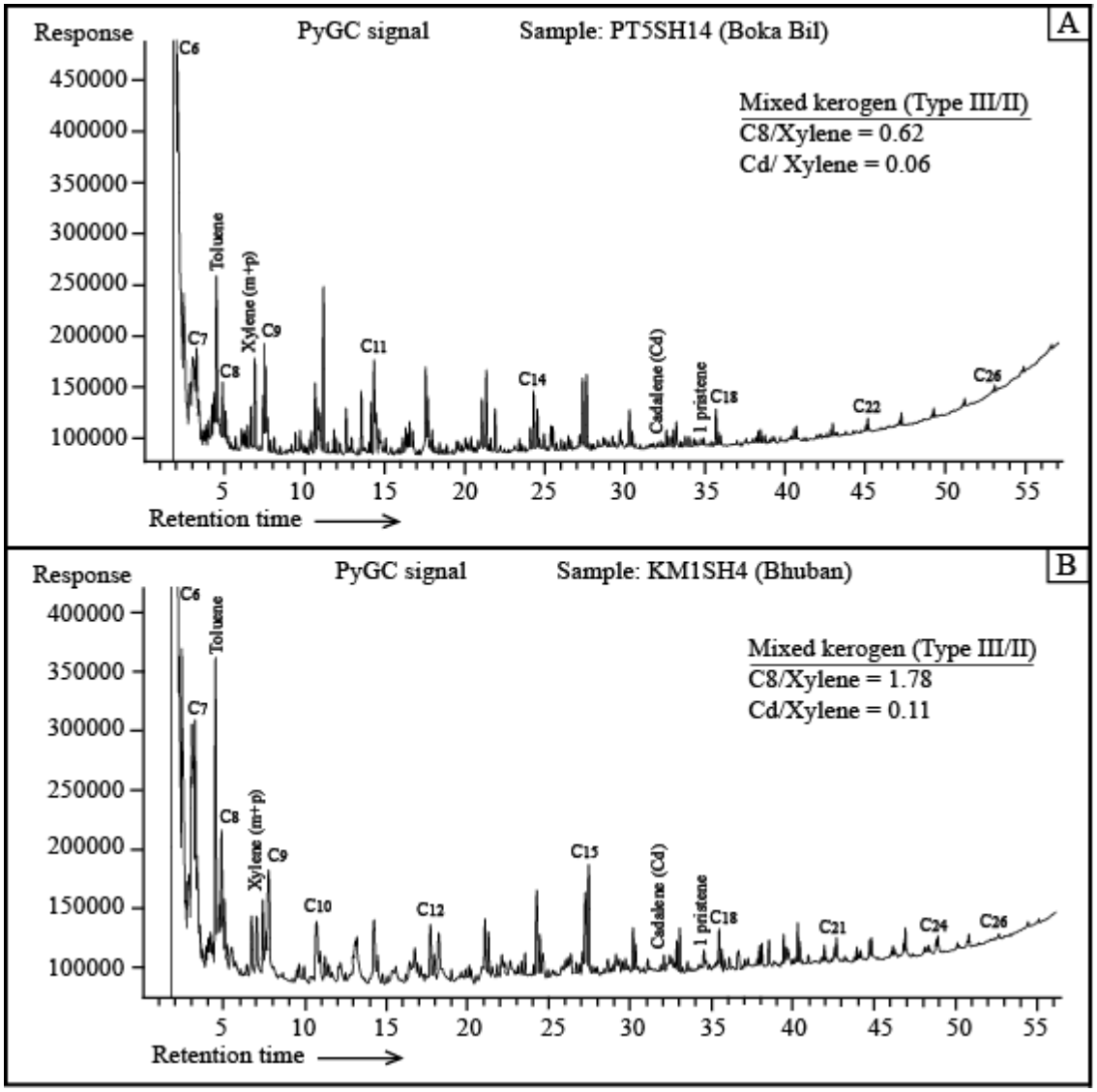

Appendix C4: Pictorial presentation of CPI values shows that the members of odd-numbered and even-numbered n-alkanes alternately predominate each other in both of the analyzed Bhuban and Boka Bil samples.

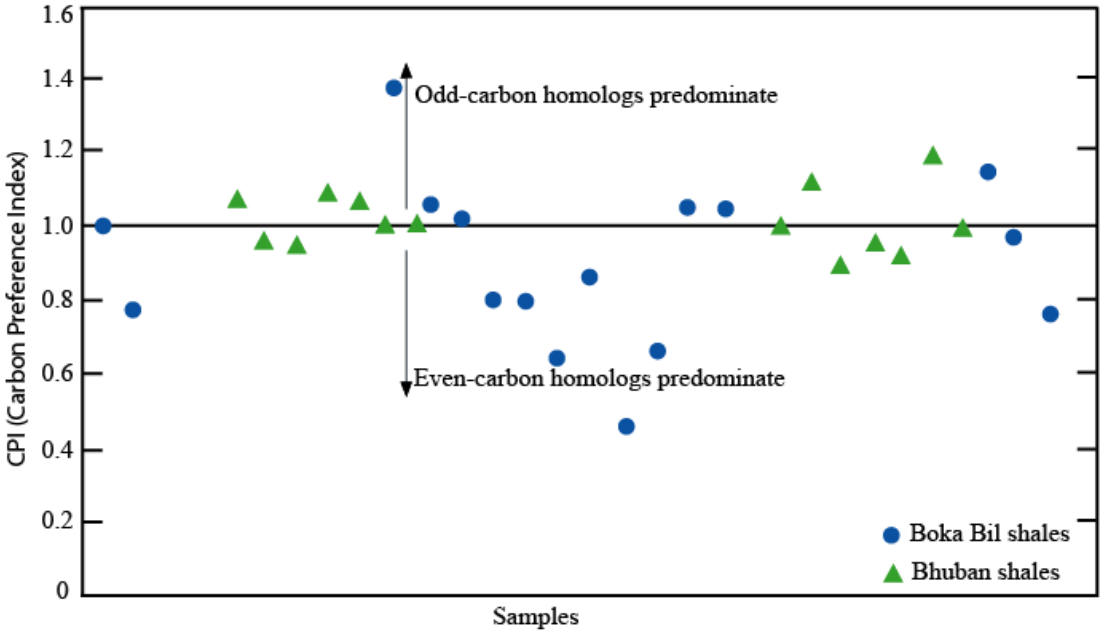

Appendix C5: Gas chromatogram (TIC) and mass fragmentograms m/z 191 and m/z 217 of aliphatic fraction of a studied Boka Bil sample (PT5SH10). It represents immature oil window (peak i.d. in Appendix B).

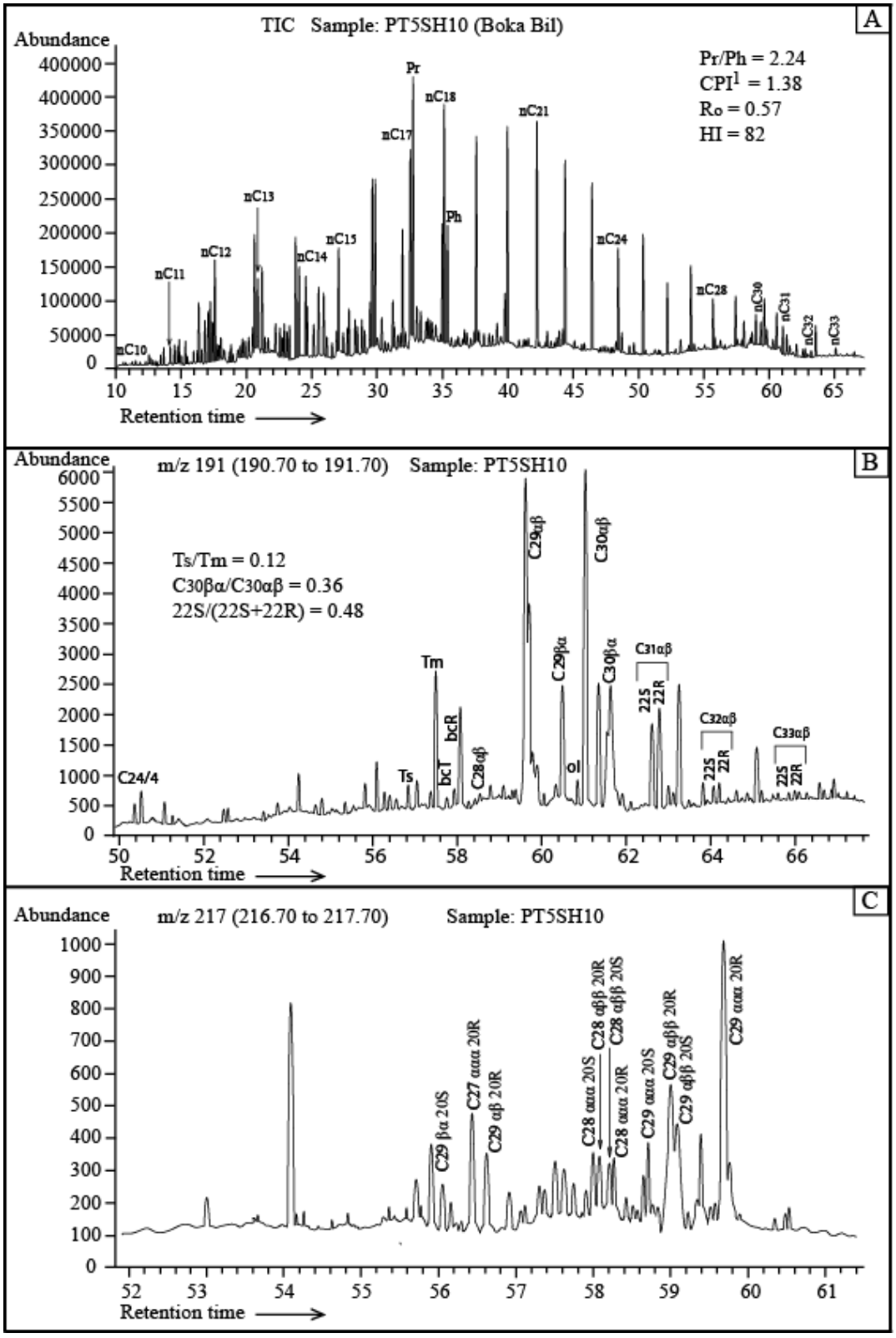

Appendix C6: Gas chromatogram (TIC) and mass fragmentograms m/z 191 and m/z 217 of aliphatic fraction of a studied Boka Bil sample (BK9SH71). It represents mature oil window (peak i.d. in Appendix B).

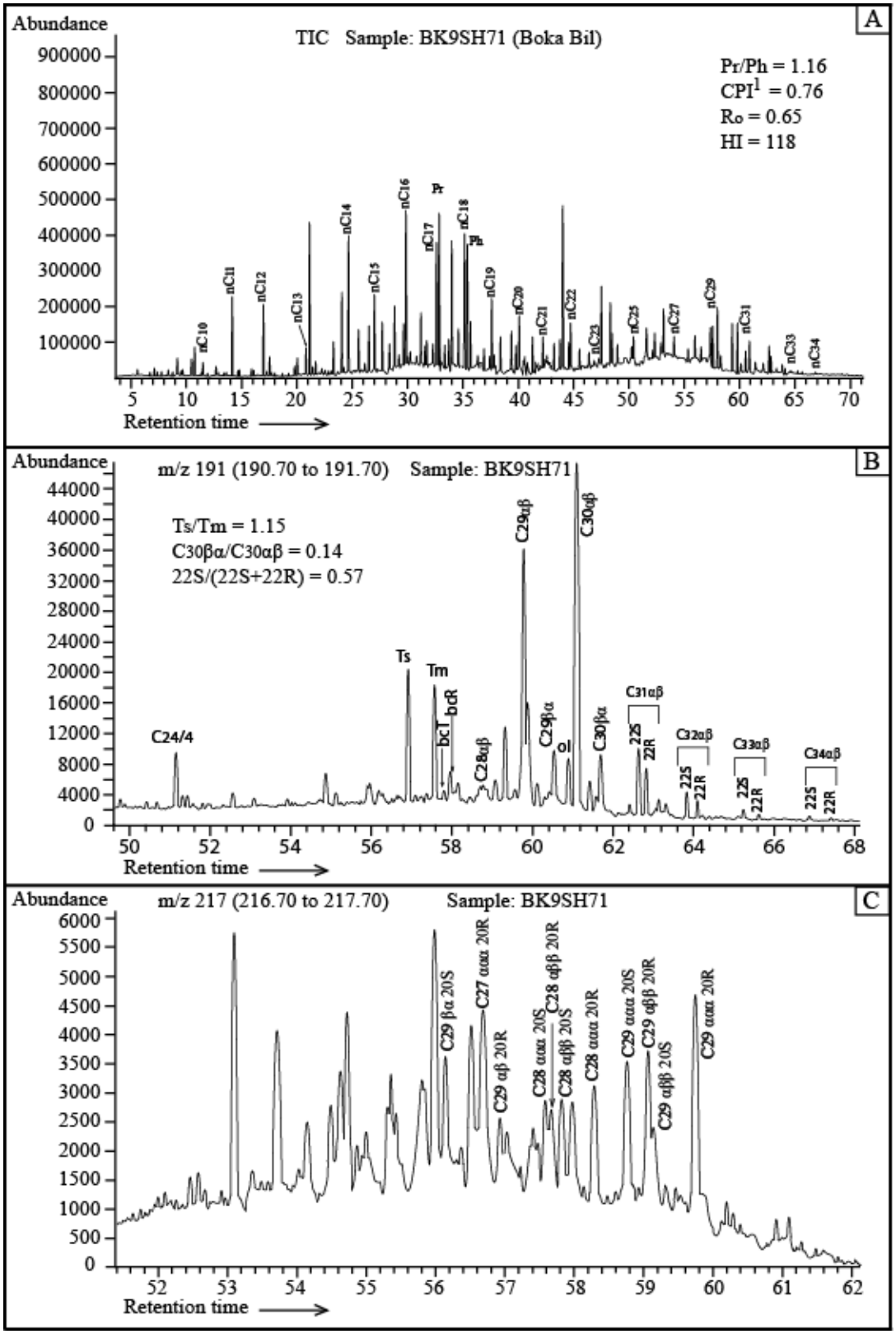

Appendix C7: Gas chromatogram (TIC) and mass fragmentograms m/z 191 and m/z 217 of aliphatic fraction of a studied Bhuban sample (FN2SH7). It represents immature oil window (peak i.d. in Appendix B).

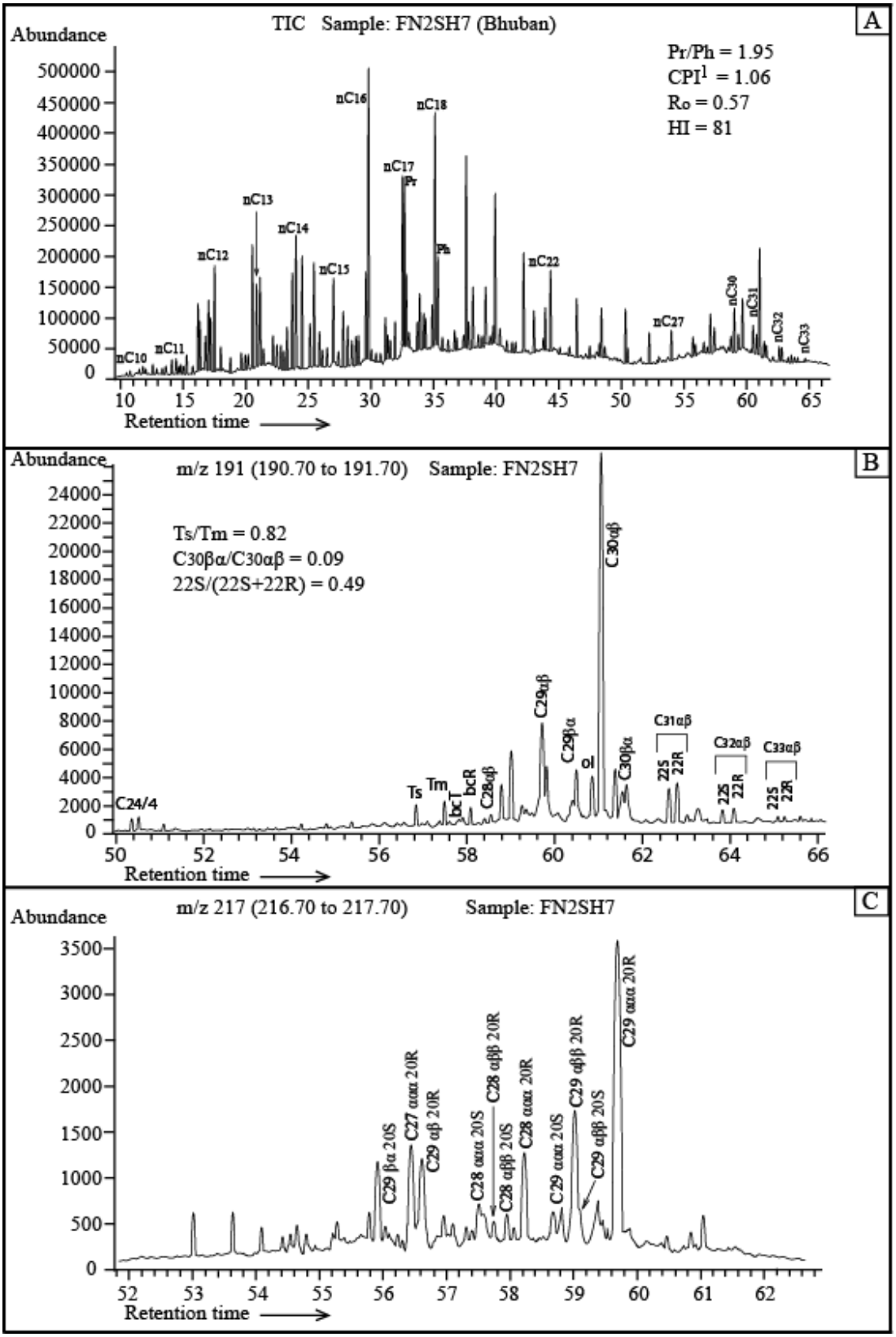

Appendix C8: Gas chromatogram (TIC) and mass fragmentograms m/z 191 and m/z 217 of aliphatic fraction of a studied Bhuban sample (BG1SH6). It represents mature oil window (peak i.d. in Appendix B).

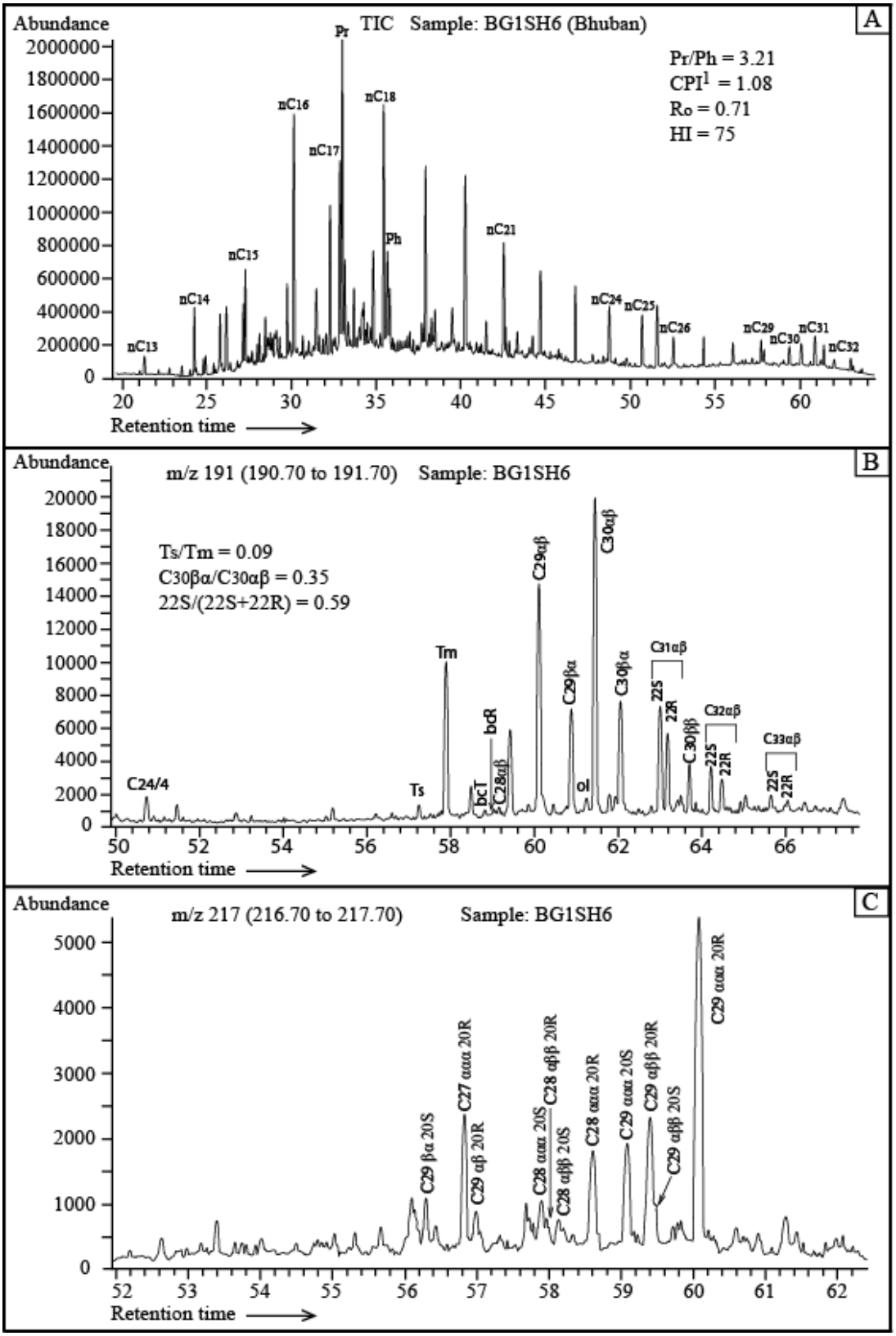

Appendix C9: Cross-plot of bc/C_{30}-hopane and ol/C_{30}-hopane (oleanane index) with respective depth (samples) shows that bc/C_{30}-hopane ratio decreases and ol/C_{30}-hopane ratio increases with depth. It indicates the relative maturity increase with depth.

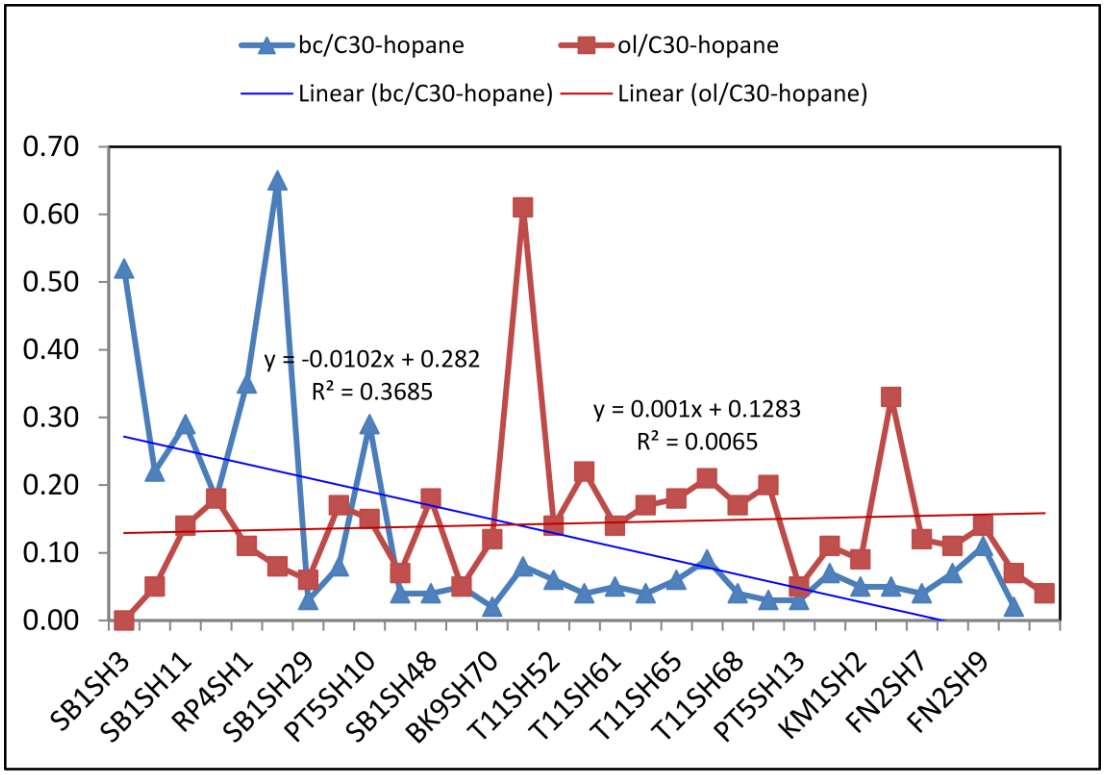

Depth → (1000-3600m)

Appendix C10: The identified similar organic geochemical and organic petrological properties of the analyzed Bhuban and Boka Bil Formations, Bengal Basin, Bangladesh.

Similar property	Bhuban	Boka Bil
S2 value (mg HC/ g Rock)	0.13-3.76	0.16-0.40
Tamx value (degree C)	420-441	420-440
HI value (mg HC/g TOC)	55-231	55-162
Production index	0.11-0.40	0.15-0.30
TOC content (% wt.)	0.14-1.42	0.14-0.57
Maturity	Immature-Early mature	Immature-Early mature
Source rock potential	poor-fair	poor-fair
Organic matter type	III/II	III/II
Elemental C/S ratio	4.2-128.6	2.4-53.3
Hydrocarbon in EOM (%)	27-61	22-62
Solubale hydrocarbon yield (mg HC/g TOC)	16-139	35-282
Pr/Ph ratio	0.99-3.41	0.58-3.65
Sterane C29 (%)	36-59	33-62
Vitrinite reflectance range	0.48-0.71	0.48-0.70
Abundance of vitrinite macerals (vol. %, mineral free basis)	62-80	64-83
TAI values	2.5-2.8	2.5-2.8

Appendix D1: Bar diagram displaying the concentrations of macerals and minerals (vol. %) of the studied Permian coals of Bangladesh.

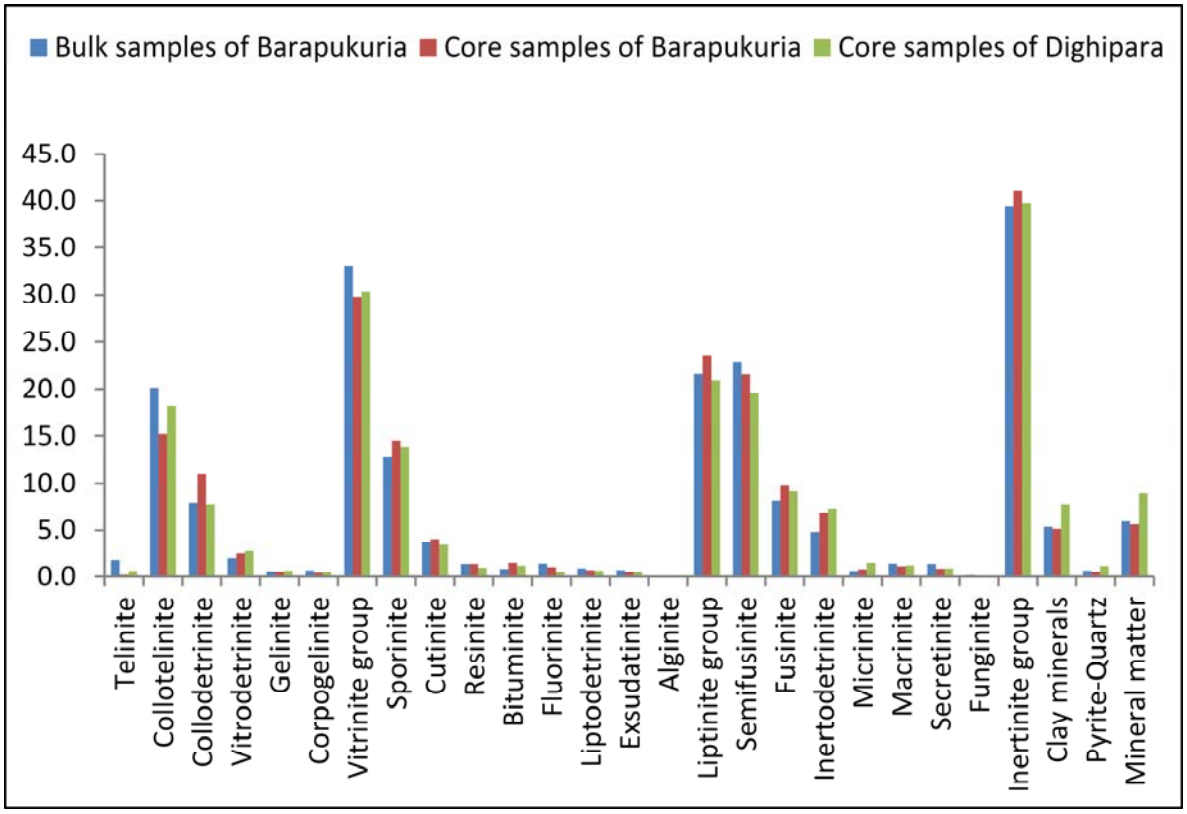

Appendix D2: Bar diagram displaying the concentrations of microlithotypes (maceral associations) and carbominerites (vol. %) of the studied Permian coals of Bangladesh.

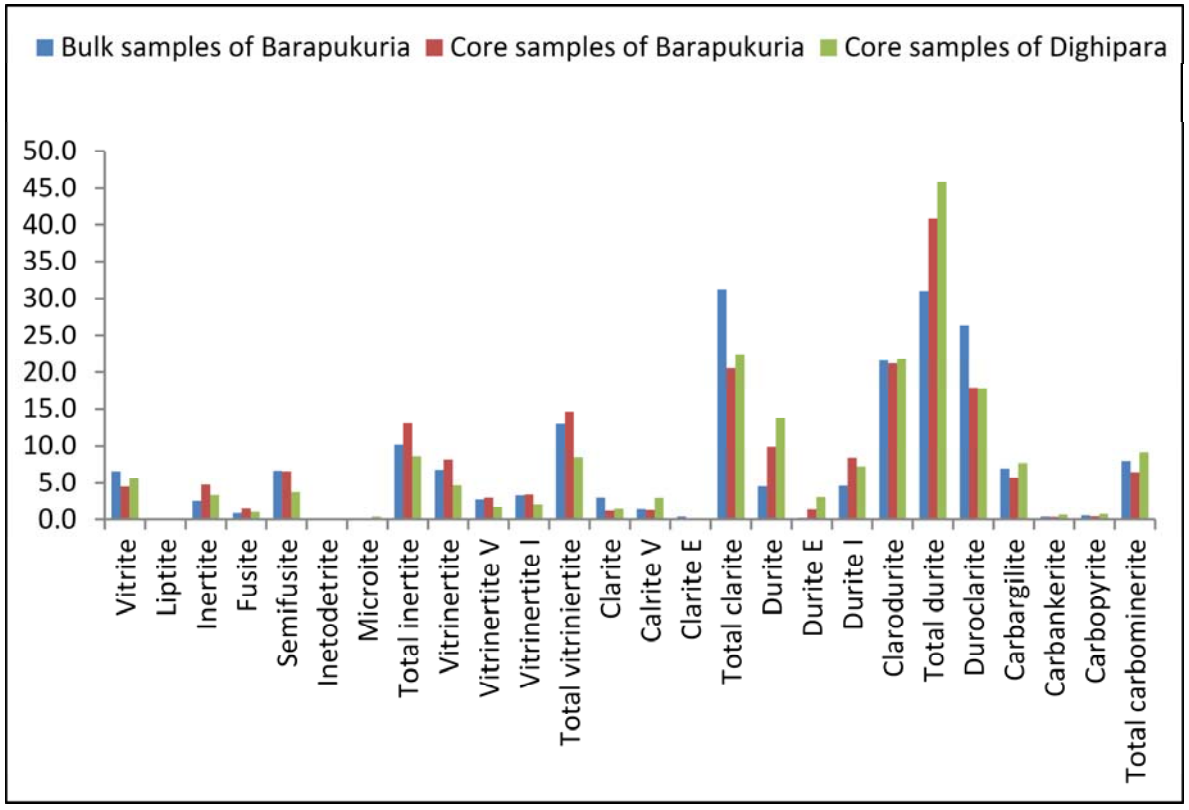

Appendix E1: Comparison between SRA and RE results of the analyzed coal, carbargillite and mudstone samples (refer to Appendix B1).

Sample no.	TOC		Tmax		S1		S2		S3		HI		OI	
	SRA	RE	SRA	RE	SRA	RE	SRA	RE	SRA	RE	SRA	RE	SRA	RE
BPCL9	73.87	72.68	430.2	430	4.92	3.77	187.64	153.63	6.21	8.56	254	211	8	12
BPCR11	24.87	25.20	431.3	431	1.78	0.14	76.44	72.95	0.58	1.63	307	289	2	6
BPCL15	64.24	64.32	430.1	434	3.41	2.34	92.03	90.42	3.86	4.55	143	141	6	7
BPCL18	69.05	67.83	433.9	434	4.05	3.84	145.28	137.08	6.24	8.66	210	202	9	13
BPMT21	5.06	5.12	438.1	441	0.08	0.03	3.84	2.81	0.88	0.59	76	55	17	12
BPMT22	6.16	5.94	439.2	440	0.09	0.03	4.03	3.20	0.79	0.91	65	54	13	15
BPCL25	63.12	63.70	435.4	436	2.32	2.06	71.11	76.67	7.89	7.94	113	120	13	12
BPCR26	38.81	39.13	429.6	431	1.88	1.15	106.56	95.52	4.64	5.32	275	244	12	14
BPCL28	59.53	58.95	430.7	432	4.06	3.80	127.86	126.30	5.05	7.71	215	214	8	13
BPCR29	25.22	25.74	431.6	432	1.05	0.11	65.26	61.14	2.80	3.70	259	238	11	14
DPCL31	70.29	69.78	434.2	433	5.95	4.99	138.06	114.96	3.82	5.06	196	165	5	7
DPCL38	44.04	44.61	436.3	434	0.69	0.58	108.94	123.02	1.84	2.13	247	276	4	5
DPCL40	54.88	53.75	435.8	435	2.01	0.45	150.73	90.13	3.68	4.49	275	168	7	8
DPCR42	38.14	38.41	434.4	434	1.84	0.11	99.20	94.54	1.56	1.16	260	246	4	3
DPCL44	63.07	63.58	436.7	436	0.88	0.97	115.92	120.02	6.03	2.18	184	189	10	3

Appendix E2: Gas chromatogram (TIC) and mass fragmentograms m/z 191 and m/z 217 of aliphatic fraction of a studied coal sample (DPCL35) of Dighipara Coal Basin (peak i.d. in Appendix B2).

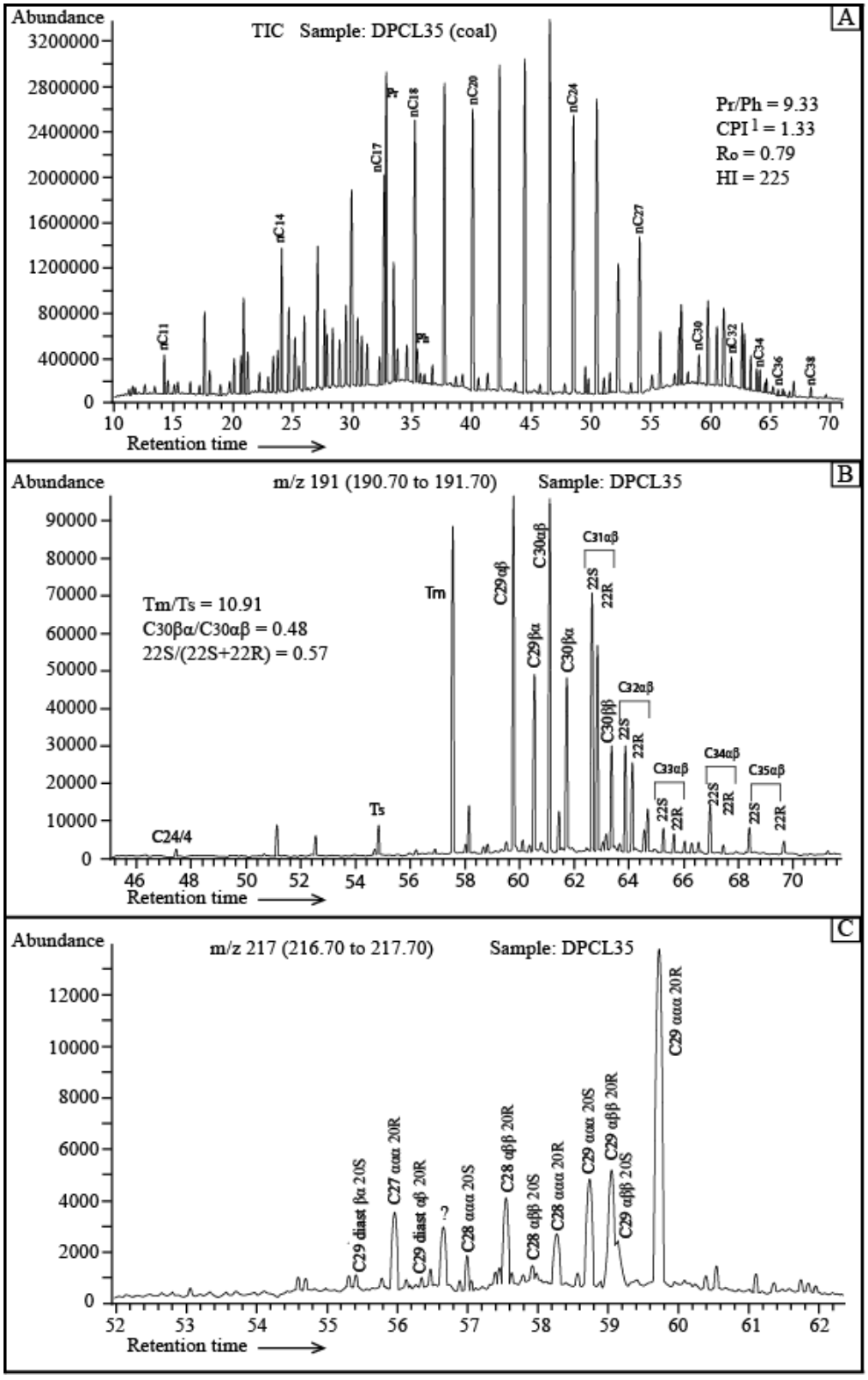

Appendix E3: Gas chromatogram (TIC) and mass fragmentograms m/z 191 and m/z 217 of aliphatic fraction of a studied carbargillite sample (BPCR11) of Barapukuria Coal Basin (peak i.d. in Appendix B2).

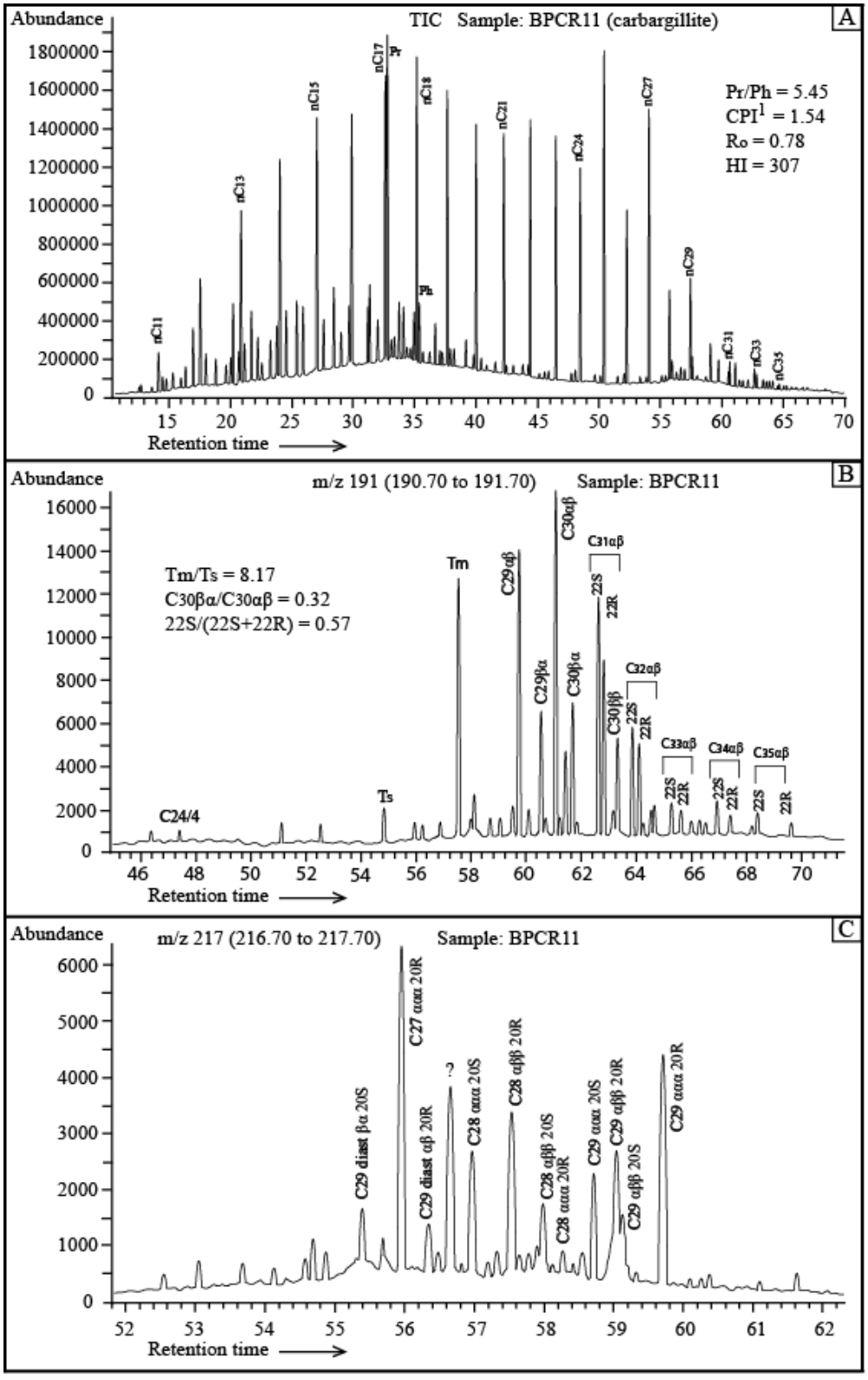

Appendix E4: Pictorial presentation of CPI values whereby all of the analyzed coal, carbargillite and mudstone samples show the dominance of odd carbon numbered n-alkanes. It indicates the terrestrial dominated organic facies in the depositional system.

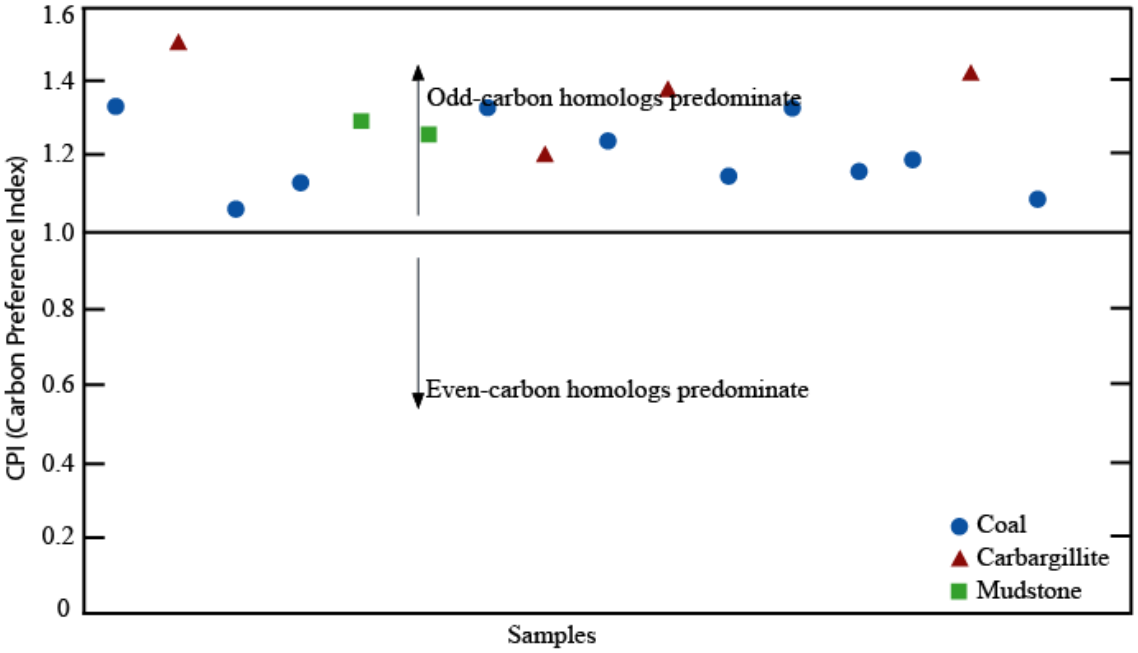

Appendix F1: A sample report of a reference management software EndNote X5 that has been used for the thesis.

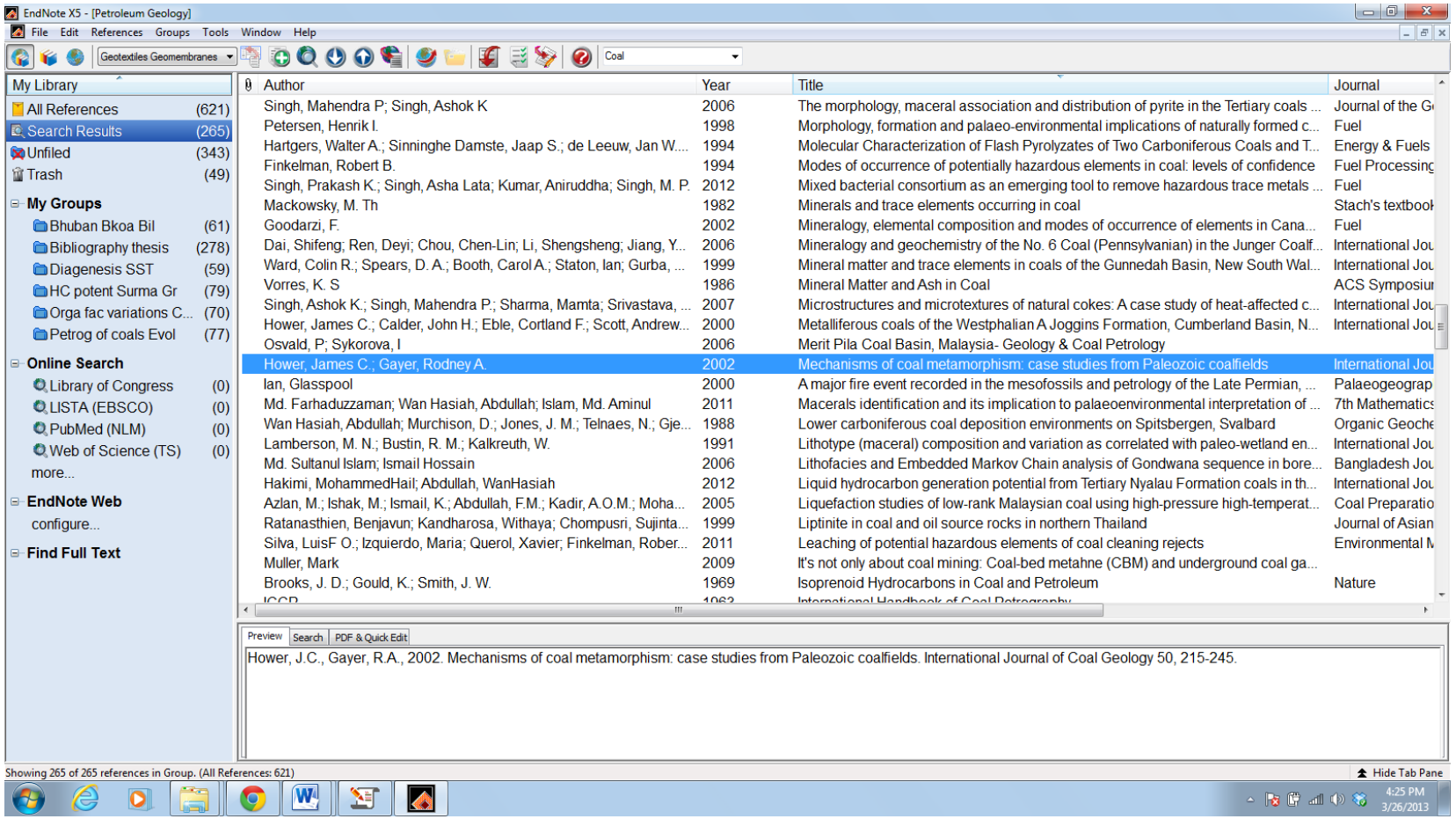

Appendix F2: A standard report of StyleWriter 4 software for checking English Language. It shows the status of English used in the thesis is “Excellent”.

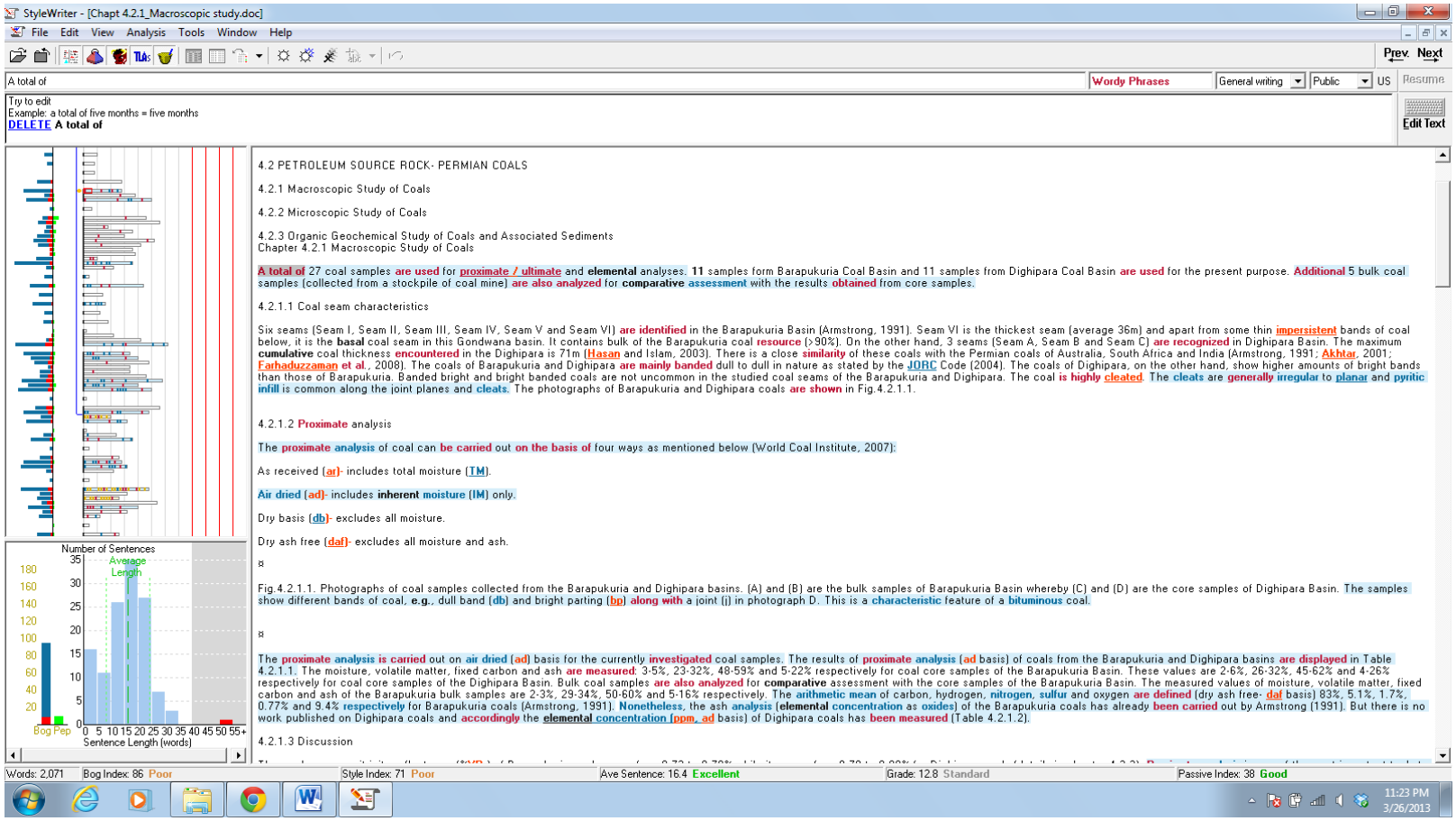

Appendix F3: A sample report for checking the originality using Turnitin software. It reports 19% similarity index with the thesis whereas more than 5% comes from the publication of author himself based on present research.

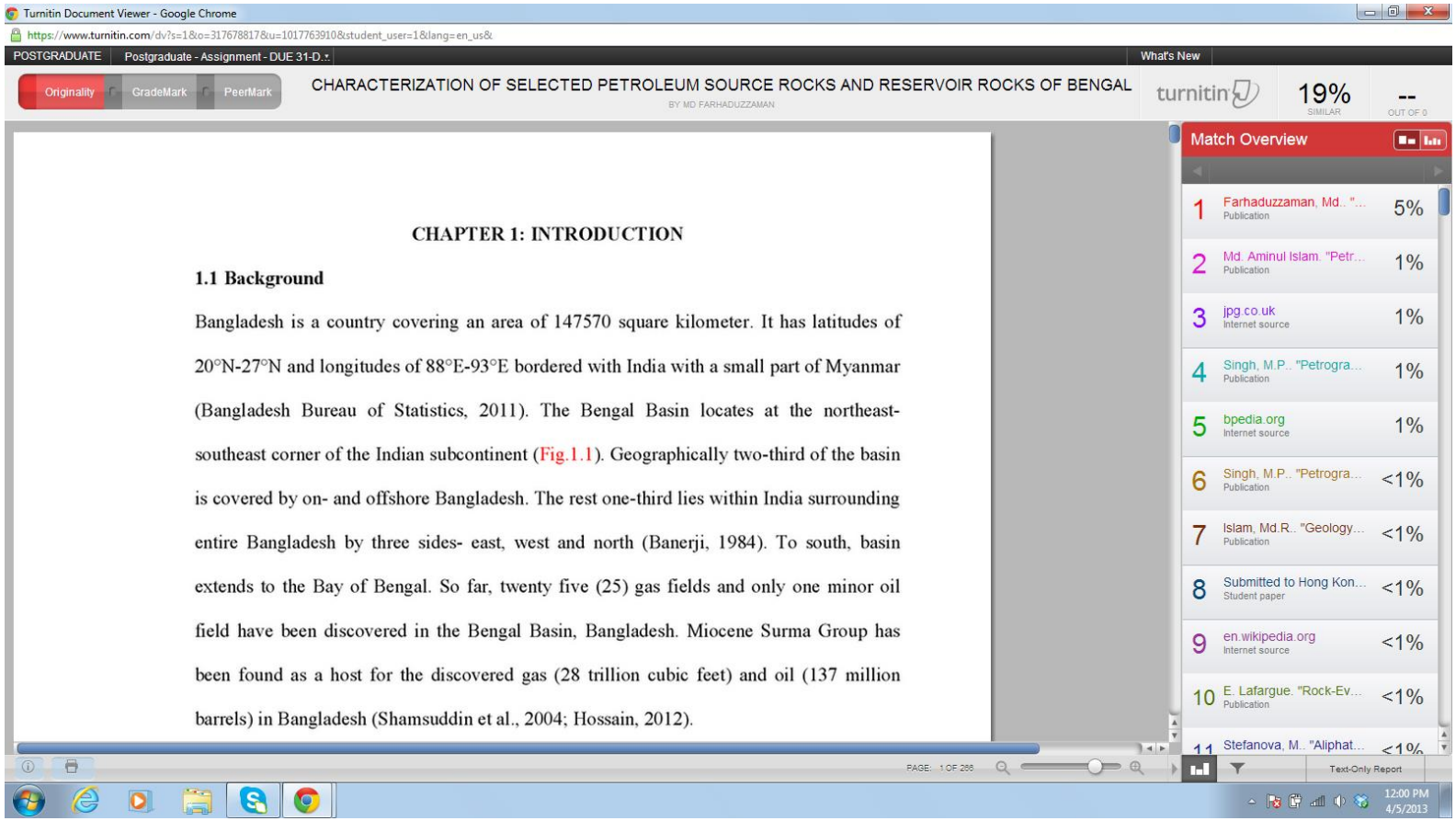

Appendix G: Contributors of the thesis.

 Author: Md. Farhaduzzaman	I received BSc (Honors) and MSc in Geology in the year 2001 and 2002 respectively from Jahangirnagar University, Dhaka, Bangladesh. I have 5 years working experience with Asia Energy Corporation Pty Ltd (UK base company) as an Assistant Geologist (Exploration) from August 2004 to June 2009. After leaving Asia Energy, I have been working with Sylhet Gas Fields Limited, a company of Petrobangla as an Assistant Manager (Development Geology) since July 2009. I've prepared this thesis partly based on the petroleum systems of Bengal Basin, Bangladesh as part of my PhD research at the Department of Geology, UM. Some of my research papers have already been published in different national and international high impact journals. I am a member of AAPG, SEG, GSM, BGS and SEAPEX.
 Supervisor: Prof. Wan Hasiah Binti Abdullah	Prof. Wan received her BSc (Honors) in Geology from University of Malaya, Malaysia. She accomplished her MSc and PhD in Petroleum Systems of North Sea from the New Castle Upon Tyne University, UK. After PhD, she joined as a faculty member at Geology Department, UM in 1989 and now continuing here as a Professor of Petroleum Geoscience and Coal. She has already published around one hundreds research articles in national and international high impact journals. More than 10 PhD students already graduated under her supervision and 15 more PhD students are continuing their researches. The areas of her expertise include Petroleum Geology (Petroleum Systems), Petroleum Geochemistry and Coal Petrology. She is a member of AAPG, TSOP, ICCP, GSM, IGM, SEAPEX and SPE. Currently she is the coordinator of the MSc Petroleum Geology Program at UM.
 Co-supervisor: Dr. Md. Aminul Islam	After BSc (Honors) and MSc in Geology and Mining from Rajshahi University, Bangladesh, Dr. Aminul joined as a Geologist in Petrobangla, the state-owned oil/gas organization. He joined as a faculty member in Geology and Mining Department, RU in 2001 after 8 years' service with Petrobangla. Based on Petroleum Geoscience and Geophysics, he did his MSc from NUST, Norway and PhD from Tsukuba University, Japan. He was a faculty member of Geology Department, UM and after that he joined in the Petroleum Geoscience Department, UBD, Brunei in 2011. He has already published around sixty research articles in national and international high impact journals. The areas of his expertise include Petroleum Geology and Geophysics. He is a member of AAPG, GSM, BGS, SEAPEX and SPE.

BIBLIOGRAPHY

Aarssen, B.G.K., Hessels, J.K.C., Abbink, O.A., de Leeuw, J.W., 1992. The occurrence of polycyclic sesqui-, tri-, and oligoterpenoids derived from a resinous polymeric cadinene in crude oils from southeast Asia. Geochimica et Cosmochimica Acta 56, 1231-1246.

AAPG, 2011. One day course review: hydrocarbon prospect in Western Indonesia. Gadjah Mada University, Indonesia, AAPG Student Chapter, p.37.

Abeed, Q., Alkhafaji, A., Littke, R., 2011. Source rock potential of the Upper Jurassic-Lower Cretaceous succession in the Southern Mesopotamian Basin, Southern Iraq. Journal of Petroleum Geology 34, 117-134.

Adams, A.E., MacKenzie, W.S., Guilford, C., 1988. Atlas of sedimentary rocks under the microscope, 1st ELBS ed. English Language Book Society, Longman, UK.

Adams, R.S., Bustin, R.M., 2001. The effects of surface area, grain size and mineralogy on organic matter sedimentation and preservation across the modern Squamish Delta, British Columbia: the potential role of sediment surface area in the formation of petroleum source rocks. International Journal of Coal Geology 46, 93-112.

Ahmed, M., Volk, H., George, S.C., Faiz, M., Stalker, L., 2009. Generation and expulsion of oils from Permian coals of the Sydney Basin, Australia. Organic Geochemistry 40, 810-831.

Ahmed, S.T., 1968. Cenozoic Fauna of the Cox's Bazar Coastal Cliff, Department of Geology. University of Dhaka, Unpublished, p. 68.

Akhtar, A., 2001. Gondwana Sediment of Bangladesh and its correlation with those of other regions of the world on the basis of spore-pollen. Gondwana Research 4, 135-136.

Akhtar, A., Kosanke, R.M., 2000. Palynomorphs of Permian Gondwana coal from borehole GDH-38, Barapukuria Coal Basin, Bangladesh. Journal of African Earth Sciences 31, 107-117.

Alam, K.M., 2010. A note on the coal resources in Bangladesh, their prospects and problems in development and uses. http://www.scribd.com, Document no. 99686014, Dhaka, p. 18.

Alam, M., Alam, M.M., Curray, J.R., Chowdhury, M.L.R., Gani, M.R., 2003. An overview of the sedimentary geology of the Bengal Basin in relation to the regional tectonic framework and basin-fill history. Sedimentary Geology 155, 179-208.

Alam, M., Pearson, M.J., 1990. Bicadinanes in oils from the Surma Basin, Bangladesh. Organic Geochemistry 15, 461-464.

Archie, C.E., 1942. The electrical resistivity log as an aid in determining some reservoir characteristics. Journal of Petroleum Technology 69, 54-62.

Asquith, G.B., Gibson. C. R., 1982. Basic well log analysis for geologist. The AAPG, Methods in Exploration Series, p.216.

Al-Gailani, M.B., Ala, M.A., 1984. Effects of epidiagenesis on reservoir characteristics of rocks beneath concealed unconformities in England and the Western Desert, Iraq. Journal of Petroleum Geology 7, 189-212.

Al-Juboury, A.I., Al-Ghrear, J.S., Al-Rubaii, M.A., 2010. Petrography and diagenetic characteristics of the Upper Oligocene-Lower Miocene Ghar Formation in SE Iraq. Journal of Petroleum Geology 33, 67-85.

Al-Ramadan, K.A., Hussain, M., Imam, B., Saner, S., 2004. Lithologic characteristics and diagenesis of the Devonian Jauf sandstone at Ghawar Field, Eastern Saudi Arabia. Marine and Petroleum Geology 21, 1221-1234.

Amijaya, H., Schwarzbauer, J., Littke, R., 2006. Organic geochemistry of the Lower Suban coal seam, South Sumatra Basin, Indonesia: Palaeoecological and thermal metamorphism implications. Organic Geochemistry 37, 261-279.

Armstrong, W., 1991. Barapukuria Coal Deposits, Stage 2, Feasibility Study, Geological Survey Bangladesh- UK Coal Project (unpublished). Petrobangla, Dhaka.

Banerjee, S., Dutta, S., Paikaray, S., Mann, U., 2006. Stratigraphy, sedimentology and bulk organic geochemistry of black shales from the Proterozoic Vindhyan Supergroup (central India). Journal of Earth System Science 115, 37-47.

Banerji, R.K., 1981. Cretaceous-Eocene sedimentation, tectonism and biofacies in the Bengal Basin, India. Palaeogeography, Palaeoclimatology, Palaeoecology 34, 57-85.

Banerji, R.K., 1984. Post-eocene biofacies, palaeoenvironments and palaeogeography of the Bengal Basin, India. Palaeogeography, Palaeoclimatology, Palaeoecology 45, 49-73.

Barakat, A.O., Mostafa, A., El-Gayar, M.S., Rullkötter, J., 1997. Source-dependent biomarker properties of five crude oils from the Gulf of Suez, Egypt. Organic Geochemistry 26, 441-450.

Bashari, A., 1998. Diagenesis and reservoir development of sandstones in the Triassic Rewan Group, Bowen Basin, Australia. Journal of Petroleum Geology 21, 445-465.

Bateman, R.M., Konen, C.E., 1977. The Log Analyst and the Programmable Pocket Calculator. The Log Analyst 18, 3-11.

BBS, 2011. Population and housing census of Bangladesh: Preliminary results. Bangladesh Bureau of Statistics, Dhaka.

Bechtel, A., Markic, M., Sachsenhofer, R.F., Jelen, B., Gratzer, R., Lücke, A., Püttmann, W., 2004. Paleoenvironment of the upper Oligocene Trbovlje coal seam (Slovenia). International Journal of Coal Geology 57, 23-48.

Belkin, H.E., Tewalt, S.J., Hower, J.C., Stucker, J.D., O'Keefe, J.M.K., 2009. Geochemistry and petrology of selected coal samples from Sumatra, Kalimantan, Sulawesi, and Papua, Indonesia. International Journal of Coal Geology 77, 260-268.

Berner, R.A., 1980. Early diagenesis. Princeton University Press, Princeton, Ney Jersey.

Berner, R.A., Raiswell, R., 1984. C/S method for distinguishing freshwater from marine sedimentary rocks. Geology 12, 365-368.

Bjorlykke, K., 1983. Diagenetic reactions in sandstones, in: Parker, A., Sellwood, B.W. (Eds.), Sediment diagenesis. D. Reidel, Dordrecht, The Netherlands, pp. 169-213.

Bjorøy, M., Mørk, A., Vigran, J.O., 1981. Organic geochemical studies of the Devonian to Triassic succession on Bjørnøya and the implications for the Barents Shelf, in: Bjorøy, M., Mørk, A., Vigran, J.O. (Eds.), Advances in Organic Geochemistry 1981. John Wiley, London, pp. 49-59.

Blatt, H., 1979. Diagenetic processes in sandstones, in: Scholle, P.A., Schluger, P.R. (Eds.), Aspects of diagenesis. The Society of Economic Paleontologists and Mineralogists, pp. 141-157.

Blatt, H., Middleton, G., Murray, R., 1980. Origin of sedimentary rocks. Prentice Hall Inc., Englewood Cliffs, New Jersey.

Boggs, S.J., 2009. Petrology of Sedimentary Rocks, 2nd ed. Cambridge University Press, New York.

Bordenave, M.L., Durand, B., 1993. Applied petroleum geochemistry. Editions Technip, Paris.

Bostick, N.H., Betterton, W.J., Gluskoter, H.J., Nazrul Islam, M., 1991. Petrography of Permian “Gondwana” coals from boreholes in northwestern Bangladesh, based on semiautomated reflectance scanning. Organic Geochemistry 17, 399-413.

Boulin, J., 1981. Afghanistan structure, Greater India concept and Eastern Tethys evolution. Tectonophysics 72, 261-287.
BPDB, 2012. Key statistics of power generation in Banagladesh, Power generation capacity on the basis of fuel type. Bangladesh Power Development Board, Dhaka.
Bradley, H., 1987. Petroleum engineering handbook- Properties of reservoir rocks. Society of Petroleum Engineering, USA, 418p.
Brock, J., 1986. Applied open-hole log analysis. Gulf Publishing Company, USA, p.284.
Brooks, J.D., Gould, K., Smith, J.W., 1969. Isoprenoid hydrocarbons in coal and petroleum. Nature 222, 257-259.
Brooks, P.W., 1986. Unusual biological marker geochemistry of oils and possible source rocks, offshore Beaufort-Mackenzie Delta, Canada. Organic Geochemistry 10, 401-406.
Burollet, P.F., 1984. Intracratonic and pericratonic basins in Africa. Sedimentary Geology 40, 1-11.
Calder, J.H., Gibbing, M.R., Mukhopadhyay, P.K., 1991. Peat formation in a Westphalian B piedmont setting. Cumberland Basin, Nova Scotia: implication for the maceral based interpretation of rheotrophic and raised palaeomires. Bulletin de la Societe Geologique de France 162, 283-298.
Casshyap, S.M., Tewari, R.C., 1987. Depositional model and tectonic evolution of Gondwana basins. Palaeobotanist 36, 59-66.
Chandra, S., Chandra, A., 1987. Vegetational changes and their climatic implications in coal-bearing Gondwana. Palaeobotanist 36, 74-86.
Chisholm, Hugh, 1911. Petroleum, in: Chisholm, Hugh (Eds.), Encyclopædia Britannica Eleventh Edition. Cambridge University Press, London.
Chowdhury, S.Q., 1982. Palynostratigraphy of the Neogene sediments of the Sitapahar anticline (western flank), Chittagong Hill Tracts, Bangladesh. Bangladesh Journal of Geology 1, 35-49.
Clifton, C.G., Walters, C.C., Simoneit, B.R.T., 1990. Hydrothermal petroleums from Yellowstone National Park, Wyoming, U.S.A. Applied Geochemistry 5, 169-191.
Coates, G., Dumanoir, J. L., 1973. A new approach to improve log-derived permeability. In: proceedings, the 14th Annual Logging Symposium, Trans. paper R, Society of Professional Well Log Analysts.
Connan, J., Bouroullec, J., Dessort, D., Albrecht, P., 1986. The microbial input in carbonate-anhydrite facies of a sabkha palaeoenvironment from Guatemala: A molecular approach. Organic Geochemistry 10, 29-50.
Cook, A.C., Hutton, A.C., Sherwood, N.R., 1981. Classification of oil shales. . Bull Centre Rech Explor Prod Elf-Aquitaine 5.
Curiale, J.A., Covington, G.H., Shamsuddin, A.H.M., Morelos, J.A., Shamsuddin, A.K.M., 2002. Origin of petroleum in Bangladesh. The AAPG Bulletin 86, 625-652.
Curray, J.R., 1991. Possible greenschist metamorphism at the base of a 22 km sedimentary section, Bay of Bengal. Geology 19, 1097-1100.
Curray, J.R., Moore, D.G., 1974. Sedimentary and tectonic processes in the Bengal Deep-Sea Fan and Geosyncline, in: Burk, C.A., Drake, C.L. (Eds.), The Geology of Continental Margins. Springer Verlag, New York, pp. 617-627.
Curtis, C.D., Coleman, M.L., 1986. Controls on the precipitation of early diagenetic calcite, dolomite and siderite concretions in complex depositional sequences, in: Gautier, D.L. (Ed.), Roles of organic matter in sediment diagenesis. The Society of Economic Paleontogists and Mineralogists, pp. 23-33.

Dai, S., Ren, D., Chou, C.-L., Li, S., Jiang, Y., 2006. Mineralogy and geochemistry of the No. 6 Coal (Pennsylvanian) in the Junger Coalfield, Ordos Basin, China. International Journal of Coal Geology 66, 253-270.

Dai, S., Ren, D., Chou, C.-L., Finkelman, R.B., Seredin, V.V., Zhou, Y., 2012. Geochemistry of trace elements in Chinese coals: A review of abundances, genetic types, impacts on human health, and industrial utilization. International Journal of Coal Geology 94, 3-21.

Das, G., 1977. Geology of Assam-Arakan region. Oil Commentary, India 15, 4-34.

Das, G., 1982. Synthesis and review on faunal records from the Surma Basin. Rec. Geol. Surv. India 112, 31-38.

Daulay, B., Cook, A.C., 1988. The petrology of some Indians coals. Journal of Southeast Asian Earth Sciences 2, 45-64.

Davies, G.R., Nassichuk, W.W., 1988. An Early Carboniferous (Viséan) lacustrine oil-shale in Canadian Arctic Archipelago. The American Association of Petroleum Geologists Bulletin 72, 8-20.

Dembicki, H.J., 2009. Three common source rock evaluation errors made by geologists during prospect or play appraisals. AAPG Bulletin 93, 341-356.

Dembicki, H.J., Horsfield, B., Thomas, T.Y.H., 1983. Source Rock Evaluation by Pyrolysis-Gas Chromatography. AAPG Bulletin 67, 1094-1103.

Dickinson, W.R., 1985. Interpreting provenance relations from detrital modes of sandstones, in: Zuffa, G.G. (Ed.), Provenance of arenites. D. Reidel Publishing Company, Dordrecht, The Netherlands, pp. 333-361.

Diessel, C.F.K., 1986. On the correlation between coal facies and depositional environments. 8th Commonwealth Mining and Metallurgical Congress, Australia pp. 669-677.

Dresser Atlas, 1979. Log Interpretation Charts: Houston. Dresser industries. Inc.,107p.

Dutta, S., Mathews, R.P., Singh, B.D., Tripathi, S.M., Singh, A., Saraswati, P.K., Banerjee, S., Mann, U., 2011. Petrology, palynology and organic geochemistry of Eocene lignite of Matanomadh, Kutch Basin, western India: Implications to depositional environment and hydrocarbon source potential. International Journal of Coal Geology 85, 91-102.

Dutton, S.P., Diggs, T.N., 1990. History of quartz cementation in the Lower Cretaceous Travis Peak Formation, East Texas. Journal of Sedimentary Petrology 60, 191-202.

Earnest, C., M, 1988. Compositional analysis by thermogravimetry. American Society for Testing and Materials, Philadelphia.

Espitalie, J., Madee, M., Tissot, B., Menning, J.J., Leplat, P., 1977. Source rock characterization methods for petroleum exploration. 9th Annual Offshore Technology Conference, Houston, pp. 439-444.

Estupiñan, J., Marfil, R., Scherer, M., Permanyer, A., 2010. Reservoir sandstones of the Cretaceous Napo Formation U and T Members in the Oriente Basin, Ecuador: links between diagenesis and sequence stratigraphy. Journal of Petroleum Geology 33, 221-245.

Evans, P., 1932. Tertiary succession in Assam. Trans. Min. Geol. Inst. India 27, 155-260.

Fabiańska, M.J., Kruszewska, K.K.J., 2003. Relationship between petrographic and geochemical characterisation of selected South African coals. International Journal of Coal Geology 54, 95-114.

Farhaduzzaman, M., Rahman, J. J. M., Rahman, M., 2008. Some Aspects of the Geology of Phulbari Coal Basin, Dinajpur District, Northwest Bangladesh: Implications for Mining. In: abstract, XII Geological Conference, Dhaka, Bangladesh Geological Society, Bangladesh, pp. 34.

Farhaduzzaman, M., 2010. Lithology Interpretation from Downhole Geophysical Well Logs of Phulbari Coal Basin, Northwest Bangladesh. Jahangirnagar University Journal of Science 33, 09-22.

Farhaduzzaman, M., Wan Hasiah A., Islam, M. A., 2011a. Petroleum source rock evaluation of the Permian coal of the Barapukuria Basin, Bangladesh. In: abstract, 2nd International Geosciences Student Conference, Krakow, Poland, pp. 132-135.

Farhaduzzaman, M., Wan Hasiah A., Islam, M. A., 2011b. Macerals identification and its implication to palaeoenvironmental interpretation of Permian Gondwana coals of the Barapukuria basin of Bangladesh. In: abstract, 7th Mathematics and Physical Sciences Graduate Congress, Singapore, pp. 74.

Farhaduzzaman, M., 2012. Hydrocarbon source rock characteristics of the Gondwana coals from Barapukuria Basin, Bangladesh. In: proceedings, Petroleum Geoscience Conference and Exhibition PGCE 2012, Kuala Lumpur, Malaysia, pp.1-5.

Farhaduzzaman, M., Wan Hasiah A., Islam, M. A., 2012a. Depositional environment and hydrocarbon source potential of the Permian Gondwana coals from the Barapukuria Basin, Northwest Bangladesh. International Journal of Coal Geology 90-91, 162-179.

Farhaduzzaman, M., Wan Hasiah A., Islam, M. A., Pearson, M.J., 2012b. Source rock potential of the organic-rich shales in the Tertiary Bhuban and Boka Bil Formations, Bengal Basin, Bangladesh. Journal of Petroleum Geology 35 (4), 357-376.

Farhaduzzaman, M., Wan Hasiah A., Islam, M. A., 2012c. Petroleum generation potential of the Permian coals from Barapukuria Basin, Bangladesh. In: poster, University of Malaya Researchers' Conference, Kuala Lumpur, Malaysia, pp. 30.

Farhaduzzaman, M., Wan Hasiah A., Islam, M. A., 2012d. Petroleum source rock potential of Boka Bil shales of the Bengal Basin, Bangladesh. In: abstract, 8th Mathematical and Physical Sciences Graduate Congress (MPSGC), Chulalongkorn University, Thailand.

Farhaduzzaman, M., Wan Hasiah A., Islam, M. A., 2013a. Petroleum generation potential of the Miocene Bhuban shales of Bengal Basin, Bangladesh. In: proceedings, International Conference on Engineering Research, Innovation and Education, Shahjalal University of Science and Technology, Bangladesh, pp.1055-1061.

Farhaduzzaman, M., Wan Hasiah A., Islam, M. A., 2013b. Hydrocarbon source potential and depositional environment of the Surma Group shales of Bengal Basin, Bangladesh. Journal of the Geological Society of India (accepted).

Farhaduzzaman, M., Wan Hasiah A., Islam, M. A., Pearson, M. J., 2013c. Organic facies variations and hydrocarbon generation potential of Permian Gondwana coals and associated sediments, Barapukuria and Dighipara Basins, NW Bangladesh. Journal of Petroleum Geology 36 (2), 117-138.

Farhaduzzaman, M., Wan Hasiah A., Islam, M. A., 2013d. Petrographic characteristics and paleoenvironments of the Permian coal resources of the Barapukuria and Dighipara Basins, Bangladesh. Journal of Asian Earth Sciences 64, 272-287.

Farhaduzzaman, M., Wan Hasiah A., Islam, M. A., 2013e. Hydrocarbon generation potential, organic matter input and depositional condition of the Miocene Bhuban Formation shales, Bengal Basin, Bangladesh. Bangladesh Journal of Geology (under review).

Farhaduzzaman, M., Wan Hasiah A., Islam, M. A., 2013f. Petroleum source rock properties of Surma Group shales of Bengal Basin, Bangladesh. In: proceedings, Petroleum Geoscience Conference and Exhibition PGCE 2013, Malaysia, pp.148-153.

Farhaduzzaman, M., Wan Hasiah A., Islam, M. A., 2013g. Petroleum source rock characteristics of the Tertiary Bhuban Formation of the Bengal Basin, Bangladesh. In: proceedings, 4th International Geosciences Student Conference, Germany, pp.1-3.

Farhaduzzaman, M., Wan Hasiah A., Islam, M. A., 2013h**.** Organic geochemical and petrological evaluation of the Early Pliocene Boka Bil shales of the Bengal Basin, Bangladesh**.** Malaysian Journal of Science (under review).

Farhaduzzaman, M., Wan Hasiah A., Islam, M. A., 2013i. Petroleum source rock properties of the Neogene Bhuban shales, Bengal Basin, Bangladesh. Sains Malaysiana (under review).

Farhaduzzaman, M., Wan Hasiah A., Islam, M.A., 2013j. Hydrocarbon generation potential and organic matter sources of the Bhuban Formation shales, Bengal Basin, Bangladesh. Bangladesh Geoscience Journal (under review).

Farhaduzzaman, M., Islam, M. A., Wan Hasiah A., 2013k. Petrography and diagenesis of the Tertiary Surma Group reservoir sandstones, Bengal Basin, Bangladesh. Geosciences Journal (under review).

Farrimond, P., Taylor, A., Telnaes, N., 1998. Biomarker maturity parameters: the role of generation and thermal degradation. Organic Geochemistry 29, 1181-1197.

Fertl, W. H., 1975. Shaly-sand analysis in development wells. In: proceedings, the 16th Annual Logging Symposium, Trans. paper A, Society of Professional Well Log Analysts.

Fertl, W.H., Vercellino, W.C., 1978. Predict water cut from well logs. In: Practical log analysis – 4. Oil and Gas Journal.

Fertl, W.H., 1987. Log-derived evaluation of shaly clastic reservoirs. Journal of Petroleum Technology 39, 175-194.

Finkelman, R.B., 1994. Modes of occurrence of potentially hazardous elements in coal: levels of confidence. Fuel Processing Technology 39, 21-34.

Finkelman, R.B., 2004. Potential health impacts of burning coal beds and waste banks. International Journal of Coal Geology 59, 19-24.

Finkelman, R.B., Orem, W., Castranova, V., Tatu, C.A., Belkin, H.E., Zheng, B., Lerch, H.E., Maharaj, S.V., Bates, A.L., 2002. Health impacts of coal and coal use: possible solutions. International Journal of Coal Geology 50, 425-443.

Folk, R.L., 1980. Petrology of sedimentary rocks, Reprinted ed. Hemphill Publishing Company, Texas.

Friedman, G.M., Sanders, J.E., 1978. Principles of sedimentology. John Wiley & Sons, New York, Brisbane, Toronto.

Frielingsdorf, J., Aminul Islam, S., Block, M., Mizanur Rahman, M., Golam Rabbani, M., 2008. Tectonic subsidence modelling and Gondwana source rock hydrocarbon potential, Northwest Bangladesh Modelling of Kuchma, Singra and Hazipur wells. Marine and Petroleum Geology 25, 553-564.

Garrels, R.M., Mackenzie, F.T., 1971. Evolution of sedimentary rocks. W. W. Norton, New York.

Giraud, A., 1970. Application of pyrolysis and gas chromatography to geochemical characterization of kerogen in sedimentary rocks. AAPG Bulletin 54, 439-455.

Goodarzi, F., Nassichuk, W.W., Snowdon, L.R., Davies, G.R., 1987. Organic Petrology and Rock-Eval analysis of the Lower Carboniferous Emma Fjord Formation in Sverdrup Basin, Canadian Arctic Archipelago. Marine and Petroleum Geology 4, 132-145.

Goodarzi, F., 2002. Mineralogy, elemental composition and modes of occurrence of elements in Canadian feed-coals. Fuel 81, 1199-1213.

Guha, D.K., 1978. Tectonic framework and oil and gas prospects of Bangladesh. 4th Annual Conference. Bangladesh Geological Society, Dhaka, pp. 65-75.

Gupta, D.C., 1999. Environmental aspects of selected trace elements associated with coal and natural waters of Pench Valley coalfield of India and their impact on human health. International Journal of Coal Geology 40, 133-149.

Gupta, S., Shen, F., Lee, W.-J., O'Brien, G., 2012. Improving coke strength prediction using automated coal petrography. Fuel 94, 368-373.

Hacquebard, P.A., Donaldson, J.R., 1969. Carboniferous coal deposition associated with flood plain and limnic environments in Nova Scotia, in: Dapples, E.C., Hopkins, M.E. (Eds.), Environments of coal deposition Geological Society of America USA, pp. 143-191.

Hakimi, M.H., Wan Hasiah, A., Shalaby, M.R., 2010. Organic geochemistry, burial history and hydrocarbon generation modelling of the Upper Jurassic Madbi Formation, Masila Basin, Yemen. Journal of Petroleum Geology 33, 299-318.

Hakimi, M.H., Wan Hasiah, A., Shalaby, M.R., 2011. Organic geochemical characteristics and depositional environments of the Jurassic shales in the Masila Basin of Eastern Yemen. GeoArabia 16, 47-64.

Harwood, L.M., Moody, C.J., 1989. Experimental organic chemistry: principles and practice. Wiley-Blackwell, UK.

Hasan, M.N., Islam, M.N., 2003. Geophysical exploration for sub-surface geology and mineral resources in the Rangpur Platform, Bangladesh. GSB/AGID International Conference NESDA. GSB/AGID, Dhaka, Bangladesh, pp. 1-8.

Hildebrand, R.T., 2010. Challenges of coalbed natural gas development in Northwest Bangladesh. AAPG International Conference and Exhibition, Alberta, Canada.

Hilchie, D.W., 1978. Applied open-hole log interpretation. Douglas W. Hilchie Inc., USA.

Hiller, K., Elahi, M., 1988. Structural growth and hydrocarbon entrapment in the Surma basin, Bangladesh, in: Wagner, H.C., Wagner, L.C., Wang, F.F.H., Wong, F.L. (Eds.), Petroleum Resources of China and Related Subjects. Circum-Pacific Council for Energy and Mineral Resources, Houston, Texas.

Hoholick, J.D., Metarko, T.A., Potter, P.E., 1982. Weighted contact packing - improved formula for grain packing of quartz arenites. The Mountain Geologist 19, 79-82.

Holland, M.J., Cadle, A.B., Pinheiro, R., Falcon, R.M.S., 1989. Depositional environments and coal petrography of the Permian Karoo Sequence: Witbank Coalfield, South Africa. International Journal of Coal Geology 11, 143-169.

Holtrop, J.F., Keiser, J., 1970. Some aspects of the stratigraphy and correlation of the Surma Basin wells, East Pakistan. ECAFE Mineral Resources Development Series 36, 143-154.

Hood, A., Gutjahr, C.M., Heacock, R.L., 1975. Organic metamorphism and the generation of petroleum. AAPG Bulletin 59, 986-996.

Hossain, M.M.A., 2012. Pump oil, outshine debate. Fortnightly Magazine Energy & Power 9, 9-12.

Hossain, Z.M., Roser, B.P., Kimura, J.I., 2010. Petrography and whole-rock geochemistry of the Tertiary Sylhet succession, northeastern Bengal Basin, Bangladesh: Provenance and source area weathering. Sedimentary Geology 228, 171-183.

Hossain, Z.M., Sampei, Y., Roser, B.P., 2009. Characterization of organic matter and depositional environment of Tertiary mudstones from the Sylhet Basin, Bangladesh. Organic Geochemistry 40, 743-754.

Hossain, Z.H., Sultan-ul-Islam, M., Ahmed, S., Hossain, I., 2002. Analysis of sedimentary facies and depositional environments of the Permian Gondwana sequence in borehole GDH-45, Khalaspir Basin, Bangladesh. Geosciences Journal 6, 227-236.

Houseknecht, D.W., 1987. Assessing the relative importance of compaction processes and cementation to reduction of porosity in sandstones. AAPG Bulletin 71, 633-642.
Hower, J. C., Robertson, J. D., 2003. Clausthalite in coal. International Journal of Coal Geology, 53(4), 219-225.
Hower, J.C., Calder, J.H., Eble, C.F., Scott, A.C., Robertson, J.D., Blanchard, L.J., 2000. Metalliferous coals of the Westphalian A Joggins Formation, Cumberland Basin, Nova Scotia, Canada: petrology, geochemistry, and palynology. International Journal of Coal Geology 42, 185-206.
Hower, J.C., Bland, A.E., 1989. Geochemistry of the Pond Creek coal bed, Eastern Kentucky coalfield. International Journal of Coal Geology 11, 205-226.
Hower, J.C., Gayer, R.A., 2002. Mechanisms of coal metamorphism: case studies from Paleozoic coalfields. International Journal of Coal Geology 50, 215-245.
Hower, J.C., O'Keefe, J.M.K., Eble, C.F., 2008. Tales from a distant swamp: Petrological and paleobotanical clues for the origin of the sand coal lithotype (Mississippian, Valley Fields, Virginia). International Journal of Coal Geology 75, 119-126.
HSE, 2003. Cadmium and you- Working with cadmium: Are you at risk? Health and Safety Executive, UK.
Huang, H., Pearson, M.J., 1999. Source rock palaeoenvironments and controls on the distribution of dibenzothiophenes in lacustrine crude oils, Bohai Bay Basin, eastern China. Organic Geochemistry 30, 1455-1470.
Huang, W.-Y., Meinschein, W.G., 1979. Sterols as ecological indicators. Geochimica et Cosmochimica Acta 43, 739-745.
Hunt, J.M., 1991. Generation of gas and oil from coal and other terrestrial organic matter. Organic Geochemistry 17, 673-680.
Hunt, J.W., 1982. Relationship between microlithotype and maceral composition of coals and geological setting of coal measures in the Permian basins of Eastern Australia. Australian Coal Geology 4, 484-502.
Hunt, J.W., 1996. Petroleum Geochemistry and Geology, 2nd ed. W.H. Freeman, San Francisco.
Hunt, J.W., Hennet, R.J.-C., 1991. Modeling petroleum generation in sedimentary basins, in: Farrington, J., Whelan, J. (Eds.), Organic matter productivity, accumulation and preservation in Recent and Ancient sediments. Columbia University Press.
Hunt, J.W., Smyth, M., 1989. Origin of inertinite-rich coals of Australian cratonic basins. International Journal of Coal Geology 11, 23-46.
ICCP, 1963. International Handbook of Coal Petrography, 2nd ed. International Committee for Coal Petrology, Center National De La Recherche Scientifique, Paris-France.
ICCP, 1998. The new vitrinite classification (ICCP System 1994). Fuel 77, 349-358.
ICCP, 2001. The new inertinite classification (ICCP System 1994). Fuel 80, 459-471.
IEA, 2010. World Energy Outlook 2010. International Energy Agency.
Imam, B., 2005. Energy Resources of Bangladesh. University Grants Commission, Bangladesh.
Imam, M.B., 1986. Scanning electron microscope study of the quartz overgrowths within Neogene sandstones of Bengal Basin, Bangladesh. Journal of the Geological Society of India 28, 407-413.
Imam, M.B., 1989. Comparison of burial diagenesis in some deltaic to shallow marine reservoir sandstones from different basins. Journal of the Geological Society of India 33, 524-537.
Imam, M.B., Hussain, M., 2002. A review of hydrocarbon habitats in Bangladesh. Journal of Petroleum Geology 25, 31-52.

Imam, M.B., Rahman, M., Akhter, S.H., 2002. Coalbed methane prospect of Jamalganj coalfield, Bangladesh. Arabian Journal for Science and Engineering 27, 17-27.

Imam, M.B., Shaw, H.F., 1985. The diagenesis of Neogene clastic sediments from the Bengal Basin, Bangladesh. Journal of Sedimentary Research 55, 665-671.

Imam, M.B., Shaw, H.F., 1987. Diagenetic controls on the reservoir properties of gas bearing Neogene Surma Group sandstones in the Bengal Basin, Bangladesh. Marine and Petroleum Geology 4, 103-111.

Islam, M. A., 2009. Diagenesis and reservoir quality of Bhuban sandstones (Neogene), Titas Gas Field, Bengal Basin, Bangladesh. Journal of Asian Earth Sciences 35, 89-100.

Islam, M. A., 2010a. Petrophysical evaluation of subsurface reservoir sandstones of Bengal Basin, Bangladesh. Journal of the Geological Society of India 76, 621-631.

Islam, M. A., 2010b. Petrography and provenance of subsurface Neogene sandstones of Bengal Basin, Bangladesh. Journal of the Geological Society of India 76, 493-504.

Islam, M. A., Farhaduzzaman, M., Wan Hasiah A., Dutta, J., 2013. Log based petrophysical analysis of Mio-Pliocene sandstone reservoir encountered in Well Rashidpur 4, Bengal Basin, Bangladesh. Journal of the Geological Society of India (under review).

Islam, M. A., Sultan-ul-Islam, M., Hasan Latif, M., Mondal, D., Abdullah-Al-Mahbub, 2006. Petrophysical analysis of shaly sand gas reservoir of Titas Gas Field using well logs. Bangladesh Journal of Geology 25, 106-124.

Islam, M. R., Hayashi, D., 2008. Geology and coal bed methane resource potential of the Gondwana Barapukuria Coal Basin, Dinajpur, Bangladesh. International Journal of Coal Geology 75, 127-143.

Islam, M. R., Kamruzaman, A.B.M., 2006. Geochemical and Techno-environmental Behaviour of Gondwana Coals from the Barapukuria Coal Mine, Bangladesh. Bangladesh Journal of Geology 25, 48-63.

Islam, M. R., Sultan-ul-Islam, M., 2005. Water Inrush Hazard in Barapukuria Coal Mine, Dinajpur District. Bangladesh Journal of Geology 24, 1-17

Islam, M.S., Hossain, I., 2006. Lithofacies and Embedded Markov Chain analysis of Gondwana sequence in boreholes GDH-40 and 43, Barapukuria Coal Field, Bangladesh. Bangladesh Journal of Geology 25, 64-80.

Islam, M. S., Rahman, M.J.J., 2009. Geochemical analysis of the Miocene Surma Group sediments from the Meghna Gas Field, Bengal Basin, Bangladesh. Jahangirnagar University Journal of Science 32, 29-46.

Jamaluddin, M., Nasrin, N., Rahman, M., Anwara, H., Bygdevold, J., 2001. Bangladesh petroleum potential and resource assessment 2001. Hydrocarbon Unit and Norwegian Petroleum Directorate, Dhaka (unpublished), p. 200.

Jasper, K., Hartkopf-Fröder, C., Flajs, G., Littke, R., 2010. Palaeoecological evolution of Duckmantian wetlands in the Ruhr Basin (western Germany): A palynological and coal petrographical analysis. Review of Palaeobotany and Palynology 162, 123-145.

Jiang, C., Alexander, R., Kagi, R.I., Murray, A.P., 1998. Polycyclic aromatic hydrocarbons in ancient sediments and their relationships to palaeoclimate. Organic Geochemistry 29, 1721-1735.

Jones, R.W., Edison, T.A., 1978. Microscopic observations of kerogen related to geochemical parameters with emphasis on thermal maturation, in: Oltz, D.F. (Ed.), Low temperature metamorphism of kerogen and clay minerals. Society of Economic Paleontologist and Mineralogist, Los Angeles, pp. 1-12.

Johnson, S.Y., Alam, A.N., 1991. Sedimentation and tectonics of Sylhet Trough, Bangladesh. Geological Society of America Bulletin 103, 1513-1527.

JORC, 2004. Australian code for reporting of exploration results, mineral resources and ore reserves. The Joint Ore Reserves Committee of The Australasian Institute of Mining and Metallurgy, Australian Institute of Geoscientists and Minerals Council of Australia, p. 20.

Jorjani, E., Hower, J.C., Chehreh Chelgani, S., Shirazi, M.A., Mesroghli, S., 2008. Studies of relationship between petrography and elemental analysis with grindability for Kentucky coals. Fuel 87, 707-713.

Kalkreuth, W., Holz, M., Cazzulo-Klepzig, M., Marques-Toigo, M., Utting, J., Semkiwa, P., 1999. A comparative study of the geology, petrology and palynology of Permian coals in Tanzania and southern Brazil. Journal of African Earth Sciences 29, 91-104.

Kashirtsev, V.A., Moskvin, V.I., Fomin, A.N., Chalaya, O.N., 2010. Terpanes and steranes in coals of different genetic types in Siberia. Russian Geology and Geophysics 51, 404-411.

Ketris, M.P., Yudovich, Y.E., 2009. Estimations of Clarkes for Carbonaceous biolithes: World averages for trace element contents in black shales and coals. International Journal of Coal Geology 78, 135-148.

Khalequzzaman, M., 2010. Assessment of coalfields in Bangladesh. Lock Haven University, Lock Haven, p. 33.

Khan, A. A., Chouhan, R. K. S., 1996. The crustal dynamics and the tectonic trends in the Bengal Basin. Journal of Geodynamics 22, 267-286.

Khan, F.H., 1991. Geology of Bangladesh. University Press Ltd., Dhaka, Bangladesh.

Khan, M.R., Muminullah, M., 1980. Stratigraphy of Bangladesh. Petroleum and Mineral Resources Seminar and Exhibition, Dhaka, pp. 35-40.

Khan, R.A., 2006. An interneeship report on the geological and drilling activities taken by Geological Survey of Bangladesh, Department of Geological Sciences. Jahangirnagar University, Savar, Dhaka, Bangladesh.

Khandelwal, M., Singh, T.N., 2010. Prediction of macerals contents of Indian coals from proximate and ultimate analyses using artificial neural networks. Fuel 89, 1101-1109.

Koeverden, J.H., Karlsen, D.A., Backer-Owe, K., 2011. Carboniferous non-marine source rocks from Spitsbergen and Bjørnøya: comparison with the Western Arctic. Journal of Petroleum Geology 34, 53-66.

Larter, S.R., Douglas, A.G., 1980. A pyrolysis-gas chromatographic method for kerogen typing. Physics and Chemistry of The Earth 12, 579-583.

Leder, F., Park, W.C., 1986. Porosity reduction in sandstone by quartz overgrowth. AAPG Bulletin 70, 1713-1728.

Lee, M., Aronson, J.L., Savin, S.M., 1989. Timing and conditions of Permian Rotliegende sandstone diagenesis, Southern North Sea: K/Ar and oxygen isotopic data. AAPG Bulletin 73, 195-215.

Lindsay, J.F., Holliday, D.W., Hulbert, A.G., 1991. Sequence stratigraphy and the evolution of the Ganges-Brahmaputra Delta complex. AAPG Bulletin 75, 1233-1254.

Littke, R., Horsfield, B., Leythaeuser, D., 1989. Hydrocarbon distribution in coals and in dispersed organic matter of different maceral compositions and maturities. Geologische Rundschau 78, 391-410.

Luo, J.L., Morad, S., Salem, A., Ketzer, J.M., Lei, X.L., Guo, D.Y., Hlal, O., 2009. Impact of diagenesis on reservoir-quality evolution in fluvial and lacustrine-deltaic sandstones: evidence from Jurassic and Triassic sandstones from the Ordos Basin, China. Journal of Petroleum Geology 32, 79-102.

Mackenzie, A.S., Patience, R.L., Maxwell, J.R., Vandenbroucke, M., Durand, B., 1980. Molecular parameters of maturation in the Toarcian shales, Paris Basin, France-I.

Changes in the configurations of acyclic isoprenoid alkanes, steranes and triterpanes. Geochimica et Cosmochimica Acta 44, 1709-1721.
Mackowsky, M.T., 1982. Minerals and trace elements occurring in coal, in: Stach, E.e.a. (Ed.), Stach's textbook of coal petrology. Gebruder Borntraeger, Berlin-Stuttgart, pp. 153-171.
Marchioni, D., Kalkreuth, W., 1991. Coal facies interpretations based on lithotype and maceral variations in Lower Cretaceous (Gates Formation) coals of Western Canada. International Journal of Coal Geology 18, 125-162.
Marchioni, D.L., 1980. Petrography and depositional environment of the liddell seam, upper hunter valley, New South Wales. International Journal of Coal Geology 1, 35-61.
Mello, M.R., Telnaes, N., Gaglianone, P.C., Chicarelli, M.I., Brassell, S.C., Maxwell, J.R., 1988. Organic geochemical characterisation of depositional palaeoenvironments of source rocks and oils in Brazilian marginal basins. Organic Geochemistry 13, 31-45.
Mishra, H.K., Chandra, T.K., Verma, R.P., 1990. Petrology of some Permian coals of India. International Journal of Coal Geology 16, 47-71.
Moinul, H., Chowdhury, H.A., Fazlul, K., Mansur, A., Morsheduddin, A., 1977. Geological/completion report on Begumganj Well no.1 and Muladi Well no.1, Begumganj Gas Field, Bangladesh. Petrobangla, Dhaka (unpublished), p. 37.
Moldowan, J.M., Seifert, W.K., Arnold, E., Clardy, J., 1985. Relationship between petroleum composition and depositional environment of petroleum source rocks. AAPG Bulletin 69, 1255-1268.
Moldowan, J.M., Sundararaman, P., Schoell, M., 1986. Sensitivity of biomarker properties to depositional environment and/or source input in the Lower Toarcian of SW-Germany. Organic Geochemistry 10, 915-926.
Moore, D.M., Reynolds, R.C.J., 1979. X-Ray Diffraction and the Identification and Analysis of Clay Minerals. Oxford University Press, USA.
Moore, T.A., Shearer, J.C., 2003. Peat/coal type and depositional environment—are they related? International Journal of Coal Geology 56, 233-252.
Morad, S., Aldahan, A.A., 1987. Diagenetic replacement of feldspars by quartz in sandstones. Journal of Sedimentary Petrology 57, 488-493.
Morad, S., Bergan, M., Knarud, R., Nystuen, J.P., 1990. Albitization of detrital plagioclase in Triassic reservoir sandstones from the Snorre Field, Norwegian North Sea. Journal of Sedimentary Petrology 60, 411-425.
Morris, R.L., Biggs, W.P., 1967. Using log-derived values of water saturation and porosity. In: proceedings, the 8th Annual Logging Symposium, Trans. Paper O, Society of Professional Well Log Analysts.
Mukhopadhyay, P.K., 1986. Petrography of selected Wilcox and Jockson Group lignites from Tertiary of Texas, in: Finkelman, R.B., Casagrande, D.J. (Eds.), Geology of Gulf Coast Lignites. Geological Society of America, Coal Geology Division, Field Trip, USA, pp. 126-145.
Muller, M., 2009. It's not only about coal mining: Coal-bed metahne and underground coal gasification potential in Bangladesh. Mines and Communities, London, p. 38.
Murchison, D.G., 1987. Recent advances in organic petrology and organic geochemistry: an overview with some reference to ‘oil from coal’. Geological Society, London, Special Publications 32, 257-302.
Najman, Y., Bickle, M., BouDagher-Fadel, M., Carter, A., Garzanti, E., Paul, M., Wijbrans, J., Willett, E., Oliver, G., Parrish, R., Akhter, S.H., Allen, R., Ando, S., Chisty, E.,

Reisberg, L., Vezzoli, G., 2008. The Paleogene record of Himalayan erosion: Bengal Basin, Bangladesh. Earth and Planetary Science Letters 273, 1-14.
Nazim, M.U., Khalid, M.H., Boul, M.A., Akkas, A., Murtoza, A.G., Jamaluddin, M., 1982. Geological/completion report on Kamta Well no.1, Kamta Gas Field, Bangladesh. Petrobangla, Dhaka (unpublished), p. 63.
Nawab, M.M., Islam, M. A., 2005. Estimation of shale volume using a combination of the tree porosity logs: case study of selected gas fields of Bangladesh. B.Sc (Hons) Project Report, Department of Geology and Mining, University of Rajshahi.
Newman, J., Price, L.C., Johnston, J.H., 1997. Hydrocarbon source potential and maturation in Eocene New Zealand vitrinite-rich coals. Journal of Petroleum Geology 20, 137-163.
Paul, D.K., 2005. Petrology and geochemistry of the Salma dike, Raniganj coalfield (Lower Gondwana), eastern India: linkage with Rajmahal or Deccan volcanic activity? Journal of Asian Earth Sciences 25, 903-913.
Pearson, M.J., Alam, M., 1993. Bicadinanes and other terrestrial terpenoids in immature Oligocene sedimentary rocks and a related oil from the Surma Basin, N.E. Bangladesh. Organic Geochemistry 20, 539-554.
Peters, K.E., 1986. Guidelines for evaluating petroleum source rock using programmed pyrolysis. AAPG Bulletin 70, 318-329.
Peters, K.E., Cassa, M.R., 1994. Applied source rock geochemistry, in: Magoon, L.B., Dow, W.G. (Eds.), The Petroleum System -From Source to Trap. AAPG Memoir, pp. 93-120.
Peters, K.E., Moldowan, J.M., 1993. The biomarker guide- interpreting molecular fossils in petroleum and ancient sediments. Prentice-Hall, Inc., Englewood Cliffs, New Jersey.
Peters, K.E., Moldowan, J.M., Schoell, M., Hempkins, W.B., 1986. Petroleum isotopic and biomarker composition related to source rock organic matter and depositional environment. Organic Geochemistry 10, 17-27.
Peters, K.E., Walters, C.C., Moldowan, J.M., 2005. The biomarker guide- biomarkers and isotopes in the environment and human history, 2nd ed. Cambridge University Press, Cambridge, UK.
Petersen, H.I., 2002. A re-consideration of the "oil window" for humic coal and kerogen Type III source rocks. Journal of Petroleum Geology 25, 407-432.
Petersen, H. I., 2006. The petroleum generation potential and effective oil window of humic coals related to coal composition and age. International Journal of Coal Geology 67, 221-248.
Petersen, H.I., Nytoft, H.P., 2006. Oil generation capacity of coals as a function of coal age and aliphatic structure. Organic Geochemistry, 37, 558-583.
Petersen, H.I., Andsbjerg, J., Bojesen-Koefoed, J.A., Nytoft, H.P., 2000. Coal-generated oil: source rock evaluation and petroleum geochemistry of the Lulita Oilfield, Danish North Sea. Journal of Petroleum Geology 23, 55-90.
Petersen, H.I., Nytoft, H.P., Ratanasthien, B., Foopatthanakamol, A., 2007. Oils from Cenozoic rift-basins in central and northern Thailand: source and thermal maturity. Journal of Petroleum Geology 30, 59-78.
Petersen, H.I., Tru, V., Nielsen, L.H., Duc, N.A., Nytoft, H.P., 2005. Source rock properties of lacustrine mudstones and coals (Oligocene Dong Ho Formation), onshore Song Hong Basin, northern Vietnam. Journal of Petroleum Geology 28, 19-38.
Pettijohn, F.J., Potter, P.E., Siever, R., 1987. Sand and sandstone, 2nd ed. Springer-Verlag, New York.

Philp, R.P., 1985. Fossil fuel biomarkers: applications and spectra. Elsevier Science Publishers B.V, Amsterdam.
Philp, R.P., Gilbert, T.D., 1986. Biomarker distributions in Australian oils predominantly derived from terrigenous source material. Organic Geochemistry 10, 73-84.
Pittman, E.D., 1979. Recent advances in sandstone diagenesis. Annual Review of Earth and Planetary Sciences 7, 39-62.
Powell, M.C., 1979. A speculative tectonic history of Pakistan and surroundings: Some constraints from the Indian Ocean, in: Farah, A., Jong, D.K.A. (Eds.), Geodynamics of Pakistan. Geological Survey of Pakistan, Quetta, pp. 5-24.
Powell, T., McKirdy, D.M., 1973. Relationship between ratio of pristane to phytane, crude oil composition and geological environments in Australia. Nature 243, 37-39.
Powell, T.G., 1978. An assessment of the hydrocarbon source rock potential of the Canadian Arctic Islands. Geological Survey of Canada, Ottawa, Canada.
Powell, T.G., Boreham, C.J., Smyth, M., Russell, N., Cook, A.C., 1991. Petroleum source rock assessment in non-marine sequences: pyrolysis and petrographic analysis of Australian coals and carbonaceous shales. Organic Geochemistry 17, 375-394.
Price, L.C., Baker, C.E., 1985. Suppression of vtrinite reflectance in amorphous rich kerogen - a major unrecognized problem. Journal of Petroleum Geology 8, 59-84.
Rahman, M., 2004. Coal: Revisiting its utility and importance. Bangladesh Journal of Geology 23, 129-137.
Rahman, M., Faupl, P., Alam, M., 2009. Depositional facies of the subsurface Neogene Surma Group in the Sylhet Trough of the Bengal Basin, Bangladesh: record of tidal sedimentation. International Journal of Earth Sciences 98, 1971-1980.
Rahman, M.J.J., Faupl, P., 2003. The composition of the subsurface Neogene shales of the Surma group from the Sylhet Trough, Bengal Basin, Bangladesh. Sedimentary Geology 155, 407-417.
Rahman, M.J.J., McCann, T., 2012. Diagenetic history of the Surma Group sandstones (Miocene) in the Surma Basin, Bangladesh. Journal of Asian Earth Sciences 45, 65-78.
Rahman, M.J.J., Suzuki, S., 2007a. Composition of Neogene shales from the Surma Group, Bengal Basin, Bangladesh: implications for provenance and tectonic setting. Austrian Journal of Earth Sciences 100, 54-64.
Rahman, M.J.J., Suzuki, S., 2007b. Geochemistry of sandstones from the Miocene Surma Group, Bengal Basin, Bangladesh: Implications for Provenance, tectonic setting and weathering. Geochemical Journal 41, 415-428.
Ramanampisoa, L., Radke, M., Schaeffer, R.G., Littke, R., Rullkötter, J., Horsfield, B., 1990. Organic-geochemical characterisation of sediments from the Sakoa coalfield, Madagascar. Organic Geochemistry 16, 235-246.
Ratanasthien, B., Kandharosa, W., Chompusri, S., Chartprasert, S., 1999. Liptinite in coal and oil source rocks in northern Thailand. Journal of Asian Earth Sciences 17, 301-306.
Reed, J.K., Gipson, M., Neese, D.G., 1993. Hydrocarbon potential of sandstone reservoirs in the Neogene East Slovakian Basin Part I: a petrographic examination of lithology, porosity, and diagenesis. Journal of Petroleum Geology 16, 89-108.
Reimann, K.U., 1993. Geology of Bangladesh, Gebruder Borntraeger, Berlin-Stuttgart, Germany.
Ren, D., Xu, D., Zhao, F., 2004. A preliminary study on the enrichment mechanism and occurrence of hazardous trace elements in the Tertiary lignite from the Shenbei coalfield, China. International Journal of Coal Geology 57, 187-196.

RPS Energy, 2009. Resources estimation for the Rashidpur Field: reservoir management project 2. Report for Petrobangla, RPS Energy, Dhaka, p37.
Ruhovets, N., 1990. A log analysis technique for evaluating laminated reservoirs in the Gulf Coast area. The Log Analyst 31, 294-303.
Sachse, V.F., Leythaeuser, D., Grobe, A., Rachidi, M., Littke, R., 2012. Organic geochemistry and petrology of a Lower Jurassic (Pliensbachian) petroleum source rock from AÏT Moussa, Middle Atlas, Morocco. Journal of Petroleum Geology 35, 5-23.
Sakurai, S., Grimaldo-Suarez, F.M., Aguilera-Gomez, L.E., Rodriguez-Larios, J.A., 2002. Estimate of lithology and net gas sand from wireline logs: Veracruz and Macuspana Basins, Mexico. Gulf Coast Association of Geological Societies Transactions 52, 871-881.
Sampei, Y., Matsumoto, E., 2001. C/N ratios in a sediment core from Nakaumi Lagoon, southwest Japan -usefulness as an organic source indicator. Geochemical Journal 35, 189-205.
Sawada, K., 2006. Organic facies and geochemical aspects in Neogene neritic sediments of the Takafu syncline area of central Japan: Paleoenvironmental and sedimentological reconstructions. Island Arc 15, 517-536.
Schiøler, P., Rogers, K., Sykes, R., Hollis, C.J., Ilg, B., Meadows, D., Roncaglia, L., Uruski, C., 2010. Palynofacies, organic geochemistry and depositional environment of the Tartan Formation (Late Paleocene), a potential source rock in the Great South Basin, New Zealand. Marine and Petroleum Geology 27, 351-369.
Schlumberger, 1972. Log interpretation manual/principles. Schlumberger Well Services Inc., Houston.
Schlumberger, 1975. A guide to well site interpretation of the Gulf Coast. Schlumberger Well Services Inc., Houston, p.85.
Schlumberger, 1977. Log Interpretation charts. Schlumberger Well Services Inc., Houston.
Schmidt, V., McDonald, D.A., 1979. Secondary reservoir porosity in the course of sandstone diagenesis. AAPG, Tulsa, USA.
Seifert, W.K., Moldowan, J.M., 1986, 1986. Use of biological markers in petroleum exploration, in: Johns, R.B. (Ed.), Biological markers in the sedimentary record. Elsevier, Amsterdam, pp. 783-794.
Shamsuddin, A.H.M., Brown, T.A., Lee, S., Curiale, J.A., 2001. Petroleum Systems of Bangladesh. SEAPEX Exploration Conference, Singapore, pp.35.
Shamsuddin, A.K.M., Huq, M.M., Faruque, M.A., Chudhury, Z., Akhteruzzaman, M., Rahman, M., Haque, A., Talukder, M.W., Bygdevoll, J., Rafdal, J., 2004. Bangladesh gas reserve estimation 2003. Hydrocarbon Unit of Bangladesh and Norwegian Petroleum Directorate of Norway, Dhaka (unpublished), p. 254.
Shaver, S.A., Eble, C.F., Hower, J.C., Saussy, F.L., 2006. Petrography, palynology, and paleoecology of the Lower Pennsylvanian Bon Air coal, Franklin County, Cumberland Plateau, southeast Tennessee. International Journal of Coal Geology 67, 17-46.
Sherwood, N.R., Cook, A.C., 1986. Organic matter in the Toolebuc Formation, in: Gravestock, D.I., Moore, P.S., Pitti, G.M. (Eds.), Contribution to the geology and hydrocarbon potential of the Eromanga Basin. Geological Society of Australia, Australia, pp. 255-265.
Sia, S.G., Wan Hasiah, A., 2011. Concentration and association of minor and trace elements in Mukah coal from Sarawak, Malaysia, with emphasis on the potentially hazardous trace elements. International Journal of Coal Geology 88, 179-193.

Simandoux, P., 1963. Measures dielectriques en milieu poreux, application a measure des saturations en eau: Etude du Comportement des Massifs Argleux. Revue de I'institut Francais du Petrole, Supplementary Issue.

Singh, B.D., Singh, A., 2004. Observations on Indian Permian Gondwana Coals Under Fluorescence Microscopy: An Overview. Gondwana Research 7, 143-151.

Singh, M.P., Shukla, R.R., 2004. Petrographic characteristics and depositional conditions of Permian coals of Pench, Kanhan, and Tawa Valley Coalfields of Satpura Basin, Madhya Pradesh, India. International Journal of Coal Geology 59, 209-243.

Singh, M.P., Singh, G.P., 1995. Petrological evolution of the Paleogene coal deposits of Jammu, Jammu and Kashmir, India. International Journal of Coal Geology 27, 171-199.

Singh, M.P., Singh, P.K., 1994. Indications of Hydrocarbon generation in the coal deposits of the Rajmahal basin, Bihar: Revelation of Fluorescence microscopy. Journal of the Geological Society of India 43, 647-658.

Singh, M.P., Singh, P.K., 1996. Petrographic characterization and evolution of the Permian coal deposits of the Rajmahal basin, Bihar, India. International Journal of Coal Geology 29, 93-118.

Singh, P.K., Singh, M., Singh, A., Naik, A., Singh, V., Singh, V., Rajak, P., 2012a. Petrological and geochemical investigations of Rajpardi lignite deposit, Gujarat, India. Energy, Exploration & Exploitation 30, 131-152.

Singh, P.K., Singh, M., Singh, A., Naik, A., 2012b. Petrographic and geochemical characterization of coals from Tiru valley, Nagaland, NE India. Energy, Exploration & Exploitation 30, 171-192.

Singh, P.K., Singh, M.P., Prachiti, P.K., Kalpana, M.S., Manikyamba, C., Lakshminarayana, G., Singh, A.K., Naik, A.S., 2012c. Petrographic characteristics and carbon isotopic composition of Permian coal: Implications on depositional environment of Sattupalli coalfield, Godavari Valley, India. International Journal of Coal Geology 90–91, 34-42.

Singh, P.K., Singh, M.P., Singh, A.K., Arora, M., 2010a. Petrographic characteristics of coal from the Lati Formation, Tarakan basin, East Kalimantan, Indonesia. International Journal of Coal Geology 81, 109-116.

Singh, P.K., Singh, M.P., Singh, A.K., 2010b. Petro-chemical characterization and evolution of Vastan Lignite, Gujarat, India. International Journal of Coal Geology 82, 1-16.

Smyth, M., 1984. Coal microlithotypes related to sedimentary environments in the Cooper Basin, Australia. Special Publication of the International Association of Sedimentologists 7, 333-347.

Smyth, M., 2009. Coal microlithotypes related to sedimentary environments in the Cooper Basin, Australia, Sedimentology of coal and coal-bearing sequences. Blackwell Publishing Ltd., pp. 331-347.

Snowdon, L.R., 1995. Rock-Eval T_{max} suppression: documentation and amelioration. AAPG Bulletin 79, 1337-1348.

Snowdon, L.R., Powell, T.G., 1982. Immature oil and condensate- modofication of hydrocarbon generation model for terrestrial organic matter. AAPG Bulletin 66, 775-788.

Solli, H., Bjorøy, M., Leplat, P., Hall, K., 1984. Analysis of organic matter in small rock samples using combined thermal extraction and pyrolysis—gas chromatography. Journal of Analytical and Applied Pyrolysis 7, 101-119.

Spears, D.A., Zheng, Y., 1999. Geochemistry and origin of elements in some UK coals. International Journal of Coal Geology 38, 161-179.
Stach, E., Mackowsky, M.T., Teichmüller, M., Taylor, G.H., Chandra, D., Teichmüller, R., 1982. Stach's Textbook of Coal Petrology, 3rd ed, Gebruder Borntraeger, Berlin.
Steckler, M.S., Akhter, S.H., Seeber, L., 2008. Collision of the Ganges–Brahmaputra Delta with the Burma Arc: Implications for earthquake hazard. Earth and Planetary Science Letters 273, 367-378.
Swaine, D.J., 1990. Trace elements in coal. Butterworth, London and Boston.
Takeda, N., Kato, S., Fujiwara, M., Alam, M.N., Hossain, M.M., Khan, M.A.E., Rahman, M.M., M.A.H, S., 2011. Geochemistry of gas and condensate in the Surma basin, Bangladesh. Abstract. Petroleum Geology Conference and Exhibition, Malaysia.
Taylor, J.M., 1950. Pore-space reduction in sandstones. AAPG Bulletin 54, 1748-1749.
Teichmüller, M., 1974a. Generation of petroleum-like substances in coal as seen under the microscope, in: Tissot, B., Bienner, F. (Eds.), Advances in organic geochemistry 1973. Editions Technip, Paris, pp. 321-348.
Teichmüller, M., 1974b. Entstehung und Veranderung bituminoser Substanzen in Kohlen in Beziehung zur Entstehung und Umwandlung der Erdols. Fortschr. Geol. Rheinld. Westf. 24, 65-112.
Teichmüller, M., 1974c. Uber neue Macerale der Liptinit-Gruppe und die Entstehung des Micrinits. Fortschr. Geol. Rheinld. Westfalen 24, 37-64.
Teichmüller, M., Durand, B., 1983. Fluorescence microscopical rank studies on liptinites and vitrinites in peat and coals, and comparison with results of the Rock-eval pyrolysis. International Journal of Coal Geology 2, 197-230.
Teichmüller, M., Teichmüller, R., 1982. The geological basis of coal formation, in: Stach, E., Mackowsky, M.T., Teichmüller, M., Taylor, G.H., Chandra, D., Teichmüller, R. (Eds.), Stach's textbook of coal petrology, Gebruder Borntraeger, Stuttgart, pp. 5-86.
Thomas, B.M., 1982. Land plant source rocks for oil and their significance in Australian basins. Journal of Australian Petroleum Exploration Association 22, 164-178.
Thompson, S., Cooper, B.S., Morely, R.J., Barnard, P.C., 1985. Oil generating coals, in: Thomas, B.M. (Ed.), Petroleum geochemistry in exploration of the Norwegian Shelf. Graham & Trotman, London, pp. 59-73.
Thompson, S., Morley, R.J., Barnard, P.C., Cooper, B.S., 1985. Facies recognition of some Tertiary coals applied to prediction of oil source rock occurrence. Marine and Petroleum Geology 2, 288-297.
Thyberg, B., Jahren, J., 2011. Quartz cementation in mudstones: sheet-like quartz cement from clay mineral reactions during burial. Petroleum Geoscience 17, 53-63.
Tiab, D., Donaldson, E.C., 1996. Theory and practice of measuring reservoir rock and fluid transport properties. Gulf Publishing Company, Houston, p.706.
Tissot, B.P., Welte, D.H., 1984. Petroleum formation and occurrence, 2nd ed. Springer, Berlin.
Uddin, A., Lundberg, N., 2004. Miocene sedimentation and subsidence during continent-continent collision, Bengal Basin, Bangladesh. Sedimentary Geology 164, 131-146.
Uddin, M.N., Islam, M.S.U., 1992. Depositional environments of the Gondwana rocks in the Khalaspir basin, Rangpur District, Bangladesh. Bangladesh Journal of Geology 11, 31-40.
UNDP, 2008. Coal development in Bangladesh. UNDP, Dhaka, p. 32.
Wan Hasiah, A., 1997a. Evidence of early generation of liquid hydrocarbon from suberinite as visible under the microscope. Organic Geochemistry 27, 591-596.

Wan Hasiah, A., 1997b. Common liptinitic constituents of Tertiary coals from the Bintulu and Merit-Pila coalfields, Sarawak, and their relation to oil generation from coal. Bulletin of the Geological Society of Malaysia 41, 85-94.

Wan Hasiah, A., 1999a. Oil-generating potential of Tertiary coals and other organic-rich sediments of the Nyalau Formation, onshore Sarawak. Journal of Asian Earth Sciences 17, 255-267.

Wan Hasiah, A., 1999b. Organic facies variations in the Triassic shallow marine and deep marine shales of central Spitsbergen, Svalbard. Marine and Petroleum Geology 16, 467-481.

Wan Hasiah, A., 2003. Coaly source rocks of NW Borneo: role of suberinite and bituminite in oil generation and expulsion. Bulletin of the Geological Society of Malaysia 47, 153-163.

Wan Hasiah, A., Abolins, P., 1998. Organic petrological and organic geochemical characterisation of the Tertiary coal-bearing sequence of Batu Arang, Selangor, Malaysia. Journal of Asian Earth Sciences 16, 351-367.

Wang, L., Wang, C., Li, Y., Zhu, L., Wei, Y., 2011. Organic geochemistry of potential source rocks in the Tertiary Dingqinghu Formation, Nima Basin, Central Tibet. Journal of Petroleum Geology 34, 67-85.

Waples, D.W., Machihara, T., 1991. Biomarkers for geologists: a practical guide to the application of steranes and triterpanes in petroleum geology. AAPG, Tulsa, USA.

Waseda, A., Nishita, H., 1998. Geochemical characteristics of terrigenous- and marine-sourced oils in Hokkaido, Japan. Organic Geochemistry 28, 27-41.

Waxman, W.H., Smits, I.J.M., 1968. Electrical conductivities in oil-bearing sands. Society of Petroleum Engineers Journal 8, 107-122.

Welz, B., Sperling, M., 2007. Frontmatter, Atomic Absorption Spectrometry. Wiley-VCH Verlag GmbH.

Wilkins, R.W.T., George, S.C., 2002. Coal as a source rock for oil: a review. International Journal of Coal Geology 50, 317-361.

Wolf, K.H., Chlingaraian, G.V., 1976. Diagenesis of sandstones and compaction, in: Chlingaraian, G.V., Wolf, K.H. (Eds.), Compaction of coarse grained sediments II. Elsevier, Amsterdam, pp. 69-444.

Worden, R.H., Burley, S.D., 2003. Sandstone diagenesis: the evolution of sand to stone, in: Burley, S.D., Worden, R.H. (Eds.), Sandstone diagenesis: Recent and ancients. Blackwell Publishing Ltd, UK, pp. 1-46.

Worden, R.H., Morad, S., 2009. Clay Minerals in Sandstones: Controls on Formation, Distribution and Evolution, Clay Mineral Cements in Sandstones. Blackwell Publishing Ltd., pp. 1-41.

Wyllie, M.R.J., Rose, W.D., 1950. Some theoritical considerations related to the quantitative evaluations of the physical characteristics of reservoir rock from electric log data. Journal of Petroleum Technology 189, 105-110.

Zahid, K.M., Uddin, A., 2005. Influence of overpressure on formation velocity evaluation of Neogene strata from the eastern Bengal Basin, Bangladesh. Journal of Asian Earth Sciences 25, 419-429.

Zhang, X., Lin, C.-M., Cai, Y.-F., Qu, C.-W., Chen, Z.-Y., 2012. Pore-lining chlorite cements in lacustrine-deltaic sandstones from the Upper Triassic Yanchang Formation, Ordos Basin, China. Journal of Petroleum Geology 35, 273-290.